University of Alberta

Endoplasmic Reticulum Chaperone Proteins Calnexin and ERp57: Structure and Function

by

Helen Patricia Coe

A thesis submitted to the Faculty of Graduate Studies and Research
in partial fulfillment of the requirements for the degree of

Doctor of Philosophy

in

Medical Sciences

Pediatrics

Fall 2010

Edmonton, Alberta

Examining Committee

Marek Michalak, Biochemistry

Jason Dyck, Pediatrics

Bernard Thebaud, Pediatrics

Paul Melancon, Cell Biology

Kursad Turksen, Biochemistry

I would like to dedicate this thesis to
the two hardest working people I know:
my parents, Yashu and Patricia Coe.

ABSTRACT

The endoplasmic reticulum is responsible for folding of newly synthesized proteins. Chaperone proteins, calreticulin and calnexin, with the thiol-oxidoreductase ERp57, interact with nascent proteins in a cycle of quality control to ensure proteins are folded correctly. In this study, we investigated the tissue-specific expression of both calnexin and ERp57 throughout embryonic development. We found that calnexin is primarily expressed in neurological tissue and cartilage which is not surprising considering that targeted deletion of calnexin results in live mice with severe motor defects. Targeted deletion of the *Pdia3* gene, which encodes ERp57, in mice is embryonic lethal at embryonic day 13.5. ERp57 expressed mainly in lung, liver and neurological tissue suggesting that ERp57 may have a critical role in the development of these tissues. Both calnexin and ERp57 play a role in quality control and my findings suggest that calnexin- and ERp57-deficient cells are under persistent stress and adapt to maintain ER homeostasis during. We also show here that STAT3-dependent signalling is increased in the absence of ERp57 and this can be rescued by expression of ER-targeted ERp57 but not by cytoplasmic-targeted protein, indicating that ERp57 affects STAT3 signalling from the lumen of the ER. ERp57 effects on STAT3 signalling are enhanced by ER luminal complex formation between ERp57 and calreticulin.

We also used site-specific mutagenesis to disrupt cysteine and histidine residues in the N- and P-domains of calnexin. We identified that disruption $Cys^{161/195}$ in calnexin resulted in significant loss of its chaperone activity for glycoyslated substrates. Disruption of $Cys^{361/367}$ also had minor impacts on the function of calnexin as chaperone for glycosylated substrates. Mutations to H^{202}, $Cys^{161/195}$ and $Cys^{361/367}$ resulted in enhanced binding of ERp57 to calnexin. In conclusion, these observations suggest that the cysteine residues within calnexin are important to the structure and function of calnexin.

Research presented in this thesis highlights the diversity of the functions of ER proteins calnexin and ERp57 and understanding the ER-associated molecular mechanisms within a cell will undoubtedly give us essential knowledge regarding healthy and normal development.

AKNOWLEDGEMENTS

I would first like to thank my supervisor, Dr. Marek Michalak. Thank you for encouraging me to enter the PhD program and supporting me throughout. I will always appreciate everything I have learned from you in terms of science, writing, leadership and work-life balance. Without your guidance and mentorship I do not think I would appreciate and love science as much as I do today! Thank you!

I would also like to thank my supervisory committee, Dr. Jason Dyck and Dr. Bernard Thebaud, for all your feedback and helpful comments over the past 5 years as well as my examination committee members, Dr. Paul Melancon and Dr. Kursad Turksen, for feedback and editing of this thesis.

I am also very grateful to the Michalak lab members both past and present. It was easy to come to the lab everyday when you are surrounded by amazing people! Thank you to Jody for always answering questions! You are a role model for all students aspiring to achieve success in science and in life. I hope one day you will hire me! Thank you to Monika for teaching me about organization and always being available to show me new techniques. Thank you to my twin sister, Asia, for all our tissue culture talks and being a great teammate for writing papers and reviews! Thanks to Allison for being a great bench neighbour, to Alison for all the fantastic scrapbooks and help with the mice, to Daniel for being Dr. Calcium and making great mixtapes, to Dukgyu for interesting discussions and being a good neighbour, to Hao-Dong for always smiling and being so encouraging and to Ola for always making me laugh. Also thanks to Jeannine, Karen, Yuan and Sandi for all your help and guidance in the past.

I would also like to thank my family, Yashu, Patricia, Anna, Nick and Stephen Coe, Beau Lark, Li Li Chung and Zach Su. Your patience, support and encouragement has never gone unnoticed. I am the luckiest person in the world to have such an amazing family! I would also like to thank my friends, Cecilia Lee, Colleen So, Craig Robb, Dejan Ozegovic, Elisa Lee, Ersilia Coccaro, Fatima Mraiche, Grace Kim, James Ng, Kathy Tse, Kerry Tham, Linda Chung, Marjorie Hitschfeld, Mo Salama, Rob Golden, Sharon Lee, Vivi Trinh, Vince Kong and Ying-Ying Lee. Between accompanying me to the lab late at night or on weekends, to being there to listen to a practice talk, to being so supportive, you guys are the absolute best!

TABLE OF CONTENTS

LIST OF TABLES

Chapter One

Chapter Three

Chapter Four

LIST OF FIGURES

Chapter One

Chapter Two

Chapter Three

Chapter Four

Appendix

LIST OF ABBREVIATIONS

AMPA	α-amino-3-hydroxy-5-methyl-4-isoxazolepropionate
APMSF	4-amidinophenyl-methanesulfonyl fluoride hydrochloride monohydrate
AARE	amino acid response elements
ARE	antioxidant response elements
ATF3	activating transcription factor-3
ATF4	activating transcription factor-4
ATF6	activating transcription factor-6
ATP	adenosine triphosphate
Bap31	B cell receptor-associated protein 31
Bcl-2	B-cell lymphoma 2
BFA	brefeldin A
BGS	bovine growth serum
bp	base pair
BPD	bronchopulmonary dysplasia
BSA	bovine serum albumin
bZip	basic leucine zipper domain
CDK	casein kinase II
CFTR	cystic fibrosis transmembrane conductance regulator
CGHC	catalytically active motifs
ChIP	chromatin immunoprecipitation
CHOP	CCAAT/enhancer binding protein (C/EBP) homologous protein
CMV	cytomegalovirus

CNFT	ciliary neurotrophic factor
CNS	central nervous system
CNX	calnexin
Col2α1	collagen alpha type II
COMP	cartilage oligomeric matrix protein
ConA	concanavalin A
COO^-	carboxyl-terminal
COUP-TF1	chicken ovalbumin upstream transcription factor 1
CTLs	cytotoxic T-lymphocytes
CRE	cAMP response element
CRT	calreticulin
Cst	castanospermine
Cx40	connexin 40
Cx43	connexin 43
DAG	diacylglycerol
DMEM	Dulbecco's modified eagle medium
dHMNV	distal hereditary motor neuropathy type V
E64	(2S,3S)-3-(N-{(S)-1-[N-(4-guanidinobutyl)carbamoyl]3-methylbutyl}carbamoyl)oxirane-2-carboxylic acid
ECL	electro chemiluminescence
EDC	1-Ethyl-3-(3-dimethyl-aminopropyl) carbodiimide HCl
EDEM	ER degradation-enhancing α-mannosidase
EDTA	ethylene diamine tetraacetic acid
EGF	epidermal growth factor

EGTA	ethylene glycol tetraacetic acid
eIF2α	eukaryotic initiation factor 2α
ER	endoplasmic reticulum
ERAD	ER-associated degradation
ERSE	ER response element
Evi1	ecotropic viral integration site 1
FACs	fluorescence-activated cell sorting
FBS	fetal bovine serum
FITC	fluorescein isothiocyanate
Fura 2-AM	fura-2-acetoxymethyl ester
GAPDH	glyceraldehyde 3-phosphate dehydrogenase
GATA6	GATA-binding protein 6
GFP	green fluorescent protein
GlucI/II	glucosidase 1 and II
GLSs	Golgi localization sites
GMEM	Glasgow minimal essential medium
gp130	glycoprotein 130
GRp78	glucose-regulated protein-78
GRp94	glucose-regulated protein 94
HCN1	hyperpolarization-activated cyclic nucleotide-gated channel 1
icm	inner cell mass
IL6	interleukin-6
$InsP_3$	inositol 1,4,5-triphosphate
$InsP_3R$	inositol 1,4,5-triphosphate receptor

IRE1	inositol-requiring kinase 1
ISG	type I interferon (IFN) stimulation, lipopolysaccharide stimulation
ISRE/GAS	interferon-gamma activation sequence
JAK	Janus kinase
K_A	association tendency
K_a	rate of association
K_D	disassociation tendency
K_d	rate of disassociation
KDEL	lysine-aspartate-glutamate-leucine
Keap1	Kelch-like Ech-associated protein 1
Krox-20 (Egr2)	early growth response protein 2
LIF	leukemia inhibitory factor
LLVY	leucine-leucine-valine-tyrosine
Maf-2 homolog 2	V-maf musculoaponeurotic fibrosarcoma oncogene
α1,2-man	α1,2-mannosidase
MARRS	membrane associated, rapid response steroid binding
MDH	malate dehydrogenase
MED	multiple epiphyseal dysplasia
MEFs	mouse embryonic fibroblasts
MEF2C	myocyte enhancer factor 2C
MEKK1-C	MEK kinase1-C
MHC	major histocompatibility complex
MIP-1	macrophage inflammatory protein 1

MLC2v	ventricular myosin light chain 2
M-MLV	Moloney Murine Leukemia Virus
MOPS	3-(N-morpholino)propanesulfonic acid
MPO	myeloperoxidase
NCX	Na^{+}/Ca^{2+} exchanger
NFAT	nuclear factor of activated T-cells
NFkappa B	nuclear factor kappa B
NH^{3+}	amino-terminal
NHS	N-Hydroxysuccinimide
Ni-NTA	Ni^{2+}-nitrilotriacetic acid-agarose
Nkx2.5	NK2 transcription factor related locus 5
NMDA	N-methyl-D-aspartic acid
NMR	nuclear magnetic resonance
NP-40	nonyl phenoxylpolyethoxylethanol
NRF2	nuclear respiratory transcription factor 2
OCA1	oculocutaneous albinism type 1
OCT	optimal cutting temperature compound
OST	oligosaccharyltransferase
P0	protein zero
Pax-6	paired box gene 6
PBS	phosphate-buffered saline
PCR	polymerase chain reaction
PDI	protein disulfide isomerase
PDK	proline-directed kinase

PERK ER kinase	double-stranded RNA-activated protein kinase-like
PIP_2	phosphatidylinositol 4,5-bisphosphate
PKC	protein kinase C
PL-C	phospholipase C
PLC	peptide loading complex
PLP	proteolipid protein
PMCA	plasma membrane Ca^{2+} ATPase
PMP22	peripheral myelin protein 22
PMSF	phenylmethylsulfonyl fluoride
PNS	peripheral nervous system
PrP^{SC}	misfolded prion proteins
PSACH	pseudoachondroplasia
P-STAT3	phosphorylated-STAT3
QDEL	glutamine-aspartate-glutamate-leucine
RANTES (CCL5)	chemokine (C-C motif) ligand 5
RER	rough endoplasmic reticulum
RFUs	relative fluorescence units
RIP	regulated intramembrane proteolysis
RKPRRE	arginine-lysine-proline-arginine-arginine-glutamate
RLUs	relative light units
R_{max}	maximum RUs
RT	room temperature
RT-PCR	reverse transcriptase –PCR
RUs	resonance units

RyR	ryanodine receptor
S1P	site-1 protease
S2P	site-2 protease
SDS-PAGE electrophoresis	sodium dodecyl sulfate polyacrylamide gel
SER	smooth endoplasmic reticulum
SERCA	sarcoplamsic/endoplasmic reticulum Ca^{2+}-ATPase
SH2	Src homology-2
siRNA	small interfering RNA
SNS	sympathetic nervous system
SOC	store-operated Ca^{2+}
Sox9	Sry-related HMG box 9
SP	signal peptidase
SPR	surface plasmon resonance
SRP	signal recognition particle
STAT3	signal transducer and activator of transcription 3
STAT3-C	constitutively active STAT3
STIM1	stromal interaction molecule 1
SUMO	small ubiquitin like modifier
TAP	peptide transporter
Tg	thapsigargin
TLCK	Nα-tosyl-Lys-chloromethylketone
TPCK	Tosyl-phenylalanyl-chloromethylketone
TRPC	transient receptor potential channels
Tn	tunicamycin

TSE	transmissible spongiform encephalopathy
UGGT	UDP-glucose:glycoprotein glucosyltransferase
UPR	unfolded protein response
UPRE	UPR element
VWF	von Willebrand factor
wt	wild-type
Xbp1	X-box binding protein
X-gal	5-bromo-4-chloro-3-indoyl-β-D-galactopyraonoside

Table 1 – Primers used in this study

Primers for RT-PCR			
Gene	**Forward**	**Reverse**	**Chapter**
Xbp1	5′- CCTTGTGGTTGAG ACCAGG-3′	5′-CTAGAGGCTTGGT GTATAC-3′	2,3
calnexin	5′-CATGATGGACATG ATGATGACAC-3′	5′- GGTCTTCAGACTTG CATCT GGC-3′	2
GRp78	5′-TGGTATTCTCCGA GTGACA GC-3′	5′-AGTCTTCAATGTC CGCAT CC-3′	2,3
GAPDH	5′-AACTTTGGCATTG TGGAA GG-3′	5′-ACACATTGGGGGT AGGAAC A-3′	2,3
tubulin	5′-CCGGACAGTGTGG CAACCA GATCGG-3′	5′-TGGCCAAAAGGAC CTGAGCG AACGG-3′	2
STAT3	5′-AGTCACATGCCAC GT TGGTGT TTC-3′	5′-CGGGCAATTTCCAT TGGCTTC TCA -3′	3
Primers used for identifying cassette insertion			
Gene	**Forward**	**Reverse**	**Chapter**
ERp57	INVF1 5′-GTTCCCAACG ATCAAGGCGAG-3′	INVR1 5′ AAGCCATAC CAAACGACGAGCG-3′	3
	INVF2 5′- TCAAGGCG AGTTACATGATCCC-3′	INVR2 5′-CGAGCGTGAC ACCACGATGC-3′	3
Primers used for genotyping			
Gene	**Forward**	**Reverse**	**Chapter**
ERp57	F2 5′-GGACAGTTTTGA GCTGCCAT-3′	R3 5′-TCTCCATTATCAT CGTACTCC-3′	3
	F1 5′-TCAAGGCGAGT TACATGA TCCC-3′		3
Lentivirus Primers *att*B1(forward) *att*B2 (reverse) recombination site (bold), Kozak sequence for expression in mammalian cells (italics) ,gene specific nucleotides (underlined)			
Gene	**Forward**	**Reverse**	**Chapter**
full-length ERp57	5′-GGGG**ACAAGTTTG TACAAAAAAGCAGGC T**AT*ACCATG*CGCTTCAG CTGCCTAGCT-3′	5′-GGGG**ACCACTTTG TACAAGAAAGCTGGG T**CCTAGAGGTCTCTTGT GCCTTCTT-3′	3
no signal sequence ERp57	5′- GGGG**ACAAGTTT GTACAAAAAAGCAGG CT**AT*ACCATGG*ATGTGT	5′-GGGG**ACCACTTTG TACAAGAAAGCTGGG T**CCTAGAGGTCTCTTGT	3

	TGGAACTGACGGACGA-3′	GCCTTCTT-3′	
calnexin	5′GGGG**ACAAGTTTGT ACAAAAAAGCAGGCT** TC*ACCATG*GAAGGGAA GTGGTTACT-3′	5′-GGGG**ACCACTTTGT ACAAGAAAGCTGGGT** CTCACTCTCTTCGTGGC TTTCT′-3′	4
Mutagenesis Primers for Mouse Calnexin (mutation in bold)			
Mutation	**Forward**	**Reverse**	**Chapter**
$C^{161}A$	5′-GGAATAGAA**GCT**GG TGGTG CCTATGTGAA GCTGCTT TCC-3′	5′- GGAAAGCAGCTTC ACATAGCACCACCAGC TTCTAT-3′	4
$C^{195}A$	5′- GGTCCAGATAAG **GCT**GGAGAG GACTAC AAA CTG CAT TTC -3′	5′- GAAATGCAGTTTG TAGTCCTCTCCAGCCTT ATCTGGACC – 3′	4
$H^{202}A$	5′-GGAGAGGACTACA AACTG**GCA**TTCATCTTT CGACACAAAAATCCC– 3′	5′- GGGATTTTTGTG TCGAAAGATGAATGCC AGTTTGTAGTCCTCTCC - 3′	4
$H^{219}A$	5′- GGTGTATATGAAGA AAAACAT**GCA**AAGAG GCCAGATGCAGATCTG – 3′	5′- CAGATCTGCATCTG GCTTCTTTGCTCGTTTTT CTTCATATACACC-3′	4
$C^{360}A$	5′- GCCAACCCCAAG **GCT**GAGTCA GCCCCT GGG-3′	5′- CCCAGGGGCTGAC TCAGCCTT GGGGTT GGC-3′	4
$C^{366}A$	5′- GCCCCTGGG**GCT**GG TGTCTGGCAGCGACCT ATG-3′	5′- CATAGGTCGCTGC CAGACACCAGCCCCAG GGGC-3′	4
Mutagenesis Primers for Soluble Dog Calnexin (mutation in bold)			
Mutation	**Forward**	**Reverse**	**Chapter**
$C^{161}A$	5′-GGAATAGAA**GCT** GGTGGTGCCGCCTATG TGAAACTGCTTTCC-3′	5′-GGAAAGCAGTTTC ACATAGGCGGCACCAC CAGCTTCTATTCC-3′	4
$C^{195}A$	5′-GGTCCAGATAAA **GCT**GGAGAAGCATATA AACTGCACTTC-3′	5′-GAAGTGCAGTTTAT AGTCTTCTCCAGCTTTA TCTGGACC-3′	4
$H^{202}A$	5′-GGAGAAGACTATA AACTG**GCT**TTCATCTTC CGCCACAAAAACCCC-3′	5′-GGGGTTTTTGTGGC GGAAGATGAAAGCCA GTTTATAGTCTTCTCC-3′	4
$H^{219}A$	5′-ACAGGCGTATATGA	5′-ATCTGCATCTGGCC	4

	AAAG**GCT**GCTAAGAG GCCACATGCAGAT-3′	TCTTAGCAGCCTTTTCT TCATATACGCCTGT-3′	
$C^{361}A$	5′-CAACCCTAAG**GCT**G AGTCGGC CCCTG-3′	5′-CAGGGGCCGACTCA GCCTTA GGGTTG-3′	4
$C^{367}A$	5′-GGCCCCTGGG**GCT**G GTGTCTG GCAG-3′	5′-CTGCAAGACACCA GCCCCAG GGGCC-3′	4
Mutagenesis Primers for Insertion of Restriction Sites (restriction sites underlined)			
template	**forward**	**reverse**	**Chapter**
IRE1α	5′- GCTAGCTCTAGAGA ATTCGATATCATGGCT ACCATTATCCTGAGC ACCTTCCTGC -3′	5′- GGGCCCGAGGGCTG CCCTAGCTCAGAGGGC ATATGGAATCAC TGG -3′	appendix
mouse CNX	5′- GCTAGCATGGAAG GGAAGTGG TTAC-3′	5′- GAATTCCAAAATG TAGACCACCCAAAGCC -3′	appendix
mouse ERp57	5′- TCTAGAATGCGCTT CAGCTGCC TA G-3′	5′ – GATATCGAGGTCCT CTTGTG CCTT C-3′	appendix
GST	5′ – GCTAGCATGTCCC CTATACTA GG -3′	5′ – TCTAGACGATGAA TTCCCG GGGATC -3′	appendix

Table 2 – Antibodies used in this study

Antibody Name	Western Blot Dilution	Immunostaining Dilution	Source	Chapter
rabbit anti-calnexin	1:1000	1:100	StressGen Inc.	2,3,4
rabbit anti-PDI	1:1000	1:50	generated in our laboratory	2,3
goat anti-calreticulin	1:500	-	generated in our laboratory	2,3
rabbit anit-ERp57	1:300	1:100 1:150 (FACs)	generated in our laboratory	2,3
rabbit anti-GAPDH	1:1000	-	Abcam	2
mouse anti-IRE1	1:500	-	Dr. R. Kaufman	2
rabbit anti-GRp78	1:1000	1:50	StressGen Inc.	2,3
rabbit anti-GRp94	1:1000	1:50	StressGen Inc.	2
goat anti-rabbit	1:10000	-	Invitrogen	2,3,4
rabbit anti-goat	1:10000	-	Invitrogen	2,3,4
rabbit anti-ERp41	1:1000	-	generated in our laboratory	3
rabbit anti-ERp54	1:1000	-	generated in our laboratory	3
rabbit anti-β-tubulin	1:1000	-	StressGen Inc.	3
rabbit-anti-phospho-STAT3 (Y^{705})	1:1000	-	Cell Signalling	3
rabbit anti-STAT3	1:1000	-	Cell Signalling	3
rabbit conjugated-fluorescein isothiocyanate (FITC)	-	1:100 1:200	Invitrogen	3,4
anti-rabbit Alexa Fluor 546	-	1:100	Invitrogen	2

Table 3 – Cell lines generated and/or used in this study

cell line	abbreviation	reference	Chapter
calnexin wild-type MFs	*wt*	generated in this study	2
calnexin-deficient MFs	*cnx*$^{-/-}$	generated in this study	2
calnexin wild-type MEFs	*wt*	generated in this study	2
calnexin-deficient MEFs	*cnx*$^{-/-}$	generated in this study	2,3,4
ERp57 and calreticulin wild-type MEFs	wild-type	Mesaeli, N., et al., J. Cell Biol., 1999. **144**	3
ERp57-deficient MEFs	*ERp57*$^{-/-}$	generated in this study	3
calreticulin-deficient MEFs	*crt*$^{-/-}$	Mesaeli, N., et al., J. Cell Biol., 1999. **144**	3
ERp57-deficient MEFs expressing:			
full-length ERp57	*ERp57*$^{-/-}$ *-ERp57*$_{ER}$	generated this study	3
no signal sequence ERp57	*ERp57*$^{-/-}$ *-ERp57*$_{cyt}$	generated this study	3
green florescent protein	*ERp57*$^{-/-}$ *-ERp57*$_{GFP}$	generated this study	3
calreticulin-deficient MEFs expressing:			
full-length calreticulin	*crt*$^{-/-}$ *-CRT*	Nakamura, K., et al., J. Cell Biol., 2001. **154**	3
full-length calreticulin that has loss of ERp57 binding	*crt*$^{-/-}$ *-CRT*^{E239R}	Martin, V., et al., J Biol Chem, 2006. **281**	3
full-length calreticulin that has ERp57 binding	*crt*$^{-/-}$ *-CRT*^{G242A}	Martin, V., et al., J Biol Chem, 2006. **281**	3
calnexin-deficient MEFs expressing:			
full-length calnexin	*cnx*$^{-/-}$*-CNX*	generated in this study	4
cysteine 161 to alanine mutant of calnexin	*cnx*$^{-/-}$*-C*^{161}	generated in this study	4
cysteine 195 to alanine mutant of calnexin	*cnx*$^{-/-}$*-C*^{195}	generated in this study	4
histidine 202 to alanine mutant of calnexin	*cnx*$^{-/-}$*H*^{202}	generated in this study	4
histidine 219to alanine mutant of calnexin	*cnx*$^{-/-}$*H*^{219}	generated in this study	4
cysteine 360 to alanine mutant of calnexin	*cnx*$^{-/-}$*-C*^{360}	generated in this study	4
cysteine 366 to alanine mutant of calnexin	*cnx*$^{-/-}$*-C*^{366}	generated in this study	4
cysteine 161 and 195 to alanine mutant of calnexin	*cnx*$^{-/-}$*-C*$^{161/195}$	generated in this study	4
cysteine 360 and 366 to alanine mutant of calnexin	*cnx*$^{-/-}$*-C*$^{360/366}$	generated in this study	4

Table 4 – Plasmids used in this study

Plasmid Description	Name	Source	Chapter
Xbp1 splicing *Firefly* luciferase, CMV *Renilla* luciferase	pRL-XFL	Dr. R. Kaufman	2,3
Firefly luciferase reporter driven by a 311 bp fragment (-304 to +4) of the GRp78 promoter	pGL3-GRp78-luciferase	Dr. R. Kaufman	2,3
Renilla luciferase reporter plasmid	pRL-CMV	Promega	2,3
full-length ERp57 in destination lentiviral vector with blasticidine resistance	p2K7-ERp57$_{ER}$	generated in this study	3
no signal sequence ERp57 in destination lentiviral vector blasticidine resistance	p2K7-ERp57$_{cyt}$	generated in this study	3
soluble dog calnexin with His-tag	pBAD-CNX	previously generated in our laboratory	4
full-length calnexin in destination lentiviral vector blasticidine resistance	p2K7-CNX	generated this study	4, appendix
full-length mouse IRE1α with zeocin resistance	IRE1α-pcDNA3.1	Dr. K. Myoshi	appendix
target plasmid with multiple cloning site, CMV promoter and zeocin resistance	pcDNA3.1/zeo	Invitrogen	appendix
mouse IRE1α-mini-multiple cloning site with zeocin resistance	IRE1α-mini-MCS	generated in this study	appendix
mouse calnexin with EcoR1/Nhe1 restriction sites	soluble calnexin-RS	generated in this study	appendix
mouse ERp57 with Xba1/EcoRV restriction sites	ERp57-RS	generated this study	appendix
GST-containing plasmid	pGEX-3X	GE Healthcare	appendix
GST with Nhe1 and Xba1 restriction sites	GST-RS	generated this study	appendix
mouse IRE1α-mini-multiple cloning site and deletion of luminal domain with zeocin resistance	IRE1$\alpha\Delta$luminal-mini-MCS	generated this study	appendix

p2K7-calnexin mutant plasmids:			
Plasmid Description	**Name**	**Source**	**Chapter**
cysteine 161 to alanine, blasticidine resistance	p2K7-$C^{161}A$	generated in this study	4
cysteine 195 to alanine, blasticidine resistance	p2K7-$C^{195}A$	generated in this study	4
histidine 202 to alanine, blasticidine resistance	p2K7-$H^{202}A$	generated in this study	4
histidine 219 to alanine, blasticidine resistance	p2K7-$H^{219}A$	generated in this study	4
cysteine 360 to alanine, blasticidine resistance	p2K7-$C^{360}A$	generated in this study	4
cysteine 366 to alanine, blasticidine resistance	p2K7-$C^{366}A$	generated in this study	4
cysteine 161 and 195 to alanine, blasticidine resistance	p2K7-$C^{161/195}A$	generated in this study	4
cysteine 360 and 366 to alanine, blasticidine resistance	p2K7-$C^{360/366}A$	generated in this study	4
pBAD-calnexin mutant plasmids for purification:			
Plasmid Description	**Name**	**Source**	**Chapter**
cysteine 161 to alanine, His-tag	pBAD-$C^{161}A$	generated in this study	4
cysteine 195 to alanine, His-tag	pBAD-$C^{195}A$	generated in this study	4
histidine 202 to alanine, His-tag	pBAD-$H^{202}A$	generated in this study	4
histidine 219 to alanine, His-tag	pBAD-$H^{219}A$	generated in this study	4
cysteine 361 to alanine, His-tag	pBAD-$C^{361}A$	generated in this study	4
cysteine 367 to alanine, His-tag	pBAD-$C^{367}A$	generated in this study	4
cysteine 161 and 195 to alanine, His-tag	pBAD-$C^{161/195}A$	generated in this study	4
cysteine 361 and 367 to alanine, His-tag	pBAD-$C^{361/367}A$	generated in this study	4

Chapter One
Introduction

Introduction

The Dynamics of the Endoplasmic Reticulum - The endoplasmic reticulum (ER) is a large membrane-bound network that is continuous with the nuclear envelope and found throughout the cytoplasm of all eukaryotes [1, 2]. The word "endoplasmic" means within the cytoplasm and "reticulum" is derived from the word meaning "network." The two types of ER, rough endoplasmic reticulum and smooth endoplasmic reticulum (SER) are morphologically and functionally distinct. The rough ER is studded with ribosomes giving it a rough appearance in electron microscope images while the smooth ER is markedly absent of ribosomes. The ER lumen milieu is distinctly different from the rest of the cell allowing it to have diverse roles such as protein folding, synthesis and degradation and trafficking, post-translational modifications, lipid and steroid metabolism, Ca^{2+} storage and release and intracellular signalling and cellular response to stress [2-6]. Additionally, the ER of mammalian cells is a major site of Ca^{2+} storage and has a very high Ca^{2+} content relative to the Ca^{2+} content in the cytosol. This high intra-luminal Ca^{2+} content is mediated by numerous ER Ca^{2+} buffering proteins and is critical to the protein folding reactions as well as the protein folding machinery [7, 8]. High luminal Ca^{2+} also allows the ER to play a role in intracellular signalling by releasing its Ca^{2+} content into the cytosol resulting in large increase in cytosolic Ca^{2+} concentrations [7]. Often, Ca^{2+} buffering proteins are also components of the protein folding machinery within the ER. The collection of activities involved protein synthesis, folding and degradation is termed quality control. Molecular chaperones and foldases are major components of quality control and they are involved in ensuring newly

synthesized proteins obtain their correct functional conformation. When looking at major redox buffer of the cell, glutathione, the cytosol has a ratio of reduced (GSH) to oxidized glutathione (GSSG) from 30:1 to 100:1 while the ER has a ratio of 1:1 to 3:1 [9]. This allows the ER to uniquely provide an oxidizing environment where disulfide bonds can be formed in newly synthesized proteins. Not only it is a major folding compartment of the eukaryotic cell, but is also the first compartment in the secretory pathway [6]. Terminally misfolded proteins are sent for proteasomal degradation by a mechanism termed ER-associated degradation (ERAD). If misfolded proteins escape both quality control and ERAD, the increase in misfolded proteins within the ER lumen is dealt with by several ER sensors that make up the unfolded protein response (UPR.) Taken together, the ER has developed numerous mechanisms to ensure that it is functioning correctly and efficiently and can mediate responses to deal with fluctuations and shortcomings of the cell.

The contributions of the ER to the coordination of cellular processes is dictated by the numerous proteins that mediate its functions to make it major Ca^{2+} store of the cell as well as the site of protein synthesis and folding. Studies of animal and cellular models of deficiencies in these molecular players will also us to gain insight into structure and function of the proteins and, ultimately, the ER. This introduction will focus on the molecular cast that takes the stage to carry out numerous ER functions.

1.0 Ca^{2+} Signalling of the Endoplasmic Reticulum - Cytoplasmic Ca^{2+} acts as a versatile and powerful second messenger impacting cellular events such as exocytosis, contraction, metabolism, transcription and fertilization [10].

The ER is the major Ca^{2+} store of the cell with a total (free and bound) ER Ca^{2+} concentration estimated to be 2 mmol/l while the free ER Ca^{2+} varies from 50 to 500 μmol/l [11]. These fluctuations in ER luminal Ca^{2+} also impact numerous cellular functions including secretion, contraction–relaxation, motility, metabolism, protein synthesis, modification and folding, gene expression, cell-cycle progression and apoptosis [12]. The enormous capacity of the ER for Ca^{2+} is mediated by the Ca^{2+} buffering capacity of the resident proteins [12, 13]. The constantly fluctuating free Ca^{2+} concentrations within the ER is maintained by a balance of uptake and release into the cytoplasm [13]. Overload and depletion of ER Ca^{2+} stores can have detrimental effects on the entire cell [14].

1.1 Ca^{2+} buffering proteins - Ca^{2+} buffering proteins of the ER (Table 1-1) are unique in a sense that they often possess dual functions and are also molecular chaperones or folding enzymes involved in protein folding and posttranslational modification [13, 14]. This fascinating trick of evolution has resulted in proteins whose folding capability is directly influenced by intraluminal Ca^{2+} fluctuations [13]. This allows the ER to have fine control over its folding capacity by modifying Ca^{2+} concentration within the lumen [13]. Perhaps the most widely studied Ca^{2+} buffering protein of the ER is calreticulin [15]. Calreticulin has been known to be involved in many cellular processes and this is in part due to its role as a Ca^{2+} buffering protein [15]. Calreticulin has a very specific domain structure with an N-terminal globular domain, a P-arm domain and a C-terminal tail domain [15]. *In vitro* studies have defined two domains of calreticulin with one site each that are involved in Ca^{2+} binding; the P-domain binds Ca^{2+} with a high affinity (K_d = 1 μmol/l) and low capacity (1 mol of Ca^{2+} per mol of

protein) [16] and the C-domain binds Ca^{2+} with a low affinity (2 mol/l) and high capacity (25 mol of Ca^{2+} per mol of protein) [16, 17]. The C-domain consists of a large stretch of acidic amino residues interrupted, at regular interval, with one or more basic lysine or arginine residues. It was found that disruption of these basic residues results in a decrease in Ca^{2+} binding capacity and this can be directly attributed to the lysine amino group sidechains [18]. In fact, the C-domain of calreticulin alone is responsible for binding over 50% of Ca^{2+} within the ER [17]. In order to effectively understand the Ca^{2+} binding properties of calreticulin and its unique role within the cell, it is important to investigate cellular and animal models looking calreticulin-deficiency and over-expression. For example, in calreticulin-deficient mouse embryonic fibroblasts (MEFs) there is a significant decrease in Ca^{2+} storage and when full-length calreticulin or the P + C (the domains involved in Ca^{2+} binding) domains of calreticulin are expressed, there is full recovery of Ca^{2+} of the ER [17]. It is likely that this is due specifically to the high capacity C-domain because expression of the N + P domain of calreticulin does not recover Ca^{2+} capacity of calreticulin-deficient MEFs [17]. The impact that the presence or absence of calreticulin has on ER Ca^{2+} capacity and the influence that Ca2+ fluctuations is known to have in the regulation of cellular processes, makes it not surprising that alteration in calreticulin protein levels ultimately impact tissue development *in vivo* (See '*2.2b-iii-Mouse models*') [15, 19-22]. Calreticulin is also studied as a molecular chaperone involved in protein folding and quality control (See '*2.1 Quality Control in the Endoplasmic Reticulum*') [3]. Interestingly, monoglucosylated carbohydrate binding to calreticulin is dependent of the presence of Ca^{2+} [23]. Compelling evidence tying

together the dual functionality of calreticulin as Ca^{2+} binding protein and molecular chaperone comes from studies involving limited proteolysis trypsin digestion [24]. When ER Ca^{2+} levels are low (<100 μmol/l) calreticulin is rapidly degraded by trypsin, however under high ER Ca^{2+} concentrations (500 μmol/l to 1 mmol/l) calreticulin forms a N-domain protease resistant core [24]. This suggests that Ca^{2+} fluctuations are able to affect the conformation of calreticulin and, ultimately, impacting function [24].

Aside from calreticulin, there are other Ca^{2+} binding proteins resident within the ER lumen and showing variance in their Ca^{2+} binding affinity as well as Ca^{2+} capacity [13, 15, 22, 25]. Some of these Ca^{2+} binding chaperones and foldases include calnexin, BiP/GRp78, glucose-regulated binding protein 94 (GRp94), protein disulfide isomerase (PDI)/Calcistorin and ERp72 [25-30]. Calnexin also binds Ca^{2+} but it does not appear to play a role of Ca^{2+} buffer in the ER [31, 32]. Outside of the ER, the cytoplasmic, highly acidic C-terminal domain of calnexin binds Ca^{2+} with moderate affinity and may affect the function of calnexin (See "*2.2a-i-Structure*") [31]. BiP/GRp78 binds Ca^{2+} with a very low capacity (1-2 mol of Ca^{2+} per mol of protein) but is surprisingly responsible for as much as 25% of the Ca^{2+} binding capacity of the ER [25]. It is thought that, unlike calreticulin, the BiP chaperoning domain and Ca^{2+} domain may be intermixed as there is no obvious domain segregation as determined by the polypeptide sequence [25]. The ATPase activity of BiP is regulated under depletions of ER Ca^{2+} providing another example of Ca^{2+} fluctuations and protein function [33]. BiP has also been shown to be involved in the transport of Ca^{2+} from the ER to the mitochondria through transient associations with

the ER membrane sigma-1 receptor (Sig-1R) [33]. As well, BiP plays a role in Ca^{2+} efflux into the ER through its association with Sec61 to keep it closed during protein translocation or in the absence of translocation [33]. GRp94 is also known to bind ER Ca^{2+} through its 15 site, 4 with moderate affinity (K_d ~ 2 μM) and low capacity (1 mol of Ca^{2+} per mol of protein) and 11 with low affinity (K_d~600 μM) and high capacity (10 mol of Ca^{2+} per mol of protein) [26]. The function of GRp94 is thought to be regulated by ER Ca^{2+} and studies showing, *in vitro,* 100 nM of free Ca^{2+} can result in dramatic conformational changes the protein structure [26]. Indeed, it has been suggested that GRp94 may have a role in myocardial cell differentiation and heart development and it has been found that a selective increase in GRp94 expression in response to Ca^{2+} levels is able to protect cardiomyocytes from ischemia [26-28]. Additionally, through its modulation of ER Ca^{2+} stores, it has been suggested that GRp94 has a role in anti-oxidant cytoprotection [34]. Finally, it is also thought that Ca^{2+} binding to GRp94 regulate its interactions with other proteins [26]. For example, in a non-physiological system, GRp94 is able to bind calmodulin in the presence of Ca^{2+}, thereby inhibiting GRp94 from binding actin filaments [26].

The ER is also home to a number of oxidoreductases that have dual functions as ER Ca^{2+} buffering proteins in addition to being folding enzymes. PDI is a 58-kDa protein that binds Ca^{2+} with a high capacity (19 mol Ca^{2+} per mol of protein) and weak affinity (K_d=2-5 mM) [29]. PDI is thought to bind to Ca^{2+} through a cluster of paired acidic residues in the C-terminal of the protein [35]. Function of PDI may also be associated with Ca^{2+} binding as UV spectral analysis show that there are conformational

Table 1-1: Calcium buffering proteins of the endoplasmic reticulum

Protein	Ca^{2+} affinity	Ca^{2+} capacity (per mol of protein)
PDI	**weak** - 2-5 mM	**high** - 20 mol of Ca^{2+}
GRp94	**high** – 2 μM (4 sites) **low** – 600 μM (11sites)	**low** - 1 mol of Ca^{2+} **high** - 10 mol of Ca^{2+}
GRp78/BiP	-	**low** - 1-2 mol of Ca^{2+}
CNX	-	**low** capacity
CRT	**high** – 1 μM (P-domain) **low** – 2 mM (C-domain)	**low** - 1 mol Ca^{2+} **high** - 25 mol Ca^{2+}
calcistorin	**low** – 1 mM	**high** - 23 mol Ca^{2+}
ERp72	**low**	**high** - 12 mol Ca^{2+}

changes in the protein induced by Ca^{2+} binding [29]. ERcalcistorin/PDI is an ER-luminal calsequestrin-like protein that binds Ca^{2+} with a high capacity (23 mol of Ca^{2+} per mol of protein) and low affinity (K_d ~ 1 mM) [35]. Mutagenesis studies have also suggested that clusters of paired acidic residues within the C-terminal end of ERcalcistornin/PDI may constitute, in part, the low affinity binding sites for Ca^{2+} [35]. ERp72 (also known as Ca^{2+} binding protein 2 or CaBP2) is a 72-KDa PDI-like family member that binds Ca^{2+} with a high capacity (12 mol of Ca^{2+} per mol of protein) and low affinity [30]. Taken together, a number of ER chaperones and foldases are responsible for the Ca^{2+} capacity of the ER. The supply of Ca^{2+} to these Ca^{2+} buffering ER resident proteins is tightly controlled by a number of ER transmembrane channels and receptors.

1.2 Regulation of ER Ca^{2+} homeostasis - The ER is equipped with a number of ER Ca^{2+} handling proteins that are involved in Ca^{2+} uptake and release (Figure 1-1) [36]. Release of Ca^{2+} from stores is controlled by the inositol 1,4,5-triphosphate ($InsP_3$) receptor and the ryanodine receptor (RyR) to produce a sustained increase in cytosolic ER Ca^{2+} concentrations that can impact cellular events such as transcriptional activity [36-38]. The binding of specific hormones and growth factors to specific receptors at the plasma membrane, lead to activation of phospholipase C (PLC) which catalyses the hydrolysis of phosphatidylinositol 4,5-bisphosphate (PIP_2) to produce the intracellular messengers inositol 1,4,5-trisphosphate ($InsP_3$) and diacylglycerol [39]. $InsP_3$ diffuses throughout the cell where it comes into contact with large homo- or hetero-tetramers of the $InsP_3$ receptor resulting in conformational changes to cause channel opening and allowing Ca^{2+} to enter the cytoplasm [39]. Interestingly, although $InsP_3$

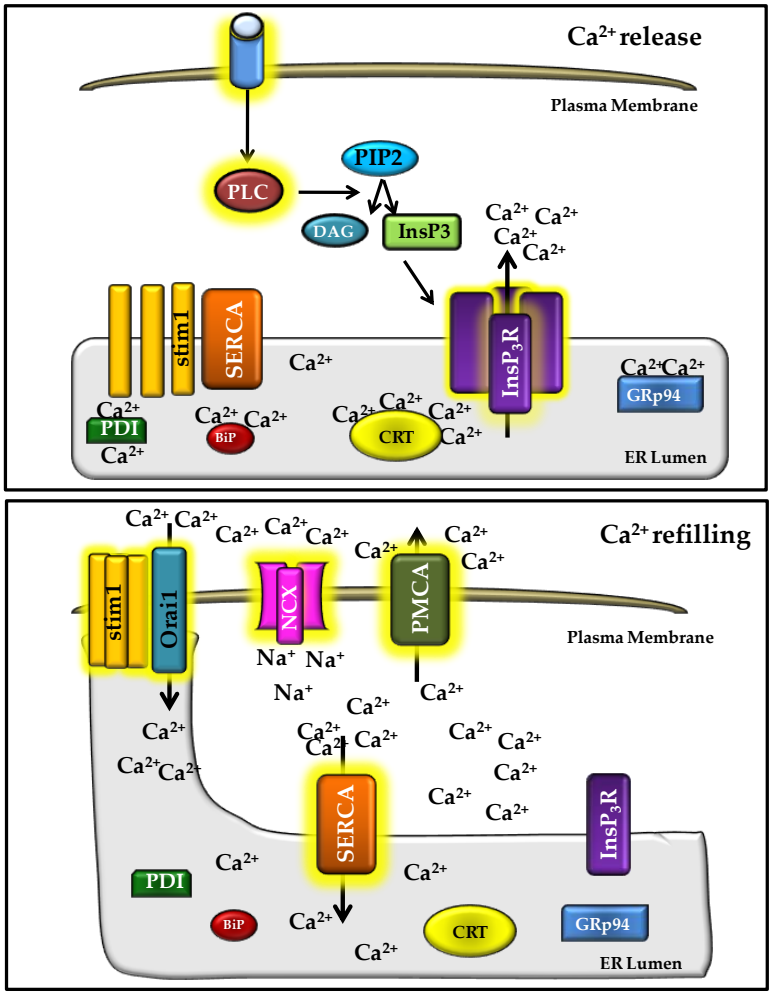

Figure 1-1

Figure 1-1 - Regulation of Ca^{2+} from intracellular ER stores. Ca^{2+} release (*top panel*) involves the binding of specific hormones (blue circle) to specific receptors (blue rectangle) at the plasma membrane resulting in activation of PLC to hydrolyse PIP2 to produce InsP3 and DAG. InsP3 activates the InsP3 receptor and Ca^{2+} is released. Ca^{2+} refilling (*bottom panel*) involves ER localized SERCA and plasma membrane NCX and PMCA to remove cytosolic Ca^{2+}. Stim1 accumulates at the plasma membrane to activate plasma membrane store operated channels (Orai1, for example) to refill ER Ca^{2+} stores. PLC: phospholipase C; PIP_2: phosphatidylinositol 4,5-biphosphate; $InsP_3$: inostiol 1,4,5-triphosphate; DAG: diacylglycerol; $InsP_3R$: $InsP_3$ receptor; SERCA: sarco/endoplasmic reticulum Ca^{2+}-ATPase; NCX: Na^+/Ca^{2+} exchanger; PMCA: plasma membrane Ca^{2+} - ATPase; STIM1: stromal interaction molecule 1

receptors require $InsP_3$ for opening, this opening can be modulated by Ca^{2+} concentrations at the cytoplasmic surface [39]. Modest increases in cytoplasmic Ca^{2+} (0.5-1.0 μM) enhance channel opening while high concentrations (>1.0 μM) inhibits channel opening [39]. The careful manipulation of ER Ca^{2+} release by both second messenger and cytosolic Ca^{2+} suggest how tightly controlled Ca^{2+} release is for complex signalling events [39]. RyRs form homotetramers and also act to refill ER Ca^{2+} in response to μM concentrations of cytoplasmic Ca^{2+}. RyRs are activated by low cytoplasmic Ca^{2+} concentrations (1-10 μM) and are inhibited by high cytoplasmic Ca^{2+} concentrations (>10 μM) [39]. RyRs are also sensitive to the plant alkyaloid ryanodine (hence the name) and while in the activated state, low concentrations (1–10 μM) of ryanodine binding locks the RyRs into a long-lived subconductance state, whereas higher concentrations (~100 μM) irreversibly inhibit channel opening [39]. Interestingly, RyRs are also sensitive to caffeine and can be activated my millimolar amounts [39]. ER luminal Ca^{2+} stores are then refilled through the action of the ER transmembrane protein sarcoplasmic/endoplasmic reticulum Ca^{2+}-ATPase (SERCA) which removes Ca^{2+} from the cytoplasm in an ATP-dependent manner [38, 40]. Cytosolic Ca^{2+} stores are also emptied through the action of the Na^+/Ca^{2+} exchanger (NXC) and the plasma membrane Ca^{2+} ATPase (PMCA) [41]. Taken together, it is the action of both plasma membrane and ER localized pumps and exchangers that can exert powerful effects of ER Ca^{2+} on varied cellular functions [22]. Store-operated Ca^{2+} (SOC) influx results from a depletion of ER Ca^{2+} stores by activation of the channels in the plasma membrane to refill intracellular stores [22, 40, 42]. The molecule that has been recently shown to be involved in the

communication of intracellular Ca^{2+} stores to the plasma membrane is the stromal interaction molecule 1 (Stim1) [22, 40]. Stim1 has two specific functions and they are acting (1) as the first sensor to detect ER lumen Ca^{2+} concentrations and (2) as a messenger to translocate to the plasma membrane to activate store-operated channels [40]. Upon store depletion, Stim1 accumulates in punctate and clusters at the plasma membrane with the store operated Ca^{2+} channel (CRAC, Orai1 or transient receptor potential channels (TRPC), depending on cell type) to increase Ca^{2+} influx into the cell [40]. This fine control of Ca^{2+} transients is critical to downstream cellular functions.

A sustained increase in cytosolic Ca^{2+} from intracellular ER Ca^{2+} stores is important for downstream events. For example, calcineurin, a Ca^{2+}/calmodulin-dependent phosphatase, dephosphosphorylates a number of transcription factors, one being nuclear factor of activated T-cells (NFAT) whose nuclear translocation and DNA-binding activities requires de-phosphorylation [40]. The nuclear import of NFAT is important for the induction of a genetic program for proliferation [40]. The calcineurin/NFAT pathway provides an excellent example of how Ca^{2+} fluctuations can directly and powerfully affect a downstream transcriptional pathway [40]. Aberrant Ca^{2+} signalling can impact both the neurological and cardiovascular system [15, 43]. The importance of Ca^{2+} signalling from the ER is underscored by the number of diseases that can result when it is altered.

2.0 Protein Folding in the Endoplasmic Reticulum - The ER has specific characteristics that make it a unique folding compartment different from

the cytosol and mitochondria [9, 22]. It has a highly oxidized environment, a high intracellular concentration of Ca^{2+} and it houses a number of chaperones and foldases [6, 9, 44]. The hydrophobic effect, or the minimization of hydrophobic amino acid residues at the surface of the protein, is the driving force of both cytosolic and ER based protein folding [45]. Proteins can obtain a number of different conformations determined by a variety of interactions between their amino acid residues [6, 45]. Each conformation yields a different free energy and the desired conformation is the one resulting in the lowest free energy and, often, this is the native conformation of the protein [6]. Unfolded proteins are defined as proteins with a higher number of hydrophobic patches on their surface resulting in increased chances of forming aggregates with other unfolded proteins in the crowded ER lumen (~100 g/l or 2 mM) [45]. However, a number of ER specific events result in limiting the number of potential conformations of a protein and allows for a certain amount of kinetic control of protein folding [45]. This kinetic control is critical because of the temporal discrepancy of protein folding and translation [6]. Protein folding happens very quickly with individual structures such as β-sheets and α-helices folding with 0.1-1 μs with small proteins folding in as little time as 50 μs [6, 46]. Translation of mRNAs, on the other hand, is a slow process and proceeds at ~ 4-6 amino acid residues/second [6]. To ensure that the correct conformation is obtained with amino acid residues that are far apart, the ER must maintain the newly synthesized protein in a folding competent intermediate state [6]. The ER has unique mechanisms to ensure correct protein folding occurs. The first delay actually occurs outside the ER in the cytoplasm. During translation, approximately the

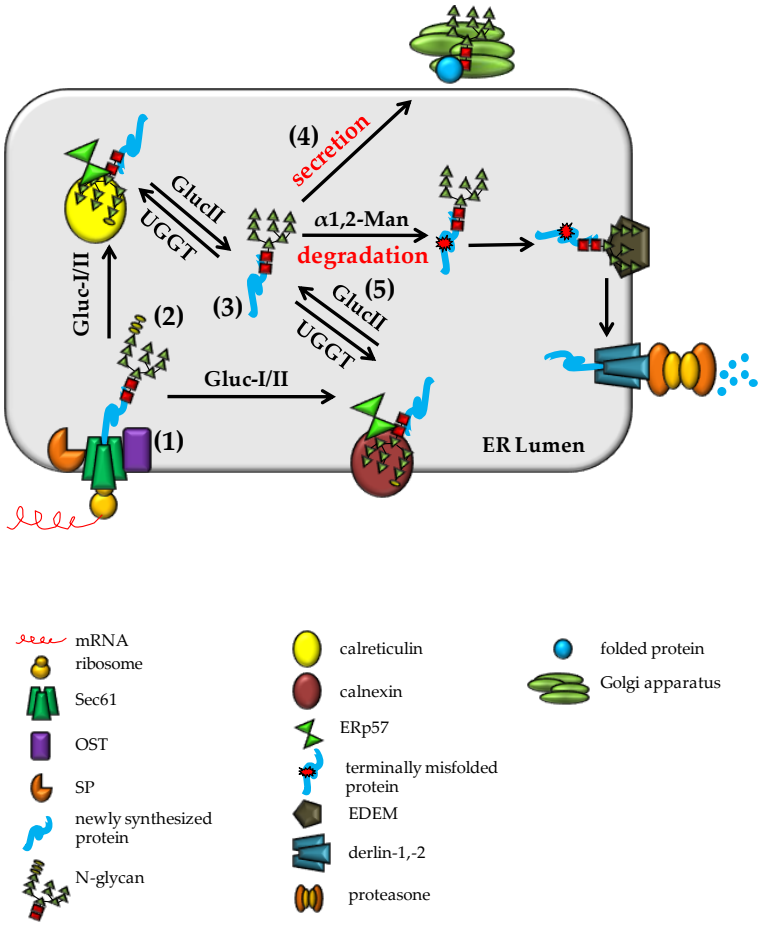

Figure 1-2

Figure 1-2 - The quality control cycle. (1) protein translated from mRNA is inserted into the ER through the Sec61 channel where its signal sequence is cleaved by SP and it is N-glycosylated (Glc3Man9GlcNAc2) by OST. (2) The N-glycan is sequentially cleaved by GlucI/II (GlucMan9GlcNAc2) allowing it to interact with chaperones CRT, CNX and the foldase ERp57. (3) The final glucose is cleaved by GlucII (Man9GlcNAc2) . The misfolded protein is recognized by UGGT and re-associates with calnexin (CNX), calreticulin (CRT) and ERp57. (4) if the protein is correctly folded, it exits the ER to the Golgi apparatus for secretion. (5) Terminally misfolded proteins are cleaved by α1,2-man to remove the innermost mannose (Man8GlcNAc2) and the protein is recognized by EDEM and sent for proteasomal degradation. SP: signal peptidase; OST: oligosachharyltransferase; GlucI/II: glucosidase 1 and II; CNX: calnexin; CRT: calreticulin; UGGT: UDP-glucose:glycoprotein glucosytransferase; α1,2-man: α1,2-mannosidase; EDEM: ER degradation-enhancing α-mannosidase-like lectins.

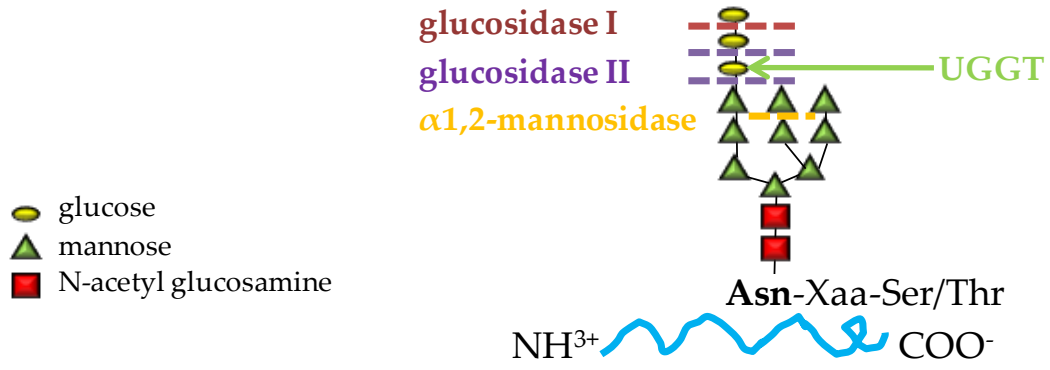

Figure 1-3

Figure 1-3 - Processing of N-glycan for regulation of the quality control cycle. Glucosidase I cleaves the outermoust glucose residue followed by the cleavage of the next glucose residue by glucosidase II to mediate interaction with chaperones. Interaction is lost when the innermost glucose is cleaved by glucosidase II. α-1, 2-mannosidase cleaves the inner mannose to target the protein for degradation. UGGT re-glucosylates the protein.

first 20 amino acids constituting the signal sequence, are immediately bound by the signal recognition particle (SRP) which not only targets the ribosome for the ER membrane but also temporarily halts translations and only resumes once the ribosome has attached to the ER membrane (via the SRP-receptor) [47]. This delay in translation provides the first level of control where folding cannot occur until the protein is in the ER. The second level of control is N-linked glycosylation, a post-translational modification obtained when proteins are translated into the ER through the Sec61 translocon. This modification provides a level of control in protein folding because not only does it dictate protein attachment sites to chaperone proteins but it also shields newly synthesized unfolded proteins from interacting and potentially forming aggregates [45]. N-linked glycosylation also instils an irreversibility onto the subsequent protein folding reactions because it directs their attachment sites to the surface of the protein and shields the vicinity of the attachment sites from hydrophobic interactions with other proteins [45]. Thirdly, formation of disulfide bonds takes precedence over the hydrophobic folding and this slow process limits the number of energy stable conformations possible [6, 45]. Finally, molecular chaperones partially act to reduce the amount of unfolded aggregates by binding to these hydrophobic surface patches and physically shielding proteins from interacting [45]. Therefore, the primary amino acid sequence dictates the 3-dimensional structure of the protein (as first discussed in Anfinsen's dogma) [6].

2.1 Quality Control in the Endoplasmic Reticulum - (Figure 1-2) Proteins are transolocated into the ER lumen through a proteinaceous channel, Sec 61 translocon complex [48, 49]. A number of proteins are transiently

associated with the translocon such as the signal peptidase (SP), GRp78/BiP and the oligosacharyltransferase (OST) [48]. GRp78/BiP is thought to mediate proteins translocating across the membrane by potentially acting as the molecular motor to power this process [48]. GRp78/BiP has also been shown to be involved in blocking the translocon channel after protein translation is complete [50]. Following cleavage of the signal sequence by the SP, the OST enzyme catalyzes the addition of a preassembled oligosaccharide core (N-acetylglucosamine$_2$-mannose$_9$-glucose$_3$ or $Glc_3Man_9GlcNAc_2$) at selective asparagine (Asn-Xaa-Ser/Thr) residues on the nascent polypeptide in a process termed N-glycosylation (Figure 1-3) [48, 51]. Although the OST has no impact on the activity of the translocon, N-glycosylation can occur at either end of the protein so the OST remains associated to the translocon for the entire translation process [48]. As the newly synthesized, N-glycosylated protein translates into the ER lumen, it is further modified by the ER enzymes, α-glucosidases I and II. They sequentially cleave terminal glucose residues with glucosidase I removing the initial glucose residue and glucosidase II cleaving a further glucose residues on the oligosaccharide core to reveal a monoglucosylated core glycan ($GlcMan_9GlcNAc_2$) (Figure 1-3) [52]. The monoglucosylated glycoprotein is now able to enter the quality control cycle through interaction with the lectin like ER chaperones, calnexin and calreticulin that associate with the oxidoreductase, ERp57 [53]. The protein is released from the folding machinery and the innermost glucose residue is removed by glucosidase II [3]. If the protein is correctly folded, it can now exit the ER through the Golgi to their correct location within the cell [3, 8]. If the protein has not obtained its correct conformation, it can re-renter the

calnexin/calreticulin cycle through re-glucosylation by the ER enzyme UDP-glucose:glycoprotein glucosyltransferase (UGGT) [54]. UGGT is a folding sensor as it only recognizes incompletely folded glycoproteins as its substrate [54]. However, if the protein is terminally misfolded it is marked for ER associated degradation (ERAD) due to the action of ER mannosidase I which cleaves the α1,2-linked mannose from the inner branch of the N-glycan ($Man_8GlcNAc_2$) (Figure 1-3) [55]. These misfolded proteins are then recognized by ER degradation-enhancing α-mannosidase-like lectins (EDEMs) proteins that target substrates for ERAD. EDEMs associate with derlin-2, derlin-3 and Sec61 that are all candidates for retro-translocation channel. After dislocation to the cytoplasm, the protein is polyubiquitinated and degraded via the 26S cytosolic proteasome [55].

2.2 Protein Folding Machinery - Protein folding in the ER is carried out by a number of different chaperones, foldases or folding enzymes and sensors. Specifically, the lectin-like ER chaperones, calnexin and calreticulin, and the oxidoreductase, ERp57. In the following sections, these proteins, in terms of the structure function, mouse model and clinical relevance, will be discussed.

2.2a Calnexin

2.2a-i- Structure - Calnexin is a type 1 integral membrane protein with a cytoplasmic C-terminal RKPRRE (Arg-Lys-Pro-Arg-Arg-Glu) ER-retention signal and an N-terminal signal sequence (Figure 1-4) [15]. It can be divided into four structural and functional domains: the N-globular domain, the P-arm domain, a short transmembrane domain and a C-

terminal cytoplasmic domain [56]. The N+P domains comprise the soluble form of calnexin and are responsible for the lectin-like chaperone function of the protein [56]. The P-domain extends away from the N-globular domain and is responsible for binding the oxidoreductase ERp57 [56, 57]. The C-terminal cytoplasmic domain binds Ca^{2+} and also contains phosphorylation sites [32, 58]. The crystal structure of the luminal, soluble domain of calnexin (N+P) has been solved and this study has allowed us to gain great insight into the function of the protein [57]. The N-globular domain of calnexin (amino acid residues 1-270 and 418-482) comprises a concave β sheet with 6 strands and a convex β sheet with 7 strands [56, 57]. Strands from opposing sheets are arranged anti-parallel forming a hydrophobic core through interactions of hydrophobic residues [57]. The carbohydrate binding site has been mapped to the N-domain and structural studies have suggested that amino acids Met^{189}, Tyr^{165}, Lys^{167}, Tyr^{186}, Glu^{217} and Glu^{246} and Cys^{161} and Cys^{195} may be involved in coordination [57, 59]. Recent mutagenesis studies also show that the Trp^{428} residue in the globular domain may also be involved in glycosylated substrate binding [60]. Studies also suggest that there is a Ca^{2+} binding site (Asp^{118} and Asp^{437}) in the N-globular domain [57]. However, because this site is located far away from the carbohydrate site and calnexin is known to undergo Ca^{2+}-dependent changes it is thought that Ca^{2+} ion bound here is likely to have a structural role rather than a ligand binding role [57, 58]. ATP has also been shown to bind calnexin in the N-globular domain resulting in conformational changes and is also required for substrate-calnexin interactions [58]. There are also Zn^{2+} binding sites within the N-terminal domain (residues 1-270) and they induce conformational changes

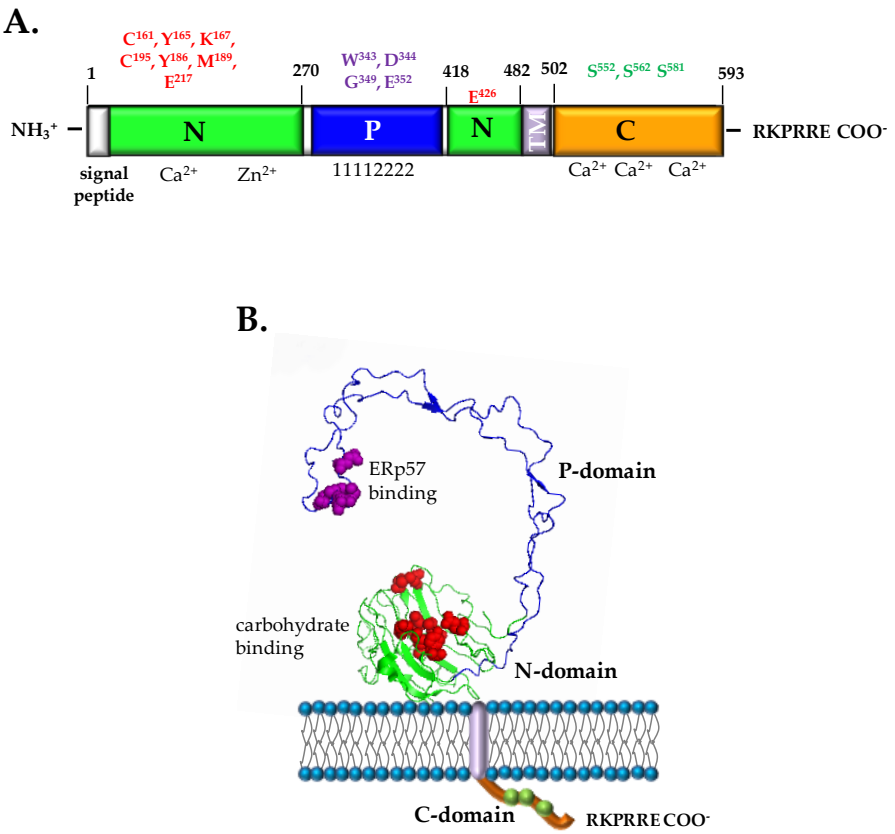

Figure 1-4

Figure 1-4 - Linear model and crystal structure of calnexin (A) A linear model of calnexin domains is shown. The N-terminal signal sequence (white box), N-domain (green box), P-domain (blue box) and the C-domain (orange box) and the C-terminal ER retention sequence are shown (RKPRRE). Amino acid residues involved in carbohydrate binding (red), amino acid residues involved in ERp57 binding (purple) and amino acid residues involved in phosphorylation (green). Zn^{+} and Ca^{2+} binding sites are indicated and the repeat motifs are indicated in the P-domain (repeat 1:PXXIXDPDAXXPEPWDE and repeat 2: GXWXPPXIXNPXYX). **(B)** The three-dimensional structure of the N- and P-domain of calnexin based on crystallographic studies with calnexin (Schrag, JD et al (2001)) (PDB code 1JHN). The extended P-domain (blue) contains residues involved in ERp57 binding (purple spheres) and loops around to meet the globular N-domain (green) which contains residues involved in carbohydrate binding (red spheres). There is a single transmembrane (grey) that passes through a membrane to give rise to the Ca^{2+} binding C-tail (orange) that contains phosphorylation sites (green spheres).

that are thought to expose its hydrophobic residues [59]. The P-arm domain (amino acid residues 270-414) of calnexin is a proline-rich tandem repeat domain [57]. It contains four copies of two proline-rich repeat domains arranged in linear pattern of 11112222 (motif 1: PXXIXDPDAXKPEPWDE and motif 2: GXWXPPXIXNPXYX). Together these amino acid sequences form an extended, flexible arm with repeat motif 1 extending away from the N-globular domain and repeat motif 2 folding back on motif 1 to return to the N-globular domain [57]. This extended arm forms a large hairpin because of head-to-tail interactions between one copy of motif 1 and one copy of motif 2 [57]. Each of the two repeat motifs has a 3 residue long β-strand and this is the only secondary structure of the P-domain [57]. The P-domain has been shown to be responsible for interactions with the oxidoreductase, ERp57 [59, 61, 62]. Mutagenesis studies in the P-domain have shown that amino acid residues located in the tip of the P-domain (Trp^{343}, Asp^{344}, Gly^{349}, and Glu^{352}) are involved in ERp57 binding [61]. Recent studies in our lab also indicate that Glu^{351} may also have a role in ERp57 binding [60]. Although the arm domain of calnexin has not been shown to be directly involved in substrate binding, it has been shown to enhance the folding function of the globular domain it is speculated that it may have a role in physically constraining the glycoprotein when bound to the N-domain [59]. The transmembrane domain of calnexin (amino acid residues 482-502) anchors calnexin to the ER membrane [56]. The role of the transmembrane domain, aside from its role in anchoring calnexin to the ER membrane, remains unclear and it has been suggested that it may promote association of calnexin with membrane proteins by holding it at the ER membrane or it

may directly bind the transmembrane domains of substrates [63]. Studies with proteolipid protein (PLP) [63] as well as CD82 [64] suggest a role for calnexin in recognizing misfolded transmembrane domains. The polytopic protein PLP is rich in polar residues in its transmembrane domains and it is thought that calnexin may be able to recognize misfolded transmembrane domains through exposure of these polar residues in the hydrophobic lipid bilayer. Calnexin is localized near the translocon during translation [48], so it is possible that calnexin samples transmembrane domains as they are integrated into the ER membrane, binding stably to those that mis- or unfolded [63]. The C-terminal domain of calnexin (amino acid residues 502-593) forms an acidic, charged cytoplasmic tail [56]. Although the function of the C-tail is not well established, it is known to be phosphorylated at Ser^{552} and Ser^{562} by casein kinase II (CDK) and at Ser^{581} by protein kinase C (PKC) or proline-directed kinase (PDK) [32]. The highly acidic domains in the C-tail are high capacity Ca^{2+} binding sites [31]. Phosphorylated calnexin is known to interact with major histocompatibility complex (MHC) class 1 molecules to effect their transport through the ER [65]. Calnexin is known to interact with misfolded null Hong Kong mutant of α-1-antitrypsin in a Ca^{2+}-dependent manner [66]. Together, these data suggest that the phosphorylation status or Ca^{2+} regulation of the C-tail may affect the function of calnexin. In fact, rhodopsin maturation in *Drosophila* has been found to be mediated by calnexin in a Ca^{2+}-dependent manner [67]. Perhaps this is not surprising as many ER chaperones function dually as Ca^{2+} proteins and it has been found that often their protein folding function is mediated by their Ca^{2+} buffering. For example, monoglucosylated carbohydrate binding to

calnexin and calreticulin is dependent of the presence of Ca^{2+} and the absence of Ca^{2+} results in these interactions being broken [14, 23]. Interestingly, the cytoplasmic C-tail has also been shown to interact with membrane- bound ribosome binding and it is speculated that this binding may, in part, regulate the chaperone activity of calnexin [68]. Overall, it is thought that modifications to the C-tail of calnexin through phosphorylation, Ca^{2+} binding or interacting partners regulate the function of calnexin.

2.2a-ii-Function - Calnexin's role as molecular chaperone is well-established and highly studied (See '*Section 2.1')* [51, 69, 70]. Thus, because it has been established that calnexin has a great number of substrates, it is not surprising that calnexin has roles in many other cellular processes [56] such as Ca^{2+} regulation [67, 71, 72], cell-cell adhesion [73], phagocytosis [74] and apoptosis [75-77].

It has been elucidated that calnexin may play a minor role in the regulation of Ca^{2+} in the ER [31, 71]. As discussed earlier (see '*Sections 1.0 and 2.1'*) ER lumen Ca^{2+} regulation is key to the maintenance of Ca^{2+} sensitive folding machinery [72]. Regulation of ER luminal proteins in a Ca^{2+}-dependent manner has been suggested in studies where depletion of intracellular Ca^{2+} resulted in extracellular transport of ER resident proteins [78-80]. It has been previously thought that calnexin may bind Ca^{2+} in the ER membrane thus regulating the retention of ER proteins [71]. In *Xenopus,* it was demonstrated that calnexin physically interacts with an Asp^{1036} in the C-terminus of SERCA2b to inhibit its function [72]. This interaction is calnexin C-tail phosphorylation-dependent; where

phosphorylation dictates interaction with SERCA2b and there is loss of interaction upon de-phosphorylation [72, 81]. SERCA2b, faces the ER lumen and impacts of $InsP_3$ -mediated Ca^{2+} release into the ER lumen [72, 81]. The localization of calnexin to the ER membrane brings a unique platform to ER Ca^{2+} regulation because it has the ability to transmit information regarding Ca^{2+} within in the ER lumen to the membrane itself [71].

Calnexin is also involved in cell-cell adhesion through its interaction with integrins [73]. Cell-cell adhesion and adhesion to proteins to the extracellular matrix and plasma membrane during differentiation is mediated by heterodimers of $\alpha\beta$-integrins [73]. β_1-integrins, the largest subgroup of the β-chain family, are known to bind many adhesion proteins such as collagen, laminin, fibronection, vitronectin and VCAM-1 [73]. Calnexin associates only with β_1-integrins and is not only involved β_1-integrin assembly but also in retention of the immature form in the ER. By retaining β_1-integrins in the ER, calnexin provides a steady supply of β_1-integrins that are readily available to associate with α-chains [73]. This intracellular pool of β_1-integrin, that calnexin maintains, contributes to the efficiency of the regulation of expression of different heterodimers of $\alpha\beta_1$-integrins [73].

A significant pool of the NMDA (N-methyl-D-aspartic acid) receptor subunit NR1 has been found to be associated with calnexin [82]. Similar to its function in the maintenance of the β1-integrin pool calnexin may serve to retain unassembled NR1 subunits until there are sufficient levels of NR2 subunits [82]. NR1 then disassociates with calnexin and assembles

with NR2 for its transport to the Golgi apparatus for further processing and eventual surface expression as a heteromeric complex (NMDA) [82] . Studies have shown that prenatal exposure to ethanol may affect NMDA receptor assembly and transport from the ER [82].

The role calnexin plays in the apoptotic pathway of the ER has been demonstrated using cell lines deficient in calnexin [76, 77]. Although calnexin-deficient cells are fairly resistant to ER stress-induced apoptosis, the absence of calnexin resulted in a decrease in caspase 12 expression as well as an inhibition of Bap31 cleavage [76, 77]. This suggested that calnexin forms complexes and promotes cleavage of Bap31 into its pro-apoptotic, p20, fragment [76]. This pro-apoptotic p20 fragment promotes effector caspase induction and apoptosis via the intrinsic pathway [83]. Calnexin-deficiency, however, does not affect caspase-3, caspase-8 or cytochrome c release suggesting that the calnexin may not be important in initiating apoptosis but have more of a role in the induction of the latter effects of apoptosis [76]. Moreover, calnexin itself is known to be cleaved by ER-stress-inducing and non-inducing conditions and this cleavage is known to attenuate apoptosis [75].

The role that calnexin has in the outlined cellular functions by no means suggests that these roles are mutually exclusive. In fact, the ability of calnexin to interact with proteins and interpret the protein itself and its microenvironment is the foundation of its biological functionality in Ca^{2+} regulation, phagocytosis, adhesion, apoptosis and quality control. Moreover, calnexin's role as a chaperone or a Ca^{2+} binding protein (outside

of the ER) may overlap, it is unsurprising that the calnexin-deficient mouse model has severe outcomes [84].

2.2a-iii- Mouse Models - Although calnexin-deficient mice are viable, they have a severe ataxic phenotype (Table 2) [84, 85]. These live mice are 30-50% smaller than their wild-type littermates, they show gait disturbance and splaying of the hindlimbs [84, 85]. Electron micrographs of the spinal cord and sciatic nerve indicate that there is severe dismyelination in the peripheral nervous system (PNS) [84, 86]. Thus, it is not surprising that there is reduced nerve conduction velocity in the calnexin-deficient mice [84]. Recent and on-going studies in our lab have shown that misfolded and non-functional myelin specific proteins, protein zero (P0) and peripheral myelin protein 22 (PMP22) are found in cells-derived from calnexin-deficient mice [84-86]. These misfolded proteins contribute to the non-compacted myelin sheath, poor conductance of nerve velocity and resulting phenotype [86]. Calnexin-deficient mice expressing a mutated and truncated (15-kDa smaller) form of calnexin have also been created [85]. The expressed calnexin mutant is an N-globular domain mutant where the Cys^{161} and Cys^{195} residues and the Tyr^{165} and Lys^{167} residues in the carbohydrate binding pocket are disrupted [85]. This mutant mouse was phenotypically identical to the calnexin-deficient mouse suggesting that the chaperone function of calnexin is responsible for the observed phenotype [85]. Although, the calnexin-deficient mouse model demonstrates the importance of calnexin in peripheral neuropathies more work needs to be carried out [85].

2.2a-iv- Possible Medical Applications - The central role of calnexin in the quality control cycle of newly synthesized proteins implicate it in numerous protein folding diseases, specifically, neuropathologies (Table 3). The Schwann cell-derived polytopic integral membrane protein, PMP22, is a major component of myelin which is responsible for the proper transmission of nerve signals [87]. PMP22 forms complexes with calnexin and has been shown to have role in correct folding of PMP22 to effect function [86, 88]. A number of defects in the gene encoding PMP22 such as intrachromosomal duplications and deletions as well as point and missence mutations result in mutant PMP22 continually interacting with calnexin and being retained in the ER [88-90]. This extended interaction with calnexin causes its sequestration in myelin-like figures (aggresomes) in the ER preventing it from carrying out chaperoning and calcium regulation duties [88, 91]. This sequestration presents itself as a number of neuropathies such as Trembler and Trembler-J in mice as well as Charcot-Marie-Tooth disease and Dejerine-Sottas syndrome in humans [88-92]. Lack of transport of the NR1 receptor out of the ER may result in sequestration of calnexin leaving it unavailable to carry out its other chaperoning duties. Tyrosinase is a type I integral membrane protein that is the rate limiting enzyme involved in melanin biosynthesis [93, 94]. This protein is known to associate with calnexin as well as calreticulin to obtain its correct functional conformation [93]. While mis- or unfolded protein is targeted for degradation, correctly folded tyrosinase is targeted to the pigmentation site organelle, the melanasome [93]. Oculocutaneous albinism type 1 (OCAI) is the absence of pigmentation and it results from over 100 known mutations in the tyrosine gene [95]. OCAI has been

referred to as an ER retention disease, where misfolded tyrosinase proteins are retained in the ER by association with calnexin and calreticulin [93]. Calnexin also has a lingering interaction with mutant vasopressin receptor that is implicated in diabetes insipidus [2, 96] and with cartilage oligomeric matrix protein (COMP) [97]. COMP is another protein that's selective retention in ER may be associated with numerous skeletal dysplasias such as osteoarthritis, pseudoachondroplasia (PSACH) and multiple epiphyseal dysplasia (MED) [97-99]. Amino acid deletions, substitutions or additions have been proposed to alter COMP structure and cause it retention in the ER possibly by calnexin [2, 100]. The $R^{273}W$ von Willebrand factor (VWF) mutant has decreased expression at the plasma membrane due to increased retention in the ER membrane and this results in bleeding disorders [101]. This mutant has been shown to have prolonged association with calnexin perhaps causing its retention in the ER [101]. Perhaps the most widely known disease associated with aberrant retention in the ER by calnexin, is retention of the ΔF508 protein, a mutant of the CFTR (cystic fibrosis transmembrane conductance regulator) chloride channel [2]. This results in the CFTR channel not being localized to the plasma membrane and this dysfunction is known to contribute to the disease [96, 102]. Immunoprecipitation experiments have shown that calnexin interacts with type I and III $InsP_3$ receptor [103]. In the mouse model of Niemann-Pick A disease, SERCA levels as well as $InsP_3R$ levels are reduced [104]. Aberrant calnexin could lead to IP_3 receptor unfolding and subsequent degradation and possible disease phenotype [103, 104].

MHC class I and II associate quantitatively with calnexin and it assists in both the assembly and/or retention [105, 106]. MHC class I molecules have a role in presenting antigenic peptides to T cells. They recognize the peptide and carry out an immune response against viruses, intracellular bacteria and tumors [107]. However, calnexin-deficient cell lines do not show aberrant transport rate of MHC class I to the surface [106]. This indicates that calnexin may not have an important role in the transport and surface expression of MHC class I molecules [106]. It has been suggested, however, that calnexin may have a more prominent role in the degradation of misfolded MHC class I molecules [107].

α-antitrypsin is a soluble, secretory protein that interacts with calnexin [108]. It is a member of the serine protease inhibitor family and its function is to prevent lung elastin fibers from elastolytic destruction [109]. Mutations to α-antitrypsin, to the Z-allele or the null-Hong-Kong variant, the protein, along with the bound calnexin, is ubiquitinated and targeted for proteasomal degradation [108]. Both these mutations result in lack of α-antitryspsin surface expression, causing degradation of lung elastin fibers and resulting in pulmonary emphysema [109].

Meprins are multidomain, oligomeric glycoproteins that are secreted from the brush border of kidney and intestinal epithelial cells [110]. The role of meprins is to activate or degrade bioactive peptides, growth factors, hormones, cytokines, and matrix proteins [110]. Wild-type meprin A and its mutant form, ΔMAM, both interact with calnexin [111]. The wild-type form is secreted while the deletion mutant is degraded implicating calnexin in a both a secretory and degradation role [111].

Another protein that calnexin is known to bind is α-amino-3-hydroxy-5-methyl-4-isoxazolepropionate (AMPA) receptor that mediates fast excitatory transmission in the central nervous system (CNS) [112]. Interaction has been observed in the cell body and dendrites of hippocampal pyramidal neurons [112]. Because it has been observed that calnexin associates with both the immature and mature form of the receptor, it has been suggested that calnexin may also have an additional and more specialized role in the maturation and targeting of AMPA [112]. Chang et al showed that when they co-transfected nicotinic receptors with calnexin they were able to stimulate the assembly and surface expression of nicotinic receptors [113]. Additionally, they also found that calnexin only associated with the immature form nicotinic receptors [113]. These two discoveries, when taken together, imply that calnexin, to some degree is able to control the composition and number of functional receptors [113]. Although a direct function of calnexin in regards to the nicotinic receptors is unknown, there have been many speculations. Calnexin may have a protective role where its binding serves to prevent newly synthesized nicotinic receptors from being degraded increasing the pool of subunits in the folding/assembly pathway [113]. Also, calnexin could successfully shield degradation signals present on the monomeric form of the receptor until ready to form its mature assembled form [113]. Calnexin also interacts with myeloperoxidase (MPO) a neutrophil lysosome hemeprotein [114]. It is able to associate with glycosylated precursor MPO, with enzymatically, heme binding pro-MPO as well as having extended binding to MPO mutants that could not incorporate heme suggesting a role for calnexin in maturation of MPO [114].

The number of substrates that calnexin is known to associate within quality control, dictates the high clinical relevance of this protein and its implication in diseases, specifically, neuropathologies.

2.2b Calreticulin

2.2b-i- Structure - Calreticulin is a 46-kDa soluble ER luminal protein with a N-terminal cleavable signal sequence and an ER retention sequence, KDEL (Lys-Asp-Glu-Leu) (Figure 1-5) [15]. It is the major Ca^{2+} buffering protein (See '*Section 1.1 Ca^{2+} Buffering Proteins')* of the ER and also acts as a molecular chaperone as a part of quality control (See '*Section 2.1 Quality Control in the Endoplasmic Reticulum')* [15]. Similar to calnexin, calreticulin is composed of distinct structural and functional domains: the N-globular domain, the P-arm domain and the C-domain [15]. Together, the N+P domain contain oligosaccharide and polypeptide binding regions and are important for the chaperone activity of calreticulin [59]. The C-domain is responsible for the majority of the Ca^{2+} binding of calreticulin [17].

The N-globular domain (amino acid residues 1-170) is predicted, based on the secondary structure of calnexin, to be comprised of eight anti-parallel β-strands [22, 24, 115]. The N-domain also contains the oligosaccharide and polypeptide binding domain with specific amino acids contributing to the oligosaccharide binding and conformational stability of the protein [116-119]. Mutations to residues Tyr^{109} and Asp^{135} in the N-domain were shown to completely abolish oligosaccharide binding and a number of other amino acids (Lys^{111}, $Tyr^{128}$and Asp^{317}) have also been found to be important for sugar-binding in the N-domain [116, 119, 120]. Trp^{302} and His^{153} in the N-domain have been shown to be critical for chaperone

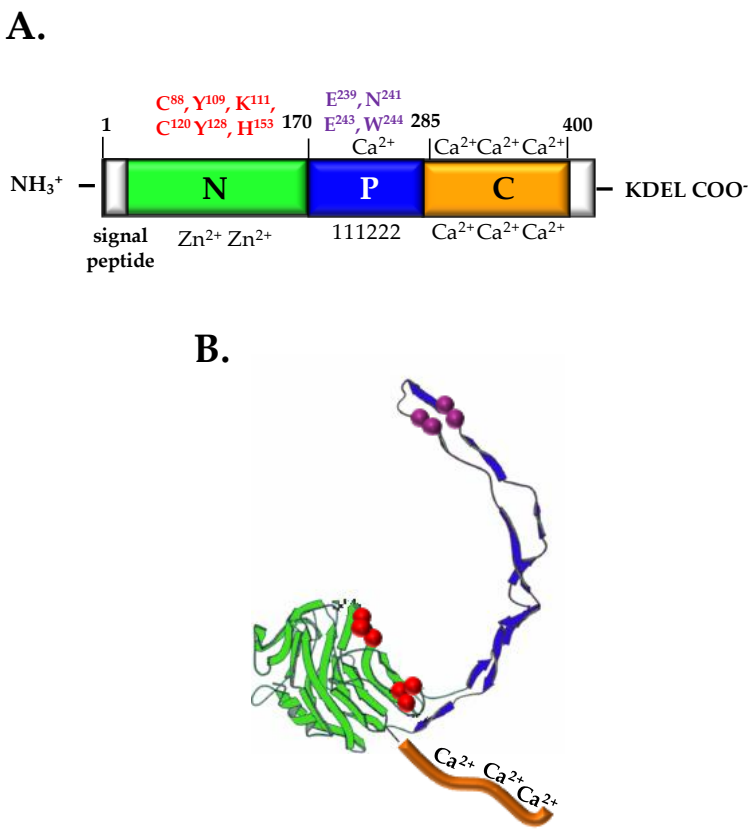

Figure 1-5

Figure 1-5 - Linear model and crystal structure of calreticulin (A) Linear model of calreticululin is shown. The N-terminal signal sequence (*white box)* N-domain (*green box)*, P-domain (*blue box)* and the C-domain (*orange box*) and the C-terminal ER retention sequence is shown (KDEL). Amino acid residues involved in carbohydrate binding *(red*), amino acid residues involved in ERp57 binding (*purple*), Zn^{+} and Ca^{2+} binding sites are indicated and the repeat motifs are indicated in the P-domain (repeat 1:IXDPXA/DXKPEDWDX and repeat 2: GXWXPPXIXNPXYX). (**B)** The three-dimensional structure of calreticulin based on crystallographic studies of the P-arm domain of calreticulin and calnexin (Ellgaard, L et al (2001) (PDB code 1HHN), Schrag, JD et al (2001) (PDB code IJHN)). The P-domain (*blue)* contains residues involved in ERp57 binding (*purple)* and loops around to meet the N-globular domain *(green)* which contains residues involved in carbohydrate binding (*red).* The C-domain (*orange*) immediately follows and has a high capacity for binding Ca^{2+}.

function with His^{153} also effecting the structure of calreticulin [118, 121]. Surprisingly, when Cys^{88} and Cys^{120} were mutated to disrupt a disulfide bridge, there was only partial disruption of the chaperone function of calreticulin [118]. The N-domain also forms a proteolysis stable core in the presence of Ca^{2+} and this may have specific physiological and pathophysiological implications [24]. In autoimmune diseases, auto-antibodies against calreticulin are produced and this proteolysis resistant N-domain fragment contains most of the antigenic sites [24]. It is speculated that during cellular stresses, the proteolytic resistant N-domain (in the presence of high levels of Ca^{2+}) would be presented to proteolotyic enzymes increasing the amounts of protease resistant calreticulin with a highly antigenic conformation [24]. The N-domain of calreticulin also binds Zn^{2+} and this may have structural effects on calreticulin to affect function [118, 122]. The N-domain of calreticulin is of interest because of its critical role in the chaperone function; however, it is important to note that for full chaperone function, the N-domain requires the P-domain [15]. The P-arm domain (amino acid residues 170-285) of calreticulin immediately follows the N-domain and forms a flexible arm domain [123, 124]. It has a very similar structure to calnexin also comprising of proline-rich amino acid sequences [124]. Although it also has two repeat amino acid sequences (motif 1: IXDPXA/DXKPEDWDX, and motif 2: GXWXPPXIXNPXYX) it has only three copies of each (as opposed to four in calnexin) [124]. Similar to calnexin, they are arranged in a "111222" pattern and are thought to be involved in oligosaccharide binding with the N-domain [124]. It is also thought that these repeats may be involved in

the binding of the oxidoreductase, ERp57 [125]. NMR (nuclear magnetic resonance) studies in conjunction with mutagenesis and surface plasmon resonance (SPR) analysis have shown that ERp57 can dock onto the tip of the P-domain and may involve specific amino acids (Glu^{239}, Asp^{241}, Glu^{243} and Trp^{244}) [59, 118, 126]. The P-domain, interestingly, has been found to bind Ca^{2+} with a high affinity (K_d = 1 μmol/l) and a low capacity (1 mol of Ca^{2+} per mol of protein) *in vitro* [16]. The C-domain (amino acid residues 285-400) of calreticulin is responsible for binding 50% of ER Ca^{2+} with a low affinity (K_d = 2 mol/l) and high capacity (25 mol of Ca^{2+} per mol of protein) [16, 17]. The C-domain has large stretches of acidic amino acid clusters that are interspersed with the basic residues lysine and arginine. It is the side-chains of the lysine residues that mediate the Ca^{2+} binding [18].

2.2b-ii- Function - Calreticulin has been widely studied for its role in protein folding and for its role as the major Ca^{2+} buffering chaperone of the ER [15]. Thus, it is not surprising that calreticulin, like calnexin, has other roles within the cells, many of which are extensions of its roles as a Ca^{2+} buffering and chaperone protein.

Calreticulin is the most potent buffer of ER Ca^{2+} and is responsible for binding over 50% of ER luminal Ca^{2+} [17]. This ability to essentially regulate ER luminal Ca^{2+} concentrations inevitably affects other biological functions within the cell [15, 127-134]. Cytotoxic T-lymphocytes (CTLs) release Ca^{2+}-activated perforin, granzymes/proteases
and calreticulin that, upon interaction with a target cell, cause lysis and apoptosis [127]. Calreticulin regulates this process through Ca^{2+} binding and it has been found the increased levels of calreticulin result in

increased amounts of chelated Ca^{2+} and a decrease in activated perforin involved in penetration of the plasma membrane of the target cell [127]. Calreticulin has a major role in targeting of CTL to the target cell [127]. Modulation of ER Ca^{2+} stores by calreticulin also impacts apoptosis which needs ER Ca^{2+} release for activation of transcriptional cascades [128]. Studies have shown that an increase in calreticulin results in a sensitivity to apoptosis while a decrease in calreticulin results in a resistance to apoptosis [129]. Ca^{2+} fluctuations via calreticulin are the molecular switch that negatively regulates the commitment to adipocyte differentiation by down-regulating expression and transcriptional activation of pro-adipocyte factors [133]. In 3T3 cells pre-adipocyte cells and embryonic stem cells, increases in cytoplasmic Ca^{2+} results in an inhibition of adipogenesis [133]. Additionally, calreticulin overexpression has been shown to impact osteocyte and chondrocyte differentiation important for proper skeletal development and this is thought to occur through the calcineurin pathway [134]

Calreticulin has also been found outside the ER and, subsequently, is involved in other biological functions within the cell [130, 135]. The exposure of calreticulin to the cell surface is critical for immunogenic cell death [135]. Calreticulin co-translocates to the cell surface with ERp57 allowing for presentation to T-cells, initiation of the immune response and apoptosis of the target cell [135]. Cell surface calreticulin is also important for focal adhesion assembly for migration and impacts phagocytosis and pro-inflammatory response [130, 136]. The N-terminal fragment of calreticulin is also known as vasostatin and has been found in the media of Epstein-Barr immortalized cells lines [131]. Extracellular

calreticulin/vasostatin affects angiogenesis by blocking laminin from interacting with endothelial cells preventing matrix attachment thus inhibiting growth [131]. Calreticulin also induces the migration and motility of keratinocytes, fibroblasts, monocytes and macrophages all important in wound healing [132]. Finally, during embryonic development, high expression of calreticulin is observed in the cerebral cortex and retina suggesting that calreticulin may be important for proper development of the central nervous system [137].

In order to understand the role of calreticulin within the cell, it is important to examine different animal models that are both deficient and over express calreticulin. This will allow us to gain insight into the critical functions of calreticulin within the cell.

2.2b-iii- Mouse Models - The importance of calreticulin as a Ca^{2+} buffering protein is highlighted by animal models that are deficient in calreticulin and over-express calreticulin (Table 2) [19-21]. These studies further demonstrate the critical role that calreticulin plays in Ca^{2+} homeostasis suggesting that it may be far more important than its role in protein folding [15].

Unlike the calnexin-deficient mouse model, the calreticulin-deficient mouse is embryonic lethal at 14.5 post-coitum [21]. This provides further evidence that calnexin and calreticulin, although having similar domain structure, may have different roles *in vivo*. Calreticulin is expressed at very low levels in the adults mouse and also at low levels throughout mouse embryonic development except in the heart, liver and some central nervous tissue [21]. Therefore, embryonic lethality of the calreticulin-

deficient mouse due to impaired cardiac development specifically, a marked decrease in ventricular wall thickness and deep intrabecular ventricular walls was not surprising [21]. In fact, electron microscope analysis revealed that the myofibrils of the ventricles were "wavy" and thin ventricular walls when compared to wild-type littermates [138]. Calreticulin-deficient embryos also have aberrant formation of the intercalated disc which are adherens-type junctions of cardiac muscle [138]. Adherens junctions contain catenins, vinculin and N-cadherin and they are involved in cardiac development [139]. Perhaps unsurprisingly, the levels of N-cadherin are down-regulated in the calreticulin-deficient mouse [138]. Embryonic fibroblasts derived from calreticulin-deficient embryos show a significant decrease in ER Ca^{2+} capacity but surprisingly, free ER Ca^{2+} remains unchanged [17]. Further studies carried out with calreticulin-deficient fibroblasts demonstrate that they have an inhibition of bradykinin-induced Ca^{2+} release likely due to bradykinin being unable to bind to its bradykinin receptor indicating that calreticulin chaperones the bradykinin receptor [17]. Regardless, inability of bradykinin-induced Ca^{2+} release results in aberrant nuclear localization of a number of factors, specifically NFAT (nuclear factor of activated T-cells), MEF2C (myocyte enhancer factor 2C), Nkx2.5 (NK2 transcription factor related locus 5), COUP-TF1 (chicken ovalbumin upstream transcription factor 1), GATA6 (GATA-binding protein 6) and Evi-1 (ecotropic viral integration site 1)[21, 140, 141]. Interestingly, these factors have been identified in being essential for correct vertebrate cardiac morphogenesis and hypertrophy [141-144]. Bradykinin-binding as well as bradykinin Ca^{2+} release is restored by the expression of full-length calreticulin as well as the N+P-

domains of calreticulin but is not restored by expression of the P+C-domains [17]. Expression of the P+C-domains did, however, rescue the Ca^{2+} storage capacity of the ER. These results show that the C- domain of calreticulin is important in determining Ca^{2+} storage capacity of the ER while the N+P domain are important in the chaperone function of calreticulin [17]. Taken together, this suggests that the Ca^{2+} buffering function of calreticulin, not its chaperone function, are what causes the lethality observed in calreticulin-deficient mice [15, 17]. Further studies provide support for the critical function of the Ca^{2+} buffering function as over expression of the serine/threonine phosphatase, calcineurin, rescues the lethality of the calreticulin-deficient mice [141, 145]. Although, these mice have rescued cardiac development they show impeded growth, hypoglycaemia, increased levels of serum triacylglycerols and cholesterol [145]. Regardless, activated calcineurin expression is able to rescue the nuclear translocation of both NFAT and MEF2C that is a result of the absence of calreticulin [141, 145]. These two factors are directly responsible for the normal cardiac development *in utero* with MEF2C having an additional role in regulating the transcription of calreticulin [141, 145]. Nkx2.5 activates the calreticulin gene during cardiac differentiation, COUP-TF1 is expressed during embryonic development and acts to repress the calreticulin gene, GAT6 activates the calreticulin gene in the heart and Evi-1 is thought to have a role in the decline of calreticulin in the postnatal heart [15, 140, 146]. The relationship between calreticulin and calcineurin stresses the importance of Ca^{2+} signalling pathways in critical cardiac development [15, 145].

In order to further investigate the molecular mechanisms involved in the heart failure observed in calreticulin-deficient embryos, embryonic stem (ES) cells were derived from calreticulin-deficient and wild-type embryos and differentiated into cardiomyocytes [147]. By day 8 of differentiation, there is less beating areas in the calreticulin-deficient ES-derived cardiomyocytes compared to the wild-type despite normal expression of cardiac transcription factors [147]. During differentiation, the calreticulin-deficient ES-derived cardiomyocytes have a severe disruption of myofibrillogenesis due to insufficient expression and Ca^{2+}-dependent phosphorylation of ventricular myosin light chain 2 (MLC2v) [147]. Myofibrillogenesis is rescued in calreticulin-deficient ES-derived cardiomyocytes when they are supplied with a Ca^{2+} ionophore highlighting the importance of calcium signalling in cardiac development [147]. This is due to a rescue of the nuclear translocation of MEF2C which goes on to activate the expression of MLC2v resulting in normal myofibrillogenesis [147]. Studies at the embryonic stem cell level also demonstrate how critical the Ca^{2+} buffering function of calreticulin is to cardiac development [138, 147].

Studies looking at the molecular and functional consequences on the over-expression of calreticulin have also been carried out and they result in a significant increase in the Ca^{2+} capacity of the ER [19, 148, 149]. Transgenic mice over-expressing calreticulin in the heart display bradycardia, complete heart block and sudden death, cardiac edema and abnormal sarcomere structure of the heart, dilated ventricular chamber and atria, thinner ventricular walls and disarray cardiomyocytes [19, 148]. These mice also have a reduced HCN1 (hyperpolarization-activated cyclic

nucleotide-gated channel 1) and this is significant because of the role of HCN1 in the regulation of cardiac pacemaker activity [148]. Calreticulin over-expression in the heart also results in a decrease in the protein expression levels of connexin 40 (Cx40) and connexin 43 (Cx43) which are gap junction components and the cardiac transcription factor, MEF2C [148]. Together, decreased levels of HCN1, Cx40 and MEF2C results impaired structure and function of the heart in calreticulin over-expressing mice [148]. Mice over-expressing calreticulin in heart have a very similar phenotype to children suffering from congenital heart block and, interestingly, patients suffering from congenital heart block have calreticulin autoantibody [19, 148, 150, 151]. Together, this suggests a role for calreticulin in the pathogenesis of both adult and paediatric congenital heart block [150, 151].

2.2b-iv-Possible Medical Applications - Calreticulin impacts a variety of biological pathways and that can lead to a range of disease phenotypes (Table 3) [15]. Calreticulin has been detected in the serum of people suffering from autoimmune diseases such as systemic lupus erythematosus (SLE), coeliac disease, rheumatic disease and a number of parasitic diseases [15]. Calreticulin can be an important auto-antigen for some individuals, however, in others it may be involved in the pathology of immune diseases by forming unfavourable complexes [15]. In order for tumours to grow, they need a steady blood supply, thus, require angiogenesis [131, 152]. Calreticulin/vasostatin have been shown to be good candidates for tumour suppressor drugs as they inhibit angiogenesis and are small, soluble, stable and easy to produce [131, 152]. However, caution needs to be taken as vasostatin treatment has also been shown to

result in enhanced malignant behaviour of some tumour cell lines [153]. Calreticulin is also useful in wound healing as it is temporally and spatially expressed in fibroblasts of injured dermis and has been shown to promote healing [132]. In fact, when calreticulin is topically applied to the wounds of diabetic mice or cortisone-impaired pigs, their wounds heal faster compared to wild-type controls [15]. Calreticulin has also been implicated in cardiac disease and this is through its modulation of intracellular Ca^{2+} stores (See *"2.2b-iii-Mouse Models"*) [15]. The numerous functions of calreticulin within the cell not only implicate it in many disease phenotypes but also heighten the interest to exploit calreticulin for treatment of disease and understanding of normal development.

2.2c ERp57

2.2c-i- Structure - ERp57 is a thiol-oxidoreductase and has been referred to as GRp58, ERp60, ERp61, PDI-Q2, Pdia3 and 1,25D3-MARRS (Membrane Associated, Rapid Response Steroid binding) [154]. Similar to calnexin and calreticulin, ERp57 is also defined by clear structural and functional domains (Figure 1-6) [154]. ERp57, like calreticulin and calnexin, has a C-terminal ER retention/retrieval sequence (QEDL) as well as an N-terminal signal sequence [154]. ERp57 contains several modification sites such as two thioredoxin-like domains, six protein kinase C phosphorylation sites, seven casein kinase II phosphorylation sites, three tyrosine phosphorylation sites, two sulfation sites and one N-myristoylation site [154]. ERp57 has a domain architecture very similar to that of another oxidoreductase, PDI sharing 33% overall identity and the same four thioredoxin-like domains arranged: *a b b′ a′* [155]. Also similar to PDI is

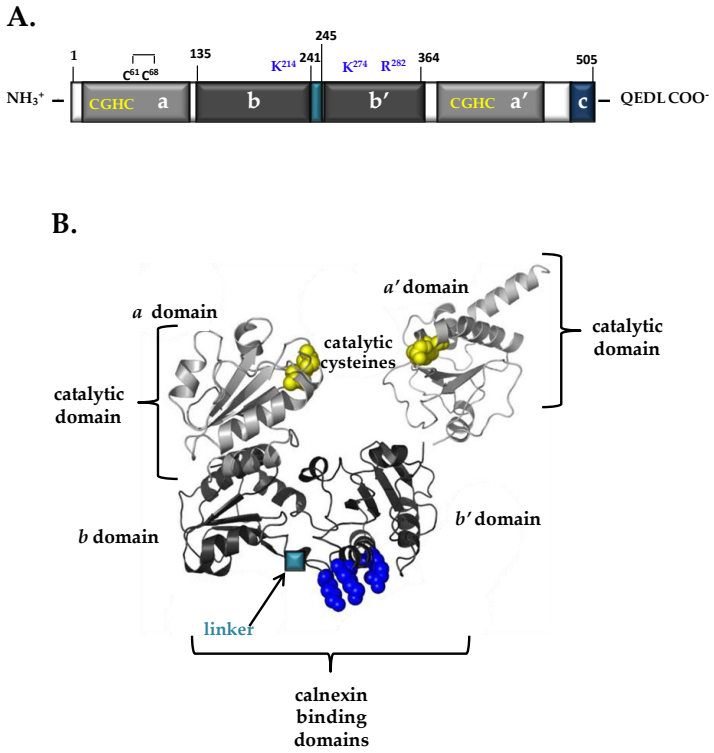

Figure 1-6

Figure 1-6 - Linear model and crystal structure of ERp57. **(A)** A linear model of ERp57 domains is shown. The protein has N-terminal amino acid signal sequence (*white box),* catalytic *a* and *a′* domains (*light grey boxes*) with catalytic residues (CGHC, *yellow*), substrate binding *b* and *b′* domains (*dark grey boxes*) connected with a linker region *(turquoise box),* a basic C-terminal (*navy blue box)* and a C-terminal ER-retention signal (QEDL). Amino acids involved in calnexin binding are indicated in blue and disulfide bond in the *a* domain is marked. **(B)** The three-dimensional structure of ERp57 based on NMR studies of the *a* and *a′* domain of protein disulfide isomerase (PDI) (Tian et al (2006)) and the *b* and *b′* domains of ERp57 (Kozlov et al (2006)). The catalytic *a* domain (*light grey*) is followed immediately by the *b* domain (*dark grey*) that contains calnexin binding residue K ^{214} which is linked *(turquoise box)* to the *b′* domain (*dark grey*) that contains the calnexin binding residues K^{274} and K^{282} (*blue).* Immediately following, is the *a′* domain containing catalytic residues (*yellow*). A version of this figure was published previously : Coe, H and Michalak, M, 2010. ERp57, a multifunctional ER oxidoreductase. Molecule in Focus: The International Journal of Biochemistry and Cell Biology. Doi:10.1016/j.biocel.2010.01.009

that, via NMR studies, ERp57 has been shown to have an overall U shape with the catalytic sites of the two active thioredoxin domains facing each other [155]. However, what is unique to ERp57 is that it has a basic carboxyl terminal domain while PDI has an acidic carboxyl domain [156]. This difference has been thought to mediate the substrate binding specificity of ERp57 [156]. The *a* and *a′* catalytic domains of ERp57 share over 50% of amino acid identity to PDI [155]. These domains contain catalytically active motifs (CGHC) and, as such, are redox active domains [155]. The redox potential of the these domains is -0.167V in the a domain and -0.156V in the *a′* domain which is comparable to the redox activity of PDI (-0.175V) [157]. The disulfide reductase and isomerase activities of ERp57, however, are 20 times lower than those of PDI [157]. The a domain also contains a structural disulfide between cysteine residues 61 and 68 [157]. The *b* and *b′* domains of ERp57 are thioredoxin-like domains that are connected by a short linker and they mediate the binding to the lectin-like chaperone calnexin [155]. X-ray diffraction techniques have allowed us to gain insight into the structure of this region [155]. The *b* and *b′* domains each consist of a five-stranded β-sheet core enclosed by four α-helices on either side and are separated by a short three residue linker that has a role in interdomain contacts [155]. Although the *b* and *b′* domains share 20% amino acid identity to PDI, the *b′* domain of ERp57 has a long deletion while the *b′* domain has two 6-7 residue inserts. These inserts, one comprising helix α3 and the second insert enlarging the β4-β5 loop, serve novel structural and functional roles to ERp57 [155]. The extended loop not only increases contact between the *b* and *b′* domains it also increases the rigidity of the *b* and *b′* pair [155]. Interestingly, this loop is also the site

of calnexin binding and when a mutation is made to K^{214} in the β4-β5 loop, there is an 8-fold loss of affinity for calnexin [155]. Another difference between the *b* and *b'* domains of ERp57 and PDI, is the surface charge, +4 and -4, respectively [155]. The positive charge of ERp57 mediates the binding of the negative P-domain tip of calnexin and when positive residues of ERp57 are mutated to neutral residues ($K^{274}A$ and $R^{282}A$), binding of ERp57 to calnexin is lost [155]. It seems that the *b'* domain of ERp57 is critical for binding to calnexin while the *b* domain strengthens this interaction [155].

2.2c-ii- Function - The promiscuous localization of ERp57 implicates it in a number of different functions within the cell [158]. The most widely studied functions of ERp57 in the ER and its role in quality control with calnexin and calreticulin in the folding of newly synthesized proteins (See '*Section 2.1 Quality Control of the Endoplasmic Reticulum)* and its involvement for the assembly of the MHC class I molecules [23, 158, 159]. New studies, however, suggest that ERp57 may be found outside of the ER in the nucleus, cytoplasm and cell surface and involved in gene regulation [158].

Newly synthesized proteins obtain correct conformation and posttranslational modifications critical to functionality through the assistance of chaperone proteins and foldases in the ER lumen [23]. ERp57 is a major protein in this process as it associates with the lectin-like ER chaperones calreticulin and calnexin to catalyze the isomerization of disulfide bonds of newly synthesized glycoproteins with unstructured disulfide-rich domains [23]. Proteins are synthesized into the ER where they are N-glycosylated and sequentially trimmed to form a mono-

glucoslyated protein that interacts with either calnexin or calreticulin [23]. ERp57, instead of binding substrates directly, is thought to be recruited and the *b* and *b'* domains of ERp57 interact with the extended P-domains of both calnexin and calreticulin [23]. It has been suggested that the role of calnexin and calreticulin is to bring ERp57 into close proximity to substrate, effectively increasing their local concentration, resulting in an enhancement of ERp57 activity [160]. Although the isomerase activity of ERp57 has been shown to be low when compared to PDI, this activity increases drastically when ERp57 forms complexes with either calnexin or calreticulin reinforcing further the role ERp57 has in quality control [160, 161].

ERp57 is also known to have a role in the immune system where it is important for the early and late stages of the folding of the heavy chain MHC class I [162]. The importance of ERp57 in MHC class I assembly is emphasized by studies with the ERp57 B cell specific knockout (See "*2.2c-iv-Mouse Models*") [163]. First, in the early stage ERp57, in complex with calnexin, binds the glycosylated heavy chain and catalyzes disulfide bind formation allowing the heavy chain to assemble with the β_2-microglobulin (β_2-m). Next, at the late stage, heterodimer complexes of heavy chain and β_2-m acquire peptides and associate with calreticulin, ERp57, TAP (peptide transporter), tapasin (a glycoprotein critical for peptide loading of MHC class I) forming the peptide loading complex (PLC) [159]. The catalytic *a* and *a'* domains of ERp57 then form a stable heterodimer with tapasin, load the peptides onto MHC class 1 and resulting in the β2-m-heavy chain heterodimer dissociating from the PLC and being exported to the cell surface [159, 164]. Mutagenesis studies have shown that ERp57 can

act independently from calnexin and calreticulin to gain access to the heavy chain arguing against the theory that MHC class I assembly is an example of quality control [164]. It is also appears that the catalytic activity of ERp57 is not required for MHC class I assembly as catalytically inactive ERp57 is able to promote peptide loading in a similar manner to wild-type ERp57 [164].

Most recently, ERp57 has been localized outside the ER to the nucleus, cell surface and cytoplasm suggesting that it may have other functions other than the ones indicated above [165]. ERp57 has been localized to the nucleus as it has a C-terminus putative nuclear localization signal and, via DNA-protein cross-linking studies in mammalian cells, has been shown to interact with DNA [165, 166]. Specifically, ERp57 has been shown to interact with signal transducer and activator of transcription 3 (STAT3) [165, 167, 168]. It has been unclear how STAT3 and ERp57 interact but data has shown that ERp57 may be involved in the regulation of STAT3 and may bind both active and inactive STAT3 [165, 167, 168]. ERp57/1,25D3-MARRS has also recently been shown to interact with the transcription factor, nuclear factor kappa B (NFkappaB) in differentiating NB4 leukaemia cells [169]. This suggests a role for ERp57/1,25D3-MARRS in gene expression and the differentiation of these cells [169].

2.2c-iii- Mouse Models - A global deletion of ERp57 in mice has been reported to be embryonic lethal, however, when a tissue-specific deletion of ERp57 in B cells is created, these mice are born live (Table 2) [163]. These mice have normal B cell development, proliferation and antibody production but have aberrant assembly of the PLC [163]. This provides

further evidence for the role of ERp57 in MHC class I antigen presentation *in vivo* [163]. Small interfering (si)RNA studies of ERp57 have been carried out in numerous cell lines to study the *in vivo* function of ERp57 [170-172]. siRNA studies have been carried out in fibroblasts and they show that although there is no effect of disulfide bond formation in co-translational synthesis of glycoproteins into the ER, there is significant loss of post-translational oxidative folding [170]. This suggests that although ERp57 is important for disulfide bond formation, there is some level functional redundancy amongst ER oxidoreductases [170]. In neuroblastoma cells, siRNA knockdown studies showed that a decrease of ERp57 results in an enhancement of toxicity of misfolded prion proteins (PrP^{SC}) while increased expression of ERp57 decreases sensitivity [171]. ERp57 protein expression was knocked down in human epithelial cells by siRNA and these cells had a decrease in tunicamycin- or hyperoxia-induced apoptosis but an increase in UPR [172]. This suggests that ERp57 may have a role in paediatric lung injury by providing cellular protection against oxidative insult-induced apoptosis [172].

2.2c-iv- Possible Medical Applications - ERp57 has been implicated in many human diseases such as cancer, prion disorders, Alzheimer's disease and hepatitis (Table 3) [171, 173-177]. In transformed cells, there is an increase in ERp57 expression [178]. Its oncogenic properties are thought to be due to its ability to control intracellular and extracellular redox activities through its thiol-dependent reductase activity [178]. However, the role ERp57 has with the modulation of STAT3 could also contribute to its oncogenic properties [168, 179]. ERp57 has also been linked to the early stages of prion disease and it may have a neuroprotective role in cellular

response to prion infection [171]. ERp57 and prion protein interact and there is enhancement of this interaction in prion infected mouse scrapies [171]. Targeting of this interaction may have applications for the development of a treatment as well as early diagnosis of prion diseases [171]. When looking at the cerebrospinal fluid (CSF) of Alzheimer's patients, ERp57, together with calreticulin, are found to be the carrier proteins that prevent the aggregation of β-amyloids, a major component of the toxic plaques found in Alzheimer's patients. They keep β-amyloids in solution and prevent them from forming the toxic aggregates that contribute to the neuronal dysfunction seen in Alzheimer's patients [176]. Ingestion of the common anaesthetic halothane can result in liver failure and, eventually, hepatitis [173]. It has been found that ingestion of halothane results in triflouroacetylated ERp57 which is non-functional in quality control leading to aberrant protein folding and liver failure [173]. The numerous functions of ERp57 link it to many disease states and make it a probable candidate for targeting and manipulation in developing treatment and diagnosis of diseases.

Table 1-2: Animal models of chaperone proteins

protein	mouse model	phenotype	references
calnexin(cnx)	*cnx* $^{-/-}$	viable, ataxic, 30-50% smaller then wild-type, gait disturbance, splaying of hind-limbs, severe dysmyelination, misfolded myelin proteins	• Denzel, A. et al (2002) *Mol. Cell Biol.* 22, 7398-7404 • Kraus, A. et al (2010) • Jung, J. et al (2010)
	cnx $^{-/-}$ + CNX $Cys^{161}Cys^{195}Tyr^{165}Lys^{167}$	identical to calnexin $^{-/-}$	• Denzel, A. et al (2002) *Mol. Cell Biol.* 22, 7398-7404
calreticulin (crt)	*crt*$^{-/-}$	embryonic lethal at 14.5 post-coitum, malformation of cardiac system, decreased Ca^{2+} capacity, down-regulated CaN, loss of NFAT/MEF2C translocation	• Mesaeli, N. et al (1999) *J. Cell Biol.* 144, 857 -868 • Lozyk, M.D. et al (2006) *BMC Dev. Biol.* 6, 54 • Guo, L. et al (2001) *J. Biol. Chem.* 276, 2797-2801
	crt $^{-/-}$ + activated CaN	viable, rescued cardiac development, impeded growth, hypoglycaemia, increased serum triglycerols and cholesterol	• Lynch, J. et al (2005) *J. Cell Biol.* 170, 37-47
	crt $^{-/-}$ + CRT O/E embryonic heart	viable, death at latest 5 weeks, dilated atria, ventricular chamber and wall, ECG abnormalities, model for A-V block	• Nakamura, K. et al (2001) *J. Cell Biol,* 154, 961-972. • Hattori, K. et al (2007) *Mol. Genet. Metab.* 91, 285-293.
	crt $^{-/-}$ + CRT O/E adult heart	dilated cardiomyopathy, heart failure	• Lee, D. et al (2010)
ERp57	*ERp57*$^{-/-}$	embryonic lethal	• Garbi, N. et al (2006) *Nat. Immunol* 7, 93-102
	ERp57$^{-/-}$ in B cells	viable, normal B cell development, proliferation and antibody production, aberrant assembly of PLC	• Garbi, N. et al (2006) *Nat. Immunol* 7, 93-102

Table 1-3: Summary of protein function and disease relevance

Protein	Localization	Function	Possible Disease Relevance	Reference
Calnexin	ER transmembrane	chaperone, Ca^{2+} signalling outside lumen, apoptosis	Charcot-Marie-Tooth (CMT), Dejerine-Sottas, Oculocutaneous albinism type 1 (OCA1), osteaoarthritis, pseudoachondroplasia (PSACH), Cystic Fibrosis, pulmonary emphysema,	2,88-95,97-114
Calreticulin	ER lumen, cell surface, cytoplasm	chaperone, Ca^{2+} buffering and signalling	systemic lupus erythemataosus (SLE), celiac disease, rheumatic disease, parasitic disease, cardiac hypertrophy, wound healing	15, 131,132, 138, 145, 152, 153
ERp57	ER lumen, cell surface, cytoplasm, nucleus	thiol-oxidoreductase, MHC class I assembly, STAT3 modulation	cancer, prion diseases, Alzheimer's disease, hepatitis	171, 173-177

3.0 Unfolded Protein Response - Disturbances to any of the players involved in quality control can results in an increase in misfolded proteins in the ER lumen and this is termed ER stress [6]. To effectively deal with the increased load of misfolded proteins in the ER lumen, the cell has evolved a sophisticated system called the unfolded protein response (UPR) (Figure 1-7) [6, 180]. UPR is directed by three ER transmembrane protein sensors called activating transcription factor-6 (ATF6), inositol-requiring kinase 1 (IRE) and double-stranded RNA-activated protein kinase-like ER kinase (PERK) [181]. Together, through three simple adaptive mechanisms ATF6, IRE1 and PERK alleviate stress on the ER: (1) there is an up-regulation of chaperone proteins and foldases and an increase in the size/capacity of the ER (2) there is an inhibition of translation of newly synthesized proteins into the ER and (3) there is an increase in degradation machinery to rapidly clear misfolded proteins from the ER lumen [181]. Activation of the three sensors is maintained by the regulatory "master" protein, glucose-regulated protein-78(GRp78) or BiP [4]. BiP has been given the name "master regulator" of the ER because this role in the ER that prevents aggregation of newly synthesized proteins and associates with UPR sensors to prevent their activation [3, 4, 182].

Genetic screens of the budding yeast, *Saccharomyces cerevisiae*, resulted in the identification of the first component of the UPR pathway, Ire1p/Ern1p, an ER transmembrane protein kinase [183, 184]. It has since been shown that Ire1p is a bi-functional protein with not only a cytosolic carboxy-terminal kinase domain but also an endoribonuclease (RNase) domain [185]. Under conditions of no stress, Ire1p is maintained as an inactive homodimer by the protein chaperone Kar2p/BiP/GRp78. However, when

misfolded proteins accumulate in the ER lumen, Ire1p is released from the Kar2p/BiP/GRp78 protein and it homodimerizes and *trans*-autophosphorylates to activate its endoribonuclease (RNase) activity [8]. The RNase domain of Ire1p targets the mRNA of the basic leucine zipper domain (bZIP) containing transcription factor, Hac1p [8]. The splicing of the mRNA results in the synthesis of a potent protein transcription factor, *HAC1*, that translocates to the nucleus where it activates the transcription of UPR element (UPRE) containing genes to alleviate ER stress [8]. Interestingly, the Ire1p branch of the UPR pathway has been found to be conserved in all eukaryotic cells. There are two mammalian homologues of yeast Ire1p and they are IREα and IREβ [186, 187]. As well, the bZIP-containing transcription factor X-box binding protein (Xbp1) has been shown to be the mRNA target of the endoribonuclease activity of mammalian IRE1 [185]. Similar to the yeast system, when UPR is activated by an accumulation of misfolded proteins within the ER lumen, a 26-nucleotide intron is cleaved from the mRNA of Xbp1(us) causing a translational frameshift to an active and stable transcription factor, Xbp1(s) [8, 185]. This transcription factor, Xbp1(s) goes on to activate the transcription of UPRE containing genes involved in ERAD in order to alleviate the build up of misfolded proteins in the ER lumen [185].

PERK is an ER transmembrane kinase whose function to transiently attenuate mRNA translation decreasing the load of newly synthesized proteins into the already stressed ER, serves as the first line of defence in mammalian UPR [8, 188]. When there is an accumulation of misfolded proteins in the ER lumen, BiP/GRp78 goes on to bind these misfolded proteins thus, disassociating from PERK freeing PERK to dimerize which

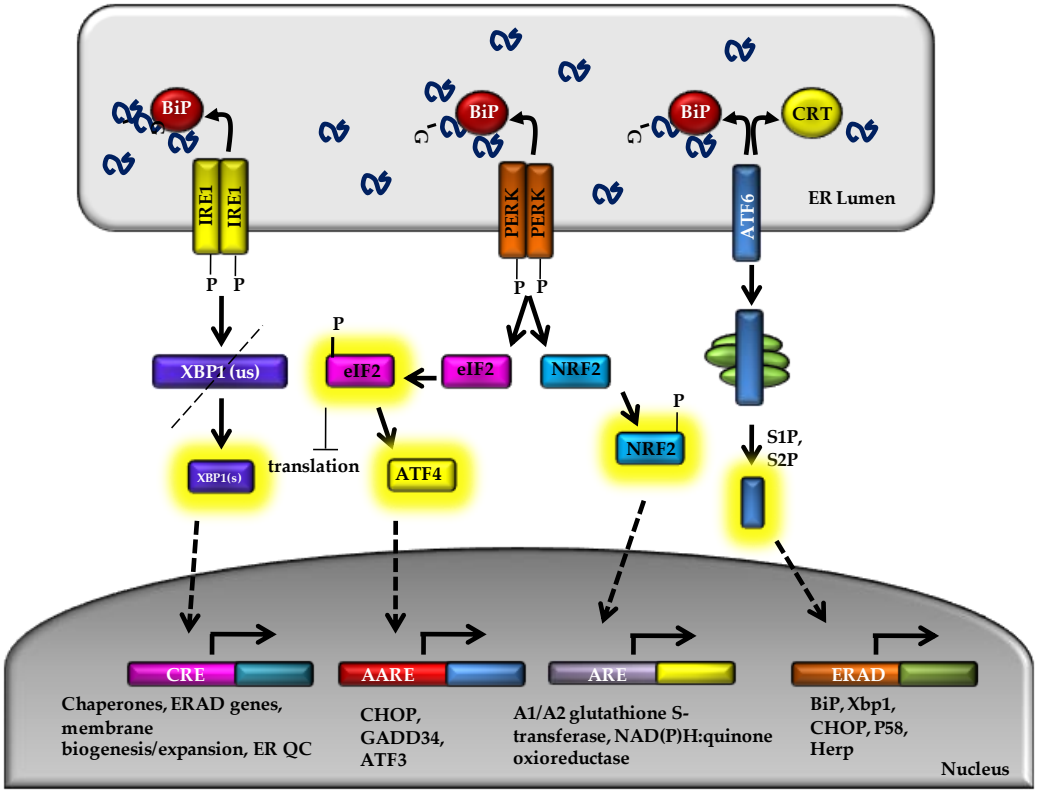

Figure 1-7 (legend on following page)

Figure 1-7 - The unfolded protein response (UPR). UPR is activated as a result of misfolded proteins (blue squiggles) in the ER (light grey box). BiP is titrated off the transmembrane sensors IRE1, PERK and ATF6 to bind non-glycosylated and glycosylated misfolded proteins accumulating in the ER. IRE1 is free to homodimerize resulting in autophosphorylation that activates its endoribonuclease activity. It then splices 26-nucleotides from Xbp1 mRNA which activates the spliced form, Xbp1(s). Xbp1(s) translocates to the nucleus where it binds to CRE promoters resulting in the activation of ERAD genes, genes involved in membrane biogenesis and quality control. PERK is also free to homodimerize and autophosphorylate activating its phosphorylation activity. It phosphorylates eIF2α activating it to decrease overall translation but increase the translation of ATF4. Increased ATF4 protein translocates to the nucleus where it binds genes with AARE promoters causing an increase in transcription of CHOP, GADD34 and ATF3. PERK also phosphorylates NRF2 activating it as a transcription factor where it translocates to the nucleus to bind genes with ARE to increase the transcription of genes responding to oxidative stress. ATF6 is released by BiP and CRT and it translocates to the Golgi apparatus where it is cleaved by S1P and S2P to release the active transcription factor, ATF6-N, that translocates to the nucleus to bind ERSE containing promoters to activate transcription of genes such as BiP, Xbp1, P58 and CHOP. These three sensors work together to decrease ER stress. IRE1: inositol requiring enzyme 1; Xbp1: X-box binding protein 1; CRE: cAMP response element; ERAD: ER associated degradation; PERK: double-stranded RNA-activated protein kinase-like ER kinase; P: phosphorylation; eIF2α: eukaryotic elongation factor 2 α; ATF4: activating transcription factor 4; AARE: amino acid response elements; ATF3: activating transcription factor 3; NRF2: nuclear respiratory factor 2; ARE: antioxidant response element; ATF6: activating transcription factor 6; S1P: site-1 protease; S2P: site-2 protease; ERSE: ER-response element. A version of this figure has been previously published: Jung, J. et al. 2009, Quality control in the secretory pathway. Handbook of Molecular Chaperones, Durante, P. And Colucci, L. eds, Nova Science Publishers.

results in its *trans*-autophosphorylation [8]. Subsequently, the cytoplasmic kinase

domain of PERK phosphorylates the α-subunit of eukaryotic initiation factor 2 (eIF2α) on Ser^{51} [8, 188]. Phosphorylated eIF2α binds the guanine nucleotide exchange factor eIF2B resulting in interference of the assembly of the 43S translation initiation complex to shut down general translation initiation consequently reducing protein synthesis [189]. Phosphorylated eIF2α also plays a selective role in the transcription by activating ATF4 (activating transcription factor 4) which results in the transcription of genes involved in mechanisms such as apoptosis and anti-oxidative stress response. Activated PERK also targets, nuclear respiratory transcription factor 2 (NRF2) which, in unstressed cells, is maintained in the cytoplasm by interaction with Kelch-like Ech-associated protein 1, Keap1. However, under stressed conditions, activated PERK phosphorylates NRF2 causing it to dissociate from Keap1 and translocate to the nucleus where it binds to antioxidant response elements (ARE) to activate the transcription of genes involved in detoxifying events [190, 191]. Together, these findings are consistent with the idea that PERK may play a role in alleviating oxidative stress insult to the cell [8].

The third branch of UPR is a 90-kDa ER transmembrane protein named ATF6 with its carboxy-terminus located in the ER lumen and its amino-terminus DNA binding domain located in the cytoplasm [8, 192-194]. There are two isoforms of ATF6 (α and β) that are characterized by their divergent transcriptional activity domains (TAD) [195]. ATF6-α and –β possess highly similar domain structures with an amino-terminal TAD, a

cytoplasmic bZip domain and a single transmembrane domain with glycosylation sites in the carboxyl-domain [196, 197]. ER stress-dependent activation of both isoforms of ATF6 is monitored by the two ER resident proteins, BiP/GRp78 and calreticulin. Under normal conditions, the luminal domain of ATF6, like PERK and IRE1, is bound by BiP/GRp78 however, it is also bound by calreticulin (through its three glycosylation sites) and this binding masks Golgi localization sites (GLSs) on ATF6. In response to ER stress, the luminal domain of ATF6 is released from BiP/GRp78 and from calreticulin (due to underglycosylation of the three luminal glycosylation sites) revealing non-consensus Golgi localization sites (GLSs) [192, 194, 198]. ATF6-α and –β then translocate to the Golgi apparatus where they are subject to proteolytic processing termed regulated intramembrane proteolysis (RIP) where they are sequentially cleaved by Site-1 protease (S1P) and site-2 protease (S2P) [192, 198]. RIP results in the cleaved and activated nuclear form of ATF6 (N-ATF6) that translocates to the nucleus to directly bind ERSEs in combination with other factors like NF-Y and YY1, to induce ER stress genes such as BiP/GRp78 [199]. N-ATF6 activates genes that contain an ERSE similar to targets of Xbp1 and it is thought that ATF6 and Xbp1 may have partially overlapping target genes [194, 198]. Recent studies show that ATF6-α and –β can bind ERSEs as homodimers or as a heterodimers to modulate the ER stress response [195-197]. There appears to be "fine tuning" of the ATF6 branch of UPR so that the different isoforms, -α and –β, regulate the strength and duration of the ER stress response [199].

The molecular mechanisms that control protein folding, transport and degradation must function in perfect balance [3]. The involvement of

players such as BiP/GRp78 and calreticulin in UPR suggest that Ca^{2+} may have role in the mediation of this stress response. It is of interest that these sensors are maintained in their "off" states by binding BiP/GRp78 (PERK, IRE, ATF6) and calreticulin (ATF6) [4, 192]. When quality control and UPR fail, the outcomes can be either inappropriate retention or disposal of proteins and this is the basis of a variety of diseases [2, 70, 200]. Loss-of-function diseases, such as cystic fibrosis, can result from mutant cargo molecules (cystic fibrosis transmembrane conductance regulator) being unable to properly fold and are retained in the ER and then sent for degradation [6]. Conversely, gain-of-function diseases, such as α1-antitrypsin, results in misfolded protein being retained within the ER and forming aggregates [3]. As well, direct defects in ER folding and transport-machinery or UPR machinery also can result in diseases such as coagulation disorders and neurodegenerative diseases, respectively [3, 6]. ER stress mediated signalling pathways have also been implicated in the pathologies of neurodegenerative diseases [201].

4.0 Research Objective

The objective of my PhD Thesis was to investigate the function of calnexin and ERp57 *in vitro* and *in vivo* with an emphasis on the expression throughout development and role in the quality control cycle and intracellular signalling. Considering the surprising viable and ataxic phenotype of the calnexin-deficient mouse [85] and the embryonic lethality of the ERp57-deficient mouse [163], it is important to fully understand the critical and novel roles that these ER proteins play within the cell. Calnexin has been well established to have a role in the quality control pathway for newly synthesized proteins [202]. However the redundancy of this chaperone function may have with calreticulin needs to be elucidated. ERp57 has been established to be involved in quality control cycle in association with calnexin and calreticulin [203], have a role in MHC class I processing [204] and, most recently, suggested to have a role in gene regulation [168]. In order to fully understand the role ERp57 plays in development, how ERp57 regulates downstream genes must be investigated. It is important to investigate the principles of protein folding, export and degradation in the ER because imbalances in these activities are the foundation of protein folding diseases [205].

5.0 Research Hypothesis

The hypothesis of this study is that the chaperone proteins, calnexin and ERp57, both have an impact on cell signalling pathways that contribute to their mouse model phenotype. To address this hypothesis I focussed on the role that calnexin plays in mediation of the unfolded protein response and the role of ERp57 in STAT3 signalling. We set out to answer three main questions: (i) does the absence of calnexin result in ER stress and activation of the UPR? (ii) does the absence of ERp57 result in aberrant modulation of STAT3 signalling? and (iii) what amino acid residues are critical for the chaperone function and ERp57 binding of calnexin?

7.0 **References**

1. Lin, J.H., P. Walter, and T.S. Yen, *Endoplasmic reticulum stress in disease pathogenesis.* Annu Rev Pathol, 2008. **3**: p. 399-425.
2. Bedard, K., et al., *Cellular functions of endoplasmic reticulum chaperones calreticulin, calnexin, and ERp57.* Int Rev Cytol, 2005. **245**: p. 91-121.
3. Hebert, D.N. and M. Molinari, *In and out of the ER: protein folding, quality control, degradation, and related human diseases.* Physiol Rev, 2007. **87**(4): p. 1377-408.
4. Hendershot, L.M., *The ER function BiP is a master regulator of ER function.* Mt Sinai J Med, 2004. **71**(5): p. 289-97.
5. Ma, Y. and L.M. Hendershot, *ER chaperone functions during normal and stress conditions.* J Chem Neuroanat, 2004. **28**(1-2): p. 51-65.
6. Schroder, M. and R.J. Kaufman, *ER stress and the unfolded protein response.* Mutat Res, 2005. **569**(1-2): p. 29-63.
7. Groenendyk, J. and M. Michalak, *Calcium Buffering Proteins: ER Luminal Proteins.* Encyclopedia of Biological Chemistry, 2004. **1**: p. 226-230.
8. Malhotra, J.D. and R.J. Kaufman, *The endoplasmic reticulum and the unfolded protein response.* Semin Cell Dev Biol, 2007. **18**(6): p. 716-31.
9. Hwang, C., A.J. Sinskey, and H.F. Lodish, *Oxidized redox state of glutathione in the endoplasmic reticulum.* Science, 1992. **257**(5076): p. 1496-1502.
10. Berridge, M.J., M.D. Bootman, and H.L. Roderick, *Calcium signalling: dynamics, homeostasis and remodelling.* Nature Rev. Mol. Cell Biol., 2003. **4**(7): p. 517-529.
11. Groenendyk, J., *Protein Folding and Calcium Homeostasis in the Endoplasmic Reticulum.* Calcium Binding Proteins, 2006. **1**(2): p. 77-85.
12. Corbett, E.F. and M. Michalak, *Calcium, a signaling molecule in the endoplasmic reticulum?* Trends Biochem. Sci., 2000. **25**(7): p. 307-311.
13. Ashby, M.C. and A.V. Tepikin, *ER calcium and the functions of intracellular organelles.* Semin Cell Dev Biol, 2001. **12**(1): p. 11-7.
14. Coe, H. and M. Michalak, *Calcium binding chaperones of the endoplasmic reticulum.* Gen Physiol Biophys, 2009. **28 Focus Iss**: p. F96-F103.
15. Michalak, M., et al., *Calreticulin, a multi-process calcium-buffering chaperone of the endoplasmic reticulum.* Biochem J, 2009. **417**(3): p. 651-66.
16. Baksh, S. and M. Michalak, *Expression of calreticulin in Escherichia coli and identification of its Ca^{2+} binding domains.* J. Biol. Chem., 1991. **266**: p. 21458-21465.
17. Nakamura, K., et al., *Functional specialization of calreticulin domains.* J. Cell Biol., 2001. **154**: p. 961-972.

18. Breier, A. and M. Michalak, *2,4,6-Trinitrobenzenesulfonic acid modification of the carboxyl- terminal region (C-domain) of calreticulin.* Mol. Cell. Biochem., 1994. **130**: p. 19-28.
19. Nakamura, K., et al., *Complete heart block and sudden death in mouse over-expressing calreticulin.* J. Clin. Invest., 2001. **107**(10): p. 1245-1253.
20. Li, J., et al., *Calreticulin reveals a critical Ca(2+) checkpoint in cardiac myofibrillogenesis.* J Cell Biol, 2002. **158**(1): p. 103-13.
21. Mesaeli, N., et al., *Calreticulin is essential for cardiac development.* J. Cell Biol., 1999. **144**: p. 857-868.
22. Coe, H. and M. Michalak, *Calcium Binding Chaperones of the Endoplasmic Reticulum.* Gen. Physiol. Biophys., 2009. **28**: p. 96-103.
23. Williams, D.B., *Beyond lectins: the calnexin/calreticulin chaperone system of the endoplasmic reticulum.* J Cell Sci, 2006. **119**(Pt 4): p. 615-23.
24. Corbett, E.F., et al., *The conformation of calreticulin is influenced by the endoplasmic reticulum lumenal environment.* J. Biol. Chem., 2000. **275**: p. 27177-27185.
25. Lievremont, J.P., et al., *BiP, a major chaperone protein of the endoplasmic reticulum lumen, plays a direct and important role in the storage of the rapidly exchanging pool of Ca^{2+}.* J. Biol. Chem., 1997. **272**: p. 30873-3089.
26. Argon, Y. and B.B. Simen, *GRP94, an ER chaperone with protein and peptide binding properties.* Semin Cell Dev Biol, 1999. **10**(5): p. 495-505.
27. Barnes, J.A. and I.W. Smoak, *Immunolocalization and heart levels of GRP94 in the mouse during post-implantation development.* Anat. Embryol., 1997. **196**: p. 335-341.
28. Vitadello, M., et al., *Overexpression of the stress protein Grp94 reduces cardiomyocyte necrosis due to calcium overload and simulated ischemia.* FASEB J, 2003. **17**(8): p. 923-5.
29. Lebeche, D., H.A. Lucero, and B. Kaminer, *Calcium binding properties of rabbit liver protein disulfide isomerase.* Biochem. Biophys. Res. Commun., 1994. **202**(1): p. 556-561.
30. Lucero, H.A., D. Lebeche, and B. Kaminer, *ERcalcistorin/protein-disulfide isomerase acts as a calcium storage protein in the endoplasmic reticulum of a living cell. Comparison with calreticulin and calsequestrin.* J. Biol. Chem., 1998. **273**(16): p. 9857-9863.
31. Tjoelker, L.W., et al., *Human, mouse, and rat calnexin cDNA cloning: identification of potential calcium binding motifs and gene localization to human chromosome 5.* Biochemistry, 1994. **33**: p. 3229-3236.
32. Wong, H.N., et al., *Conserved in vivo phosphorylation of calnexin at casein kinase II sites as well as a protein kinase C/proline-directed kinase site.* J Biol Chem, 1998. **273**(27): p. 17227-35.
33. Dudek, J., et al., *Functions and pathologies of BiP and its interaction partners.* Cell Mol Life Sci, 2009. **66**(9): p. 1556-69.

34. Pizzo, P., et al., *Grp94 acts as a mediator of curcumin-induced anti-oxidant defence in myogenic cells.* J Cell Mol Med, 2009.
35. Lucero, H.A. and B. Kaminer, *The role of calcium on the activity of ERcalcistorin/protein-disulfide isomerase and the significance of the C-terminal and its calcium binding. A comparison with mammalian protein-disulfide isomerase.* J Biol Chem, 1999. **274**(5): p. 3243-51.
36. Rizzuto, R. and T. Pozzan, *Microdomains of intracellular Ca2+: molecular determinants and functional consequences.* Physiol Rev, 2006. **86**(1): p. 369-408.
37. Taylor, C.W. and A.J. Laude, *IP3 receptors and their regulation by calmodulin and cytosolic Ca2+.* Cell Calcium, 2002. **32**(5-6): p. 321-34.
38. Prins, D. and M. Michalak, *Endoplasmic reticulum proteins in cardiac development and dysfunction.* Can J Physiol Pharmacol, 2009. **87**(6): p. 419-25.
39. Bootman, M.D., et al., *Calcium signalling--an overview.* Semin. Cell Dev. Biol., 2001. **12**(1): p. 3-10.
40. Lipskaia, L., J.S. Hulot, and A.M. Lompre, *Role of sarco/endoplasmic reticulum calcium content and calcium ATPase activity in the control of cell growth and proliferation.* Pflugers Arch, 2009. **457**(3): p. 673-85.
41. Rhodes, J.D. and J. Sanderson, *The mechanisms of calcium homeostasis and signalling in the lens.* Exp Eye Res, 2009. **88**(2): p. 226-34.
42. Putney, J.W., Jr., *A model for receptor-regulated calcium entry.* Cell Calcium, 1986. **7**(1): p. 1-12.
43. Nedergaard, M., J.J. Rodriguez, and A. Verkhratsky, *Glial calcium and diseases of the nervous system.* Cell Calcium, 2009.
44. Sitia, R. and I. Braakman, *Quality control in the endoplasmic reticulum protein factory.* Nature, 2003. **426**(6968): p. 891-4.
45. Schroder, M., *Endoplasmic reticulum stress responses.* Cell Mol Life Sci, 2008. **65**(6): p. 862-94.
46. Mayor, U., et al., *The complete folding pathway of a protein from nanoseconds to microseconds.* Nature, 2003. **421**(6925): p. 863-7.
47. Stevens, F.J. and Y. Argon, *Protein folding in the ER.* Sem. Cell Dev. Biol., 1999. **10**(5): p. 443-454.
48. Johnson, A.E. and M.A. van Waes, *The translocon: a dynamic gateway at the ER membrane.* Annu Rev Cell Dev Biol, 1999. **15**: p. 799-842.
49. Oliver, J., et al., *The Sec61 complex is essential for the insertion of proteins into the membrane of the endoplasmic reticulum.* FEBS Lett, 1995. **362**(2): p. 126-30.
50. Hamman, B.D., L.M. Hendershot, and A.E. Johnson, *BiP maintains the permeability barrier of the ER membrane by sealing the lumenal end of the translocon pore before and early in translocation.* Cell, 1998. **92**(6): p. 747-58.
51. Trombetta, E.S. and A. Helenius, *Lectins as chaperones in glycoprotein folding.* Curr. Opin. Struct. Biol., 1998. **8**(5): p. 587-592.

52. Helenius, A. and M. Aebi, *Roles of N-linked glycans in the endoplasmic reticulum.* Annu Rev Biochem, 2004. **73**: p. 1019-49.
53. Oliver, J.D., et al., *ERp57 functions as a subunit of specific complexes formed with the ER lectins calreticulin and calnexin.* Mol Biol Cell, 1999. **10**(8): p. 2573-82.
54. Taylor, S.C., et al., *Glycopeptide specificity of the secretory protein folding sensor UDP-glucose glycoprotein:glucosyltransferase.* EMBO Rep, 2003. **4**(4): p. 405-11.
55. Vembar, S.S. and J.L. Brodsky, *One step at a time: endoplasmic reticulum-associated degradation.* Nat Rev Mol Cell Biol, 2008. **9**(12): p. 944-57.
56. Jung, J., Coe, H., Opas, M., and Michalak, M., *Calnexin: An Endoplasmic Reticulum Integral Membrane Chaperone.* Calcium Binding Proteins, 2006. **1**(2): p. 67-71.
57. Schrag, J.D., et al., *The structure of calnexin, an ER chaperone involved in quality control of protein folding.* Mol. Cell, 2001. **8**: p. 633-644.
58. Ou, W.J., et al., *Conformational changes induced in the endoplasmic reticulum luminal domain of calnexin by Mg-ATP and Ca2+.* J Biol Chem, 1995. **270**(30): p. 18051-9.
59. Leach, M.R., et al., *Localization of the lectin, ERp57 binding, and polypeptide binding sites of calnexin and calreticulin.* J Biol Chem, 2002. **277**(33): p. 29686-97.
60. Groenendyk, J., Dabrowska, M., and Michalak, M., *Mutational analysis of calnexin.* Biochimica et Biophysica Acta, 2010.
61. Pollock, S., et al., *Specific interaction of ERp57 and calnexin determined by NMR spectroscopy and an ER two-hybrid system.* Embo J, 2004. **23**(5): p. 1020-9.
62. Oliver, J.D., et al., *ERp57 Functions as a Subunit of Specific Complexes Formed with the ER Lectins Calreticulin and Calnexin.* Mol. Biol. Cell, 1999. **10**: p. 2573-2582.
63. Swanton, E., S. High, and P. Woodman, *Role of calnexin in the glycan-independent quality control of proteolipid protein.* Embo J, 2003. **22**(12): p. 2948-58.
64. Cannon, K.S. and P. Cresswell, *Quality control of transmembrane domain assembly in the tetraspanin CD82.* EMBO J., 2001. **20**(10): p. 2443-2453.
65. Capps, G.G. and M.C. Zuniga, *Class I histocompatibility molecule association with phosphorylated calnexin. Implications for rates of intracellular transport.* J. Biol. Chem., 1994. **269**: p. 11634-11639.
66. Le, A., et al., *Association between calnexin and a secretion-incompetent variant of human alpha 1-antitrypsin.* J Biol Chem, 1994. **269**(10): p. 7514-9.
67. Rosenbaum, E.E., R.C. Hardie, and N.J. Colley, *Calnexin is essential for rhodopsin maturation, Ca2+ regulation, and photoreceptor cell survival.* Neuron, 2006. **49**(2): p. 229-41.

68. Delom, F. and E. Chevet, *In vitro mapping of calnexin interaction with ribosomes.* Biochem Biophys Res Commun, 2006. **341**(1): p. 39-44.
69. Parodi, A.J., *The quality control of glycoprotein folding in the endoplasmic reticulum, a trip from trypanosomes to mammals.* Braz. J. Med. Biol. Res., 1998. **31**: p. 601-614.
70. Ellgaard, L. and A. Helenius, *Quality control in the endoplasmic reticulum.* Nature Rev. Mol. Cell Biol., 2003. **4**(3): p. 181-191.
71. Wada, I., et al., *SSR alpha and associated calnexin are major calcium binding proteins of the endoplasmic reticulum membrane.* J Biol Chem, 1991. **266**(29): p. 19599-610.
72. Roderick, H.L., J.D. Lechleiter, and P. Camacho, *Cytosolic phosphorylation of calnexin controls intracellular Ca^{2+} oscillations via an interaction with SERCA2b.* J. Cell Biol., 2000. **149**(6): p. 1235-1248.
73. Lenter, M. and D. Vestweber, *The integrin chains beta 1 and alpha 6 associate with the chaperone calnexin prior to integrin assembly.* J. Biol. Chem., 1994. **269**: p. 12263-12268.
74. Muller-Taubenberger, A., et al., *Calreticulin and calnexin in the endoplasmic reticulum are important for phagocytosis.* EMBO J., 2001. **20**: p. 6772-6782.
75. Takizawa, T., et al., *Cleavage of calnexin caused by apoptotic stimuli: implication for the regulation of apoptosis.* J Biochem (Tokyo), 2004. **136**(3): p. 399-405.
76. Zuppini, A., et al., *Calnexin deficiency and endoplasmic reticulum stress-induced apoptosis.* Biochemistry, 2002. **41**: p. 2850-2858.
77. Groenendyk, J., et al., *Caspase 12 in calnexin-deficient cells.* Biochemistry, 2006. **45**(44): p. 13219-26.
78. Booth, C. and G.E.L. Koch, *Perturbation of cellular calcium induces secretion of luminal ER proteins.* Cell, 1989. **59**: p. 729-737.
79. Rudolph, H.K., et al., *The yeast secretory pathway is perturbed by mutations in PMR1, a member of a Ca^{2+} ATPase family.* Cell, 1989. **58**: p. 133-145.
80. Suzuki, C.K., et al., *Regulating the retention of T-cell receptor alpha chain variants within the endoplasmic reticulum: Ca^{2+}-dependent association with BiP.* J. Cell Biol., 1991. **114**(2): p. 189-205.
81. Lee, W., et al., *Caenorhabditis elegans calnexin is N-glycosylated and required for stress response.* Biochem Biophys Res Commun, 2005. **338**(2): p. 1018-30.
82. Hughes, P.D., W.R. Wilson, and S.W. Leslie, *Effect of gestational ethanol exposure on the NMDA receptor complex in rat forebrain: from gene transcription to cell surface.* Brain Res Dev Brain Res, 2001. **129**(2): p. 135-45.
83. Breckenridge, D.G., et al., *Caspase cleavage product of BAP31 induces mitochondrial fission through endoplasmic reticulum calcium signals, enhancing cytochrome c release to the cytosol.* J. Cell Biol., 2003. **160**(7): p. 1115-1127.
84. Kraus, A., et al., *Calnexin deficiency leads to dysmyelination.* J Biol Chem, 2010.

85. Denzel, A., et al., *Early postnatal death and motor disorders in mice congenitally deficient in calnexin expression.* Mol. Cell. Biol., 2002. **22**(21): p. 7398-7404.
86. Jung, J., Janowicz, A., Coe, H., Kraus, A. and Michalak, M. , *Specialization of Endoplasmic Reticulum Chaperones for the Folding and Function of Myelin Glycoproteins P0 and PMP22.* submitted, 2010.
87. Shames, I., et al., *Phenotypic differences between peripheral myelin protein-22 (PMP22) and myelin protein zero (P0) mutations associated with Charcot-Marie-Tooth-related diseases.* J Neuropathol Exp Neurol, 2003. **62**(7): p. 751-64.
88. Dickson, K.M., et al., *Association of calnexin with mutant peripheral myelin protein-22 ex vivo: A basis for "gain-of-function" ER diseases.* Proc. Natl. Acad. Sci. U.S.A., 2002. **99**: p. 9852-9857.
89. Chance, P.F., et al., *DNA deletion associated with hereditary neuropathy with liability to pressure palsies.* Cell, 1993. **72**(1): p. 143-51.
90. Chance, P.F. and D. Pleasure, *Charcot-Marie-Tooth syndrome.* Arch Neurol, 1993. **50**(11): p. 1180-4.
91. Fontanini, A., et al., *Glycan-independent role of calnexin in the intracellular retention of Charcot-Marie-tooth 1A Gas3/PMP22 mutants.* J Biol Chem, 2005. **280**(3): p. 2378-87.
92. Roa, B.B., et al., *Dejerine-Sottas syndrome associated with point mutation in the peripheral myelin protein 22 (PMP22) gene.* Nat Genet, 1993. **5**(3): p. 269-73.
93. Popescu, C.I., et al., *Soluble tyrosinase is an endoplasmic reticulum (ER)-associated degradation substrate retained in the ER by calreticulin and BiP/GRP78 and not calnexin.* J Biol Chem, 2005. **280**(14): p. 13833-40.
94. Branza-Nichita, N., et al., *Tyrosinase folding and copper loading in vivo: a crucial role for calnexin and alpha-glucosidase II.* Biochem. Biophys. Res. Commun., 1999. **261**(3): p. 720-725.
95. Oetting, W.S., et al., *Oculocutaneous albinism type 1: the last 100 years.* Pigment Cell Res, 2003. **16**(3): p. 307-11.
96. Denning, G.M., et al., *Processing of mutant cystic fibrosis transmembrane conductance regulator is temperature-sensitive.* Nature, 1992. **358**(6389): p. 761-4.
97. Hecht, J.T. and E.H. Sage, *Retention of the Matricellular Protein SPARC in the Endoplasmic Reticulum of Chondrocytes from Patients with Pseudoachondroplasia.* J Histochem Cytochem, 2006. **54**(3): p. 269-74.
98. Posey, K.L. and J.T. Hecht, *The role of cartilage oligomeric matrix protein (COMP) in skeletal disease.* Curr Drug Targets, 2008. **9**(10): p. 869-77.
99. Posey, K.L., et al., *Model systems for studying skeletal dysplasias caused by TSP-5/COMP mutations.* Cell Mol Life Sci, 2008. **65**(5): p. 687-99.
100. Stevens, J.W., *Pseudoachondroplastic dysplasia: an Iowa review from human to mouse.* Iowa Orthop J, 1999. **19**: p. 53-65.

101. Allen, S., et al., *Endoplasmic reticulum retention and prolonged association of a von Willebrand's disease-causing von Willebrand factor variant with ERp57 and calnexin.* Biochem. Biophys. Res. Commun., 2001. **280**(2): p. 448-453.
102. Denning, G.M., L.S. Ostedgaard, and M.J. Welsh, *Abnormal localization of cystic fibrosis transmembrane conductance regulator in primary cultures of cystic fibrosis airway epithelia.* J Cell Biol, 1992. **118**(3): p. 551-9.
103. Joseph, S.K., et al., *Biosynthesis of inositol trisphosphate receptors: selective association with the molecular chaperone calnexin.* Biochem. J., 1999. **342**: p. 153-161.
104. Ginzburg, L. and A.H. Futerman, *Defective calcium homeostasis in the cerebellum in a mouse model of Niemann-Pick A disease.* J Neurochem, 2005. **95**(6): p. 1619-28.
105. Jackson, M.R., et al., *Regulation of MHC class I transport by the molecular chaperone, calnexin (p88, IP90).* Science, 1994. **263**: p. 384-387.
106. Scott, J.E. and J.R. Dawson, *MHC class I expression and transport in a calnexin-deficient cell line.* J. Immunol., 1995. **155**: p. 143-148.
107. Paulsson, K. and P. Wang, *Chaperones and folding of MHC class I molecules in the endoplasmic reticulum.* Biochim Biophys Acta, 2003. **1641**(1): p. 1-12.
108. Chevet, E., et al., *Calnexin family members as modulators of genetic diseases.* Semin Cell Dev Biol, 1999. **10**(5): p. 473-80.
109. Liu, Y., et al., *Oligosaccharide modification in the early secretory pathway directs the selection of a misfolded glycoprotein for degradation by the proteasome.* J Biol Chem, 1999. **274**(9): p. 5861-7.
110. Ishmael, F.T., et al., *Multimeric structure of the secreted meprin A metalloproteinase and characterization of the functional protomer.* J Biol Chem, 2001. **276**(25): p. 23207-11.
111. Tsukuba, T., et al., *Chaperone interactions of the metalloproteinase meprin A in the secretory or proteasomal-degradative pathway.* Arch. Biochem. Biophys., 2002. **397**(2): p. 191-198.
112. Rubio, M.E. and R.J. Wenthold, *Calnexin and the immunoglobulin binding protein (BiP) coimmunoprecipitate with AMPA receptors.* J Neurochem, 1999. **73**(3): p. 942-8.
113. Chang, W., M.S. Gelman, and J.M. Prives, *Calnexin-dependent enhancement of nicotinic acetylcholine receptor assembly and surface expression.* J Biol Chem, 1997. **272**(46): p. 28925-32.
114. Nauseef, W.M., S.J. McCormick, and M. Goedken, *Coordinated participation of calreticulin and calnexin in the biosynthesis of myeloperoxidase.* J. Biol. Chem., 1998. **273**: p. 7107-7111.
115. Michalak, M., J. M. Robert Parker and M. Opas, *Ca2+ signaling and calcium binding chaperones of the endoplasmic reticulum.* Cell Calcium, 2002. **32**(5-6): p. 269-278.

116. Kapoor, M., et al., *Mutational analysis provides molecular insight into the carbohydrate-binding region of calreticulin: pivotal roles of tyrosine-109 and aspartate-135 in carbohydrate recognition.* Biochemistry, 2004. **43**(1): p. 97-106.
117. Leach, M.R. and D.B. Williams, *Lectin-deficient calnexin is capable of binding class I histocompatibility molecules in vivo and preventing their degradation.* J. Biol. Chem., 2003. **279**(10): p. 9072-9079.
118. Martin, V., et al., *Identification by mutational analysis of amino acid residues essential in the chaperone function of calreticulin.* J Biol Chem, 2006. **281**(4): p. 2338-46.
119. Thomson, S.P. and D.B. Williams, *Delineation of the lectin site of the molecular chaperone calreticulin.* Cell Stress Chaperones, 2005. **10**(3): p. 242-51.
120. Gopalakrishnapai, J., et al., *Isothermal titration calorimetric study defines the substrate binding residues of calreticulin.* Biochem Biophys Res Commun, 2006. **351**(1): p. 14-20.
121. Guo, L., et al., *Identification of an N-domain histidine essential for chaperone function in calreticulin.* J. Biol. Chem, 2003. **278**: p. 50645-50653.
122. Baksh, S., et al., *Identification of the Zn^{2+} binding region in calreticulin.* FEBS Lett., 1995. **376**: p. 53-57.
123. Ellgaard, L., et al., *NMR structure of the calreticulin P-domain.* Proc. Natl. Acad. Sci. U.S.A., 2001. **98**(6): p. 3133-3138.
124. Ellgaard, L., et al., *Three-dimensional structure topology of the calreticulin P-domain based on NMR assignment.* FEBS Lett., 2001. **488**(1-2): p. 69-73.
125. Vassilakos, A., et al., *Oligosaccharide binding characteristics of the molecular chaperones calnexin and calreticulin.* Biochemistry, 1998. **37**: p. 3480-3490.
126. Frickel, E.M., et al., *TROSY-NMR reveals interaction between ERp57 and the tip of the calreticulin P-domain.* Proc. Natl. Acad. Sci. U.S.A., 2002. **99**: p. 1954-1959.
127. Sipione, S.e.a., *Impaired Cytolytic Activity in Calreticulin-Deficient CTLs.* The Journal of Immunology, 2005. **174**: p. 3212-3219.
128. Rong, Y. and C.W. Distelhorst, *Bcl-2 protein family members: versatile regulators of calcium signaling in cell survival and apoptosis.* Annu Rev Physiol, 2008. **70**: p. 73-91.
129. Nakamura, K., et al., *Changes in endoplasmic reticulum luminal environment affect cell sensitivity to apoptosis.* J. Cell Biol., 2000. **150**: p. 731-740.
130. Orr, A.W., M.A. Pallero, and J.E. Murphy-Ullrich, *Thrombospondin Stimulates Focal Adhesion Disassembly through Gi- and Phosphoinositide 3-Kinase-dependent ERK Activation.* J. Biol. Chem., 2002. **277**(23): p. 20453-20460.
131. Pike, S.E., et al., *Vasostatin, a calreticulin fragment, inhibits angiogenesis and suppresses tumor growth.* J. Exp. Med., 1998. **188**: p. 2349-2356.

132. Gold, L.I., et al., *Overview of the role for calreticulin in the enhancement of wound healing through multiple biological effects.* J Investig Dermatol Symp Proc, 2006. **11**(1): p. 57-65.
133. Szabo, E., et al., *Calreticulin inhibits commitment to adipocyte differentiation.* J Cell Biol, 2008. **182**(1): p. 103-16.
134. St-Arnaud, R., et al., *Constitutive expression of calreticulin in osteoblasts inhibits mineralization.* J. Cell Biol., 1995. **131**: p. 1351-1359.
135. Panaretakis, T., et al., *The co-translocation of ERp57 and calreticulin determines the immunogenicity of cell death.* Cell Death Differ, 2008. **15**(9): p. 1499-509.
136. Gardai, S.J., et al., *By binding SIRPalpha or calreticulin/CD91, lung collectins act as dual function surveillance molecules to suppress or enhance inflammation.* Cell, 2003. **115**(1): p. 13-23.
137. Zhang, X., et al., *Endoplasmic reticulum stress during the embryonic development of the central nervous system in the mouse.* Int J Dev Neurosci, 2007. **25**(7): p. 455-63.
138. Lozyk, M.D., et al., *Ultrastructural analysis of development of myocardium in calreticulin-deficient mice.* BMC Dev Biol, 2006. **6**: p. 54.
139. Goncharova, E.J., Z. Kam, and B. Geiger, *The involvement of adherens junction components in myofibrillogenesis in cultured cardiac myocytes.* Development, 1992. **114**(1): p. 173-83.
140. Guo, L., et al., *COUP-TF1 antagonizes Nkx2.5-mediated activation of the calreticulin gene during cardiac development.* J. Biol. Chem., 2001. **276**: p. 2797-2801.
141. Lynch, J., et al., *Calreticulin signals upstream of calcineurin and MEF2C in a critical Ca(2+)-dependent signaling cascade.* J Cell Biol, 2005. **170**(1): p. 37-47.
142. Chien, K.R. and E.N. Olson, *Converging pathways and principles in heart development and disease: CV@CSH.* Cell, 2002. **110**(2): p. 153-162.
143. Srivastava, D. and E.N. Olson, *A genetic blueprint for cardiac development.* Nature, 2000. **407**(6801): p. 221-226.
144. Qiu, Y. and M. Michalak, *Transcriptional control of the calreticulin gene in health and disease.* Int J Biochem Cell Biol, 2009. **41**(3): p. 531-8.
145. Guo, L., et al., *Cardiac-specific expression of calcineurin reverses embryonic lethality in calreticulin-deficient mouse.* J. Biol. Chem., 2002. **277**(52): p. 50776-50779.
146. Qiu, Y., et al., *Regulation of the calreticulin gene by GATA6 and Evi-1 transcription factors.* Biochemistry, 2008. **47**(12): p. 3697-704.
147. Li, J., et al., *Calreticulin reveals a critical Ca^{2+} checkpoint in cardiac myofibrillogenesis.* J. Cell Biol., 2002. **158**(1): p. 103-113.
148. Hattori, K., et al., *Arrhythmia induced by spatiotemporal overexpression of calreticulin in the heart.* Mol Genet Metab, 2007. **91**(3): p. 285-93.

149. Arnaudeau, S., et al., *Calreticulin differentially modulates calcium uptake and release in the endoplasmic reticulum and mitochondria.* J. Biol. Chem., 2002. **277**(48): p. 46696-46705.
150. Orth, T., et al., *Complete congenital heart block is associated with increased autoantibody titers against calreticulin.* Eur. J. Clin. Invest., 1996. **26**: p. 205-215.
151. Moak, J.P., et al., *Congenital heart block: development of late-onset cardiomyopathy, a previously underappreciated sequela.* J. Am. Coll. Cardiol., 2001. **37**: p. 238-242.
152. Pike, S.E., et al., *Calreticulin and calreticulin fragments are endothelial cell inhibitors that suppress tumor growth.* Blood, 1999. **94**(7): p. 2461-2468.
153. Liu, M., et al., *Gene transfer of vasostatin, a calreticulin fragment, into neuroendocrine tumor cells results in enhanced malignant behavior.* Neuroendocrinology, 2005. **82**(1): p. 1-10.
154. Coe, H. and M. Michalak, *Molecules in Focus ERp57, a multifunctional endoplasmic reticulum resident oxidoreductase.* Int J Biochem Cell Biol.
155. Kozlov, G., et al., *Crystal structure of the bb' domains of the protein disulfide isomerase ERp57.* Structure, 2006. **14**(8): p. 1331-9.
156. Pirneskoski, A., et al., *Molecular characterization of the principal substrate binding site of the ubiquitous folding catalyst protein disulfide isomerase.* J Biol Chem, 2004. **279**(11): p. 10374-81.
157. Frickel, E.M., et al., *ERp57 is a multifunctional thiol-disulfide oxidoreductase.* J. Biol. Chem., 2004.
158. Khanal, R.C. and I. Nemere, *The ERp57/GRp58/1,25D3-MARRS receptor: multiple functional roles in diverse cell systems.* Curr Med Chem, 2007. **14**(10): p. 1087-93.
159. Dong, G., et al., *Insights into MHC class I peptide loading from the structure of the tapasin-ERp57 thiol oxidoreductase heterodimer.* Immunity, 2009. **30**(1): p. 21-32.
160. Zapun, A., et al., *Enhanced catalysis of ribonuclease B folding by the interaction of calnexin or calreticulin with ERp57.* J Biol Chem, 1998. **273**(11): p. 6009-12.
161. Urade, R., et al., *ER-60 domains responsible for interaction with calnexin and calreticulin.* Biochemistry, 2004. **43**(27): p. 8858-68.
162. Wearsch, P.A. and P. Cresswell, *The quality control of MHC class I peptide loading.* Curr Opin Cell Biol, 2008. **20**(6): p. 624-31.
163. Garbi, N., et al., *Impaired assembly of the major histocompatibility complex class I peptide-loading complex in mice deficient in the oxidoreductase ERp57.* Nat Immunol, 2006. **7**(1): p. 93-102.
164. Zhang, Y., et al., *ERp57 Does Not Require Interactions with Calnexin and Calreticulin to Promote Assembly of Class I Histocompatibility Molecules, and It Enhances Peptide Loading Independently of Its Redox Activity.* J Biol Chem, 2009. **284**(15): p. 10160-73.

165. Coppari, S., et al., *Nuclear localization and DNA interaction of protein disulfide isomerase ERp57 in mammalian cells.* J. Cell. Biochem., 2002. **85**(2): p. 325-333.
166. Bourdi, M., et al., *cDNA cloning and baculovirus expression of the human liver endoplasmic reticulum P58: characterization as a protein disulfide isomerase isoform, but not as a protease or a carnitine acyltransferase.* Arch Biochem Biophys, 1995. **323**(2): p. 397-403.
167. Eufemi, M., et al., *ERp57 is present in STAT3-DNA complexes.* Biochem Biophys Res Commun, 2004. **323**(4): p. 1306-12.
168. Guo, G.G., et al., *Association of the chaperone glucose-regulated protein 58 (GRP58/ER-60/ERp57) with Stat3 in cytosol and plasma membrane complexes.* J Interferon Cytokine Res, 2002. **22**(5): p. 555-63.
169. Wu, W., et al., *Nuclear translocation of the 1,25D(3)-MARRS (membrane associated rapid response to steroids) receptor protein and NFkappaB in differentiating NB4 leukemia cells.* Exp Cell Res.
170. Solda, T., et al., *Consequences of ERp57 deletion on oxidative folding of obligate and facultative clients of the calnexin cycle.* J Biol Chem, 2006.
171. Hetz, C., et al., *The disulfide isomerase Grp58 is a protective factor against prion neurotoxicity.* J Neurosci, 2005. **25**(11): p. 2793-802.
172. Xu, D., et al., *Knockdown of ERp57 Increases BiP/GRP78 Induction and Protects against Hyperoxia and Tunicamycin-induced Apoptosis.* Am J Physiol Lung Cell Mol Physiol, 2009.
173. Martin, J.L., et al., *Halothane hepatitis patients have serum antibodies that react with protein disulfide isomerase.* Hepatology, 1993. **18**(4): p. 858-63.
174. Muhlenkamp, C.R. and S.S. Gill, *A glucose-regulated protein, GRP58, is down-regulated in C57B6 mouse liver after diethylhexyl phthalate exposure.* Toxicol Appl Pharmacol, 1998. **148**(1): p. 101-8.
175. Seliger, B., et al., *Characterization of the major histocompatibility complex class I deficiencies in B16 melanoma cells.* Cancer Res, 2001. **61**(3): p. 1095-9.
176. Erickson, R.R., et al., *In cerebrospinal fluid ER chaperones ERp57 and calreticulin bind beta-amyloid.* Biochem Biophys Res Commun, 2005. **332**(1): p. 50-7.
177. Tourkova, I.L., et al., *Restoration by IL-15 of MHC class I antigen-processing machinery in human dendritic cells inhibited by tumor-derived gangliosides.* J Immunol, 2005. **175**(5): p. 3045-52.
178. Hirano, N., et al., *Molecular cloning of the human glucose-regulated protein ERp57/GRP58, a thiol-dependent reductase. Identification of its secretory form and inducible expression by the oncogenic transformation.* Eur. J. Biochem., 1995. **234**(1): p. 336-342.
179. Coe, H., et al., *ERp57 modulates STAT3 signalling from the lumen of the endoplasmic reticulum.* J Biol Chem, 2009.

180. Kozutsumi, Y., et al., *The presence of malfolded proteins in the endoplasmic reticulum signals the induction of glucose-regulated proteins.* Nature, 1988. **332**(6163): p. 462-464.
181. Schroder, M. and R.J. Kaufman, *The mammalian unfolded protein response.* Annu Rev Biochem, 2005. **74**: p. 739-89.
182. Groenendyk, J. and M. Michalak, *Endoplasmic reticulum quality control and apoptosis.* Acta Biochim Pol, 2005. **52**(2): p. 381-95.
183. Shamu, C.E. and P. Walter, *Oligomerization and phosphorylation of the Ire1p kinase during intracellular signaling from the endoplasmic reticulum to the nucleus.* Embo J, 1996. **15**(12): p. 3028-39.
184. Welihinda, A.A. and R.J. Kaufman, *The unfolded protein response pathway in Saccharomyces cerevisiae. Oligomerization and trans-phosphorylation of Ire1p (Ern1p) are required for kinase activation.* J Biol Chem, 1996. **271**(30): p. 18181-7.
185. Back, S.H., et al., *ER stress signaling by regulated splicing: IRE1/HAC1/XBP1.* Methods, 2005. **35**(4): p. 395-416.
186. Tirasophon, W., A.A. Welihinda, and R.J. Kaufman, *A stress response pathway from the endoplasmic reticulum to the nucleus requires a novel bifunctional protein kinase/endoribonuclease (Ire1p) in mammalian cells.* Genes Dev., 1998. **12**: p. 1812-1824.
187. Wang, X.Z., et al., *Cloning of mammalian Ire1 reveals diversity in the ER stress responses.* Embo J, 1998. **17**(19): p. 5708-17.
188. Lin, J.H., et al., *Divergent effects of PERK and IRE1 signaling on cell viability.* PLoS ONE, 2009. **4**(1): p. e4170.
189. Harding, H.P., et al., *Perk is essential for translational regulation and cell survival during the unfolded protein response.* Mol Cell, 2000. **5**(5): p. 897-904.
190. Cullinan, S.B., et al., *Nrf2 is a direct PERK substrate and effector of PERK-dependent cell survival.* Mol Cell Biol, 2003. **23**(20): p. 7198-209.
191. Nguyen, T., P.J. Sherratt, and C.B. Pickett, *Regulatory mechanisms controlling gene expression mediated by the antioxidant response element.* Annu Rev Pharmacol Toxicol, 2003. **43**: p. 233-60.
192. Hong, M., et al., *Underglycosylation of ATF6 as a novel sensing mechanism for activation of the unfolded protein response.* J Biol Chem, 2004. **279**(12): p. 11354-63.
193. Yoshida, H., et al., *Identification of the cis-acting endoplasmic reticulum stress response element responsible for transcriptional induction of mammalian glucose-regulated proteins. Involvement of basic leucine zipper transcription factors.* J Biol Chem, 1998. **273**(50): p. 33741-9.
194. Shen, J., et al., *Stable binding of ATF6 to BiP in the endoplasmic reticulum stress response.* Mol Cell Biol, 2005. **25**(3): p. 921-32.

195. Thuerauf, D.J., L. Morrison, and C.C. Glembotski, *Opposing roles for ATF6alpha and ATF6beta in endoplasmic reticulum stress response gene induction.* J Biol Chem, 2004. **279**(20): p. 21078-84.
196. Kondo, S., et al., *OASIS, a CREB/ATF-family member, modulates UPR signalling in astrocytes.* Nat Cell Biol, 2005. **7**(2): p. 186-94.
197. Murakami, T., et al., *Cleavage of the membrane-bound transcription factor OASIS in response to endoplasmic reticulum stress.* J Neurochem, 2006. **96**(4): p. 1090-100.
198. Shen, J., et al., *ER stress regulation of ATF6 localization by dissociation of BiP/GRP78 binding and unmasking of Golgi localization signals.* Dev Cell, 2002. **3**(1): p. 99-111.
199. Thuerauf, D.J., et al., *Effects of the isoform-specific characteristics of ATF6 alpha and ATF6 beta on endoplasmic reticulum stress response gene expression and cell viability.* J Biol Chem, 2007. **282**(31): p. 22865-78.
200. Eriksson, K.K., et al., *EDEM contributes to maintenance of protein folding efficiency and secretory capacity.* J Biol Chem, 2004. **279**(43): p. 44600-5.
201. Kadowaki, H., H. Nishitoh, and H. Ichijo, *Survival and apoptosis signals in ER stress: the role of protein kinases.* J Chem Neuroanat, 2004. **28**(1-2): p. 93-100.
202. Hammond, C. and A. Helenius, *Quality control in the secretory pathway.* Curr. Opinion Cell Biol., 1995. **7**: p. 523-529.
203. Oliver, J.D., et al., *Interaction of the thiol-dependent reductase ERp57 with nascent glycoproteins.* Science, 1997. **275**: p. 86-88.
204. Hughes, E.A. and P. Cresswell, *The thiol oxidoreductase ERp57 is a component of the MHC class I peptide-loading complex.* Curr. Biol., 1998. **8**: p. 709-712.
205. Wiseman, R.L., et al., *An adaptable standard for protein export from the endoplasmic reticulum.* Cell, 2007. **131**(4): p. 809-21.

Chapter Two

Endoplasmic Reticulum Stress in the Absence of Calnexin

A version of this chapter has been published previously in:
Coe, H., Bedard, K., Groenendyk, J., Jung, J. and Michalak, M. (2008). Endoplasmic reticulum stress in the absence of calnexin. *Cell Stress and Chaperones*, **1**:67-71.

Author contributions:
K.B and J.G designed experiments; J.J. designed and performed experiments (Proteasomal Activity Assay, Figure 2-7)

Introduction

The ER is involved in many specialized functions of the cell, including synthesis of membrane and secretory proteins, regulation of protein folding and trafficking, cellular responses to stress and regulation of Ca^{2+} homeostasis. In the ER, there are several chaperones and folding enzymes that associate with newly synthesized proteins to assist with their correct folding and assembly [1]. Calnexin is a 90-kDa type I integral ER transmembrane chaperone which transiently binds newly synthesized monoglucosylated and misfolded glycoproteins, promoting their folding and oligomerization [1]. The protein, together with calreticulin, glucosidases, UGGT and ERp57, is a component of a quality control of the secretory pathway [1]. Calnexin is ubiquitously expressed in all cells containing the ER [1]. Surprisingly, calnexin-deficient mice survive but exhibit severe motor problems, develop ataxic features and growth defects [2] suggesting that expression of calnexin may play an important role during embryogenesis possibly restricted to specific organ or developmental stage.

When protein synthesis/folding is disrupted, leading to accumulation of misfolded proteins, the cell responds by eliciting UPR or ER stress response [3]. This is characterized by up-regulation of the synthesis of chaperone proteins (calreticulin, BiP/GRp78, GRp94), by a decrease in general protein synthesis, and by activation of ERAD [3] [4]. The signalling proteins that mediate UPR response are ER proteins which include ATF6, PERK and IRE1 [3]. They act as proximal sensors of a disturbed ER environment. BiP/GRp78 serves as an important UPR

regulator and under non-stress conditions, it binds to the luminal domains of ATF6, PERK and IRE1 [3]. UPR induces translocation of ATF6 to the Golgi for protease-dependent cleavage, producing a transcription factor involved in the up-regulation of expression of ER chaperones [3]. Activation of PERK/PEK induces phosphorylation of the α subunit of eIF2α to attenuate translation [3]. Finally, activation of IRE1 leads to splicing of mRNA encoding *Xbp1* producing a potent transcription factor which activates the transcription of chaperone encoding genes [3]. In addition, proteins that fail to fold correctly are translocated to the cytoplasm, ubiquitinated and degraded by ERAD [4].

In this study, I investigated activation of the calnexin gene and expression of calnexin during embryonic development as well as impact of calnexin deficiency on UPR. During embryonic development, the calnexin gene was activated in neuronal tissue at early stages of embryogenesis. There was no significant ER stress at the tissue level, suggesting compensatory mechanisms may have been developed to deal with misfolded and aggregated proteins. However, UPR was activated in cultured non-stimulated calnexin-deficient cells. Importantly, $cnx^{-/-}$ cells had increased proteasomal activity, potentially involved in adapting to the acute ER stress observed in the absence of the chaperone.

Materials and Methods

Transgenic Mice - ES cells with a deletion of one allele of the calnexin gene were created by a gene-trap approach, interrupting a coding region of the gene with a cDNA encoding β-galactosidase [5-7]. These cells (designated KST286) were created at BayGenomics [8] and used to generate $cnx^{+/-}$ mice.

ES cells were microinjected into 3.5-d-old C57BL/6J blastocysts to generate chimeric mice. Chimeric males were analyzed for germline transmission by mating with C57BL/6J females, and the progeny were analyzed by PCR, β-galactosidase staining and Western blot analyses. Rabbit anti-calnexin antibody was used at dilution of 1:1,000. *cnx*$^{+/-}$ mice used in this study were indistinguishable from wild-type littermates [5].

Staining of embryos for β-galactosidase activity - For histological analysis, wild-type and *cnx*$^{+/-}$ embryos were harvested, washed in Phosphate-Buffered Saline (PBS) and fixed in 4% paraformaldehyde in PBS, pH 7.2 for 3 hours at 4°C. The embryos were washed in PBS and saturated with 15% sucrose in PBS overnight at 4°C. The embryos were then incubated with 25% optimal cutting temperature compound (OCT, Tissue-Tek)/15% sucrose in PBS for 20-60 minutes, in 50% OCT/25% sucrose in PBS for 20-60 minutes and then in 75% OCT/15% sucrose in PBS for 20-60 minutes. The embryos were frozen in OCT by submersion into methyl butane chilled in liquid nitrogen and cryosectioned. Slides were dried overnight, washed in PBS to remove the OCT and incubated in PBS X-gal (5-Bromo-4-chloro-3-indoyl-β-D-galactopyranoside) staining solution containing 2 mM $MgCl_2$, 0.01% sodium deoxycholate, 0.02% Nonidet-P 40, 20 mM Tris, pH 8.0, 5 mM potassium ferricyanide, 1 mg/ml X-gal (bromo-chloro-indolyl-galactopyranoside) in N,N-dimethylformamide for 1-5 hours at 37°C. The slides were washed in PBS, counterstained with eosin (0.1% eosin in 0.1% acetic acid), washed in 95% ethanol, 100% ethanol, and mounted with Cytoseal (Richard-Allen Scientific).

Western Blot and Cell Culture - Proteins were isolated from mouse tissues by snap freezing the tissues in liquid nitrogen and crushing to a fine powder with a mortar and pestle. The powdered tissue was re-suspended in a buffer containing 50 mM Tris, pH 7.5, 150 mM NaCl, 1 mM EDTA, 1 mM EGTA, 1% Triton X-100, 0.1% SDS, 0.5% sodium deoxycholate with protease inhibitors (0.5 mM PMSF (phenylmethanesulfonylfluoride or phenylmethylsulfonyl fluoride), 0.5 mM benzamidine, 0.05 μg/ml aproprotin, 0.025 μg/ml phosphormidone, 0.05 μg/ml TLCK (1-Chloro-3-tosylamido-7-amino-2-heptanone HCl), 0.05 μg/ml APMSF (4-Amidinophenyl-methanesulfonyl-fluoride), 0.05 μg/ml E-64, 0.025 μg/ml leupeptin and 0.01 μg/ml pepstatin) [9]. Mouse embryonic fibroblasts were isolated from day 12 calnexin-deficient and wild-type embryos. Cells were immortalized as described previously [10] and maintained in Dulbeccos Modified Eagles Medium with 10% fetal bovine serum, 1% Penicillin/Streptomycin and 2.5 ng/ml of Plasmocin. Cells were treated with 2 μg/ml of tunicamycin or 1 μM of thapsigargin for 16 hours. Cells were lysed in a buffer containing in the same lysis buffer used for the powdered tissue (see above) [9], incubated on ice for 10 minutes and spun down at 12,100 x g for 10 minutes. Supernatant containing cellular proteins was collected and proteins were separated by SDS-PAGE. Thirty μg of protein was separated by SDS-PAGE (10% acrylamide) and transferred to nitrocellulose [11]. The nitrocellulose membrane was blocked with 5% milk powder and 0.1% Tween-20 in PBS or Odyssey Blocking Buffer followed by probing with specific antibodies. Antibodies used were: rabbit-anti-calnexin at dilution of 1:1,000, rabbit-anti-PDI at dilution of 1:1,000, goat-anti-calreticulin at dilution of 1:500, rabbit-anti-

ERp57 at a dilution of 1:300, rabbit-anti-GAPDH at a dilution of 1:1,000 (Abcam), mouse-anti-IRE1 at a dilution of 1:500 (a generous gift from Dr. R. Kaufman at the Department of Biological Chemistry, Howard Hughes Medical Institute, University of Michigan Medical Center, Ann Arbor, MI), rabbit-anti-GRp94 at dilution of 1:1000 (StressGen) or rabbit-anti-GRp78 at dilution of 1:1,000 (StressGen). Secondary antibodies used were goat anti-rabbit (1:10,000) and rabbit anti-goat (1:10,000). Blots were analyzed using the Odyssey Infrared Imaging System (Li-Cor) or by ECL reaction [11]

Immunohistochemistry - For immunocytochemistry, calnexin-deficient or wild-type cells were grown on glass coverslips. Cells were fixed with 3.7% formaldehyde in PBS for 15 minutes, permeabilized for 5 minutes in PBS containing 1% saponin and blocked for 1 hour in PBS/1% saponin containing 1% milk powder. Primary antibodies used were rabbit anti-PDI (1:50), rabbit anti-GRp78 (1:50), and rabbit anti-GRp94 (1:50). Secondary antibody was anti-rabbit Alexa Fluor 546 (1:100). The cells were also stained with FITC-Concanavalin A (Sigma). The cells were then mounted onto glass slides and fluorescent signals visualized using an inverted fluorescent microscope.

RT-PCR - Calnexin-deficient and wild-type cells were treated with thapsigargin (1 μM), tunicamycin (2 μg/μl), brefeldin-A (2.5 μM) or castanospermine (5 μg/ml) for 16 hours and total RNA was isolated using TRIzol Reagent (Invitrogen Life Technologies). cDNA was synthesized using M-MLV (Moloney Murine Leukemia Virus) Reverse Transcriptase (Invitrogen) and subsequently amplified with Taq polymerase (Sigma) with specific primers as follows: for Xbp1 forward primer 5'-

CCTTGTGGTTGAGAACCAGG-3′ and reverse primer 5′-CTAGAGGCTTGGTGTATAC-3′; for calnexin forward primer 5′-CATGATGGACATGATGATGACAC-3′ and reverse primer 5′-GGTCTTCAGACTTGCATCTGGC-3′; for GRp78 forward primer 5′-TGGTATTCTCCGAGTGACAGC-3′ and reverse primer 5′-AGTCTTCAATGTCCGCATCC-3′; for GAPDH forward 5′-AACTTTGGCATTGTGGAAGG-3′ and reverse primer 5′-ACACATTGGGGGTAGGAACA-3′; for tubulin forward primer 5′-CCGGACAGTGTGGCAACCAGATCGG-3′ and reverse primer 5′-TGGCCAAAAGGACCTGAGCGAACGG-3′. PCR products were separated on acrylamide gels containing a 7.5% acrylamide (for Xbp1 PCR products) or 1% acrylamide (for calnexin, GRp78, GAPDH and tubulin PCR products). For quantitative analysis, three independent experiments were carried out and intensities of DNA bands were quantified using ImageJ Software.

Cell transfection and luciferase assay - Wild-type and calnexin-deficient cells were transfected with pRL-XFL vector encoding *Renilla* luciferase and *Firefly* luciferase reporter genes as described previously [12]. The cells were co-transfected with pGL3-GRp78-luciferase (*Firefly* luciferase reporter driven by a 311 bp fragment (-304 to +4) of the GRp78 promoter) [13] and with *Renilla* luciferase reporter plasmid pRL-CMV (cytomegalovirus) (Promega) at 1:50 ratio, respectively, using Effectene (Qiagen) with 0.2 μg total DNA. Cells were treated with 1 μM of thapsigargin for 16 hours, lysed, diluted 1:10 in Passive Lysis Buffer (Promega) and then assayed with the Dual-Luciferase Assay Kit (Promega) using a luminometer (Berthold-Lumat LB 9501). Relative light

units (RLUs) were normalized to internal control (pRL-XF) or to *Renilla* luciferase reporter gene under control of CMV promoter (pRL-CMV or pGL3-Xbp1) [12]. Average values ± standard deviation of three independent experiments (n=3) are reported.

Proteasome activity assay - Proteasome activity of cell extracts was measured using 20S Proteasome Activity Assay Kit from Chemicon International. Cells were washed twice with PBS and lysed ($1x10^6$ cells per sample) for 30 minutes on ice in a buffer containing 50 mM Hepes, pH 7.5, 5 mM EDTA, 150 mM NaCl and 1% Triton X-100. Lysates were centrifuged at 14,000 rpm for 15 minutes at 4^oC followed by measurement of fluorescence using 380 nm excitation and 460 nm emission filters in a fluorometer (SPECTRAmax GEMINI XPS).

Results

Developmental activation of the calnexin gene - Calnexin is a ubiquitously expressed ER protein, yet calnexin-deficient mice develop specific motor disorders and neurological problems [2], suggesting an essential role for the protein during neuronal development. I used a transgenic mouse model to investigate expression of calnexin during embryonic development with a special emphasis on the nervous system. First, I generated mice expressing β-galactosidase reporter gene under control of the endogenous calnexin promoter. Second, embryos were harvested at different gestational times, fixed, frozen and stained for β-galactosidase activity. Each embryo was tested for the presence of the β-galactosidase

transgene by PCR, followed by analysis of sections prepared from transgenic and wild-type littermates. Figure 2-1 shows sagittal sections of embryos at different stages of development. At embryonic day 11 (E11.5), there was high activity of the calnexin promoter and relatively uniform β-galactosidase staining throughout the embryo (Figure 2-1A). Interestingly, there was low activity of the calnexin promoter in the E11.5 embryonic liver (Figure 2-1A). As the embryo aged, activation of the calnexin gene became more localized to specific regions. Already at day 12, specific activity of the β-galactosidase reporter was highest in the neuronal tissue and cartilage, while the signal in liver tissue remained distinctively low (Figure 2-1B, E12.5). This pattern became more apparent in later stages of embryogenesis. Figure 2-1C shows that the calnexin gene was highly activated in neuronal tissue, lungs, and cartilage. β-galactosidase activity remained low in the liver, heart, arteries and ganglions (Figure 2-1C, E13.5). At day 15 (Figure 2-1D, E15.5), the calnexin promoter remains highly active in neuronal (brain, spine) and in cartilage tissues. At this stage of embryonic development, no significant staining for β-galactosidase was detected in the heart, liver and smooth muscle (Figure 2-1D). A high level of activation of the calnexin promoter continued in the neuronal tissue and cartilage in the 17 and 18-day-old embryos (Figure 2-1E, F). In the 17-day-old embryo, there was also activation of the calnexin gene in the lungs, kidney, but very little in the liver (Figure 2-1E, E17). At day 18 of embryonic development, the calnexin gene remained highly active in the brain, spine, cartilage and lungs (Figure 2-1F, E18.5). At this stage of embryonic development, there was significant activation of the calnexin gene in the liver (Figure 2-1F, E18.5), while the activity remained

below detection in the heart, intestine and smooth muscle (Figure 2-1F, E18.5). Wild-type control embryos had no staining of β-galactosidase.

Next, I isolated RNA from a variety of mouse tissues at different stages of embryonic development as well as from newborn animals, followed by RT-PCR analysis of expression of calnexin mRNA (Figure 2-2). In agreement with observed β-galactosidase signal, calnexin was highly expressed in brain at all stages of embryonic and postnatal development compared to other tissues (Figure 2-2). At early stages of embryonic development, large quantities of calnexin mRNA were found in the liver and there was no detectable mRNA in the heart, lung and intestine (Figure 2-2, E13.5). Expression of calnexin mRNA increased at later stages of development in the lung, intestine and kidney (Figure 2-2). In the E17.5 embryos, expression of calnexin mRNA in the brain remained high and there was no detectable mRNA signal in the heart, intestine, spleen, kidney and skeletal muscle (Figure 2-2). After birth, a significant level of calnexin mRNA was also detected in the heart and other tested tissues (Figure 2-2). In conclusion, both β-galactosidase reporter gene studies (Figure 2-1) and RT-PCR analysis (Figure 2-2) indicated that throughout embryonic development, the calnexin gene is highly activated in a nervous system, especially in the brain. In order to ensure that the specific activation of the calnexin gene corresponds to the expression at the protein level, protein extracts were isolated from wild type mice and mice embryos and assessed for calnexin expression through western blot analysis (Figure 2-3). At early embryonic stages of mouse development, E.13 (Figure 2-3) calnexin is expressed in all tissues that were able to be differentiated, however, expression varies. Highest expression was

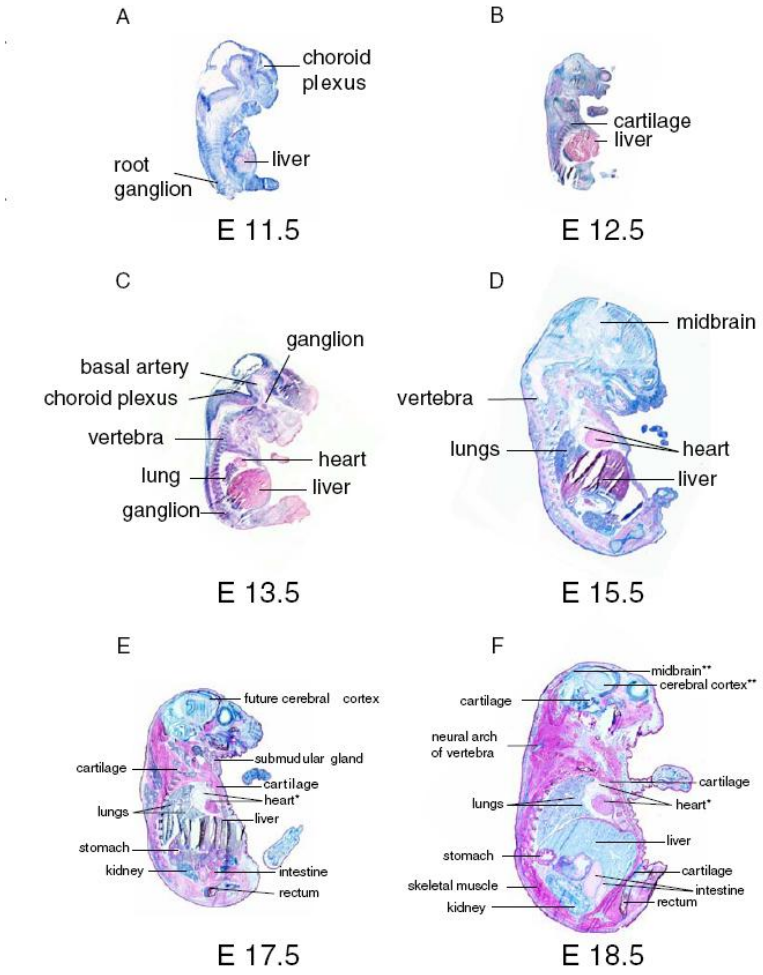

Figure 2-1

Figure 2-1 - Activation of the calnexin gene during embryogenesis. Histological analysis and detection of the β-galactosidase reporter gene activity of *cnx*$^{+/-}$ embryos was carried out as described under "Materials and Methods". ***A***, shows a ubiquitous activation of the calnexin promoter in E11.5 embryos (n=2). As early as E12.5 (n=2) (***B***) and E13.5 (n=2) (***C***) there was activation of the calnexin gene in the brain and cartilage but not in the liver. ***D***, in the E15.5 (n=4) embryo the strongest β-galactosidase signal was observed in the brain and liver but not in the heart. Activation of the calnexin promoter was also seen in the lungs. At embryonic stages E17.5 (n=5) (***E***) and E18.5 (n=2) (***F***) activation of calnexin promoter was most apparent in the brain, lungs, kidney and cartilage tissues. No significant staining was detected in the heart.

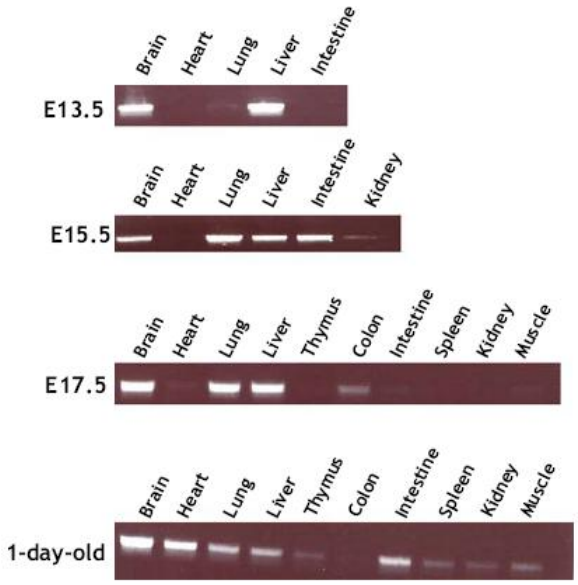

Figure 2-2

Figure 2-2 - RT-PCR analysis of calnexin mRNA in mouse embryonic tissues. RT-PCR analysis was carried out as described under "Materials and Methods". Relatively high level of calnexin mRNA was observed in the brain, lungs and liver at all stages of development tested. Tissues were isolated from greater than one embryo (E13.5 n=6; E15.5 n=3; E17.5 n=3; 1-day-old n=3)

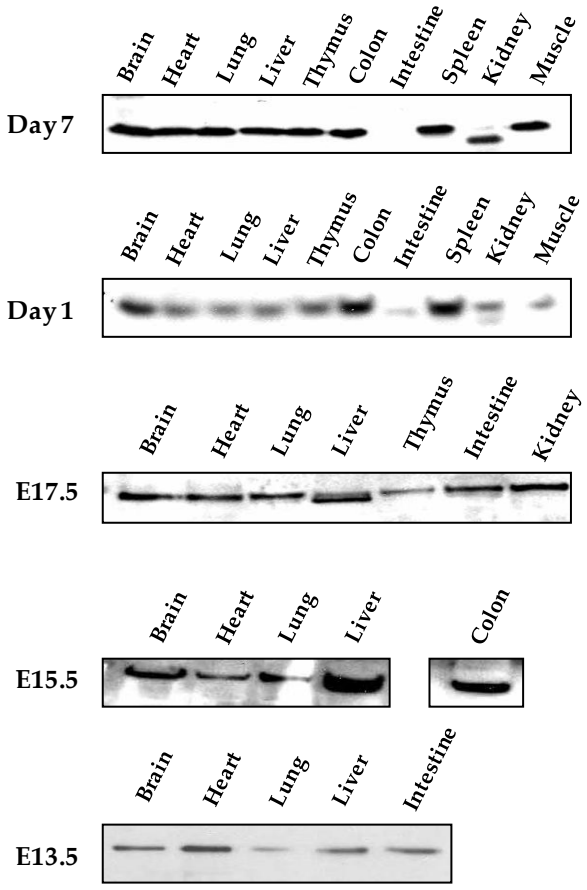

Figure 2-3

Figure 2-3 – Western blot analysis of calnexin expression in mouse embryonic tissues. Western blot analysis was carried out as described under "Materials and Methods". Relatively high level of calnexin protein was observed in the brain and liver at all stages of development tested. Each Western blot is representative from tissues isolated from 3 or more embryos or mice.

observed in the heart, lowest in the lung with brain, liver and intestine falling between highest and lowest and having relatively the same amount of expression. By E.15, expression of calnexin in the brain and liver increase from E.13 and surpass expression in the heart. However, by E.17, more tissues are able to be distinguished revealing a different expression pattern of calnexin. Expression of calnexin is high and similar in brain, heart, lung, intestine and kidney with lover expression observed in the liver and thymus. Although there is apparent discrepancy between β-galactosidase, RT-PCR and protein analysis results, the trend remains the same that there is high activation of the calnexin gene and high expression of calnexin in the brain throughout embryonic development when compared to other tissues

Calnexin-deficient mouse fibroblasts - Calnexin is an important component of the quality control of the secretory pathway involved in folding of newly synthesized (glyco)proteins [14]. It is expected that in the absence of calnexin there might be a build-up of misfolded proteins in the ER and consequently activation of the UPR. To test if the absence of calnexin affects UPR, I isolated mouse fibroblasts from wild-type and *cnx*$^{-/-}$ mice [5]. As expected, Western blot analysis revealed that wild-type cells contained immunoreactive calnexin whereas calnexin-deficient cells did not (Figure 2-4A). Densitometrical analysis revealed that there was approximately a 1-fold increase in the level of GRp94 and ERp57 in *cnx*$^{-/-}$ cells and a slight (0.5-fold) increase in GRp78 (Figure 2-4A). I found no significant difference in the level of expression of calreticulin and PDI in the absence of calnexin (Figure 2-4A). Thus, the lack of calnexin in these cells did not appear to significantly impact expression of other ER folding proteins.

Moreover, the morphological appearance of the wild-type and calnexin-deficient cells was indistinguishable (Figure 2-4B, C). The cells attached firmly to plastic and showed typical, ER-like staining with FITC-ConA, anti-PDI, anti-GRp78 and anti-GRp94 antibodies (Figure 2-4B, C).

ER stress in calnexin-deficient mouse embryonic fibroblasts - Next, I tested if calnexin deficiency led to activation of UPR in cultured cells. In the present study, we examined expression of ER resident stress-sensitive proteins (Figure 2-5A), splicing of Xbp1 (Figure 2-5B and C, 2-6A and B) and activation of the BiP promoter (Figure 2-6A and B) [3]. Upon the accumulation of misfolded proteins, IRE1, an ER, type 1 transmembrane protein, homodimerizes, undergoes trans-autophosphorylation, leading to activation of its cytoplasmic endoribonuclease function [15]. The target of this endoribonuclease is mRNA encoding Xbp1 [3, 15]. I used two ER stress inducers to test for the UPR-dependent expression of ER resident proteins in the absence of calnexin: tunicamycin (Tn), an inhibitor of N-glycosylation, and thapsigargin (Tg), an inhibitor of SERCA, an ER localized Ca^{2+}-ATPase and performed experiments in parallel and in duplicate. Figure 4A shows that both thapsigargin and tunicamycin induced expression of Grp78 (BiP), Grp94, and IRE1 in wild-type and calnexin-deficient cells. Although the same level of ER stress has been detected in non-stimulated, untreated calnexin-deficient cells as indicated by a slight up-regulation of the GRp78 and GRp94 genes, there was still a significant, tunicamycin- or thapsigargin-dependent, up-regulation of UPR in the absence of calnexin (Figure 2-5A).

UPR activation and Xbp1 splicing in calnexin-deficient cells - Next, I examined if activation of IRE1 and splicing of Xbp1 were affected in the absence of

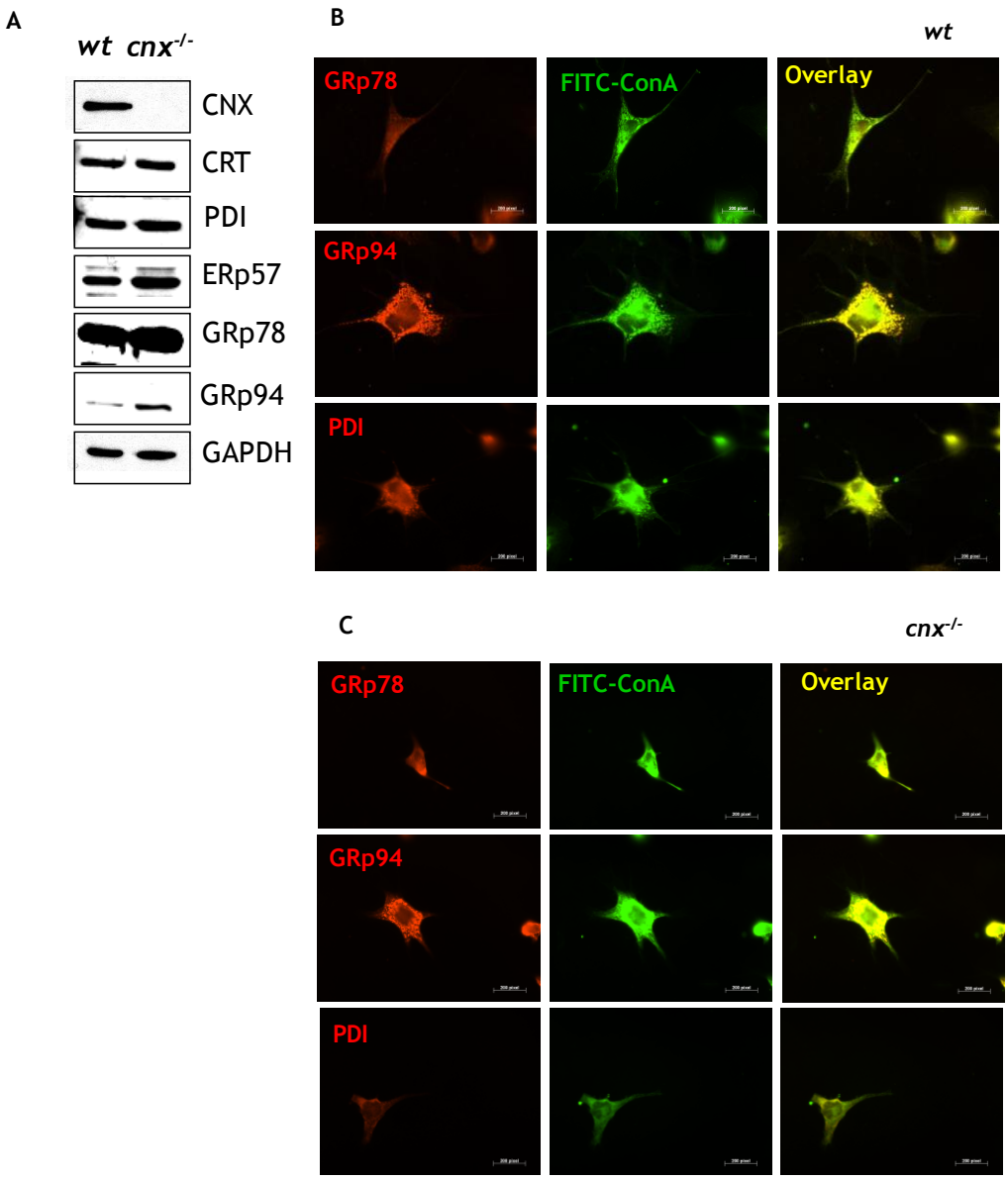

Figure 2-4

Figure 2-4 - Chaperone expression in calnexin-deficient cells. ***A***, Western blot analysis of ER folding factors in wild-type (*wt*) and calnexin-deficient (*cnx*$^{-/-}$) mouse embryonic fibroblasts. Wild-type and calnexin-deficient cells were lysed, proteins were separated by SDS-PAGE, transferred to nitrocellulose membrane, and probed with specific antibodies as indicated in the Figure. ***B*** and ***C***, immunostaining of wild-type and calnexin–deficient cells, respectively, with anti-Grp78, anti-Grp94, anti-PDI antibodies and FITC-ConA.

calnexin. I isolated RNA from mouse embryonic fibroblasts followed by RT-PCR analysis of Xbp1 mRNA. In addition to tunicamycin and thapsigargin, UPR was also induced in wild-type and *cnx*$^{-/-}$ cells with brefeldin-A (BFA), an ER-Golgi transport inhibitor, and castanospermine (Cst), an inhibitor of glucosidase I, thus inhibiting oligosaccharide processing critical for calnexin-substrate interactions [16, 17]. Treatment of cells with these drugs leads to protein accumulation in the ER and to activation of UPR [18]. Figure 2-5B shows that thapsigargin (Tg) or tunicamycin (Tn) treatment of cells strongly induced a rapid and complete splicing of Xbp1 to produce a 424 bp spliced variant. Importantly, both cell lines showed similar sensitivity to thapsigargin- and tunicamycin-induced UPR. However, under the same experimental conditions, brefeldin A and castanospermine induced only a partial splicing of Xbp1 (Figure 2-5C). Most importantly, wild-type cells were more sensitive to brefeldin A- and castanospermine-induced UPR than calnexin-deficient counterparts (Figure 2-5).

In order to quantify Xbp1 splicing, we took advantage of a luciferase reporter system developed by Kaufman's group [12]. Wild-type and *cnx*$^{-/-}$ cells were transfected with pRL-IXFL vector encoding *Renilla* luciferase (internal control) and *Firefly* luciferase reporter gene, which is activated only when the 26-nt intron from Xbp1 is removed in a UPR-dependent manner [12]. To report activation of UPR we also transfected cells with pGL3-GRp78-luciferase vector encoding *Firefly* luciferase under control of the GRp78 promoter containing ERSE element [13]. Figure 2-6 shows that in non-stimulated cells there was a significant difference in UPR activation between *cnx*$^{-/-}$ and wild-type cells as measured by splicing of Xpb1 mRNA

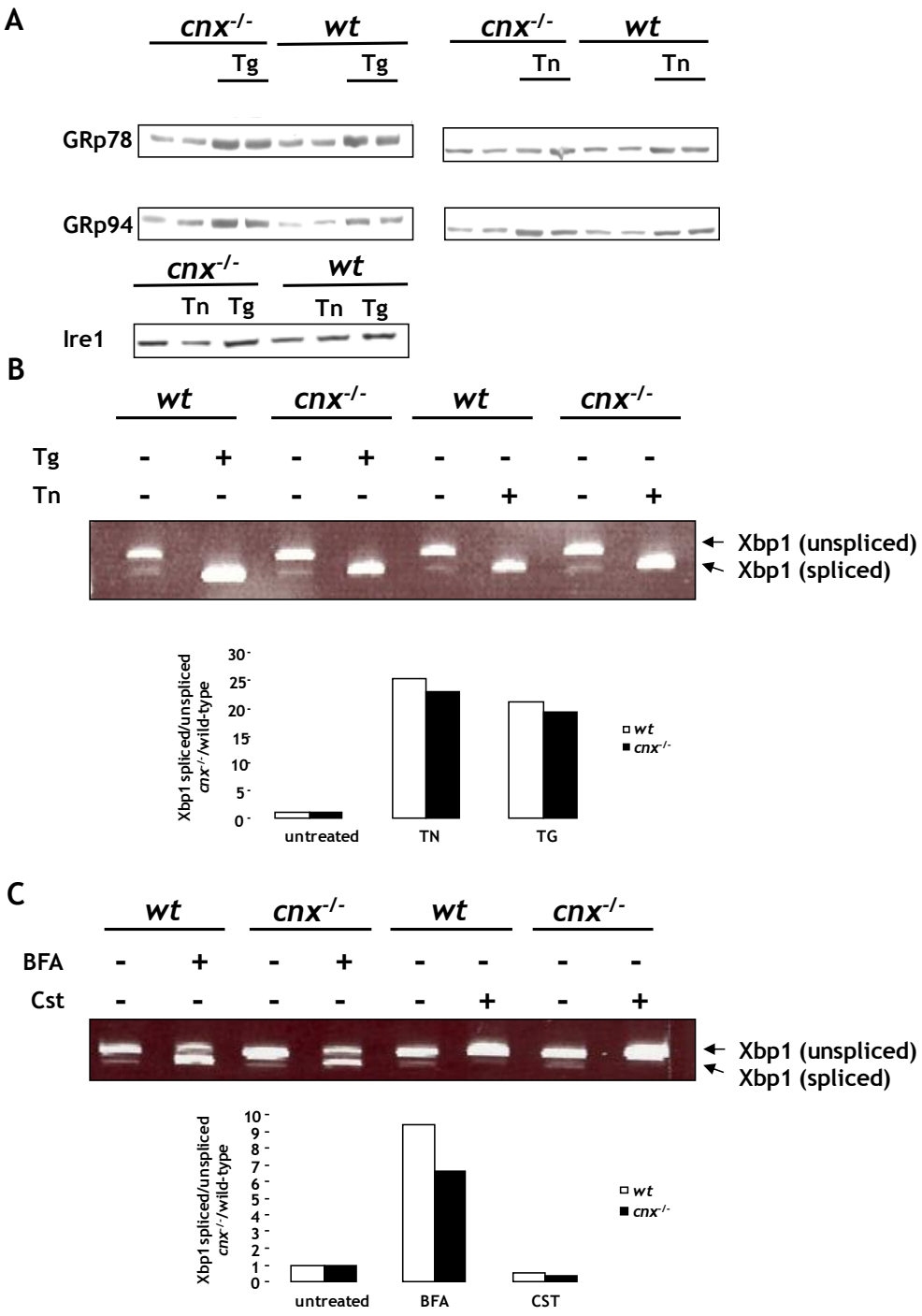

Figure 2-5 (figure legend on following page)

Figure 2-5 - Induction of UPR in calnexin-deficient cells. ***A,*** Western blot analysis of chaperone proteins in wild-type and calnexin-deficient cells treated with tunicamycin (*Tn*) and thapsigargin (*Tg*). Western blot shown represents between 3 and 5 independent experiments. Duplicate samples were analyzed by Western blotting as indicated in the Figure. Densitometry was performed using Kodak Image Software and a one-tail, two sample t-test was done to determine significant difference from untreated control. In wild-type cells treated with Tg, GRp78 increased 80% (p=0.05, n=3), GRp94 increased 139% (p=0.25, n=5) and IRE1 increased 20% (p=0.05, n=3). Wild-type cells treated with Tn, GRp78 increased 53% (p=0.05, n=5), GRp94 increased 153% (p=0.25, n=5) and IRE1 increased 7% (p=0.05, n=4). In calnexin-deficient cells treated with Tg, GRp78 increased 82% (p=0.25, n=4), GRp94 increased 75% (p=0.25, n=4) and IRE1 increased 52% (p=0.05, n=4). In calnexin-deficient cells treated with Tn, GRp78 increased 55% (p=0.05, n=5), GRp94 increased 34% (p=0.05, n=5) and IRE1 increased 3% (p=0.05, n=4). ***B*** and ***C,*** Xbp1 splicing in wild-type and *cnx*$^{-/-}$ cells. Wild-type (*wt*) and calnexin-deficient (*cnx*$^{-/-}$) cells were treated with (***B***) thapsigargin (*Tg*) and tunicamycin (*Tn*) or (***C***) brefeldin-A (*BFA*) and castanosperime (*Cst*) followed by isolation of mRNA and RT-PCR with primers specific for unspliced (*upper DNA band*) and spliced (*lower DNA band*) variant of Xbp1 mRNA. Densitometry was normalized to wt untreated and shown graphically below.

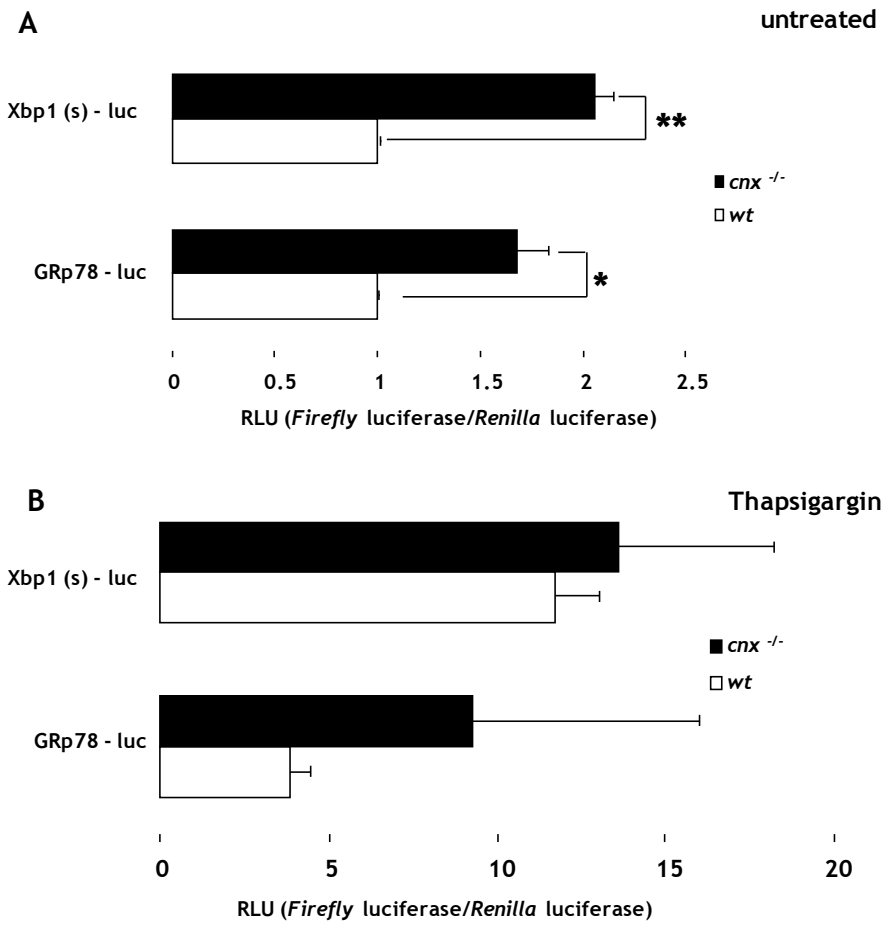

Figure 2-6

Figure 2-6 - Xbp1 splicing and activation of Grp78 promoter in calnexin-deficient cells. *Renilla* luciferase and *Firefly* luciferase activities were measured as described under "Materials and Methods" and the relative ratio of *Firefly* luciferase to *Renilla* luciferase activity in each cell lysates was calculated. ***A***, wild-type (open bars) and *cnx*$^{-/-}$ (black bars) cells were transfected with reporter plasmid for Xbp1 splicing or a plasmid DNA encoding luciferase reported gene under control of GRp78 promoter as described under "Materials and Methods". Cell lysates were assayed for luciferase activity. ***B***, Wild-type (open bars) and calnexin-deficient (black bars) cells were transfected with reporter plasmid for Xbp1 splicing or a plasmid DNA encoding luciferase reporter gene under control of GRp78 promoter as described under "Materials and Methods". Cells were treated with thapsigargin (*Tg*) followed by luciferase assay. Columns and bars represent the mean ±S.D. of nine measurements from three independent transfection experiments. *RLU*, relative light units. One tail, two-sample t-test were performed. * denotes p=0.05, ** denotes p=0.25.

and activation of the GRp78 promoter. There was 2-fold and 1.7-fold higher luciferase activity in *cnx*$^{-/-}$ cells transfected with pRL-IXFL and pGL3-GRp78-luciferase vector, respectively. Thapsigargin treatment significantly enhanced luciferase activity in wild-type and calnexin-deficient cells expressing luciferase reporter genes (Figure 2-6B). Figure 2-5B shows that thapsigargin treatment of wild-type and calnexin-deficient cells resulted in similar levels of activation of luciferase resulting from Xbp1 splicing. However, comparison of the means of wild-type untreated cells to wild-type thapsigargin treated cells revealed that thapsigargin-induced luciferase activity was increased 11-fold, whereas it was induced only 6.6-fold when comparing the means of calnexin-deficient cells that are untreated to calnexin-deficient cells that are treated with thapsigargin. This was likely due to already significantly higher luciferase activity detected in non-stimulated, untreated *cnx*$^{-/-}$ cells (Figure 2-6A). Figure 2-6B also shows that there was similar thapsigargin-dependent activation of the BiP promoter in wild-type and *cnx*$^{-/-}$ cells. By using highly sensitive Xbp1 splicing and Grp78 luciferase promoter vectors, we are able to quantify and more accurately assess small differences that may not be detected by less sensitive Western blot analysis.

Calnexin-deficient cells have increased proteasomal activity - Although calnexin-deficient cells have increased UPR, they have typical growth and survival characteristics observed under standard tissue culture conditions, suggesting they may develop adaptive mechanisms to deal with increased stress [19, 20]. One additional pathway induced by UPR is activation of ERAD and proteasomal activity leading to the removal of misfolded proteins [19-21]. Therefore, I tested if increased proteasomal activity in the

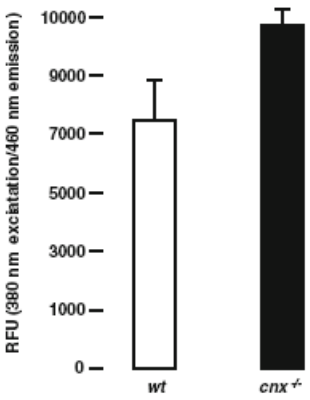

Figure 2-7

Figure 2-7 - Proteasomal activity in calnexin-deficient cells Cellular extracts were prepared from wild-type (open bar) and *cnx*$^{-/-}$ (closed bar) cells and assayed for proteasome using 20S Proteasome Activity Assay Kit from Chemicon International as described under "Materials and Methods". Fluorescence of the fluorophore 7-amino-4-methylcoumarin was measured using 380 nm excitation and 460 nm emission filters. RFU, relative fluorescence units.

absence of calnexin compensated for constitutively active UPR in these cells. Cellular extracts from wild-type and calnexin-deficient cells were prepared and tested for proteasomal activity based on detection of the fluorophore 7-amino-4- methylcoumarin after cleavage from the fluorescently labelled substrate LLVY (Leu-Leu-Val-Tyr) [22]. Figure 2-7 shows that proteasome activity was 3-fold higher in calnexin-deficient cells when compared to wild-type cells. This suggests that increased ERAD may be one mechanism of adaptation to acute ER stress seen in the absence of calnexin.

Neuronal tissue deficient in calnexin does not have increased ER stress - Next, I asked if there is any UPR activation in calnexin-deficient mouse tissues, as this may contribute to a neuronal phenotype of the calnexin-deficient mouse [2]. I examined splicing of Xbp1 in calnexin-deficient spine, brain, cerebellum and liver (Figure 2-8). Thapsigargin-induced UPR in wild-type cells was used as a positive control. Thapsigargin treatment of wild-type cells resulted in rapid and complete splicing of Xbp1 to produce a 424 bp spliced variant (Figure 2-8, *ctrl*). Although there was a different level of expression of Xbp1 in mouse tissues tested, RT-PCR analysis of mRNA showed no detectable splicing of Xbp1 in calnexin-deficient (Figure 2-8, $cnx^{-/-}$) and wild-type (Figure 2-8, *wt*) tissues.

Next, I carried out Western blot analysis of the level of BiP in cerebellum and brain from wild-type and calnexin-deficient animals. In agreement with Xbp1 splicing results, there was no significant increase in BiP expression in calnexin-deficient tissues (Figure 2-9). Collectively, these results indicate that there was no significant activation of UPR in the presence and absence of calnexin in cerebellum, brain, spine and liver.

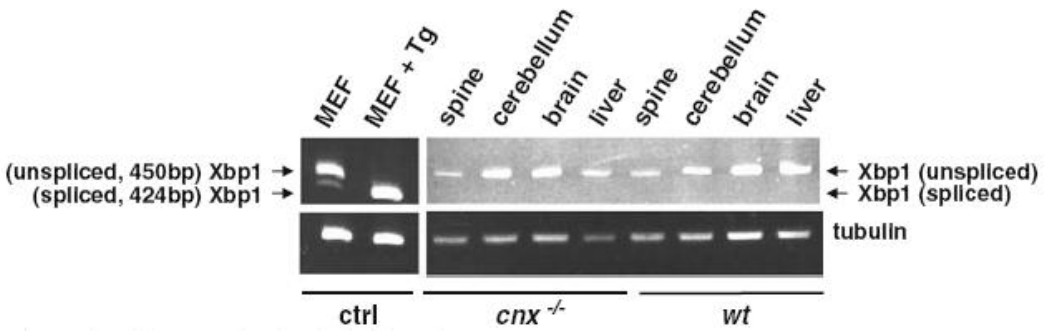

Figure 2-8

Figure 2-8 - Activation of UPR in wild-type and calnexin-deficient tissues. RNA was isolated from tissues derived from wild-type (*wt*) and calnexin-deficient (*cnx*$^{-/-}$) 21-day-old mice followed by RT-PCR analysis for Xbp1 unspliced (450bp) and splice (424bp) variants. Wild-type cells treated with thapsigargin (*Tg*) were used as a positive control (*ctrl*). RT-PCR of tubulin mRNA was used as a loading control. The arrows indicating the location of unspliced and spliced Xbp1 RT-PCR DNA fragment.

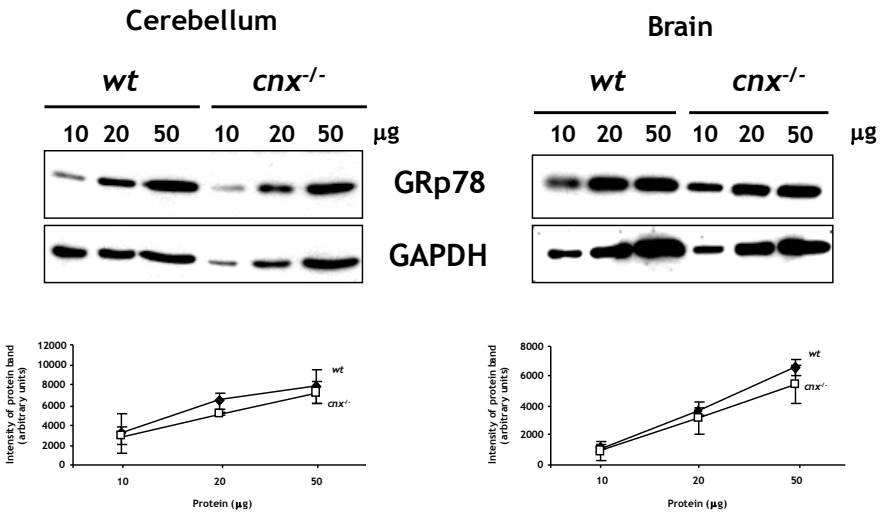

Figure 2-9

Figure 2-9 - Expression of GRp78 protein in wild-type and *cnx*$^{-/-}$ cerebellum and brain. Tissues (n=4) were solubilized in a lysis buffer and proteins were separated by SDS-PAGE as described under "Materials and Methods". Increasing amount of tissue lysates were loaded into SDS-PAGE as indicated in the Figure. Blots were normalized for expression of GAPDH.

Discussion

Despite considerable understanding of the calnexin/calreticulin cycle, virtually nothing is known about the regulation of the calnexin gene and a potential role for the protein in UPR. Here we report, for the first time, on the activation of the calnexin gene during embryonic development in mouse. One of the most striking and unexpected findings is that the calnexin gene is highly active in neuronal and cartilage tissues at relatively early stages of embryogenesis. In contrast, activation of the calnexin gene occurs relatively late in the liver and is undetectable in the heart. Only at the latest stages of embryo development is there activation of the calnexin gene in the liver with little to no activation of the gene in the heart. Neuronal specific activation of the calnexin gene is of great interest because calnexin-deficient mice exhibit motor disorders [2]. In *C. elegans*, calnexin is also highly expressed in the dorsal and ventral nerve cord, and head and tail neurons throughout development [23]. Moreover, in *Drosophila*, calnexin is required for rhodopsin maturation, with mutations in *Drosophila* calnexin leading to severe down-regulation in rhodopsin expression resulting in retinal degeneration [24]. Taken together, these observations indicate that calnexin may play an important role during neuronal development. Our finding that calnexin is highly expressed in the neuronal tissue throughout embryonic development taken together with evidence that calnexin interacts with the myelin protein, PMP22 [25], further stresses the impact calnexin may have on neurogenesis and how in its absence, the neuroprotection function it may serve could be lost, resulting in neuropathology.

Although the chaperones calnexin and calreticulin are homologous proteins with some redundant functions, they yield very different phenotypes in their mouse deficient models. The calreticulin-deficiency is embryonic lethal at day 14 of gestation due to impaired cardiac development [10]. This is not surprising because calreticulin is highly expressed in the heart during early stages of embryonic development [10]. Furthermore, this lethality is rescued by cardiac specific over-expression of calcineurin, suggesting that changes in Ca^{2+} homeostasis, in the absence of calreticulin, play an important role during cardiogenesis [26]. Importantly, calnexin is not expressed in the developing heart (this study) and does not compensate for calreticulin function during cardiogenesis, further supporting the hypothesis that the Ca^{2+} homeostasis role of calreticulin is responsible for impaired cardiac development in calreticulin-deficient mice [10]. In sharp contrast, calnexin-deficient mice survive and exhibit severe motor problems, growth defects and ataxic features, such as an unstable gait [2]. This is not surprising in view of our findings that the calnexin gene is highly activated in neuronal tissue at early stages of embryonic development. Importantly, the drastically different patterns of expression of calreticulin and calnexin during embryonic development as well as phenotypes of calreticulin- and calnexin-deficient mice suggest that the functions of these proteins are not entirely redundant and that calnexin does not have a critical role in life but an important role in quality of life.

The important finding of this study is that *cnx*$^{-/-}$ cells have constitutively active UPR as shown by luciferase reporters. This may represent chronic stress response phenomenon proposed by Kaufman's

group [19, 20]. Yet both wild-type and calnexin-deficient cells have a similar capacity for ER stress induction with commonly used drugs (thapsigargin, tunicamycin) but they differ in UPR levels in non-stimulated cells. This is supported by reporter gene and RT-PCR analyses as well as by Western blot analysis of ER stress proteins including GRp78 and GRp94. Interesting *cnx*$^{-/-}$ cells show up-regulation of ERp57, a protein that has not been associated with ER stress. Relatively high expression of ERp57 in these cells may represent an ER-stress independent adaptive mechanism for cells deficient in calnexin. Increased UPR in *cnx*$^{-/-}$ cells does not appear to have any effect on cell growth, suggesting that *cnx*$^{-/-}$ must have developed adaptive mechanisms for dealing with an increased load of misfolded proteins. Indeed, we show here that calnexin-deficient cells have significantly increased proteasomal activity, indicative of a high activity of ERAD. Therefore, we propose that increased ERAD may represent one mechanism of adaptation to chronic ER stress in the absence of calnexin. Calnexin-deficient cells do not appear to compensate for the loss of calnexin by up-regulating expression of other chaperones. Instead, they modulate specific pathways, including ERAD, to deal with increased load of misfolded proteins.

References

1. Hebert, D.N. and M. Molinari, *In and out of the ER: protein folding, quality control, degradation, and related human diseases.* Physiol. Rev., 2007. **87**(4): p. 1377-1408.
2. Denzel, A., et al., *Early postnatal death and motor disorders in mice congenitally deficient in calnexin expression.* Mol. Cell. Biol., 2002. **22**(21): p. 7398-7404.
3. Zhang, K. and R.J. Kaufman, *Signaling the unfolded protein response from the endoplasmic reticulum.* J Biol Chem, 2004. **279**(25): p. 25935-8.
4. Meusser, B., et al., *ERAD: the long road to destruction.* Nat Cell Biol, 2005. **7**(8): p. 766-72.
5. Kraus, A., et al., *Calnexin deficiency leads to dysmyelination.* J Biol Chem, 2010.
6. Mitchell, K.J., et al., *Functional analysis of secreted and transmembrane proteins critical to mouse development.* Nature Genet., 2001. **28**(3): p. 241-249.
7. Leighton, P.A., et al., *Defining brain wiring patterns and mechanisms through gene trapping in mice.* Nature, 2001. **410**(6825): p. 174-179.
8. BayGenomics, *http://baygenomics.ucsf.edu/*.
9. Milner, R.E., et al., *Calreticulin, and not calsequestrin, is the major calcium binding protein of smooth muscle sarcoplasmic reticulum and liver endoplasmic reticulum.* J. Biol. Chem., 1991. **266**: p. 7155-7165.
10. Mesaeli, N., et al., *Calreticulin is essential for cardiac development.* J. Cell Biol., 1999. **144**: p. 857-868.
11. Nakamura, K., et al., *Changes in endoplasmic reticulum luminal environment affect cell sensitivity to apoptosis.* J. Cell Biol., 2000. **150**: p. 731-740.
12. Back, S.H., et al., *Cytoplasmic IRE1{alpha}-mediated XBP1 mRNA Splicing in the Absence of Nuclear Processing and Endoplasmic Reticulum Stress.* J Biol Chem, 2006. **281**(27): p. 18691-706.
13. Yoshida, H., et al., *Identification of the cis-acting endoplasmic reticulum stress response element responsible for transcriptional induction of mammalian glucose-regulated proteins - Involvement of basic leucine zipper transcription factors.* J. Biol. Chem., 1998. **273**: p. 33741-33749.
14. Williams, D.B., *Beyond lectins: the calnexin/calreticulin chaperone system of the endoplasmic reticulum.* J Cell Sci, 2006. **119**(Pt 4): p. 615-23.
15. Back, S.H., et al., *ER stress signaling by regulated splicing: IRE1/HAC1/XBP1.* Methods, 2005. **35**(4): p. 395-416.
16. Hebert, D.N., B. Foellmer, and A. Helenius, *Calnexin and calreticulin promote folding, delay oligomerization and suppress degradation of influenza hemagglutinin in microsomes.* EMBO J., 1996. **15**: p. 2961-2968.

17. Ivessa, N.E., et al., *The Brefeldin A-induced retrograde transport from the Golgi apparatus to the endoplasmic reticulum depends on calcium sequestered to intracellular stores.* J. Biol. Chem., 1995. **270**: p. 25960-25967.
18. Pahl, H.L. and P.A. Baeuerle, *A novel signal transduction pathway from the endoplasmic reticulum to the nucleus is mediated by transcription factor NF-kB.* EMBO J., 1995. **14**: p. 2580-2588.
19. Rutkowski, D.T., et al., *Adaptation to ER stress is mediated by differential stabilities of pro-survival and pro-apoptotic mRNAs and proteins.* PLoS Biol, 2006. **4**(11): p. e374.
20. Rutkowski, D.T. and R.J. Kaufman, *That which does not kill me makes me stronger: adapting to chronic ER stress.* Trends Biochem. Sci., 2007. **32**(10): p. 469-76.
21. Yoshida, H., et al., *A time-dependent phase shift in the mammalian unfolded protein response.* Dev Cell, 2003. **4**(2): p. 265-71.
22. Meng, L., et al., *Eponemycin exerts its antitumor effect through the inhibition of proteasome function.* Cancer Res, 1999. **59**(12): p. 2798-801.
23. Lee, W., et al., *Caenorhabditis elegans calnexin is N-glycosylated and required for stress response.* Biochem Biophys Res Commun, 2005. **338**(2): p. 1018-30.
24. Rosenbaum, E.E., R.C. Hardie, and N.J. Colley, *Calnexin is essential for rhodopsin maturation, Ca2+ regulation, and photoreceptor cell survival.* Neuron, 2006. **49**(2): p. 229-41.
25. Dickson, K.M., et al., *Association of calnexin with mutant peripheral myelin protein-22 ex vivo: A basis for "gain-of-function" ER diseases.* Proc. Natl. Acad. Sci. U.S.A., 2002. **99**: p. 9852-9857.
26. Guo, L., et al., *Cardiac-specific expression of calcineurin reverses embryonic lethality in calreticulin-deficient mouse.* J. Biol. Chem., 2002. **277**(52): p. 50776-50779.

Chapter Three

ERp57 modulates STAT3 signalling from the lumen of the endoplasmic reticulum

A version of this chapter has been published previously in:

Coe, H., Jung, J., Groenedyk, J., Prins, D. and Michalak, M. (2010). ERp57 modulates STAT3 signalling from the lumen of the endoplasmic reticulum. *The Journal of Biological Chemistry* **285**: 6725–6738.

Coe, H. And Michalak, M (2010). ERp57, a multifunctional endoplasmic reticulum oxidoreductase. *The International Journal of Biochemistry and Cell Biology*. doi:10.1016/j.biocel.2010.01.009

Author contributions:
J.J. designed and performed experiments (Genotype analysis of ERp57-deficient mice, Figure 3-1A,B and Table 3-1; Lentiviral primer design; Fluorescence activated cell sorting (FACs), Figure 3-6D, Figure 3-13B). J.G designed and performed experiments (Subcellular fractionation of cytoplasm and ER membrane, Figure 3-6C; Annexin V-FITC staining, Figure 3-9). D.P. designed and performed experiments (Calcium measurements, Figure 3-7)

Introduction

The ER is involved in many cellular functions including protein synthesis and modification, regulation of Ca^{2+} homeostasis, phospholipid and steroid synthesis and regulation of the response to cellular stress [1-3]. To carry out these diverse functions, the ER is equipped with many chaperone proteins and folding enzymes [3]. For example, calreticulin, calnexin and oxidoreductase ERp57 are components of the folding machinery involved in the quality control of newly synthesized glycoproteins [3]. ERp57 forms complexes with calnexin and calreticulin to assist in chaperone functions to ensure that newly synthesized proteins are correctly folded [3]. Targeted deletion of ERp57 in B cells in mice results in normal B cell development and proliferation as well as antibody production [4]. However, there is aberrant assembly of the peptide loading complex indicating that ERp57 is involved in the assembly of the peptide loading complex and this protein contributes both qualitatively and quantitatively to MHC class I antigen presentation *in vivo* [4]. Interestingly, siRNA studies also demonstrated that ERp57 might be critical for oxidative folding of immunoglobulin heavy chain but not important for peptide loading of class one molecules [5].

Aside from its role as a folding enzyme in quality control in the secretory pathway, ERp57 also known as GRp58 [6-13] has been reported to affect STAT3 signalling via interaction with STAT3 [6, 14-17]. STATs are a family of cytoplasmic proteins with SH2 (Src Homology-2) domains that act as signal messengers and transcription factors as a part of the Janus kinase (JAK)-STAT pathway [18]. In mammals, there are 7 family

members (STAT1-7) and they are differentially activated and phosphorylated to induce transcription of specific genes in response to different cell stresses [19]. These unique factors are able to bypass second messengers and directly communicate signals from the plasma membrane to the nucleus [19].

STAT proteins are a part of the JAK-STAT signalling pathway which mediates the transduction of stress signals from the plasma membrane to the nucleus [18]. There are several modes of activation for STATs [19]. The first is the classical JAK-STAT pathway that is activated in response to cytokines (Figure 3-1A). Initiation of the JAK-STAT pathway begins by cytokine binding to cell surface cytokine receptors [18]. This results in homo- or hetero-dimerization of these receptors resulting in phosphorylation and activation of tyrosine kinase JAK proteins that are associated with the intracellular domain of the receptor [18]. These activated JAK proteins, in turn, *trans*-phosphorylate the intracellular domains of the receptors creating a docking site for the cytosolic STAT proteins via their Src-Homology 2 (SH2) domains [18, 19]. Once in close proximity, activated JAK kinases phosphorylate specific tyrosine residues of the cytoplasmic tail of STATs (Tyr^{705} for STAT3) resulting in homo- or hetero-dimerization of STATs via the phopshotyrosine of one STAT and the SH2 domain of another STAT [18, 19]. The STAT dimers dissociate from the receptors and translocate to the nucleus where they bind specific DNA sequences to activate a number of genes [18]. Some receptors have intrinsic tyrosine kinase activities and can phosphorylate STATs directly [19]. STATs can also be activated through non-receptor associated tyrosine kinases and by proteins that serve as adaptors to bring JAKs into close

proximity [19, 20]. STAT activation is a rapid event with accumulation of phosphorylated STAT1 in the nucleus by 30 minutes with faster dephosphorylation as the half-life of phosphorylated STAT1 is less than 15 minutes [19]. Nuclear import and export of STATs is a dynamic process and, when activated, there is a shift to import resulting in nuclear accumulation of STATs [19].

STAT3 is 770 amino acid residues in length and follows the same functional domain organization as all isoforms of STATs (Figure 3-2) [19]. STATs consist of a N-terminal STAT protein interaction domain, a coiled-coil domain followed by a DNA binding domain, linker domain, SH2 domain and transactivation domain [19]. STAT3 contains a conserved tyrosine (Tyr^{705}) residue to mediate dimerization and serine (Ser^{724}) residue at the C-terminus near the transactivation domain that is also phosphorylated to maximize transcriptional activation [19, 21]. In response to glycoprotein-130 (gp130) ligand binding, STAT3 is phosphorylated at its Tyr^{705} to mediate dimerization through phosphotyrosine and SH2 domains interactions [21]. Dimerized STAT3 translocates to the nucleus and binds DNA consensus sequences such as ISRE/GAS (interferon-gamma activation sequence) to activate and regulate transcription of specific genes [21]. This activation is mediated by the transactivation domain in the C-terminus and is maximized by phosphorylation of the Ser^{724} [21]. Studies have shown that STAT3 recruits co-activators and other transcription factors to its target genes to activate transcription [21]. STAT3 is involved in a wide range of physiological processes including oncogenesis, tumour growth, early embryogenesis, lymphocyte growth, wound healing and postnatal survival [21]. Many of

the target genes are known to regulate cell cycle progression, cell growth and survival and migration [21]. ChIP (chromatin immunoprecipitation) analysis has identified 34 genes regulated by STAT3 which are involved in muscle growth and differentiation [21]. Interestingly, ischemia in the heart results in an increase in interleukin-6 (IL6) cytokine which results in an activation of STAT3 [18]. This increase in STAT3 serves a cardioprotective role and results in a decrease in infarct size after ischemia/reperfusion post-conditioning perhaps through regulation of target genes or control of mitochondrial function [18]. However, persistent activation of STAT3 is also associated with malignant transformation [18]. Therefore, to use activated STAT3 for treatment of cardiovascular disease must be well controlled because of the promiscuity STAT3 has in downstream target genes [18].

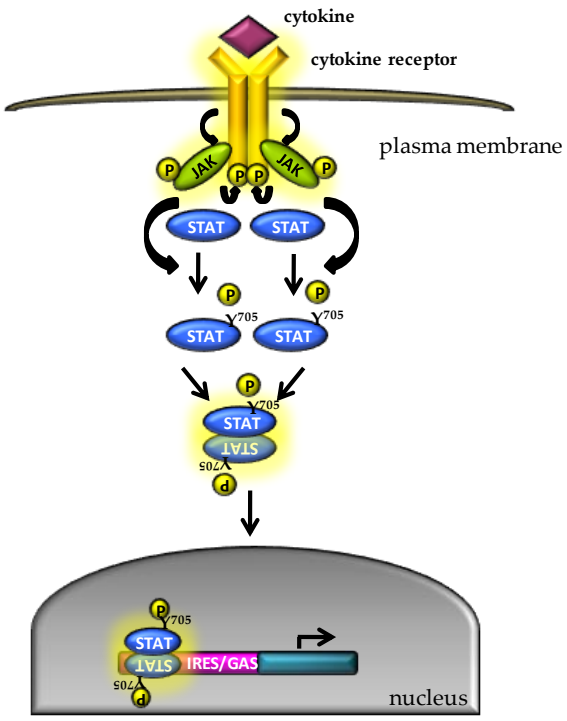

Figure 3-1

Figure 3-1 - The classical STAT3 signalling pathway. Cytokines (*purple diamond*) bind to plasma membrane cytokine receptors (*yellow).* These receptors homo- or hetero-dimerize and activating them to phosphorylate and activate receptor associated JAK proteins. Activated JAK proteins *trans*-phosphorylate intracellular sites on the receptors creating docking sites for STAT3 proteins. Bound STAT3 proteins, are phosphorylated and activated at Tyr705 by JAK kinases. Activated STAT3 proteins dimerize , translocate to the nucleus where they bind ISRE/GAS containing genes to activate transcription. JAK proteins: Janus-kinase tyrosine kinase; STAT3: signal transducer and activator of transcription 3; P: phosphate; ISRE/GAS: inteferon-gmma-activator sequence.

STAT3 has an important role in early embryogenesis so it is not surprising that STAT3-deficient mice are embryonic lethal at embryonic stage 6.5 to 7.5 [22]. It is thought that lethality may be due to nutritional insufficiency as the stage of death coincides with expression of STAT3 in visceral endoderm which is important for nutrient exchange between maternal and embryonic environments [22]. Tissue specific knockout mouse models of STAT3 in T-cells, macrophages/neutrophils, keratinocytes and mammary glands were also created by a Cre-Lox system [23]. Together, these tissue specific knockouts showed a role for STAT3 in the immune response, hair growth and apoptosis [23]. Mice expressing an allele of STAT3 with a substitution of Ser^{724} with alanine were viable however they were severely underweight and died soon after birth [24]. Studies with these mice stress the importance of transcriptional capacity of STAT3 gene regulation [24]. Mice with a cardiac-specific deletion of STAT3 do not show a decrease in infract size after ischemic-preconditioning [25].

Although it is not clear how STAT3 activity is negatively regulated by ER resident ERp57/Grp58 it has been reported that ERp57/Grp58 may sequester the inactive and active STAT3 preventing its interaction with DNA and consequently activation of STAT3-dependent genes [6, 12].

In this study we created ERp57-deficient mice and *ERp57*$^{-/-}$ cell lines. ERp57 deficiency is embryonic lethal at embryonic day (E) 13.5 and ERp57-deficient cells have significantly increased STAT3 activity. We showed that the ER, but not cytosolic, form of ERp57 is responsible for inhibition of STAT3 activity. Furthermore, ERp-57-dependent modulation of STAT3 is enhanced by ER luminal interactions between ERp57 and

calreticulin. Our results suggest that, *in vivo*, ERp57 and STAT3 may not interact and that the observed modulation of STAT3 activity may be due to ERp57-dependent signaling from the ER.

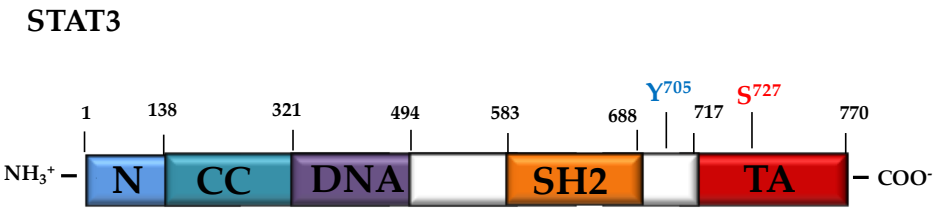

Figure 3-2

Figure 3-2 - A linear representation of the STAT3 protein. Residues separating domains are indicated above. The N-domain (*blue box*) is involved in the dimerization of the protein, the coiled-coiled domain (CC, *turquoise box)* is involved with interactions with other proteins, the DNA-binding domain (*purple box*) binds DNA, the Src-homology 2 domain (SH2, *orange box*) is involved in receptor binding and dimerization and the transactivation domain (TA, *red box)* is involved in the activation of target genes. Amino acid indicated in blue, is a conserved residue that is phosphorylated to dimerize STAT3 proteins, while the amino acid indicated in red is phosphorylated to maximize activation of genes.

Materials and Methods

Generation of ERp57-deficient mice - Gene trapping with the trap vector pGT1TMpfs was used to generate the *Pdia3* gene disrupted embryonic stem cells from the Gene Trap Resource at http://baygenomics.ucsf.edu (BayGenomics, University of San Francisco, San Francisco, California). The *Pdia3* gene encodes ERp57. Parental cell lines (CGR8 and E14Tg2A) were established from delayed blastocysts on gelatinized tissue culture dishes in embryonic stem cell medium containing leukemia inhibitory factor (LIF) [26]. Embryonic stem cells were cultured in a media containing Glasgow minimal essential medium (GMEM), 2 mM glutamine, 1 mM sodium pyruvate, non-essential amino acids, 10% fetal calf serum, β-mercaptoethanol, and 1000 U LIF [27]. Embryonic stem cells were microinjected into 3.5day old C57BL/6J blastocysts to generate chimeric mice [28]. Chimeric males were analyzed for germline transmission by mating with C57BL/6J females, and the progeny was identified by polymerase chain reaction PCR analysis, β-galactosidase staining, and Western blot analysis. All animal experimental procedures were approved by the Animal Welfare Program at the Research Ethics Office, University of Alberta and conformed to relevant regulatory standards.

Genotype analysis of ERp57-deficient mice - Genomic DNA from heterozygous mice (carrying the LacZ gene) was isolated using DNeasy Blood & Tissue kit (Invitrogen). Genomic DNA was purified using a PCR purification kit (Qiagen), and then DNA fragments were ligated using the Rapid DNA Ligation Kit (Boehringer). First PCR amplification was performed using primers specific to inserted vector INVF1, 5′-GTTCCCAACGATCAAGGCGAG-3′ and INVR1-5′

AAGCCATACCAAACGACGAGCG-3′. The product from the PCR reaction was used as a template for second PCR with specific (nested) primers: INVF2 5′- TCAAGGCGAGTTACATGATCCC-3′, and INVR2 5′-CGAGCGTGACACCACGATGC-3′. Products of the inverse PCR-driven amplification were analyze by agarose gel electrophoresis, purified using a gel purification kit (Qiagen) and sequenced. Once the integration site was identified, we designed a protocol for genotyping wild-type, heterozygote and homozygote ERp57-deficient embryos (Figure 2-3). Embryos were harvested at embryonic days 10.5-15.5 followed by the isolation of genomic The following PCR primers were used for genotyping wild-type embryos: forward primer (F2) 5′-GGACAGTTTTGAGCTGCCAT-3′ (hybridizes to the intron within the insertion of the vector site) and reverse primer (R3) 5′-TCTCCATTATCATCGTACTCC-3′ (hybridizes to intron 4 after the vector insertion site). To identify heterozygous embryos the following primers were used: forward primer (F1) 5′-TCAAGGCGAGTTACATGATCCC-3′ (hybridizes to the end of the inserted vector) and reverse primer (R3) 5′-TCTCCATTATCATCGTACTCC-3′.

Histological analysis - Blastocysts were harvested at 3 days post-coitum and whole-mount β-galactosidase staining of blastocysts was performed. Blastocysts were washed with phosphate buffered saline (PBS), fixed in 3.7% paraformaldehyde in PBS for 30 min followed by a wash with PBS. Blastocysts were then incubated for 1 h in freshly prepared staining solution in 10 ml of PBS containing 2 mM $MgCl_2$, 0.01% sodium deoxycholate, 0.02% NP40, 0.1% 5-bromo-4-chloro-3-indoyl-β-D-galactopyraonoside (X-gal) dissolved in dimethylformamide [29].

Photographs of blastocysts were taken using a Nikon Coolpix 995 camera attached to a Nikon eclipse TS100 microscope with a 10x magnification objective. β-galactosidase, hematoxilin and eosin staining of wild-type and *ERp57*$^{+/-}$ embryos was carried out as described previously (page 79-80) [2]. B-galactosidase stained slides were counterstained with eosin (0.1% eosin in 0.1% acetic acid.). Embryos were viewed with the Nikon CoolscanIV.

Cell culture, plasmid DNA, DNA cloning and lentivirus transduction - Mouse embryonic fibroblasts were isolated from day-11 wild-type and ERp57-deficient embryos, immortalized and maintained in culture as described previously [28]. When indicated, cells were treated with 1 μM thapsigargin or 2.5 μM brefeldin A for 16 hours.

cDNAs encoding full-length ERp57 or encoding mature ERp57 with no signal sequence were isolated from a mouse brain cDNA library using Gateway Cloning Technology (Invitrogen). The following forward DNA primers were used for amplification of full length ERp57 and no signal sequence ERp57: 5′-GGGG**ACAAGTTTGTACAAAAAAGCAGGCT**AT*ACCATG*CGCTTCA GCTGCCTAGCT-3′ and 5′-GGGG**ACAAGTTTGTACAAAAAAGCAGGCT**AT*ACCATG*GATGTGTT GGAACTGACGGACGA -3′, respectively. The forward primers contain an *att*B1 recombination site (bold), Kozak sequence for expression in mammalian cells (italics) and gene specific nucleotides (underlined). The same reverse primer was used for the synthesis of cDNAs encoding full-length and no signal sequence ERp57: 5′-

GGGG**ACCACTTTGTACAAGAAAGCTGGGT**CCTAGAGGTCTCTTGTGCCTTCTT-3′. The reverse primer contains an *att*B2 recombination site (bold) and the ERp57 gene specific nucleotides (underlined). Both forward and reverse primers required four guanine residues at the 5′ end. First, a BP clonase reaction was carried out as recommended by the manufacturer to generate entry clone vectors. Recombination reaction was carried out using BP Clonase Enzyme Mix to insert cDNA encoding full-length ERp57 or no signal sequence ERp57 and the promoter EF1α (cellular polypeptide chain elongation factor 1 alpha) into the destination lentiviral vector $2K7_{bsd}$ (containing a blasticidine resistance gene for cell selection). Expression vectors $p2K7ERp57_{ER}$ and $p2K7ERp57_{cyt}$ contained cDNA encoding full-length ERp57 and no-signal sequence ERp57, respectively. Lentiviral transduction techniques were used to generate *ERp57*$^{-/-}$ and wild-type fibroblast-derived cells lines stably expressing recombinant proteins ERp57 or no-signal sequence ERp57 [30]. Protein from bulk cell population was harvested with RIPA buffer containing 50 mM Tris (pH 7.5), 150 mM NaCl, 1 mM EDTA, 1 mM EGTA, 1% Triton X-100, 0.1% SDS, 0.5% sodium deoxycholate and protease inhibitors (0.5 mM phenylmethylsulfonyl fluoride [PMSF], 0.5 mM benzamidine, 0.05 μg/ml aproprotin, 0.025 μg/ml phosphormidone, 0.05 μg/ml Nα-tosyl-Lys-chloromethylketone [TLCK], 0.05 μg/ml 4-amidinophenyl-methanesulfonyl fluoride hydrochloride monohydrate [APMSF], 0.05 μg/ml (2S,3S)-3-(N-{(S)-1-[N-(4-guanidinobutyl)carbamoyl]3-methylbutyl}carbamoyl)oxirane-2-carboxylic acid [E-64], 0.025 μg/ml leupeptin and 0.01 μg/ml pepstatin)[31]. Expression of full-length ER targeted ERp57 and cytoplasmically targeted ERp57 (no signal sequence

ERp57) was monitored by Western blot analysis (page 80-81) [2, 30, 32]. ERp57-deficient cells expressing full-length ERp57 were denoted *ERp57*$^{-/-}$-57$_{ER}$ and cells expressing no signal sequence-cytoplasmic ERp57 were denoted *ERp57*$^{-/-}$-ERp57$_{cyt}$.

SDS-polyacrylamide gel electrophoresis (PAGE) and Western blot analysis - Whole cell lysates from wild-type, *ERp57*$^{-/-}$, *ERp57*$^{-/-}$-57$_{ER}$ and *ERp57*$^{-/-}$-ERp57$_{cyt}$ mouse embryonic fibroblasts were isolated as described previously [2]. Twenty μg of protein was separated by SDS-PAGE (10% acrylamide), transferred to nitrocellulose and probed with specific antibodies [33]. Antibodies used were rabbit-anti-GRp78/BiP at a dilution of 1:1000 (StressGen), rabbit-anti-calnexin at a dilution of 1:1000 (StressGen), goat-anti-calreticulin at a dilution of 1:300, rabbit-anti-ERp57 at a dilution of 1:1000, rabbit-anti-protein disulfide isomerase (PDI) at a dilution of 1:1000, rabbit-anti-ERp41 at a dilution of 1:1000, rabbit-anti-ERp54 at a dilution of 1:1000 and rabbit-anti-β-tubulin at a dilution of 1:1000 [2, 34].

For detection of phosphorylated-STAT3 (Y^{705}-phospho STAT3), *ERp57*$^{-/-}$, *ERp57*$^{-/-}$-57$_{ER}$ and *ERp57*$^{-/-}$-ERp57$_{cyt}$ cells were grown to confluency and treated with 2 mM Na_3VO_4 for 20 minutes prior to harvesting. Cells were washed with PBS containing 4 mM Na_3VO_4 and harvested in RIPA buffer. Thirty μg of protein was separated by SDS-PAGE (10% acrylamide) and transferred to nitrocellulose membrane [33]. The nitrocellulose membrane was washed with 25 ml of TBS buffer containing 20 mM Tris (pH 7.6), and 150 mM NaCl, and blocked for 1 h in TBS containing 5% milk and 0.1% Tween 20. Membranes were probed with

rabbit-anti-phospho-STAT3 (Y^{705}) antibodies (Cell Signaling) or anti-STAT3 (Cell Signaling) at 1:1000 dilutions overnight at 4°C. Secondary antibodies used were goat-anti-rabbit (1:10000 or 1:15000 for anti-phospho-STAT3 antibodies) and rabbit-anti-goat (1:10000 for anti-STAT3 antibodies). Blots were developed using a chemilumenscence system [33].

Reverse transcription (RT)-PCR - Total RNA was isolated from different tissues using TRIzol Reagent (Invitrogen Life Technologies). cDNA was synthesized using M-MLV reverse transcriptase (Invitrogen) and amplified with Taq polymerase (Sigma) using the following primers: for ERp57, forward primer 5′-GGACAGTTTTGAGCTGCCAT-3′ and reverse primer 5′-CTCTCCATTATCATCGTACTCC-3′; for Xbp1, forward primer 5′-CCTTGTGGTTGAGAACCAGG-3′ and reverse primer 5′-CTAGAGGCTTGGTGTATAC-3′; for GRp78, forward primer 5′-TGGTATTCTCCGAGTGACAGC-3′ and reverse primer 5′-AGTCTTCAATGTCCGCATCC-3′; for GAPDH, forward 5′-AACTTTGGCATTGTGGAAGG-3′ and reverse primer 5′-ACACATTGGGGGTAGGAACA-3′; and for STAT3, 5′-AGTCACATGCCACGTTGGTGTTTC-3′ and reverse primer 5′-CGGGCAATTTCCATTGGCTTCTCA -3′.

Immunohistochemistry and electron microscopy - For immunostaining, *ERp57*$^{-/-}$, *ERp57*$^{-/-}$-57_{ER} and *ERp57*$^{-/-}$-$ERp57_{cyt}$ mouse embryonic fibroblasts were grown on glass coverslips. Cells were fixed with 3.7% paraformaldehyde in PBS for 20 min at room temperature [2]. For immunostaining of ERp57, cells were permeablized with 0.1% Triton-X in PBS for 20 min at room temperature and washed twice with PBS. Cells were incubated in PBS

containing 1% bovine serum albumin (BSA) for 30 min at room temperature and then incubated with anti-ERp57 (1:100) in PBS containing 1% BSA for 1h at room temperature. The secondary antibody used was rabbit conjugated-fluorescein isothiocyanate (FITC) at a dilution of 1:100 in PBS containing 1% BSA for 45 min at room temperature [35]. All coverslips were co-stained with Alexa Flour 546-Concanavalin A at a dilution of 1:1000 (Sigma). The coverslips were mounted onto glass slides and fluorescent signals visualized using spinning disk confocal microscopy (WaveFX from Quorum Technologies, Guelph, Canada) set up on an Olympus IX-81 inverted stand (Olympus, Markham, Canada). Images were acquired through a 60X objective (N.A. 1.42) with an EMCCD camera (Hamamatsu, Japan). The fluorescent dyes, FITC and Texas Red, were excited by a 491 nm and a 561 nm laser line, respectively (Spectral Applied Research, Richmond Hill Canada). Z-slices (0.25 μm) were acquired using Volocity (Improvision) through the cells using a peizo z-stage (Applied Scientific Instrumentation, Eugene, USA.)

For electron microscopy analysis, cells were harvested, spun down and fixed at 4^{o}C for 4 hours in a freshly prepared solution containing 2.5% glutaraldehyde and 2% paraformaldehyde in 100 mM cacodylate, pH 7.2 [36]. Samples were processed for electron microscopy and examined with a Hitachi Transmission Electron Microscope H-7000.

Subcellular fractionation of cytoplasm and ER membrane - The cell lines; wild-type, ERp57$^{-/-}$, ERp57$^{-/-}$-ERp57$_{ER}$, ERp57$^{-/-}$-ERp57$_{cyt}$ were grown in three 25 cm plates to confluency. Cells were washed three times with PBS and scraped into 3 mL fractionation buffer composed of 250 mM Sucrose, 20

mM Hepes, 10 mM KCl, 1.5 mM $MgCl_2$, 1 mM EDTA, 1 mM EGTA, 1 mM fresh DTT, 200 μM PMSF, 100 μM benzamidine, and SL inhibitors (0.05 μg/mL aprotinin, 0.025 μg/mL phosphoramidone, 0.05 μg/mL TLCK, 0.1 μg/mL TPCK, 0.05 μg/mL APMSF, 0.05 μg/mL E-64, 0.025 μg/mL leupeptin, and 0.01 μg/mL pepstatin [31]). The cellular solution was incubated on ice for 10 minutes then subjected to 40 strokes with a dounce homogenizer and incubated a further 20 minutes on ice. 100 μL was removed as lysate for SDS-PAGE. The cellular solution was centrifuged at 720xg for 5 minutes at 4°C to remove nuclei, the supernatant removed and recentrifuged at 720xg for 5 minutes at 4°C to remove any remaining nuclei. The supernatant containing cytoplasm, mitochondria and ER membranes was then centrifuged at 10000xg for 10 minutes at 4°C to remove mitochondria, supernatant removed and recentrifuged at 10000xg for 10 minutes at 4°C to remove any remaining mitochondria. The supernatant containing cytoplasm and ER membranes was then subjected to a high speed centrifuge at 100000xg for 1 hour at 4C with the supernatant removed as the cytoplasmic fraction, approximately 3 mL, and the pellet washed with 3 mL of 10 mM Tris, pH 7.2 and centrifuged at 100000xg for 45 minutes at 4C. The pellet was resuspended in 1 mL of RIPA buffer (50 mM Tris, pH 7.2, 150 mM NaCl, 1 mM EDTA, 1 mM EGTA, 1% Tx-100, 0.1% SDS, 0.5% sodium deoxycholate, 200 μM PMSF, 100 μM benzamidine, and SL inhibitors (0.05 μg/mL aprotinin, 0.025 μg/mL phosphoramidone, 0.05 μg/mL TLCK, 0.1 μg/mL TPCK, 0.05 μg/mL APMSF, 0.05 μg/mL E-64, 0.025 μg/mL leupeptin, and 0.01 μg/mL pepstatin [31])) and both cytoplasmic fraction and ER fraction precipitated with ice cold acetone at a ratio of 5:1, incubated at -20°C overnight,

pelleted and washed with 5 mL of 75% EtOH. The protein pellet was dried and resuspended in 500 μL of RIPA buffer and diluted 3:1 with SDS sample buffer and run on SDS-PAGE. Gels were transferred to nitrocellulose and western blotted with rabbit anti-ERp57 antibody at a dilution of 1:1000.

Fluorescence-activated cell sorting (FACs) - Samples were analyzed on BD FACScan single laser flow cytometry (BD Bioscience, San Diego) equipped with 488nm filter. Data was collected from 10 000 cells and analyzed using CellQuest software. Cells at confluency 80-90% were harvested by scraping into PBS, resuspended in 100ul 0.1% of formaldehyde in PBS and incubate for 10 min at RT, next the primary antibody rabbit anti-ERp57 was added at the concentration 1:150 and cells were incubated on ice for 30min. Cell pellets were than washed 3 times with PBS containing 2% FBS (fetal bovine serum) followed by addition of FITC label anti-rabbit (ALEXA Fluor 488 Invitrogen) secondary antibody and incubated on ice for 30 min. Cells were washed 3 times with PBS with FBS and once with PBS alone. Staining with secondary antibodies alone was used as a negative control. All experiments were carried out at least three times. For staining of intracellular proteins cells were permeabilized with 0.05% of NP-40 in PBS for 10 min at RT.

Luciferase reporter gene assay - Generation of *crt*$^{-/-}$, *crt*$^{-/-}$-CRT^{G242A}, and *crt*$^{-/-}$-CRT^{E234R} mouse embryonic fibroblasts was described previously [37]. *ERp57*$^{-/-}$, *ERp57*$^{-/-}$-57$_{ER}$ were transfected with ER stress luciferase reporter vector [pRL-XFL, generous gift from Dr. R.J. Kaufman at the Department of Biological Chemistry, Howard Hughes Medical Institute, University of

Michigan Medical Center, Ann Arbor, MI [38] as described previously (page 83) [2]. Twenty four hours after transfection, cells were treated with thapsigargin (1 μM) or H_2O_2 (50 μM) for 16 hours. *ERp57*$^{-/-}$, *ERp57*$^{-/-}$-57$_{ER}$, *ERp57*$^{-/-}$-ERp57$_{cyt}$, *crt*$^{-/-}$, *crt*$^{-/-}$-CRT, *crt*$^{-/-}$-CRT^{G242A}, and *crt*$^{-/-}$-CRT^{E234R} cells were co-transfected with a luciferase reported gene under control of the STAT3 promoter [pLucTKS3, a kind gift from Dr. J. Jung at the Department of Microbiology and Molecular Genetics, Tumor Virology Division, New England Primate Research Center, Harvard Medical School, Southborough, MA and was described previously [39, 40]] with *Renilla* luciferase reporter at a 50:1 ratio, respectively [2]. After 48 hours cells were harvested, lysed and collected in Passive Lysis Buffer (Promega) followed by measurement of luciferase activity using the Dual-Luciferase Assay Kit (Promega) and a Berthold-Lumat 9507 luminometer [2]. RLUs were normalized to the *Renilla* luciferase under the control of the CMV promoter [2, 38]. Three or 4 independent transfection experiments were carried out equaling 9 or 12 measurements. Two-sample unpaired t-tests were carried out.

Miscellaneous procedures - Protein concentration was measured spectrophotometrically using a Bio-Rad procedure (page 80) [2]. The Annexin V-FITC cell death detection kit (BD Biosciences, San Jose, California) was used for the detection and quantification of apoptosis in *ERp57*$^{-/-}$, *ERp57*$^{-/-}$-57$_{ER}$ mouse embryonic fibroblasts. To induce apoptosis, cells were treated with 1 μM thapsigargin for sixteen hours at 37°C. FACS analysis was performed using a FACScan Instrument (BD Biosciences Inc, San Jose, California). Analysis of labeled cells was determined using the program CellQuest (BD Biosciences Inc. San Jose, California). For Ca^{2+}

fluorescence measurements were carried out using 0.5 μM Fura2-AMc [27]. Cells were treated with 600 nM bradykinin and 300 nM thapsigargin [41]. Each trial was calibrated with 1 μM ionomycin and 4 mM $CaCl_2$ fluorescence was measured at λ_{ex}=340 nm and λ_{ex}=380 nm with λ_{em}=510 nm. Ca^{2+} concentrations were calculated from the fluorescence values.

Results

ERp57 deficiency is embryonic lethal - Figure 1A summarizes the results of the gene trapping strategy used to generate the ERp57-deficient mice. The *Pdia3* gene, which encodes ERp57, was interrupted between intron 4 and 5 (nucleotides 14083-14084) with the pGT1.8TM cassette containing neomycin resistance and β-galactosidase genes (Figure 3-3A). PCR analysis of genomic DNA using the specific sets of primers depicted in the Figure 3-3A allowed for determination of the genotype of mice. Analysis of wild-type mice showed only a 797 base pair (bp) DNA product corresponding to the wild-type allele (Figure 3-3B, primers F1, R3) and no DNA product with primers F2 and R3 (Figure 3-3B). As expected, *ERp57*$^{-/-}$ mice showed a 1800 bp DNA product with primers F2, R3 and no product with primers F1, R3 (Figure 3-3B). PCR-driven amplification of genomic DNA isolated from *ERp57*$^{+/-}$ produced both the 797 bp and the 1800 bp DNA products indicating the presence of one copy of the wild-type allele and one copy of the targeted knock-out allele (Figure 3-3B). Western blot analysis revealed that interruption of both alleles of the ERp57 gene resulted in no detectable expression of ERp57 protein (Figure 3-3C).

Chimeric mice were crossed with wild-type C57BL6 females to generate the first generation of heterozygotes. *ERp57*$^{+/-}$ B6/CD-1 mice were indistinguishable from wild-type animals. *ERp57*$^{+/-}$ males were intercrossed to *ERp57*$^{+/-}$ females to generate homozygote (*ERp57*$^{-/-}$) gene knockout mice. We were unable to obtain any viable *ERp57*$^{-/-}$ pups from this cross. Living embryos were obtained at E13 or earlier (Table 3-1). Analysis of embryos at or after E13.5 showed a deficient number of *ERp57*$^{-/-}$ embryos indicating that a significant fraction of *ERp57*$^{-/-}$ embryos died earlier. We concluded that the ERp57 gene knockout was embryonic lethal and that ERp57 is essential for survival.

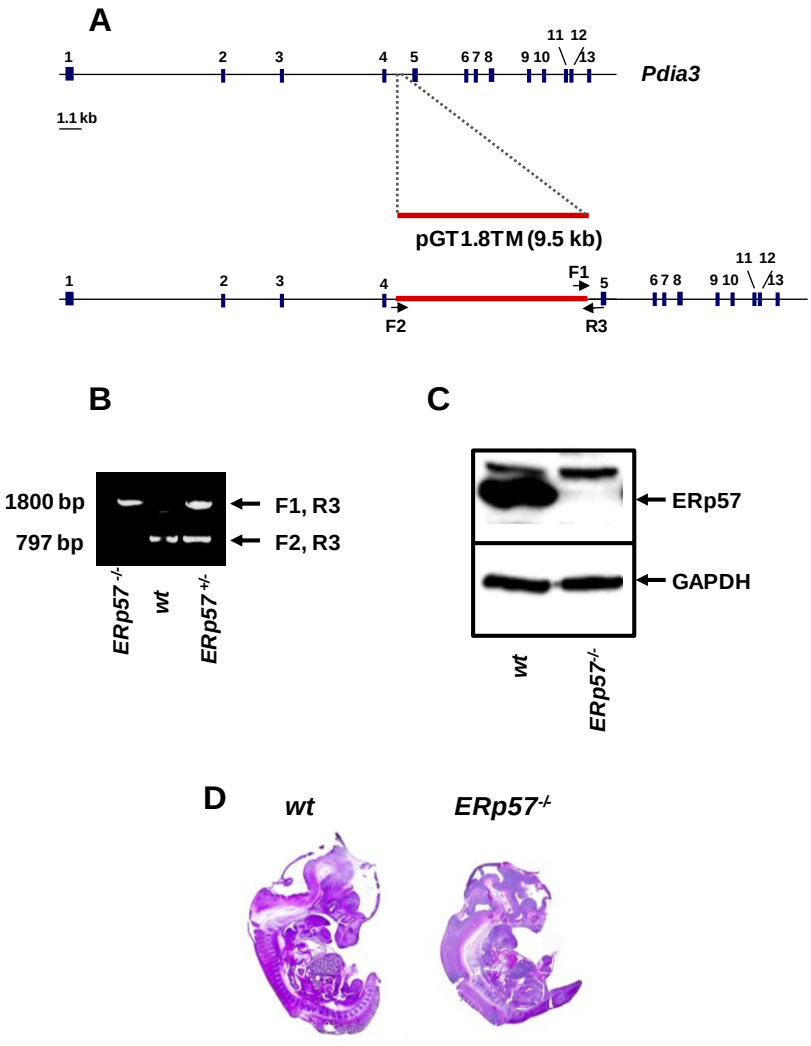

Figure 3-3

Figure 3-3 - Disruption of the ERp57 gene and generation of *ERp57*$^{-/-}$ mice. A. A linear representation of the *Pdia3* gene which encodes ERp57. The gene was interrupted by insertion of the pGT1.8TM vector (red). The location of the F1, F2, R3 DNA primers used for genotyping is indicated in the Figure. Introns are represented as blocks**. B.** PCR analysis of genomic DNA isolated from wild-type (*wt*), heterozygote ERp57$^{+/-}$ and homozygote ERp57$^{-/-}$ embryos. Primers 3R and 1F were used for detection of wild-type alleles and 3R and 2F for mutated allele. **C.** Western blot analysis with anti-ERp57 antibodies (*upper panel*) and anti-glyceraldehyde 3-phosphate dehydrogenase (GAPDH) antibodies (*lower panel*) **D.** Hematoxylin and Eosin staining of embryonic day 12.5 wild-type (*wt*) and ERp57-deficient embryos (*ERp57*$^{-/-}$).

Table 3-1
Genotyping of offspring from ERp57$^{+/-}$ intercross

Age of Mouse	Number of Progeny	ERp57 Genotype		
		+/+	+/-	-/-
E15.5	6	1	5	0
E14.5	5	2	3	0
E13.5	11	3	7	1
E12.5	8	2	5	1
E11.5	15	8	4	3
E10.5	9	2	5	2
Total	54	18	24	7

Developmental activation of the ERp57 gene - Histological analysis of E12.5 *ERp57*$^{-/-}$ embryos revealed that although there were no obvious gross morphological differences between *ERp57*$^{-/-}$ and wild-type embryos, the *ERp57*$^{-/-}$ embryos were markedly smaller than wild-type (Figure 3-3D). To gain additional insight into a potential role of ERp57 during embryonic development, we carried out β-galactosidase reporter gene analysis. The transgenic animals we created in this study were generated by insertion of a gene cassette containing β-galactosidase reporter gene (Figure 3-3A). To quantify transcriptional activation of the ERp57 gene we monitored expression of the β-galactosidase gene to evaluate ERp57 promoter activity in blastocysts and during embryonic development. Figure 3-4A shows high expression and activity of β-galactosidase in blastocysts 3-days post-coitum indicating high expression of ERp57 during the early stages of blastocyst formation. High activation of the ERp57 gene was confined to the inner cell mass (Figure 3-4A, *icm*) with relatively decreased activation of the gene in the blastocoel (Figure 3-4A, *b*) and trophoblast (Figure 3-4A, *t*). Next, *ERp57*$^{+/-}$ and wild-type embryos were harvested at different gestational stages and stained for β-galactosidase activity. Activation of the ERp57 gene, as reported by high activity of β-galactosidase, was observed as early as E13.5 (Figure 3-4B). At E13.5 there was high activation in the lung and vertebra but a relatively low activity of the gene in the liver and the heart (Figure 3-4B). At E15.5 β-galactosidase reporter gene activity was observed most strongly in the lungs with high activation also in the liver, vertebrae and intestine (Figure 3-4C). However, the activity was strikingly absent in the heart, thymus and neurological tissue including the brain (Figure 3-4C). At later stages of

embryonic development (E18.5) the pattern of activation of the ERp57 gene changed. Low activity of the ERp57 promoter was maintained in the heart, thymus and skeletal muscle and high activity was observed in the lungs and liver (Figure 3-4D). At E18.5 we now observe a significant increase in the activation of the ERp57 gene in the brain which was absent in the (Figure 3-4D). This data suggests that ERp57 may play a direct role in embryonic development specifically in lung, liver and vertebrae and, in the later developmental stages in the brain.

Next, we isolated RNA from tissues of wild-type embryos to further assess ERp57 gene activity. At early embryonic stages of embryonic development (E13.5) ERp57 mRNA was found largely in the brain, heart and liver with less expression in the lung and intestine (Figure 3-5). This is in contrast to β-galactosidase staining of the E13.5 embryo which showed low expression of ERp57 in the heart and brain and high expression in the lung (Figure 3-4B). This suggests that although there is high ERp57 mRNA accumulation in the brain, heart and liver there is a relatively low transcriptional activity of the ERp57 gene in those tissues. Similarly, while there were lower amounts of ERp57 mRNA in the lung (Figure 3), there is higher transcriptional activity of ERp57 in this tissue (Figure 3-4B). We observe that in tissues taken from embryos at developmental stage 18.5 (E18.5) that there are abundant amounts of ERp57 mRNA in the brain, lung, liver and kidney and less ERp57 mRNA in the heart, thymus, spleen and intestine (Figure 3-5). This is consistent with the activation of ERp57 in the E18.5 embryo by β-galactosidase staining which showed high activity in the brain, lung and liver and low activity in the heart (Figure 3-4D). At postnatal day 1 there was high ERp57 activation in the brain, lung,

liver and intestine (Figure 3-5). Seven days postnatal, ERp57 mRNA is observed in higher amounts in the brain, liver, thymus and spleen (Figure 3-5). In day 1 postnatal there was no detectable level of ERp57 mRNA in the thymus and in day 7 postnatal there was no detectable level of ERp57 mRNA in the muscle (Figure 3-5). One explanation for this outcome is that mRNA levels of ERp57 in these tissues are too low to detect visually. Taken together, β-galactosidase studies (Figure 3-4) and RT-PCR data (Figure 3-5) showed that ERp57 was expressed throughout embryonic development specifically in the lung and liver and postnatally with high expression particularly in the brain, lungs and liver.

The ER in ERp57-deficient mouse fibroblasts - To determine the effects of ERp57 deficiency on ER functions, we isolated mouse embryonic fibroblasts from ERp57-deficient and wild-type embryos. ERp57-deficient cells were transfected with expression vectors encoding full length, ER-targeted ERp57 or cytoplasm-targeted ERp57 with no signal sequence and were designated ERp57$^{-/-}$-ERp57$_{ER}$ or ERp57$^{-/-}$-ERp57$_{cyt}$, respectively. As expected, Western blot analysis revealed that wild-type, ERp57$^{-/-}$-ERp57$_{ER}$ or ERp57$^{-/-}$-ERp57$_{cyt}$ cells contained immunoreactive ERp57 (Figure 3-6A). Figure 3B shows that wild-type and ERp57$^{-/-}$-57$_{ER}$ cells expressed ERp57 and that the protein was localized to an ER-like network. As expected, ERp57 was localized to the cytoplasmic compartment in ERp57-deficient cells expressing ERp57 without signal sequence (Figure 3-5B, ERp57$^{-/-}$-ERp57$_{cyt}$). Cytoplasmic localization of ERp57 without signal sequence (ERp57$_{cyt}$) was further confirmed by biochemical fractionation of ERp57-deficient cells expressing ERp57 without signal sequence (ERp57$^{-/-}$-ERp57$_{cyt}$) (Figure 3-6C). Finally, we carried out FACS analysis of different

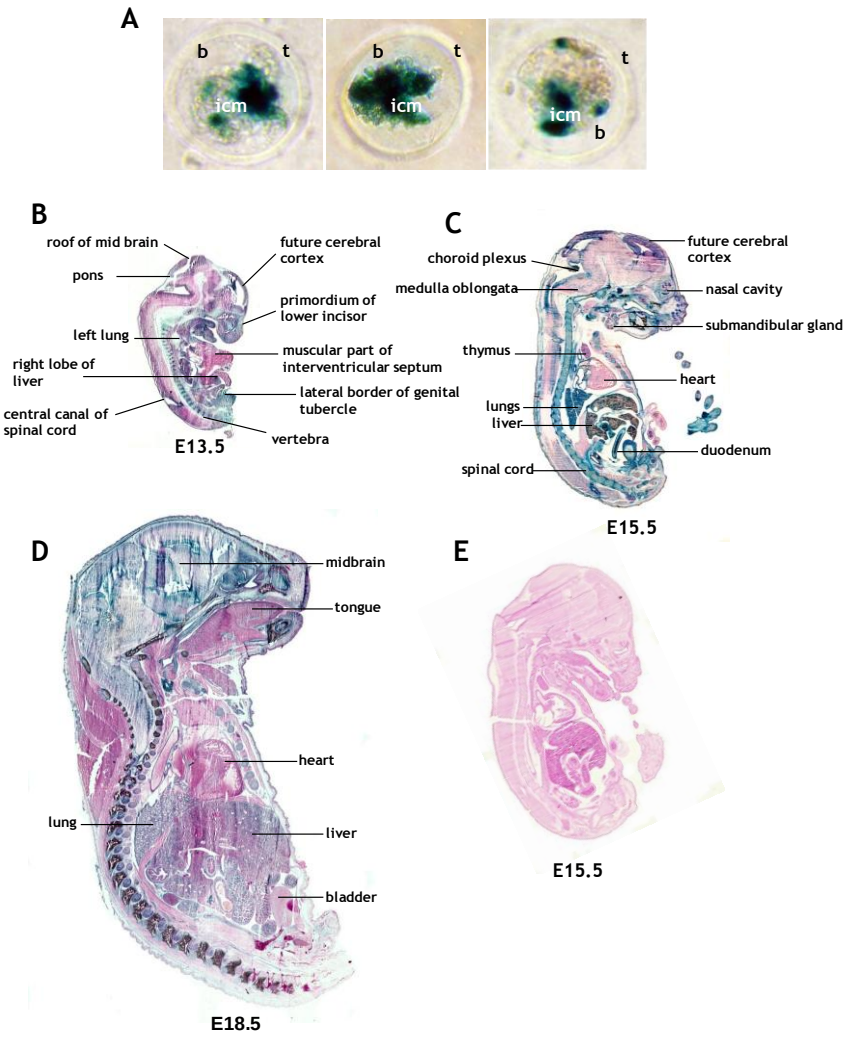

Figure 3-4

Figure 3-4- Activation of the ERp57 promoter during mouse embryogenesis. Expression of the ERp57 gene was detected as β-galactosidase activity from the β-galactosidase reporter gene inserted in the ERp57 gene within the *ERp57*$^{+/-}$ mouse (see Figure 1). **A.** Activation of the ERp57 promoter in mouse blastocysts. High activation of the ERp57 gene was detected in the inner cell mass (*icm*) of the blastocysts but not in the blastocoels (*b*) or the trophoblasts (*t*). **B.** Activation of the ERp57 promoter in lung, liver, and spine but not the heart of E13.5 (n=3) *ERp57*$^{+/-}$ mouse embryos. **C.** High activity of the ERp57 promoter in the lung, liver, gut and spinal cord in an E15.5 (n=3) *ERp57*$^{+/-}$ mouse embryo. **D.** High activity of the ERp57 promoter in the brain, lungs and liver in an E18.5 (n=3) an *ERp57*$^{+/-}$ mouse embryo. **E.** β-galactosidase staining of a wild-type E15.5 control embryo (n=2).

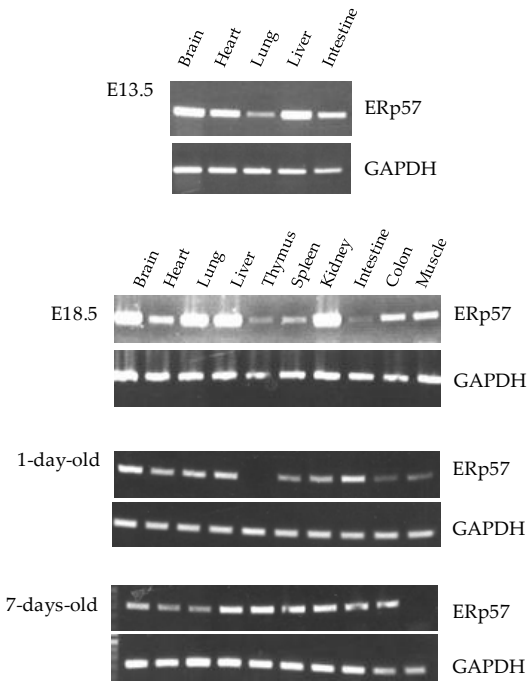

Figure 3-5

Figure 3-5 - Expression of ERp57 mRNA in mouse embryonic and postnatal tissues. RT-PCR analysis was carried out as described under "Materials and Methods." Relatively high levels of ERp57 mRNA were detected in the brain, lungs and liver at all stages of development. At E18.5, there was also high level of ERp57 mRNA in the kidney.(E13.5 n=6; E18.5 n=3; 1-day-old n=3; 7-day-old n=3)

cells lines and showed that there was a small level of immunoreactive ERp57 detected on cell surface of cell lines used in this study (Figure 3-6D).

Morphologically, the ER appeared intact in all cell lines as judged by staining with Texas Red conjugated Concanavalin A and electron microscopy (Figure 3-6B and E). Western blot analysis demonstrated that there was no significant differences in the expression of ER chaperone proteins calreticulin, calnexin, Grp78/BiP, and Grp94 in the absence of ERp57 (Figure 3-6F). Next we examined the impact of the absence of ERp57 on other oxidoreductase folding enzymes family members. Again there was no significant change in expression of PDI and PDI-like family of protein ERp19 in the absence of ERp57 (Figure 3-6F). Slight increase in the level of ERp41 and decrease in the level of ERp54 was seen in the absence of ERp57 (Figure 3-6F). Thus, the absence of ERp57 had no major impact on the expression of other ER chaperones or folding enzymes.

ER Ca^{2+} homeostasis in the absence of ERp57 - The ER is the major Ca^{2+} store of the cell and calreticulin- or Grp94-deficient cells have impaired Ca^{2+} buffering and Ca^{2+} homeostasis [41-48]. We examined, therefore, whether ERp57 deficiency had any effect on ER Ca^{2+} homeostasis. Wild-type, $ERp57^{-/-}$ and $ERp57^{-/-}$-$ERp57_{ER}$ mouse embryonic fibroblasts were stimulated with thapsigargin, an inhibitor of sarcoplasmic/endoplasmic reticulum Ca^{2+} ATPase (SERCA) type Ca^{2+} pumps or with bradykinin, a potent activator of the inositol 1,4,5-trisphosphate ($InsP_3$)-dependent Ca^{2+} release channel located in the ER. When cells were stimulated with bradykinin, the peak amplitude and the duration of enhanced cytoplasmic

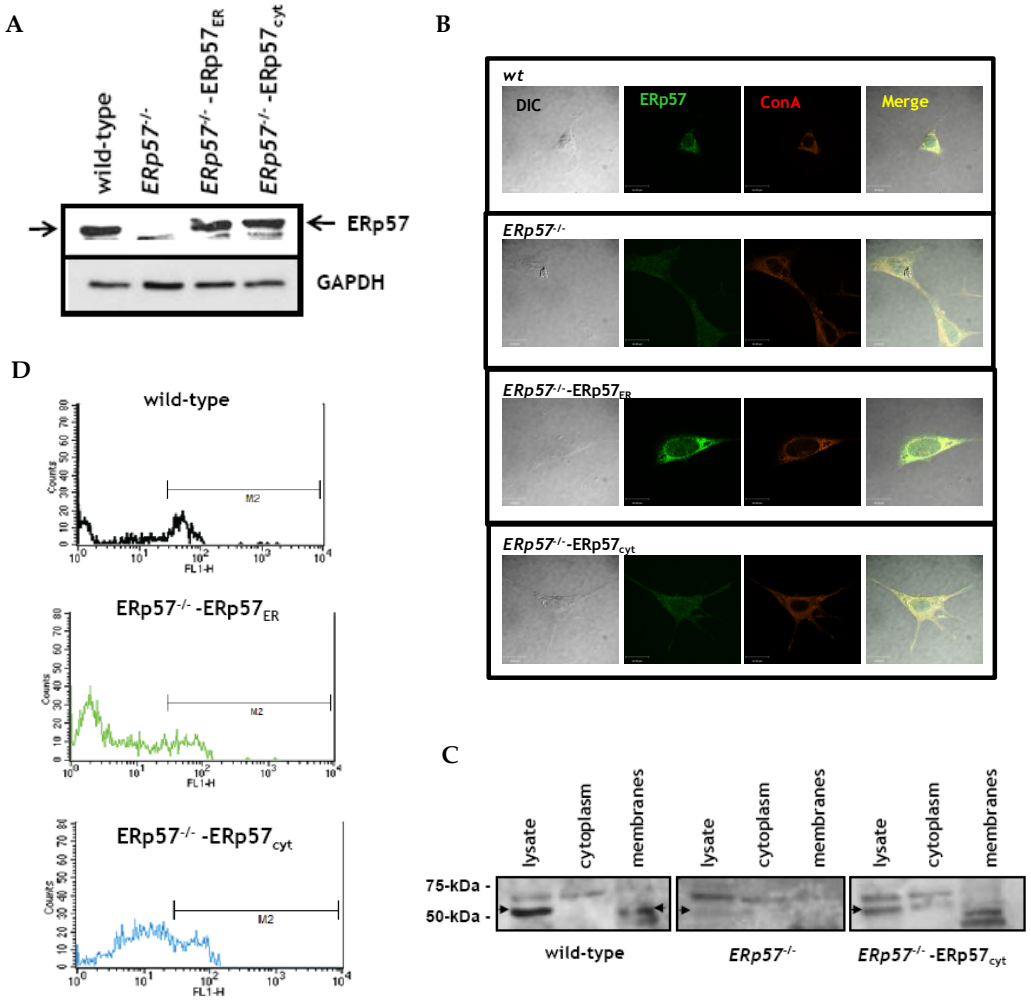

Figure 3-6 continued on the next page

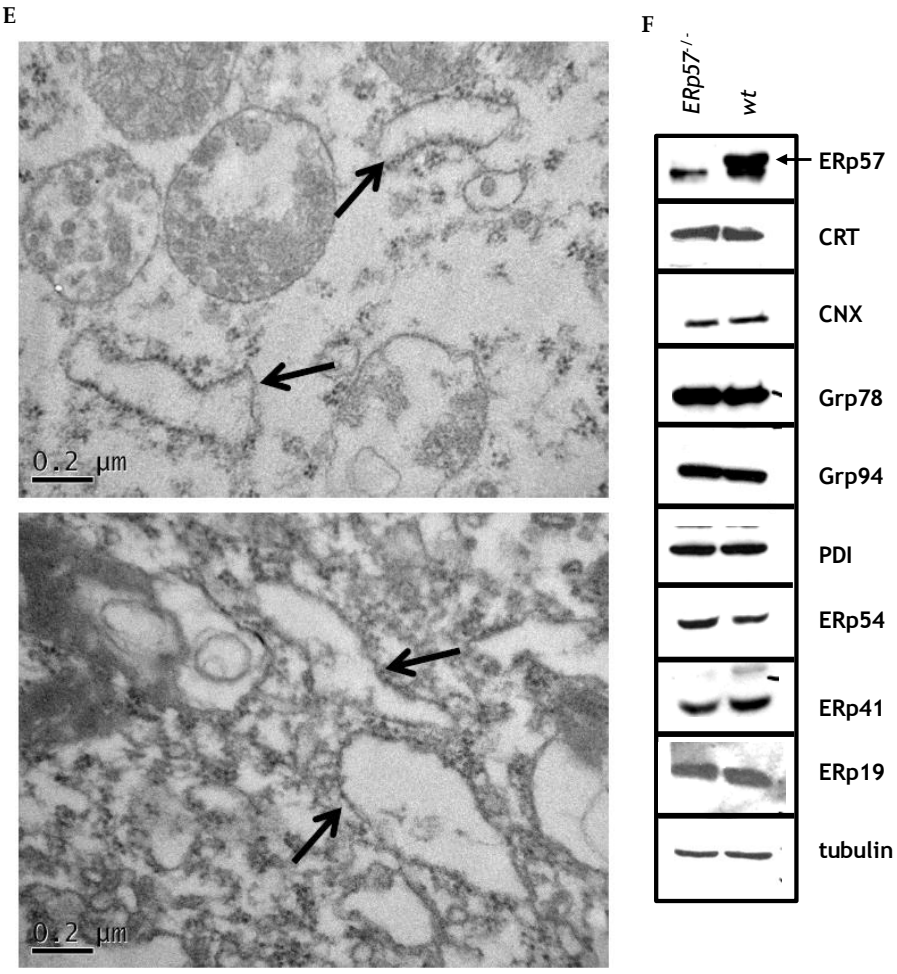

Figure 3-6 continued, legend on next page

Figure 3-6 - Western blot and microscopy analysis of ERp57-deficient cells. A. Western blot analysis of wild-type, ERp57-deficient cells (*ERp57*$^{-/-}$) and *ERp57*$^{-/-}$ cells expressing full length recombinant ERp57 (*ERp57*$^{-/-}$-*ERp57*$_{ER}$) or cytoplasmic-targeted, no signal sequence ERp57 (*ERp57*$^{-/-}$-*ERp57*$_{cyt}$)**.** Blots were probed with rabbit anti-ERp57 antibodies (lower protein band corresponds to a nonspecific immunoreactivity) and anti-GAPDH antibodies. In **B**, Immunostaining of wild-type cells (*wt*), ERp57-deficient cells (*ERp57*$^{-/-}$), ERp57-deficient cells expressing full length, ER targeted recombinant ERp57 (*ERp57*$^{-/-}$-*ERp57*$_{ER}$) and ERp57-deficient cells expressing cytoplasmically targeted recombinant ERp57 (*ERp57*$^{-/-}$-*ERp57*$_{cyt}$). Cells were stained with anti-ERp57 antibodies and with TR-ConA, Texas Red conjugated Concanavalin A. In each panel images represent staining with anti-ERp57 antibodies, ConA staining, phase) contrast and merged images of the cells. Scale bar=16 μm. **C.** Western blot analysis of cell lysate, cytoplasmic and microsomal (containing ER) fraction of wild-type, ERP-57-deficient and ERp57-deficient (*ERp57*$^{-/-}$) cell lines expressing cytoplasmic targeted ERp57 (*ERp57*$^{-/-}$-*ERp57*$_{cyt}$). **D.** Flow cytometry analysis of specific cell lines was carried out with anti-ERP57 antibodies. Wild-type, *ERp57*$^{-/-}{}_{ER}$ and *ERp57*$^{-/-}{}_{Cyt}$ cell lines were used for the analysis. Results are presented as the relative mean fluorescence intensity after subtracting unspecific staining of ERp57$^{-/-}$ cells. M2 represents the gate set on cells stained with antibody **E.** Electron microscopy analysis of wild-type and ERp57-deficient cells. The arrows indicate the location of the ER. Scale bar=16 μm. **F.** Western blot analysis of ER chaperone proteins and oxidoreductases in wild-type (wt) and ERp57-deficient (*ERp57*$^{-/-}$) mouse embryonic fibroblasts. Antibodies used to probe the Western blot are indicated to the left of each panel. Lower protein band in the ERp57 lanes corresponds to a nonspecific immunoreactivity. CNX, calnexin; CRT, calreticulin; PDI, protein disulfide isomerase

Ca^{2+} concentration was comparable in wild-type, ERp57$^{-/-}$ and ERp57$^{-/-}$-ERp57$_{ER}$ cells (Figure 3-7A). In ERp57$^{-/-}$ and ERp57$^{-/-}$-ERp57$_{ER}$ we observed a slight increase in Ca^{2+} concentration in response to thapsigargin when compared to wild-type (Figure 3-7B), suggesting that there might be minor changes in ER Ca^{2+} capacity in the absence of ERp57. This might be due to an ERp57-dependent regulation of SERCA2b activity [49].

The unfolded protein response (UPR) in ERp57-deficient cells - Next, we examined if the absence of ERp57 led to any induction of ER stress and consequently the initiation of the UPR. The UPR was examined by splicing analysis of mRNA encoding X-box binding protein (Xbp1), which is cleaved and activated by ER-stress-activated inositol-requiring enzyme (IRE)-1 [2]. As a control, ER stress was induced using a classical ER stress inducer, thapsigargin [2]. In addition, we induced UPR/ER stress in wild-type and ERp57$^{-/-}$ cells with brefeldin A (BFA), an ER-Golgi trafficking inhibitor [50].

RT-PCR analysis was carried out to test for expression of Grp78/BiP mRNA and splicing of Xbp1, both markers of UPR. Non-stimulated wild-type and ERp57$^{-/-}$ cells did not have an increased level of Grp78/BiP mRNA nor was there any observable splicing of Xbp1 mRNA (Figure 3-8A). As expected, thapsigargin induced complete splicing of Xbp1 (Figure 3-8A, *Xbp1s*) as well as a significant increase in the level of Grp78/BiP mRNA (Figure 3-8A). When wild-type and ERp57$^{-/-}$ cells were treated with BFA, there was incomplete splicing of Xbp1 with both unspliced (Figure 3-8A, *Xbp1us*) and spliced (Figure 3-8A, Xbp1s) forms of Xbp1 mRNA detected. Interestingly, both the level of Grp78/BiP mRNA and the

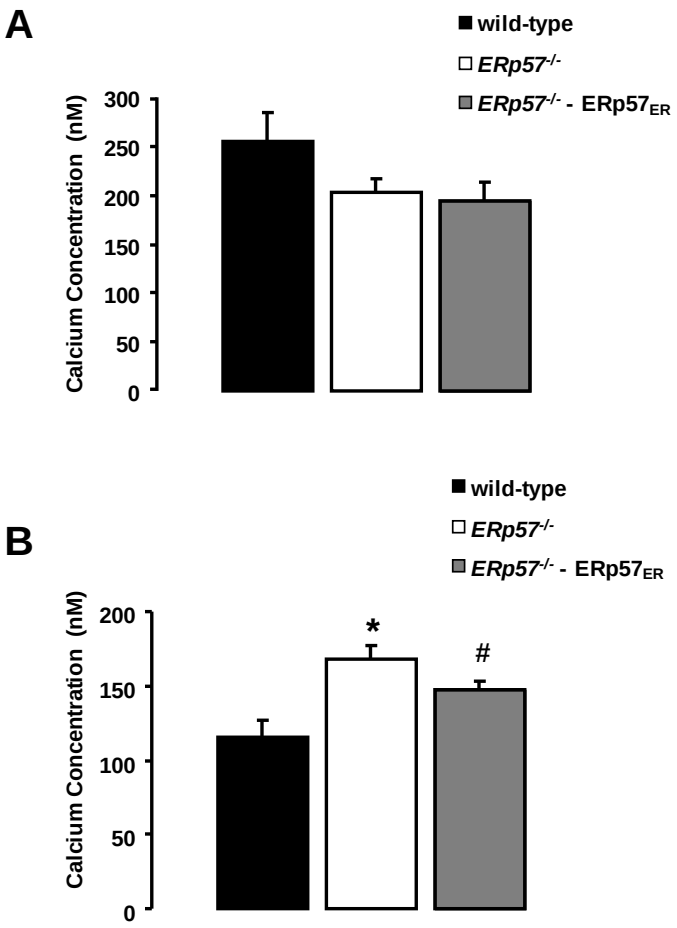

Figure 3-7

Figure 3-7 - Endoplasmic reticulum Ca^{2+} homeostasis in ERp57-deficient cells and cells expressing ER targeted ERp57. Cytoplasmic Ca^{2+} concentration was measured in the wild-type and ERp57-deficient cells as described under "Materials and Methods". **A.** Ca^{2+} released by bradykinin. In the absence of ERp57 (*white bar)* there was a decrease in bradykinin Ca^{2+} release but this not significantly different from wild-type (*black bar*). Bradykinin release is decreased in cells supplied with ER localized ERp57 ($ERp57^{-/-}$-$ERp57_{ER}$; *grey bar)* but this was not significantly different from wild-type cells. Data is presented as the mean ± SD, n=4. **B**. Ca^{2+} released by thapsigargin. In the absence of ERp57 (*$ERp57^{-/-}$*, *white bar*) and in *$ERp57^{-/-}$* cells transfected with expression vector encoding ERp57 (*$ERp57^{-/-}$-$ERp57_{ER}$*; *grey bar)*, there was significantly more Ca^{2+} release. Data is presented as the mean ± SD, n=4. Two-sample, unpaired t-test was performed. #*p*=0.01 vs. wild-type and **p*=0.0065 vs. wild-type.

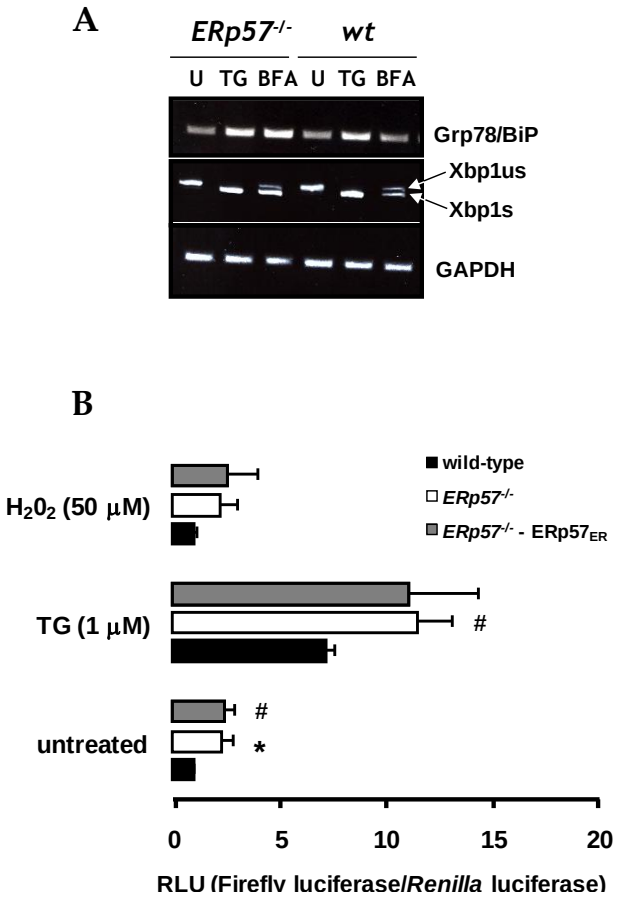

Figure 3-8

Figure 3-8 - Endoplasmic reticulum stress in the absence of ERp57. Endoplasmic reticulum (ER) stress was induced in wild-type and ERp57-deficient cells with thapsigargin (*TG;* 1 μM) or Brefeldin A (*BFA;* 2.5 μM). *U*=untreated. A. RT-PCR analysis of Grp78/BiP mRNA and splicing of Xbp1 mRNA [2]. Spliced (*Xbp1s*) and unspliced (*Xbp1us*) forms of Xbp are indicated with arrows. RT-PCR of GAPDH mRNA was carried out to normalize for loading of agarose gels. B. Quantitative analysis of splicing of the Xbp1 mRNA in wild-type and ERp57-deficient cells (ERp57$^{-/-}$). Cells were transfected with DNA plasmid reporting Xbp1 splicing. ER stress was induced with 1 μM thapsigargin (*TG*) or 50 μM H_2O_2. *Renilla* luciferase and firefly luciferase activities were measured and the relative ratio of firefly luciferase to *Renilla* luciferase activity in each cell lysate is reported. Data are presented as the mean ± SD, n=9. Experiments were performed with two different ERp57-deficient cell lines and data shown represents one of the cell lines. RLU, relative light units. Two-sample, unpaired t-test was performed. #p=0.01 vs. wild-type and *p=0.02 vs. wild-type.

spliced form of Xbp1 were increased in ERp57$^{-/-}$ compared to wild-type cells (Figure 3-8A), indicating that ERp57$^{-/-}$ cells were more sensitive to BFA- ER stress.

Next, we quantified Xbp1 splicing using a luciferase reporter system developed by Kaufman's group [38]. In this system, only the spliced form of the Xbp1 is in frame with the luciferase reporter gene, therefore, high luciferase activity reports splicing of Xbp1 and increased ER stress [38]. Figure 3-8B shows that there was a small but significant increase in the UPR in ERp57$^{-/-}$ cells when compared to wild-type cells (Figure 3-8B) and this was not rescued by expression of the recombinant ERp57 (Figure 3-8B). Thapsigargin treatment significantly enhanced luciferase activity in wild-type, ERp57$^{-/-}$ and ERp57$^{-/-}$-ERp57$_{ER}$ cells (Figure 3-8B). There was an 8-fold increase in UPR activation upon treatment with thapsigargin when compared to non-stimulated counterparts (Figure 3-8B). Although there was a significant increase in ER stress in the absence of ERp57, this did not result in increased apoptosis in ERp57$^{-/-}$ cells (Figure 3-9) indicating that ERp57-deficient cells experienced a tolerable level of ER stress [51]. ERp57 is one of the targets of oxidative stress induced by H_2O_2 [52], therefore, we also used H_2O_2 to induce ER stress in wild-type and ERp57$^{-/-}$ cells. H_2O_2 was not a very potent inducer of ER stress as there was only a slight increase in ER stress in cells treated with H_2O_2 (Figure 3-8C). We concluded that ERp57 deficiency did not have a significant effect on ER morphology; expression of ER associated chaperones and folding enzymes, ER stress, or apoptosis.

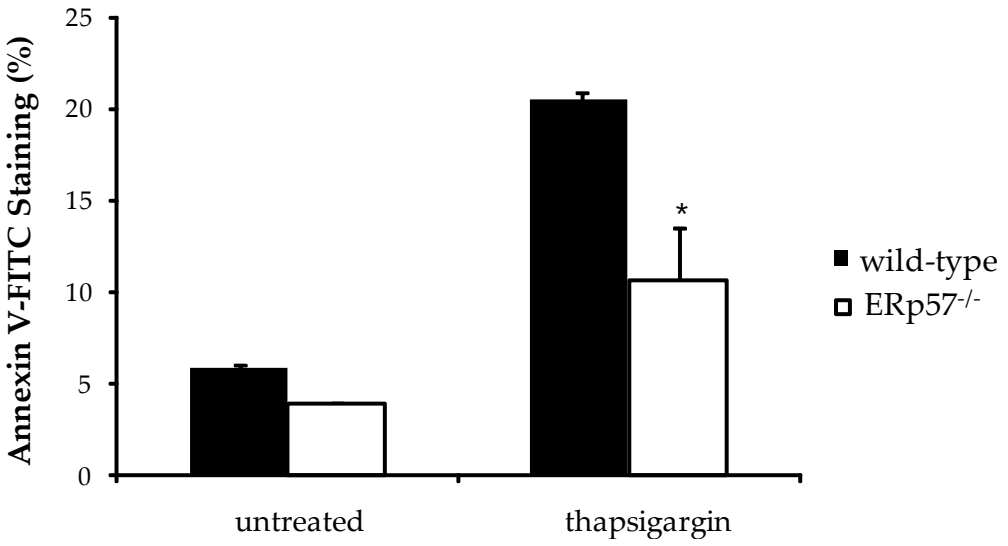

Figure 3-9

Figure 3-9 - Annexin V-FITC staining to detect apoptosis in wild-type (*black bars*) and ERp57-deficient (*open bars)* as described in "Materials and Methods." The percentage of staining is plotted. *Columns* and *bars* represent the mean ±SD of 3 or 4 measurements depending on cell type (wt: n=3;*ERp57*$^{-/-}$:n=4). Two-sample, unpaired t-test were performed. **p*=0.0009 vs thapsigargin treated wt.

STAT3 activation in the absence of ERp57 - Earlier reports indicate that ERp57, in addition to its function as an ER oxidoreductase folding enzyme, may play a role in modulation of STAT3 signalling [6, 15, 53]. It has been proposed that ERp57 forms complexes with both inactive and active STAT3, preventing STAT3 interaction with DNA and consequently leading to inhibition of STAT3-dependent signalling pathway [6, 53]. Therefore we took advantage of ERp57-deficient cells and examined whether the absence of ERp57 affected STAT3 signalling. STAT3 signalling was monitored using RT-PCR, Western blot analyses of inactive and active (phosphorylated-Y^{705}) STAT3, and luciferase activity assay for STAT3 activated promoter.

Figure 3-10A shows that expression of STAT3 mRNA was not affected in the absence of ERp57 ($ERp57^{-/-}$) nor in ERp57-deficient cells transfected with ERp57 expression vector encoding ERp57 localized to the ER ($ERp57^{-/-}$-$ERp57_{ER}$). Tubulin expression was measured as a control. However, Western blot analysis showed increased levels of STAT3 protein and phospho-STAT3 (Y^{705}) (Figure 3-10B). The level of phospho-STAT3 was not changed in $ERp57^{-/-}$-$ERp57_{ER}$ or $ERp57^{-/-}$-$ERp57_{cyt}$ suggesting that ERp57 may not affect the phosphorylation status of STAT3 (Figure 3-10B). To quantify STAT3 activation we used plucTKS3 plasmid DNA containing firefly luciferase reporter gene under the control of STAT3 binding sites [39]. Since ERp57 has been shown to inhibit STAT3 activity, we expected that STAT3-dependent activation of the promoter would result in high activity of luciferase in the absence of ERp57. Wild-type, $ERp57^{-/-}$, ERp57-deficient cells expression ER target ERp57 ($ERp57^{-/-}$-$ERp57_{ER}$), cytoplasm target ERp57 (no N-terminal signal sequence, $ERp57^{-/-}$-$ERp57_{cyt}$) and green

fluorescent protein (GFP) control were transfected with luciferase reporter plasmid followed by analysis of luciferase activity. In non-stimulated ERp57$^{-/-}$ cells, there was 2-fold increase in STAT3 activation (Figure 3-10C) indicating that there was a link between ERp57 and STAT3 activity. Since STAT3 is a cytoplasmic/nuclear transcription factor found in the cytoplasm, for ERp57 to interact directly with STAT3 to form functional complexes, ERp57 would have to be also present in the cytoplasm. ERp57 is a promiscuous protein and is found in the ER as well as the cytoplasm and nucleus [54]. There are number of possibilities as to how ERp57 could inhibit STAT3 signalling and some of these are outlined in Figure 3-11. In order to investigate this further, we tested if the ER targeted or cytoplasm targeted ERp57 was effective in modulation of STAT3 signalling. High activity of STAT3 in ERp57$^{-/-}$ cells was partially rescued in ERp57-deficient cells expressing ER targeted ERp57 (Figure 3-10C, ERp57$^{-/-}$-ERp57$_{ER}$) but not in ERp57$^{-/-}$ cells expressing cytoplasm targeted protein (Figure 3-10C, *ERp57$^{-/-}$-ERp57$_{cyt}$*). As expected, expression of the recombinant GFP in ERp57-deficient cells did not have any effect on STAT3 transcriptional activity. Figure 3-6D shows that there was a detectable level of immunoreactive ERp57 at the cell surface. However, we do not believe that this small fraction of ERp57 contributes to the modulation of STAT3 transcriptional activity since addition of purified ERp57 to cell cultures did not affect STAT3 transcriptional activity in the ERp57-deficient cells (Figure 3-12). We concluded that the ER targeted ERp57 was the most effective in influencing STAT3 signalling, suggesting that ERp57 modulates STAT3 activity from the lumen of the ER.

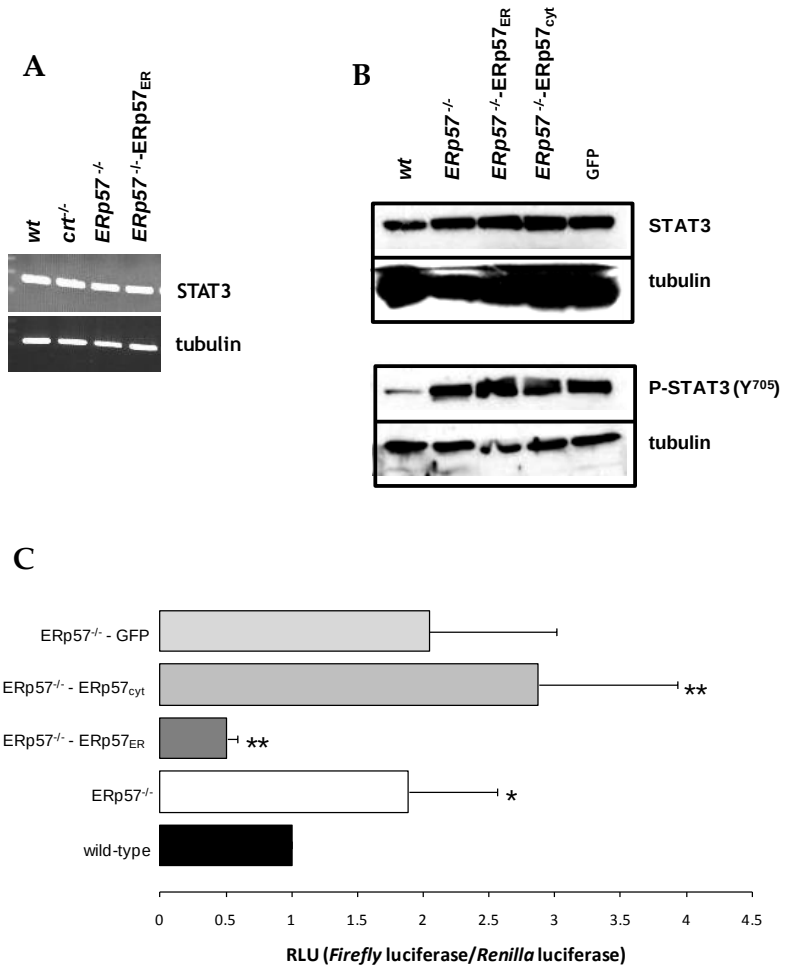

Figure 3-10

Figure 3-10 - STAT3 expression and activity in the absence of ERp57. A. RT-PCR analysis of the STAT3 mRNA in wild-type (*wt*), calreticulin deletion (*crt*$^{-/-}$), *ERp57*$^{-/-}$-ERp57$_{ER}$ and *ERp57*$^{-/-}$-ERp57$_{cys}$. **B.** Western blot analysis of STAT3 (*inactive*) and phosphorylated (Y^{705}) STAT3 (*active*) in wild-type (*wt*), *ERp57*$^{-/-}$-ERp57$_{ER}$, and *ERp57*$^{-/-}$-ERp57$_{cys}$ cells. **C.** STAT3 activity in wild-type (*wt*), *ERp57*$^{-/-}$-ERp57$_{ER}$ and *ERp57*$^{-/-}$-ERp57$_{cys}$ expressing cells. *ERp57*$^{-/-}$-GFP expressing cells were used a control. Cells were transfected with a plasmid containing the luciferase reporter gene under control of the STAT3 activated promoter. *Renilla* luciferase and firefly luciferase activities were measured as described under "Materials and Methods," and the relative ratio of firefly luciferase to *Renilla* luciferase activity in each cell lysate is presented. Data are the mean ± SD. (wild-type, n=27; *ERp57*$^{-/-}$, n=21, *ERp57*$^{-/-}$-ERp57$_{ER}$ n=12; *ERp57*$^{-/-}$-ERp57$_{cys}$ n=12; and *ERp57*$^{-/-}$+GFP n=9.) *RLU,* relative light units. Two-sample, unpaired t-test was performed. *p=0.0013 vs. wild-type and #p=0.0001 vs. wild-type. **p=.0031 vs. *ERp57*$^{-/-}$-ERp57$_{ER}$.

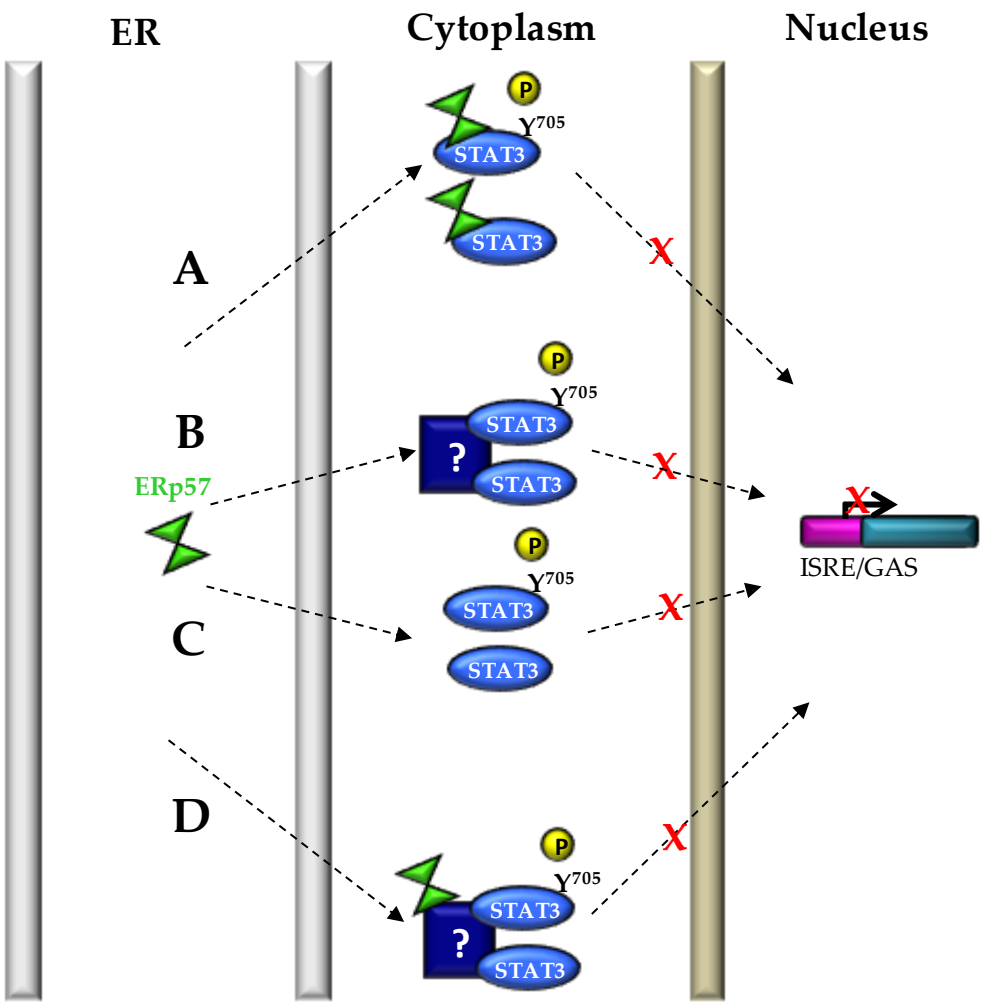

Figure 3-11

Figure 3-11 – A model of how ERp57 might affect STAT3 signalling. ERp57, forms complexes in the ER with CRT and CNX for quality control, but **A.** leaves the ER to the cytoplasm and sequesters both active (P-STAT3) and inactive (STAT3) to inhibit signalling **B.** signals from the ER to an unknown molecule (*blue square*) which binds active and inactive STAT3 to inhibit signalling **C.** signals directly to active and inactive STAT3 to inhibit signalling **D.** leaves the ER and, with an unknown molecule, binds active and inactive STAT3 to inhibit signalling. CRT: calreticulin; CNX: calnexin; ISRE/GAS: interferon-gamma activation sequence.

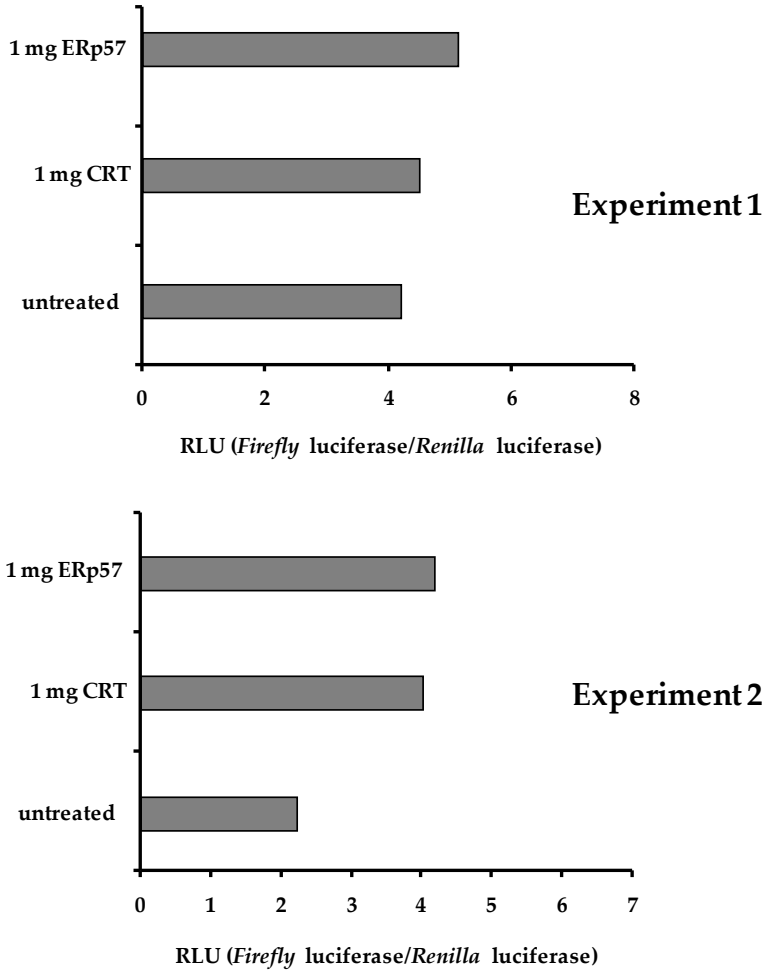

Figure 3-12

Figure 3-12 - Exogenous ERp57 and calreticulin do not affect STAT3 transcriptional activity. STAT3 activity in ERp57-deficient cells was measured using luciferase reported gene under control of STAT3 binding sites. Cells were incubated with *E. coli* expressed and purified ERp57 or calreticulin followed by measurement of *Renilla* luciferase and firefly luciferase activities as described under "Materials and Methods". The relative ratio of firefly luciferase to *Renilla* luciferase activity in each cell lysate is presented. Results of two independent experiments are presented.

Calreticulin enhances ERp57 modulation of STAT3 signalling - ERp57 forms functional complexes with calreticulin to assist in folding and posttranslational modification of newly synthesized proteins [3]. We asked whether calreticulin may influence ERp57-dependent STAT3 activity. To do this we employed *crt*$^{-/-}$ cells lines expressing wild-type calreticulin or calreticulin mutants defective in binding ERp57 [37]. In this study we used a loss of ERp57 binding calreticulin-E^{239}R mutant and a calreticulin-G^{242}A mutant that has no loss in ERp57 binding [37]. Immunostaining for ERp57 showed that these cell lines (*crt-/-*, *crt*$^{-/-}$*-CRT*, *crt*$^{-/-}$*-CRT*^{G242A} and *crt*$^{-/-}$*-CRT*^{E239R}*)* have ERp57 protein localized to the ER (Figure 3-13, A). Concanavalin A staining of these cells also show that the ER is morphologically intact (Figure 3-13, A). We also carried out FACS analysis of different cells lines and showed, like the ERp57 cell lines (Figure 3-6D), that there was a small level of immunoreactive ERp57 detected on cell surface of cell lines used in this study which was determined by subtracting ERp57 staining of *ERp57*$^{-/-}$ cells lines from all other cells lines (Figure 3-13B). Western blot analysis showed that STAT3 or phospho-STAT3 (Y^{706}) expression was not affected by expression of calreticulin or calreticulin mutants in *crt*$^{-/-}$ cells (Figure 3-14A). Surprisingly, quantitative analysis of STAT3 activity using luciferase reporter gene system showed high activity of STAT3 in *crt*$^{-/-}$ cells compared to wild-type counterparts (Figure 3-14B), indicating that calreticulin may also affect STAT3 signalling. Figure 3-14B shows that STAT3 was not affected in the absence of calnexin, a homologue of calreticulin. Expression of wild-type calreticulin (Figure 3-14B, *crt*$^{-/-}$*-CRT*) or a calreticulin mutant interacting with ERp57 (Gly^{242}Ala) (Figure 3-14B,

crt$^{-/-}$-*CRT*^{G242A}) resulted in full recovery of STAT3 activity back to the level observed in wild-type cells (Figure 3-14B, *wt*). In contrast, expression of calreticulin mutant with a loss of ERp57 binding (Glu^{239}Arg) had no effect on STAT3 activity (Figure 3-14B, *crt*$^{-/-}$-*CRT*^{E239R}), which remained high and at the same level as observed in calreticulin deficient cells (Figure 3-14B, *crt*$^{-/-}$). Taken together, these results indicate that ERp57-dependent modulation of STAT3 from the lumen of the ER requires calreticulin capable of forming complexes with ERp57.

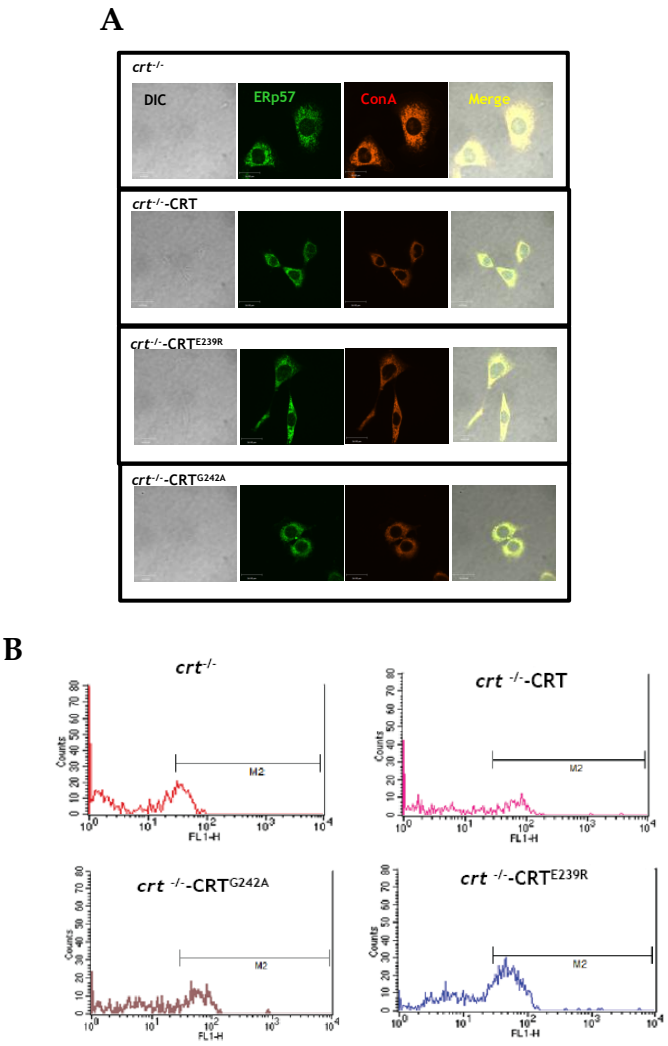

Figure 3-13

Figure 3-13 – Immunostaining and FACs analysis of crt cell lines. A. Immunostaining of CRT-deficient cells (*crt*$^{-/-}$), CRT-deficient cells expressing full length CRT (*crt*$^{-/-}$*-CRT*) and calreticulin deficient cells expressing loss of ERp57 binding mutant (*crt*$^{-/-}$*-CRT*^{E239R}) and ERp57 binding mutant of calreticulin (*crt*$^{-/-}$*-CRT*^{G242A}*)*. Cells were stained with anti-ERp57 antibodies and with TR-ConA, Texas Red conjugated Concanavalin A. In each panel images represent staining with anti-ERp57 antibodies, ConA staining, phase contrast and merged images of the cells. Scale bar=16 μm. **B.** Flow cytometry analysis of specific cell lines was carried out with anti-ERp57 antibodies. *crt*$^{-/-}$, *crt*$^{-/-}$*-CRT*, *crt*$^{-/-}$*-CRT*^{E239R} and *crt*$^{-/-}$*-CRT*^{G242A} cell lines were used for the analysis. Results are presented as the relative mean florescence intensity after subtracting unspecific staining of ERp57$^{-/-}$ cells. M2 represents the gate set on cells stained with antibody.

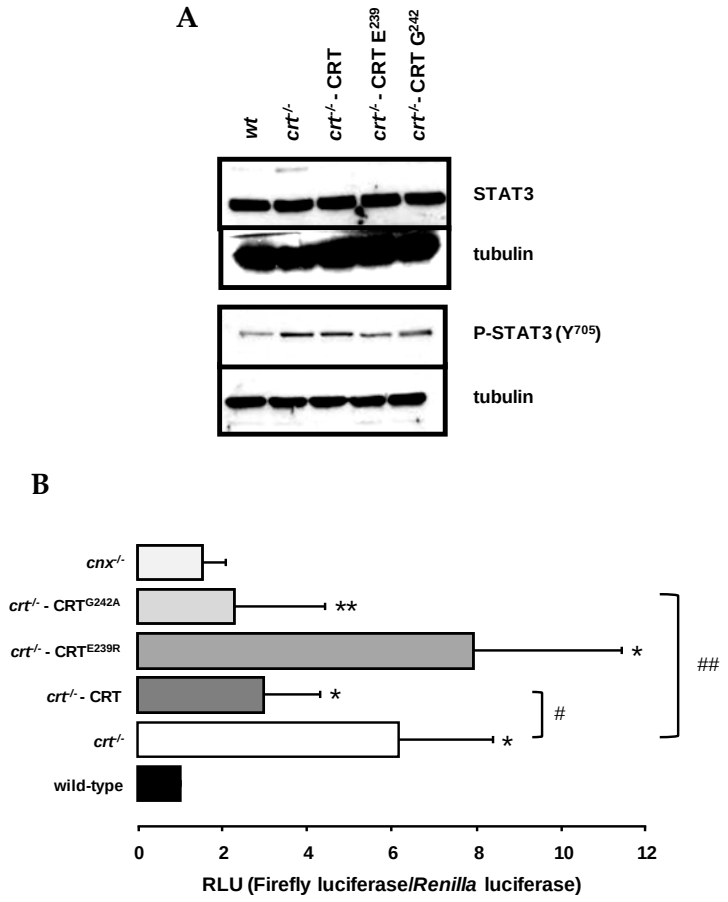

Figure 3-14

Figure 3-14 -Calreticulin enhances ERp57 effects on STAT3 activity. A. Western blot analysis of STAT3 (*inactive*) and phosphorylated (Y^{705}) STAT3 (*active*) in wild-type (*wt*), calreticulin-deficient cells ($crt^{-/-}$), calreticulin deficient cells with loss of ERp57 binding mutant ($crt^{-/-}$-CRT^{E239R}) or calreticulin-deficient cells with no loss of ERp57 binding ($crt^{-/-}$-CRT^{G242A}). Western blot analysis of tubulin was used as loading control. **B.** STAT3 activity in wild-type (*wt*), calreticulin-deficient cells ($crt^{-/-}$), calreticulin deficient cells expression loss of ERp57 binding mutant ($crt^{-/-}$-CRT^{E239R}) or ERp57 no loss of binding mutant of calreticulin ($crt^{-/-}$-CRT^{G242A}). *Renilla* luciferase and firefly luciferase activities were measured as described under "Materials and Methods" and the relative ratio of firefly luciferase to *Renilla* luciferase activity in each cell lysate is presented. Data are the mean ± SD. (wild-type, n=14; $crt^{-/-}$, n=12, $crt^{-/-}$-CRT n=12; $crt^{-/-}$-CRT^{G242A} n= 4; and $crt^{-/-}$-CRT^{E239R} n=4.) *RLU,* relative light units. Two-sample, unpaired t-test was performed. *p<0.0001 vs. wild-type and **p=0.02 vs. wild-type. #p=0.0003 vs. $crt^{-/-}$. ##p=0.0088 vs. $crt^{-/-}$.

Discussion

In this study, we showed that deletion of the *Pdia3* gene, which encodes ERp57, was embryonic lethal at E13.5. Biochemical and cell biological analysis of ERp57-deficient cells indicated that the absence of ERp57 has no impact on ER morphology or expression of ER associated chaperones and folding enzymes, s significant increase in chronic ER stress, or decrease in apoptosis. However, we show that STAT3-dependent signalling was increased in the absence of ERp57 and this could be rescued by expression of the ER targeted ERp57, indicating that ERp57 affects STAT3 signalling from the lumen of the ER. This effect of ERp57 on the STAT3 pathway is further enhanced by an ER luminal complex formation between ERp57 and calreticulin. Increased STAT3 activity in the absence of ERp57 may contribute to embryonic lethality of *ERp57*$^{-/-}$ mice.

The ERp57 gene is differentially regulated during embryonic development indicating that the protein may play a direct role in the development of specific tissues. This is in line with earlier observations of the expression of ER associated ERp57 partner proteins, calreticulin and calnexin [2, 28]. Calreticulin is predominately expressed in the heart during early stages of embryonic development and calreticulin-deficient mice die at E14.5 from impaired cardiac development [28]. In contrast the calnexin gene is highly activated in neuronal tissue [2] and calnexin-deficient mice are born with neurological abnormalities [55]. In this study, we showed that the ERp57 gene was highly active in the inner cell mass of blastocysts, an origin of the fetus formation [56] and in the lung, liver, and brain during early stages of embryogenesis, suggesting that impaired

development of these tissues may, at least in part, contribute to *ERp57*$^{-/-}$ embryonic lethality. The high expression of ERp57 in the lungs seen in this study is of interest because it has recently been reported that ERp57 is decreased in a neonatal rat model of hyperoxia-induced lung injury and cultured cells [52]. siRNA knockdown of ERp57 in human endothelial cells resulted in cellular protection against hyperoxia and tunicamycin-induced caspase-3 activation apoptosis, suggesting that ERp57 has a role in the regulation of apoptosis [52].

Garbi *et al*. [4] carried out a targeted deletion of the ERp57 gene in mouse B cells. They also reported no *ERp57*$^{-/-}$ offspring, indicating that an ERp57 deficiency might be embryonic lethal. Here we investigated embryonic development in the absence of ERp57 and showed that *ERp57*$^{-/-}$ was embryonic lethal at E13.5. Interestingly, deletion of ERp57 in B cells in mice results in normal B cell development, proliferation, and antibody production indicating that ERp57 is not required for glycoprotein folding in B cells [4]. However, there is aberrant assembly of the peptide loading complex, showing that ERp57 is involved in the assembly of the peptide loading complex and it contributes both qualitatively and quantitatively to MHC class I antigen presentation *in vivo*. This supports earlier observations that ERp57 is critically involved in the early folding events of MHC class I heavy chain [5, 14]. The role of ERp57 in MHC class I biogenesis and assembly is further supported by ERp57 siRNA studies [5, 57, 58].

In addition to its role as a folding enzyme in quality control in the secretory pathway, ERp57 is reported to affect STAT3 signalling [12]. This

may be due to formation of inhibitory complexes between ERp57 and STAT3 protein either in the cytoplasm or the nucleus [6, 15, 53, 59, 60]. Furthermore, in avian and mammalian cells, DNA-protein cross-linking experiments indicate that ERp57 is nuclear and it interacts directly with DNA [15]. *In vitro* experiments in HeLa cells showed that ERp57 preferentially binds DNA sequences having characteristic scaffold/matrix associated regions (S/MARs) [61]. Finally, the protein has also been suggested to be present on the cell surface and in the cytoplasm [6, 14-17]. Using FACS analysis we detected some immunoreactive ERp57 on the surface of cells used in this study. However, it is unlikely that the cell surface ERp57 affects STAT3 transcriptional activity as addition of extracellular ERp57 did not affected STAT3 function (Figure 3-12). The conundrum is then: how does ERp57 gain access to the cytoplasm/nucleus to influence STAT3 activity when its N-terminal signal sequence should direct it to the ER and its C-terminal QDEL ER retrieval motif should keep it there? To address this question, we took advantage of available ERp57-deficient cells and tested, for the first time, STAT3 signalling in the absence of ERp57. Analysis of STAT3-dependent expression of the luciferase reporter gene in ERp57-deficient cells revealed that ERp57 indeed affects STAT3 signalling. Most importantly, we showed that the ER but not the cytoplasmic form of ERp57 was effective in inhibition of STAT3 activity. This effect is specific to ERp57, since transfection of ER targeted GFP or calnexin did not have any effect on the STAT3 activity.

Figure 3-15 shows a model of ERp57 function in the lumen of the ER. ERp57 is an ER resident folding enzyme involved in oxidative folding of glycoproteins in the ER, biosynthesis of the MHC class I, and as a

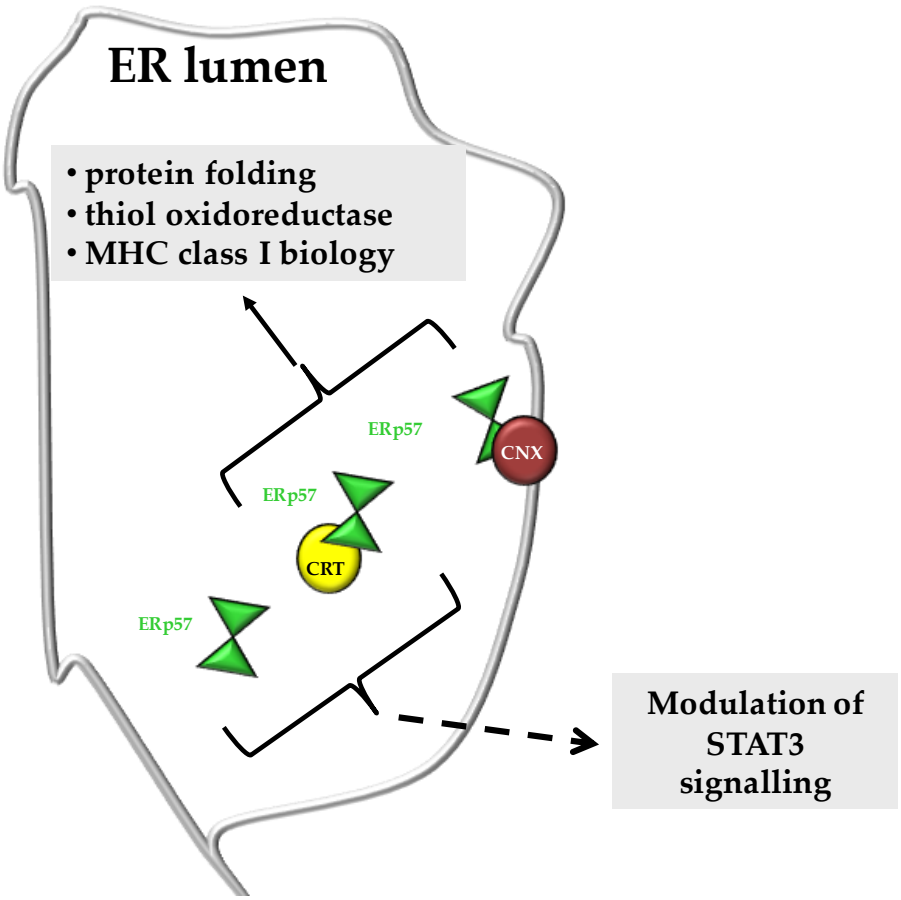

Figure 3-15

Figure 3-15 - A model of the relationship between STAT3, ERp57 and calreticulin. This model shows cross talk between ERp57, calreticulin and STAT3 signalling. ERp57 forms functional complexes with calnexin and calreticulin to promote protein folding, disulfide bond formation and isomerisation. ERp57 is also critical for MHC class I biosynthesis and assembly. A model shows that ERp57, from the lumen of the ER, also affects STAT3 singling and functions as a STAT3 inhibitor. ERp57-dependent modulation of STAT3 is enhanced by complex formation between ERp57 and calreticulin. CRT: calreticulin; CNX: calnexin; MHC: major histocompatability; STAT3: signal transducer and activator of transcription 3.

component of the loading complex [14]. In this study, we showed that ERp57 also affects STAT3 signalling from the lumen of the ER (Figure 3-15). It is not clear at present how ERp57 affected STAT3 signalling, but our work indicates that the inhibitory function of ERp57 was significantly enhanced by interaction with another ER resident luminal protein, calreticulin (Figure 3-15). The two proteins form functional complexes involved in folding and posttranslational modification of newly synthesized (glyco)proteins [47]. Our results indicate that ERp57-dependent modulation of STAT3 activity also depends on the formation of ERp57- calreticulin complexes in the lumen of the ER. Interestingly, ERp57-calreticulin complex formation might also be important for cell surface targeting of these ER proteins [54]. The molecular mechanisms of ERp57-dependent signalling from the ER are not presently clear, however, several other cellular processes are controlled by "ER signalling". For example, cholesterol homeostasis is controlled by ER-nuclear signalling via sterol-regulated proteolysis of ER membrane bound transcription factors called sterol regulatory element-binding proteins [62]. The UPR is also regulated by ER associated kinases which transduce their signals from the ER to affect gene expression in the nucleus [63]. One critical aspect of Ca^{2+} homeostasis is involved in store-operated Ca^{2+} influx resulting from ER-dependent activation of the plasma membrane Ca^{2+} channel [64]. Transcriptional activity of steroid receptors is also modulated by ER luminal proteins [65]. Here we report, for the first time, that the STAT3-dependent pathway may also be modulated by signalling from the ER.

References

1. Bedard, K., et al., *Cellular functions of endoplasmic reticulum chaperones calreticulin, calnexin, and ERp57.* Int Rev Cytol, 2005. **245**: p. 91-121.
2. Coe, H., et al., *Endoplasmic reticulum stress in the absence of calnexin.* Cell Stress Chaperones, 2008. **13**(4): p. 497-507.
3. Hebert, D.N. and M. Molinari, *In and out of the ER: protein folding, quality control, degradation, and related human diseases.* Physiol Rev, 2007. **87**(4): p. 1377-408.
4. Garbi, N., et al., *Impaired assembly of the major histocompatibility complex class I peptide-loading complex in mice deficient in the oxidoreductase ERp57.* Nat Immunol, 2006. **7**(1): p. 93-102.
5. Zhang, Y., E. Baig, and D.B. Williams, *Functions of ERp57 in the folding and assembly of major histocompatibility complex class I molecules.* J Biol Chem, 2006. **281**(21): p. 14622-31.
6. Guo, G.G., et al., *Association of the chaperone glucose-regulated protein 58 (GRP58/ER-60/ERp57) with Stat3 in cytosol and plasma membrane complexes.* J Interferon Cytokine Res, 2002. **22**(5): p. 555-63.
7. Hetz, C., et al., *The disulfide isomerase Grp58 is a protective factor against prion neurotoxicity.* J Neurosci, 2005. **25**(11): p. 2793-802.
8. Hirano, N., et al., *Molecular cloning of the human glucose-regulated protein ERp57/GRP58, a thiol-dependent reductase. Identification of its secretory form and inducible expression by the oncogenic transformation.* Eur. J. Biochem., 1995. **234**(1): p. 336-342.
9. Khanal, R.C. and I. Nemere, *The ERp57/GRp58/1,25D3-MARRS receptor: multiple functional roles in diverse cell systems.* Curr Med Chem, 2007. **14**(10): p. 1087-93.
10. Mazzarella, R.A., et al., *Erp61 is GRP58, a stress-inducible luminal endoplasmic reticulum protein, but is devoid of phosphatidylinositide-specific phospholipase C activity.* Arch Biochem Biophys, 1994. **308**(2): p. 454-60.
11. Muhlenkamp, C.R. and S.S. Gill, *A glucose-regulated protein, GRP58, is down-regulated in C57B6 mouse liver after diethylhexyl phthalate exposure.* Toxicol Appl Pharmacol, 1998. **148**(1): p. 101-8.
12. Ndubuisi, M.I., et al., *Cellular physiology of STAT3: Where's the cytoplasmic monomer?* J Biol Chem, 1999. **274**(36): p. 25499-509.
13. Wyse, B., N. Ali, and D.H. Ellison, *Interaction with grp58 increases activity of the thiazide-sensitive Na-Cl cotransporter.* Am J Physiol Renal Physiol, 2002. **282**(3): p. F424-30.
14. Wearsch, P.A. and P. Cresswell, *The quality control of MHC class I peptide loading.* Curr Opin Cell Biol, 2008. **20**(6): p. 624-31.

15. Coppari, S., et al., *Nuclear localization and DNA interaction of protein disulfide isomerase ERp57 in mammalian cells.* J. Cell. Biochem., 2002. **85**(2): p. 325-333.
16. Grillo, C., et al., *The DNA-binding activity of protein disulfide isomerase ERp57 is associated with the a(') domain.* Biochem Biophys Res Commun, 2002. **295**(1): p. 67-73.
17. Altieri, F., et al., *Purification of a 57kDa nuclear matrix protein associated with thiol:protein-disulfide oxidoreductase and phospholipase C activities.* Biochem Biophys Res Commun, 1993. **194**(3): p. 992-1000.
18. Boengler, K., et al., *The myocardial JAK/STAT pathway: from protection to failure.* Pharmacol Ther, 2008. **120**(2): p. 172-85.
19. Lim, C.P. and X. Cao, *Structure, function, and regulation of STAT proteins.* Mol Biosyst, 2006. **2**(11): p. 536-50.
20. Lim, C.P. and X. Cao, *Regulation of Stat3 activation by MEK kinase 1.* J Biol Chem, 2001. **276**(24): p. 21004-11.
21. Snyder, M., X.Y. Huang, and J.J. Zhang, *Identification of novel direct Stat3 target genes for control of growth and differentiation.* J Biol Chem, 2008. **283**(7): p. 3791-8.
22. Takeda, K., et al., *Targeted disruption of the mouse Stat3 gene leads to early embryonic lethality.* Proc Natl Acad Sci U S A, 1997. **94**(8): p. 3801-4.
23. Akira, S., *Roles of STAT3 defined by tissue-specific gene targeting.* Oncogene, 2000. **19**(21): p. 2607-11.
24. Shen, Y., et al., *Essential role of STAT3 in postnatal survival and growth revealed by mice lacking STAT3 serine 727 phosphorylation.* Mol Cell Biol, 2004. **24**(1): p. 407-19.
25. Boengler, K., et al., *Cardioprotection by ischemic postconditioning is lost in aged and STAT3-deficient mice.* Circ Res, 2008. **102**(1): p. 131-5.
26. Nichols, J., E.P. Evans, and A.G. Smith, *Establishment of germ-line-competent embryonic stem (ES) cells using differentiation inhibiting activity.* Development, 1990. **110**(4): p. 1341-8.
27. Mery, L., et al., *Overexpression of calreticulin increases intracellular Ca^{2+} storage and decreases store-operated Ca^{2+} influx.* J. Biol. Chem., 1996. **271**: p. 9332-9339.
28. Mesaeli, N., et al., *Calreticulin is essential for cardiac development.* J. Cell Biol., 1999. **144**: p. 857-868.
29. Reddy, R.K., et al., *Cancer-inducible transgene expression by the Grp94 promoter: spontaneous activation in tumors of various origins and cancer-associated macrophages.* Cancer Res, 2002. **62**(24): p. 7207-12.
30. Suter, D.M., et al., *Rapid generation of stable transgenic embryonic stem cell lines using modular lentivectors.* Stem Cells, 2006. **24**(3): p. 615-23.

31. Milner, R.E., et al., *Calreticulin, and not calsequestrin, is the major calcium binding protein of smooth muscle sarcoplasmic reticulum and liver endoplasmic reticulum.* J. Biol. Chem., 1991. **266**: p. 7155-7165.
32. Milner, R.E., M. Michalak, and L.C. Wang, *Altered properties of calsequestrin and the ryanodine receptor in the cardiac sarcoplasmic reticulum of hibernating mammals.* Biochim. Biophys. Acta, 1991. **1063**: p. 120-128.
33. Nakamura, K., et al., *Changes in endoplasmic reticulum luminal environment affect cell sensitivity to apoptosis.* J. Cell Biol., 2000. **150**: p. 731-740.
34. Knoblach, B., et al., *ERp19 and ERp46, new members of the thioredoxin family of endoplasmic reticulum proteins.* Mol. Cell. Proteomics, 2003. **2**(10): p. 1104-1119.
35. Okiyoneda, T., et al., *Delta F508 CFTR pool in the endoplasmic reticulum is increased by calnexin overexpression.* Mol Biol Cell, 2004. **15**(2): p. 563-74.
36. Lozyk, M.D., et al., *Ultrastructural analysis of development of myocardium in calreticulin-deficient mice.* BMC Dev Biol, 2006. **6**: p. 54.
37. Martin, V., et al., *Identification by mutational analysis of amino acid residues essential in the chaperone function of calreticulin.* J Biol Chem, 2006. **281**(4): p. 2338-46.
38. Back, S.H., et al., *Cytoplasmic IRE1{alpha}-mediated XBP1 mRNA Splicing in the Absence of Nuclear Processing and Endoplasmic Reticulum Stress.* J Biol Chem, 2006. **281**(27): p. 18691-706.
39. Chung, Y.H., et al., *Activation of Stat3 transcription factor by Herpesvirus saimiri STP-A oncoprotein.* J Virol, 2004. **78**(12): p. 6489-97.
40. Turkson, J., et al., *Stat3 activation by Src induces specific gene regulation and is required for cell transformation.* Mol Cell Biol, 1998. **18**(5): p. 2545-52.
41. Nakamura, K., et al., *Functional specialization of calreticulin domains.* J. Cell Biol., 2001. **154**: p. 961-972.
42. Lievremont, J.P., et al., *BiP, a major chaperone protein of the endoplasmic reticulum lumen, plays a direct and important role in the storage of the rapidly exchanging pool of Ca^{2+}.* J. Biol. Chem., 1997. **272**: p. 30873-3089.
43. Argon, Y. and B.B. Simen, *GRP94, an ER chaperone with protein and peptide binding properties.* Semin Cell Dev Biol, 1999. **10**(5): p. 495-505.
44. Lebeche, D., H.A. Lucero, and B. Kaminer, *Calcium binding properties of rabbit liver protein disulfide isomerase.* Biochem. Biophys. Res. Commun., 1994. **202**(1): p. 556-561.
45. Lucero, H.A. and B. Kaminer, *The role of calcium on the activity of ERcalcistorin/protein-disulfide isomerase and the significance of the C-terminal and its calcium binding. A comparison with mammalian protein-disulfide isomerase.* J Biol Chem, 1999. **274**(5): p. 3243-51.
46. Lucero, H.A., D. Lebeche, and B. Kaminer, *ERcalcistorin/protein-disulfide isomerase acts as a calcium storage protein in the endoplasmic reticulum of a*

living cell. Comparison with calreticulin and calsequestrin. J. Biol. Chem., 1998. **273**(16): p. 9857-9863.

47. Michalak, M., et al., *Calreticulin, a multi-process calcium-buffering chaperone of the endoplasmic reticulum.* Biochem J, 2009. **417**(3): p. 651-66.
48. Reddy, R.K., J. Lu, and A.S. Lee, *The endoplasmic reticulum chaperone glycoprotein GRP94 with Ca(2+)-binding and antiapoptotic properties is a novel proteolytic target of calpain during etoposide-induced apoptosis.* J Biol Chem, 1999. **274**(40): p. 28476-83.
49. Li, Y. and P. Camacho, *Ca2+-dependent redox modulation of SERCA2b by ERp57.* J. Cell Biol., 2004. **164**(1): p. 35-46.
50. Alvarez, C. and E.S. Sztul, *Brefeldin A (BFA) disrupts the organization of the microtubule and the actin cytoskeletons.* Eur J Cell Biol, 1999. **78**(1): p. 1-14.
51. Rutkowski, D.T., et al., *Adaptation to ER stress is mediated by differential stabilities of pro-survival and pro-apoptotic mRNAs and proteins.* PLoS Biol, 2006. **4**(11): p. e374.
52. Xu, D., et al., *Knockdown of ERp57 Increases BiP/GRP78 Induction and Protects against Hyperoxia and Tunicamycin-induced Apoptosis.* Am J Physiol Lung Cell Mol Physiol, 2009.
53. Eufemi, M., et al., *ERp57 is present in STAT3-DNA complexes.* Biochem Biophys Res Commun, 2004. **323**(4): p. 1306-12.
54. Panaretakis, T., et al., *The co-translocation of ERp57 and calreticulin determines the immunogenicity of cell death.* Cell Death Differ, 2008. **15**(9): p. 1499-509.
55. Denzel, A., et al., *Early postnatal death and motor disorders in mice congenitally deficient in calnexin expression.* Mol. Cell. Biol., 2002. **22**(21): p. 7398-7404.
56. Ghassemifar, M.R., et al., *Gene expression regulating epithelial intercellular junction biogenesis during human blastocyst development in vitro.* Mol Hum Reprod, 2003. **9**(5): p. 245-52.
57. Garbi, N., G. Hammerling, and S. Tanaka, *Interaction of ERp57 and tapasin in the generation of MHC class I-peptide complexes.* Curr Opin Immunol, 2007. **19**(1): p. 99-105.
58. Zhang, Y., et al., *ERp57 Does Not Require Interactions with Calnexin and Calreticulin to Promote Assembly of Class I Histocompatibility Molecules, and It Enhances Peptide Loading Independently of Its Redox Activity.* J Biol Chem, 2009. **284**(15): p. 10160-73.
59. Sehgal, P.B., et al., *Cytokine signaling: STATS in plasma membrane rafts.* J Biol Chem, 2002. **277**(14): p. 12067-74.
60. Kita, K., et al., *Evidence for phosphorylation of rat liver glucose-regulated protein 58, GRP58/ERp57/ER-60, induced by fasting and leptin.* FEBS Lett, 2006. **580**(1): p. 199-205.

61. Ferraro, A., et al., *Binding of the protein disulfide isomerase isoform ERp60 to the nuclear matrix-associated regions of DNA.* J Cell Biochem, 1999. **72**(4): p. 528-39.
62. Horton, J.D., J.L. Goldstein, and M.S. Brown, *SREBPs: activators of the complete program of cholesterol and fatty acid synthesis in the liver.* J. Clin. Invest., 2002. **109**(9): p. 1125-1131.
63. Schroder, M. and R.J. Kaufman, *The mammalian unfolded protein response.* Annu Rev Biochem, 2005. **74**: p. 739-89.
64. Putney, J.W., Jr., *Recent breakthroughs in the molecular mechanism of capacitative calcium entry (with thoughts on how we got here).* Cell Calcium, 2007. **42**(2): p. 103-10.
65. Burns, K., et al., *Modulation of gene expression by calreticulin binding to the glucocorticoid receptor.* Nature, 1994. **367**: p. 476-480.

Chapter Four
Site Specific Mutagenesis of Calnexin

Introduction

The ER is a large, membrane bound organelle that has many critical functions within the cell. One of the major roles of the ER is its function in the quality control cycle of newly synthesized proteins [1]. In order to carry out this critical function, the ER houses many chaperone proteins such as calnexin and calreticulin and foldases such as ERp57 [1]. Calnexin and calreticulin bind newly synthesized glycoproteins in the ER as a mechanism of slowing these proteins down [2]. Both calnexin and calreticulin form complexes with the oxidoreductase, ERp57, which catalyzes disulfide bond formation in the newly synthesiszed proteins essentially speeding up the folding. [2] Quality control requires a balance between slowing down the folding by the chaperones and speeding up the folding by foldase to be accurate. The importance of proper ER quality control is underscored by the numerous diseases that result from aberrant protein folding [1].

Calnexin is a 90-kDa, type 1 integral membrane protein that has a very specific domain structure consisting of 4 major domains: the N-globular domain, the P-arm domain, the transmembrane domain and the C-tail domain [3]. The N-globular and P-arm domains form a soluble ER lumen localized domain. Together, these domains are responsible for the folding capacity of calnexin [3]. The N-globular domain contains the primary lectin site and a Zn^{2+} binding site but requires the P-arm domain for full chaperone function [4]. The P-domain is a long, extended flexible arm domain that is involved in interaction with ERp57 [3]. In a recent study,

specific residues within the tip of the P-domain have been found to be critical for ERp57 binding [5].

Calnexin-deficient mice are born live but have severe ataxic phenotype [6, 7]. These mice are 30-50% smaller than their wild-type littermates and have peripheral and central dismyelination [6].Cells derived from these mice have increased ER stress and hyperactive proteasomes as well misfolded and non-functional myelin proteins, P0 and PMP22 [8, 9]. These observations highlight how critical the chaperone function of calnexin is in proper development of the neurological system in utero and post-natally [6, 8, 9]. Therefore, the goal of this study was to examine residues within both the N-globular domain as well as the P-arm domain and determine if they play a role in the critical chaperone function of calnexin. Mutagenesis studies with calreticulin have identified His^{153} and Trp^{302} in the N-domain and Trp^{244} in the P-domain as being critical for chaperone function [10, 11]. Additionally, mutation of Glu^{239}, Glu^{243}, Asp^{241} and Trp^{244} in the P-domain all have decreased binding of ERp57 while mutation of Trp^{302} of the N-domain has enhanced ERp57 binding [10]. In calnexin, mutations to residues Glu^{351} and Trp^{428} located in the P-domain and N-domain, respectively, showed decreased chaperone activity for glycosylated substrates [12]. Residues located at the tip of the P-domain (Trp^{343}, Asp^{344}, Gly^{349}, and Glu^{352}) have been shown via mutagenesis to be involved in ERp57 binding [5]. Mutation to the Trp^{428} in the N-globular domain (Trp^{302} in calreticulin) results in enhanced ERp57 binding [12].

In the present study I focused on the cysteine residues located within the N-globular domain (Cys^{161} and Cys^{195}) and in the P-domain (Cys^{361} and

Cys^{367}) of calnexin. These cysteine residues are conserved throughout all species and crystal modelling of calnexin has predicted that they form disulfide bonds [13]. The contribution of these predicted disulfide bonds in both the N-domain and P-domain to structure and/or function of calnexin remains unknown however, it has been suggested that disulfide bonds are important to maintaining calnexin in the proper conformation for ATP binding [14]. Also, previous studies looking at the crystal structure of calnexin show that the putative Cys^{161}-Cys^{195} disulfide bond is not only localized near the carbohydrate binding site but it is also labile and has effects on carbohydrate binding [13]. Mutations to the disulfide bridge in the N-domain of calreticulin partially disrupted chaperone function [10]. We also looked at the His^{202} residue because the conserved residue in calreticulin (His^{153}) was found to be essential for chaperone function [11] and we also studied the effects of another N-domain histidine (His^{219}). I found that the His^{202}, His^{219}, Cys^{161}, Cys^{195}, Cys^{361}, Cys^{367} had and Cys$^{361/367}$ mutations have no impact on the chaperone function of calnexin for non-glycosylated substrates. However, the double mutation Cys$^{161/195}$ seemed to accelerate the aggregation of non-glycosylated substrate. Both double mutations Cys$^{161/195}$Ala and Cys$^{361/367}$Ala partially lost their ability to thermally aggregate glycosylated substrate while the His^{202}Ala mutation had no effect. The Cys$^{161/195}$Ala and His^{202}Ala mutations resulted in slightly increased ERp57 binding while the Cys$^{361/367}$Ala mutation resulted in greatly increased ERp57 binding. These studies show the importance of the N-globular domain and P-arm domain cysteine residues in the structure and function of calnexin.

Materials and Methods

Materials – Trypsin, malate dehydrogenase (MDH), ATP-Mg^{2+}, $CaCl_2$, $ZnCl_2$ and Dulbecco's modified Eagle's medium were from Sigma. Fetal bovine serum was from Invitrogen. SDS-PAGE reagents and molecular weight markers were from Bio-Rad. Ni^{2+}-nitrilotriacetic acid-agarose beads (Ni-NTA) were from Qiagen. CM5 sensor chips, amine coupling kit and the BIA evaluation analysis program were from BIAcore Inc (GE). All chemicals were of the highest grade available.

Cloning, site-directed mutagenesis and purification of proteins – For *Escherichia coli* (*E. coli*) expression of wild-type soluble calnexin, the wild-type soluble (N and P domains with no transmembrane or C domain) domain of dog calnexin was cloned into enzyme restriction sites Nco1 and Xba1 of pBAD/glIII to generate pBad-HisCNX, as described previously [12]. Site specific mutagenesis on pBad-HisCNX was carried out using protocols from QuickChange Site-Directed Mutagenesis Kit (Stratagene). In brief, megaprimers were designed and alanine (A) mutants were created using *Pfu* DNA polymerase and Gene Amp PCR system 9700 Thermal Cycler. The following mutants were created: CNX-H^{202}A, CNX-H^{219}A, CNX-C^{161}A, CNX-C^{195}, CNX-$C^{161/195}$A, CNX-C^{361}, CNX-C^{367} and CNX-$C^{361/367}$A. Proteins were expressed in Top10F' *E. coli* and His-tagged proteins were purified by one-step Ni^{2+} -nitrilotriacetic acid-agarose affinity chromatography in native condition [10, 12]. Over 90% of the His-tagged protein was purified to homogeneity by one-step Ni^{2+}-nitrilotriacetic acid-agarose column chromatography [10, 11]. Protein concentration was determined spectrophometrically (Bio-Rad protein assay) or by Beckman System 6300

amino acid analyzer [10, 12]. All recombinant proteins were run on an SDS-PAGE gel to check for impurities and degradation products. Human ERp57 was expressed in BL21 *E.coli* and purified as described previously [15, 16].

For expression in eukaryotic cells, cDNA encoding full-length calnexin were isolated from mouse brain library using Gateway Cloning Technology (Invitrogen) [17]. The following DNA primers were used for amplification of full-length calnexin: 5'GGGG**ACAAGTTTGTACAAAAAAGCAGGCT**TC*ACCATG*GAAGGG AAGTGGTTACT-3' (forward) and 5'-GGGG**ACCACTTTGTACAAGAAAGCTGGGT**CTCACTCTCTTCGTGG CTTTCT'-3' (reverse). The forward primer contains an *att*B1 recombination site (bold), Kozak site for expression in mammalian cells (italics) and calnexin gene specific nucleotides (underlined). The reverse primer contains *att*B2 recombination site (bold) and the calnexin gene specific nucleotides (underlined). First, to generate entry clone vectors, a BP Clonase Reaction was carried out as recommended by the manufacturer. The recombination reaction was carried out using BP Clonase Enzyme Mix to insert full-length calnexin and the promoter EF1α (cellular polypeptide chain elongation factor 1 alpha) into the destination lentiviral vector $2K7_{bsd}$ (containing blasticidine resistance gene for cell selection.) This vector was called p2K7-CNX and was used as a template for site-specific mutagenesis. Using, methods from QuickChange XL Site-Directed Mutagenesis Kit (Stratagene) and *Pfu* DNA polymerase, the following mutants were created: CNX-$H^{202}A$, CNX-$H^{219}A$, CNX-$C^{161}A$, CNX-C^{195}, CNX-$C^{161/195}A$, CNX-C^{360}, CNX-C^{366} and CNX-$C^{360/366}A$. Cells

were selected with blasticidine (10μg/μL – Gibco) and protein from bulk cell population was harvested with RIPA buffer containing 50mM Tris, pH 7.5, 150mM NaCl, 1mM EDTA, 1mM EGTA, 1% Triton X-100, 0.1% SDS, 0.5% sodium deoxycholate and protease inhibitors (0.5mM PMSF, 0.5mM benzamidine, 0.05μg/ml TLCK, 0.05μg/ml APMSF, 0.05μg/ml E-64, 0.025μg/ml leupeptin and 0.01μg/ml pepstatin) [18].

Western blot analysis and immunostaining - For Western blot analysis, 30μg of protein was separated on a 10% SDS-PAGE acrylamide gel, transferred to nitrocellulose membrane and probed with rabbit-anti-calnexin (StressGen) at dilution 1:1000 and rabbit-anti tubulin (StressGen) at a dilution 1:1000 [9]. Blots were developed using a chemiluminescent system [19]. For immunostaining, wild-type, *cnx*$^{-/-}$ and *cnx*$^{-/-}$ -expressing calnexin mutants mouse embryonic fibroblasts were grown on glass converslips. Cells were fixed with 3.7% paraformaldehyde in PBS for 20 min at room temperature and washed 3 times with PBS [9]. Cells were permeabilized with Opas buffer (0.1% Triton X-100, 100mM PIPES, 1mM EGTA, 4% w/v polyethylene glycol 8000, pH 6.9) for 2 min and washed 3 times with PBS [20]. Primary antibody rabbit-anti-calnexin (StressGen) at a 1:100 dilution and the secondary antibody was rabbit conjugated-fluorescein isothiocynate (FITC) (Invitrogen) at a dilution of 1:200 in PBS. Coverslips were also co-stained with Alexa Fluor 546-Concanavalin A at a dilution of 1:1000 (Sigma) [17]. The coverslips were mounted onto glass slides and fluorescent signals visualized using spinning disk confocal microscopy (WaveFX from Quorum Technologies, Geulph, Canada) set up on an Olympus IX-81 inverted stand (Olympus, Markham, Canada.) Images were acquired through a 60X objective (N.A. 1.42) with an

EMCCD camera (Hamamatsu, Japan.) The fluorescent dyes, FITC and Texas Red, were excited by a 491nm and a 561nm laser line, respectively (Spectral Applied Research, Richmond Hill, Canada.) Z-slices (0.25μM) were acquired using Volocity Software (Improvision) through the cells using a piezo z-stage (Applied Scientific Instrumentation, Eugene, USA.)

Aggregation assays and intrinsic fluorescence – Protein aggregation was carried out using 2μM of denatured malate dehydrogenase (MDH) suspended in 50mM sodium phosphate buffer, pH 7.5 and 0.2μM of wild-type or mutant calnexin suspended in 10mM Tris pH 7.0 and 1mM EDTA. Buffer containing 50mM sodium phosphate , pH 7.5, was incubated at 45°C followed by the addition of both denatured MDH and 0.2μM of wild-type or mutant calnexin and then measured for light scattering [11, 12, 21]. Protein aggregation was also carried out using IgY isolated from chicken egg yolk using the EGG-stract IgY purification method (Promega) [11]. After denaturing, 0.25μM of IgY was suspended in a buffer containing 10mM Tris-HCl, pH 7.0, 150mM NaCl and 5mM $CaCl_2$. Buffer containing 10mM Tris-HCl, pH 7.0, 150mM NaCl and 5mM $CaCl_2$ was incubated to 45°C followed by the addition of both 0.2uM of IgY and 0.125μM of wild-type or mutant calnexin [11]. Light scattering was measured at excitation and emission at 320nm and 360nm, respectively, for 1h using a spectrofluorometer system C43/2000 (PTI) equipped with a temperature-controlled cell holder [11, 21]. Both MDH and IgY aggregation assays were performed 3 times each with wild-type or mutant calnexin and averages are plotted. For intrinsic fluorescence, 3 μM of wild-type or calnexin mutant protein was suspended in buffer containing 10 mM 3-(N-morpholino)propanesulfonic acid (MOPS), pH 7.0, 3 mM $MgCl_2$

and 150 mM KCl. The excitation wavelength was set at 286nM and the range of emission was set at 295-450nM. The effect of Zn^{2+}, Ca^{2+} and ATP on the intrinsic fluorescence of the protein was measured at 25°C using a spectrofluorometer system C43/2000 [10]. Experiments with wild-type or mutant calnexin, under each condition, were performed twice.

Proteolytic digestions – Ten μg of purified, recombinant wild-type or calnexin mutant protein was suspended in a buffer containing 10 mM Tris-HCl, pH 7.0, 1 mM $MgCl_2$ and 100 mM KCl. Proteins samples were incubated with trypsin at 1:100 (trypsin:protein w/w) in the presence or absence of 2mM $CaCl_2$, 1 mM $ZnCl_2$, or 1 mM ATP-Mg^{2+}. Samples of digested proteins were taken and loaded on a 12.5% SDS-PAGE gel at 0, 0.5, 2, 5, 10 and 20 minutes and then stained with Coomassie Blue [10].

Surface Plasmon Resonance (SPR) – A CM5 sensor chip was activated, coupled and blocked using an Amine Coupling Kit from BIAcore, as described previously [10, 12]. In brief, two lanes of a CM5 sensor chip were activated using a 1:1 mixture of 1-Ethyl-3-(3-dimethyl-aminopropyl) carbodiimide HCl (EDC) and N-Hydroxysuccinimide (NHS) for 7 min at a flow rate of 5μl/min. 1μM of purified wild-type calnexin or calnexin mutant protein was suspended in 10mM sodium acetate at pH 4.0 and coupled to 1 lane (other lane is control) at a flow rate of 5μl/min until approximately 1000-3000 RU's protein were covalently coupled. Both the ligand bound as well as the control lane were then blocked using 1M Ethanolamine HCl at pH8.5 for 7 min at a flow rate of 5ul/min. To monitor homogenous, binary interactions, kinetic analysis experiments were performed at 21°C in running buffer containing 20 mM Tris-HCl, pH 7.0,

135 mM KCl, 2 mM $CaCl_2$, 0.05% Tween-20 and protease inhibitors protease inhibitors (200 μM PMSF, 100 μM benzamidine, 0.05μg/ml TLCK, 0.05μg/ml APMSF, 0.05μg/ml E-64, 0.025μg/ml leupeptin and 0.01μg/ml pepstatin) at a flow rate of 30μl/min to reduce mass transfer effects (BIACore control software 3.2). His-tagged human ERp57 was the analyte used in a concentration series curve from 5000nm to 5nM. Kinetic analysis was performed using a 1:1 Langmuir binding with drifting baseline as a model (BIAanalysis software) to generate equilibrium and rate constants. The maximum relative response was calculated based on the predicted R_{max} and normalized to wild-type control.

Results

Expression of calnexin mutants in calnexin-deficient cells – Calnexin has a very specific domain homology consisting of 4 domains: the N-terminal globular domain, the P-arm domain, a short transmembrane domain and a cytoplasmic C-terminal domain [3]. The N-terminal globular domain is important for carbohydrate binding [3, 13] and contains a critical tryptophan (Trp^{428}) residue that impacts the structural and functional properties of calnexin [12]. As well, model building of calnexin has predicted a disulfide bridge between Cys^{161}-Cys^{195} in the N-globular domain [13]. The P-domain of calnexin forms an extended, flexible arm domain and also may be involved in the binding of carbohydrates in the ER lumen [3, 13]. Through quantitative binding studies and NMR and yeast two hybrid studies, ERp57 binding has been mapped to the arm domain of calnexin [4, 5]. Site-specific mutagenesis on mouse calnexin was carried out in order to determine if any of these mutations impacted on

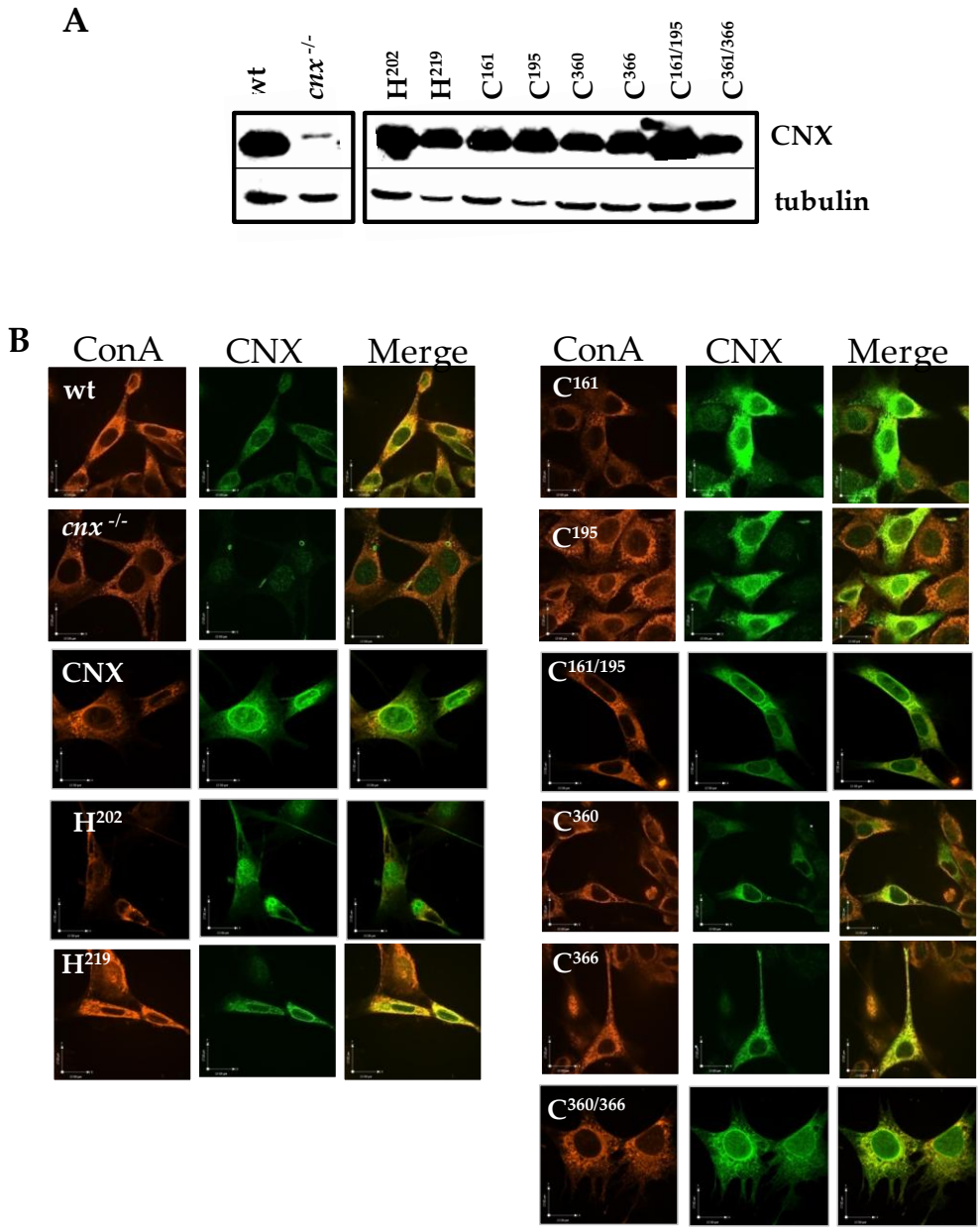

Figure 4-1

Figure 4-1 - Expression of calnexin mutants in calnexin-deficient mouse embryonic fibroblasts A. Western blot analysis of protein lysates for calnexin and for tubulin (loading control) isolated from calnexin-deficient cell lines stably expressing calnexin mutants. Proteins of all mutants are expressed **B.** Immunolocalization of calnexin and calnexin mutants in calnexin-deficient cell lines. Calnexin localizes to the ER in the wild-type and cell lines expressing calnexin mutant. Scale bar, 17μM (See "Materials and Methods".)

the localization and potentially function of calnexin. All residues were mutated to alanine residue to prevent conformational changes in the protein and impose extreme electrostatic or steric effects [22]. In the N-terminal domain, we created $Cys^{161}A$, $Cys^{195}A$ and $Cys^{161/195}A$, were created to prevent formation of the disulfide bridge. The residues $His^{202}A$ and $His^{219}A$ were also mutated. The His^{202} residue is conserved between calreticulin (His^{153}) and in calreticulin has been found to impact chaperone function [11]. The His^{219} residue is also important to investigate as it may also have a role in the chaperone function of calnexin through the coordination of divalent cations [11]. Also, mutations of the cysteine residues in the P- domain (Cys^{360}, Cys^{366} and $Cys^{360/366}$) to elucidate the importance of the disulfide bond in calnexin structure and function. Calnexin-deficient ($cnx^{-/-}$) mouse embryonic fibroblast cells were transduced with lentiviral vectors encoding wild-type calnexin or calnexin mutants followed by creation of stable cell lines (See "Materials and Methods") [9, 17]. The following cell lines were created: $cnx^{-/-}$*-CNX* (CNX), $cnx^{-/-}$*-CNX-His*^{202} (H^{202}), $cnx^{-/-}$*-CNX-His*^{219} (H^{219}), $cnx^{-/-}$*-CNX-Cys*^{161} (C^{161}), $cnx^{-/-}$*-CNX-Cys*^{195} (C^{195}), $cnx^{-/-}$*-CNX-Cys*$^{161/195}$ ($C^{161/195}$), $cnx^{-/-}$*-CNX-Cys*^{360} (C^{360}), $cnx^{-/-}$*-CNX-Cys*^{366} and *cnx-/-* -*CNX-Cys*$^{360/366}$ ($C^{360/366}$). Western blot analysis showed that all the cell lines expressed recombinant protein (Figure 4-1A) and this was confirmed by immunostaining for calnexin (Figure 4-1B). Figure 2B also shows that, morphologically, all mutant cells lines appear to have intact ER as indicated by counterstaining with Concanavalin A. Additionally, immunostaining also shows that all calnexin mutants localize to an ER-like network (Figure 4-1B.) Therefore,

mutations in residues of calnexin Cys^{161}, Cys^{195}, His^{202}, His^{219}, Cys^{360} and Cys^{366} have no impact on expression or ER-localization.

Structural analysis of calnexin mutants – Previous studies have used both limited proteolysis analysis and intrinsic fluorescence to reveal amino acid residues that cause significant conformational changes resulting differences in trypsin accessible portions of the protein [10-12]. Studies have identified residues His^{153} and Glu^{243} and Trp^{244} (in the presence of Ca^{2+}) in calreticulin as having important structural roles [10, 11]. In calnexin, a mutation in the Trp^{428} in the globular domain also has an effect on the conformation and only in the presence of Ca^{2+} was this protection recovered [12]. Thus, it is important to determine whether the histidine and the cysteine residues of calnexin used in this study contribute significantly to the structural stability of the protein. We were able to purify and express soluble dog calnexin and calnexin mutants (Figure 4-2E). I have carried out both limited proteolysis analysis and intrinsic fluorescence in the absences and presence of Ca^{2+}, Zn^{2+} and ATP on wild-type and His^{202}, His^{219}, Cys^{161}, Cys+, $Cys^{161/195}$, Cys^{361}, Cys^{367} and $Cys^{361/367}$ soluble dog calnexin mutant protein (Figure 4-2A-D.)

Soluble wild-type and mutant dog calnexin proteins were incubated with trypsin and run on a 12.5% SDS-PAGE gel and stained with Coomassie Blue to monitor the effect of the mutations on protein conformation resulting in changes in trypsin accessibility (Figure 4-3A-D). Congruent with previous studies, we also determined that calnexin is partially resistant trypsin as we observe a fraction of full-length calnexin at the 20 min time point (Figure 4-3A.) Although no ATP has been shown to bind

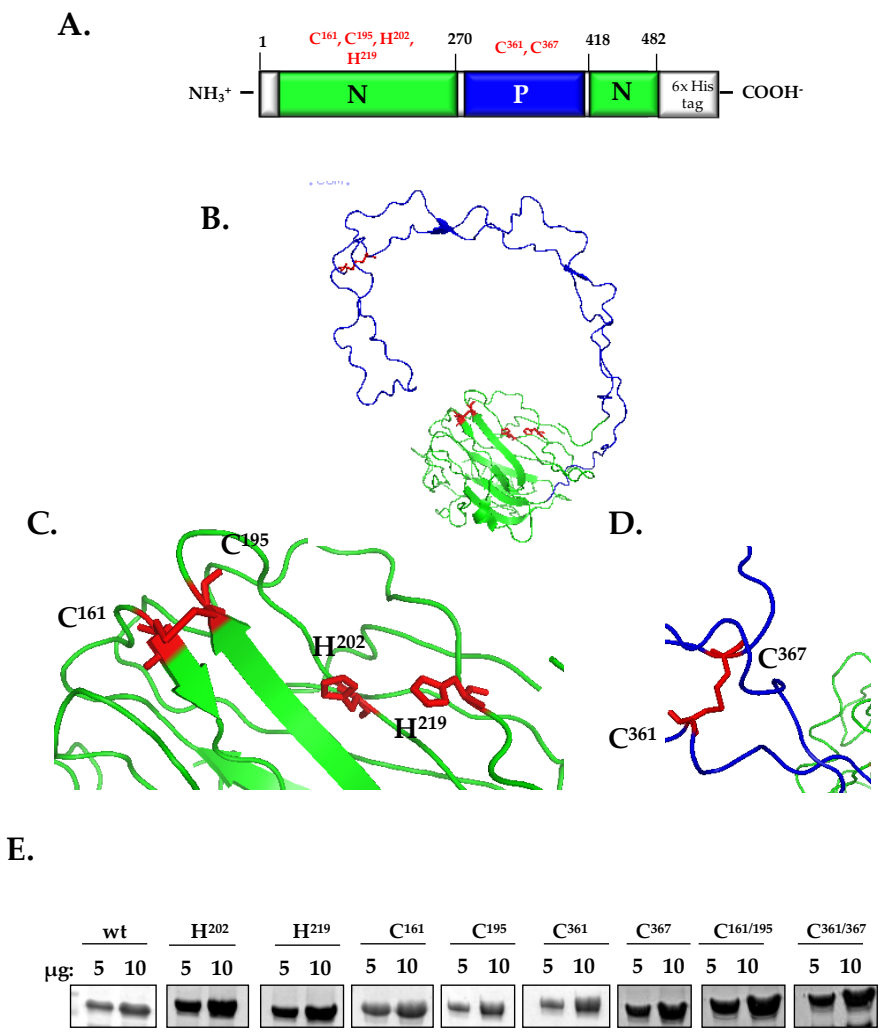

Figure 4-2

Figure 4-2 – Soluble dog calnexin and calnexin mutants expression. A. A linear model of the N-globular domain (*green)* and the P-domain (*blue)* of dog calnexin with mutations created *(red).* **B.** The crystal structure of soluble calnexin. **C.** The N-domain with mutated residues in red. **D.** The P-domain with mutated residues in red. **E.** Coomassie gel of the expressed soluble calnexin and calnexin mutants.

molecular chaperones, ATP has been shown to effect their conformation as well as their function [14]. Previous studies have shown that ATP binds to calnexin inducing a conformational change [14]. I have found that in the presence of 1 mM Mg-ATP, we also observe mutational dependent conformational changes in calnexin (Figure 4-3B.) Mutations to His^{202} and His^{219} in the globular domain of calnexin show increased protection to trypsin in the presence of ATP suggesting that the binding of ATP to calnexin may be altered with these mutations and result in a different proteolysis pattern when compared to wild-type. Interestingly, we also observe increased protection in the Cys^{367} mutation in the globular domain suggesting this residue may also impact ATP binding resulting in an altered trypsin accessible conformation (Figure 4-3B). It is interesting that the mutation in the Cys^{361} of the P-domain results in decreased protection in the presence of ATP. In the presence of ATP, there were no effects on Cys^{161}, Cys^{195} or the double mutants, $Cys^{161/195}$ and $Cys^{361/367}$ (Figure 4-3B.)

Calnexin has one Ca^{2+} binding site within the N-globular domain and this binding is known to affect the protein conformation [3, 13, 14]. In the presence of Ca^{2+}, we do not observe any striking difference in wild-type calnexin when compared to the absence of Ca^{2+} (Figure 4-3A and C.) However, in the His^{219}, Cys^{367}, $Cys^{361/367}$ and $Cys^{161/195}$ mutations we observe increased resistance to limited trypsin proteolysis when compared to wild-type calnexin (Figure 4-3C). The His^{219} and $Cys^{161/195}$ residues are located in the N-globular domain and these data suggest that they may play a role in Ca^{2+} binding. Interestingly, the Cys^{361} and Cys^{367} residues are located in the P-arm domain of calnexin and they also may have a structural role in the coordination of the Ca^{2+} binding. No dramatic effects

A.

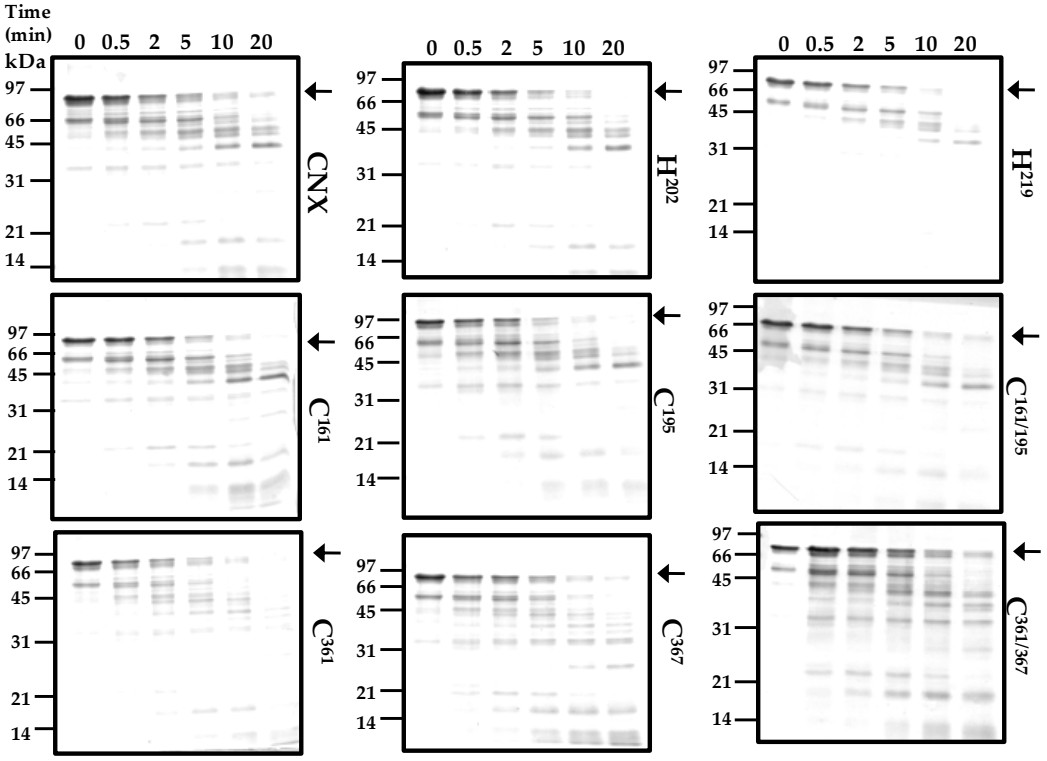
Time (min)
kDa
0 0.5 2 5 10 20
97
66
45
31
21
14
CNX
H202
H219
C161
C195
C161/195
C361
C367
C361/367

Figure 4-3

B. + 1mM Mg^{2+}-ATP

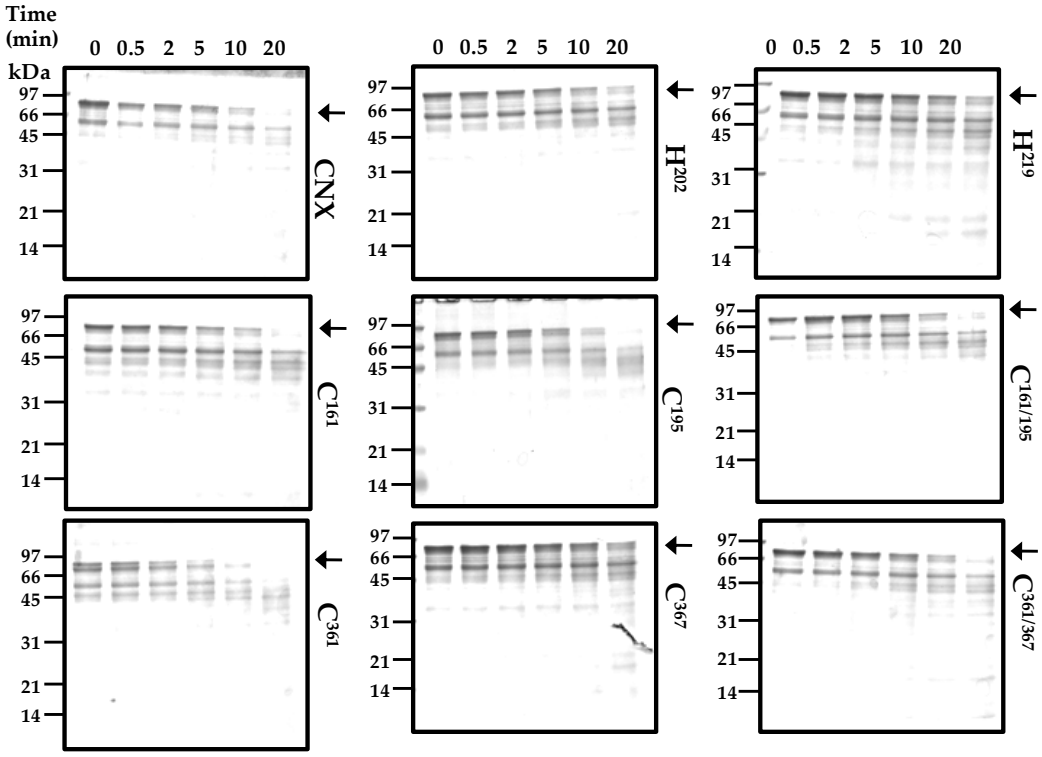

Figure 4-3

C. **+2mM Ca^{2+}**

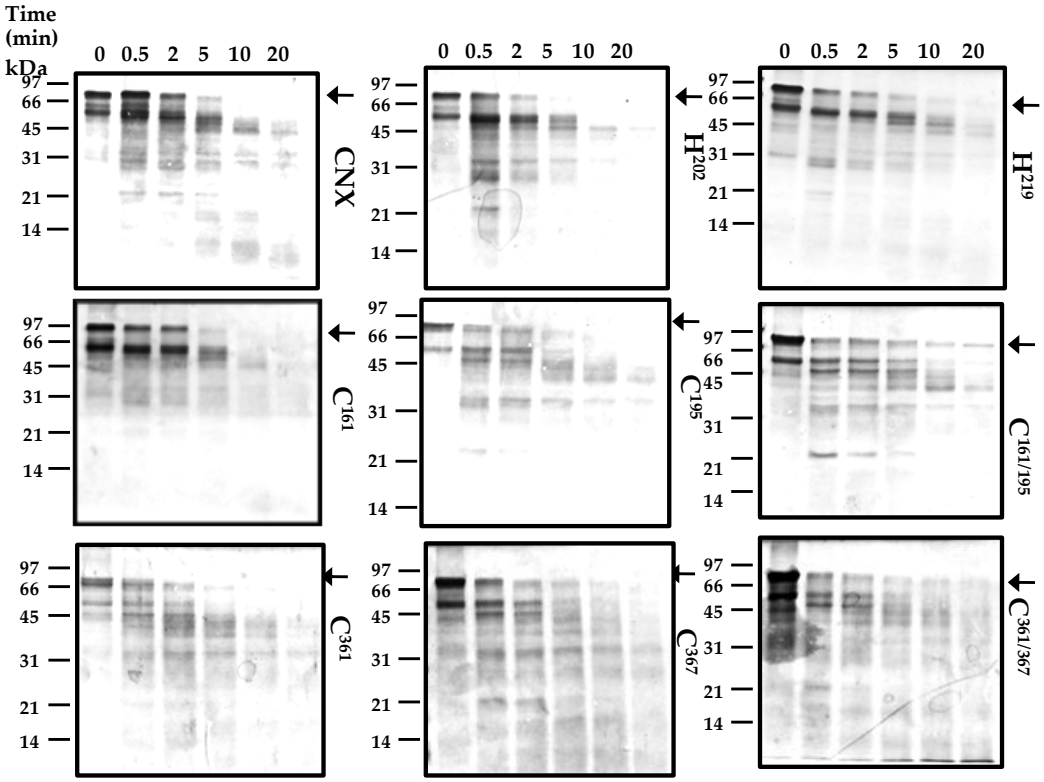

Figure 4-3

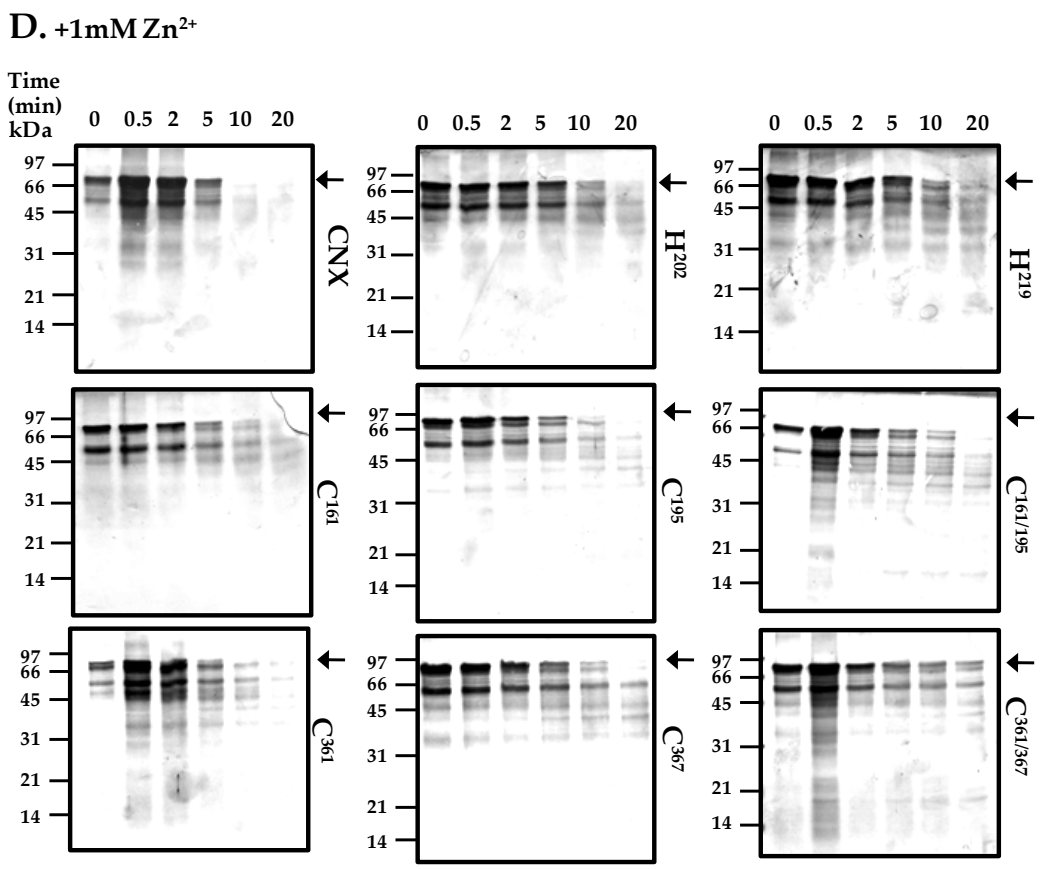

Figure 4-3

Figure 4-3 - Limited trypsin proteolysis of soluble, canine wild-type calnexin and calnexin mutants in the absence (A) or presence of ATP (B) Ca^{2+} (C) and Zn^{2+} (D) Wild-type calnexin and calnexin mutants (indicated, *right*) were digested with trypsin, aliquots taken at the time points indicated (*top,* minutes), run on an SDS-PAGE gel and Coomassie stained (See "Materials and Methods.") The arrows indicate the location of calnexin protein. *CNX,* calnexin. Each gel is representative of at least 3 experiments.

on trypsin accessibility were observed in mutations to residues His^{202}, Cys^{161}, Cys^{195} and Cys^{361} when compared to wild-type (Figure 4-3C).

Calnexin has a Zn^{2+} binding site located within its N-globular domain [4]. The importance of the co-factor Zn^{2+} in the function of calnexin has been demonstrated by studies showing Zn^{2+}-dependent ERp57 binding [4]. We wanted to investigate whether mutations within the N-globular domain or P-arm domain of calnexin resulted in conformational changes in the presence of Zn^{2+}. I found that the presence of Zn^{2+} caused greater trypsin accessibility on wild-type calnexin protein (Figure 4-3D). This is not surprising as previous studies with calreticulin have shown that in the presence of 100μM Zn^{2+}, large hydrophobic patches of the protein are exposed and this data, along with others, suggest that the binding of Zn^{2+} may also result in large hydrophobic patches of calnexin being exposed [4, 23]. N-globular domain residues, His^{202}, His^{219} and $Cys^{161/195}$ resulted in increased protection of calnexin to trypsin digestion in the presence of Zn^{2+} when compared to wild-type as determined by the presence of full-length calnexin being observed as late as 10 min (Figure 4-3D). Interestingly, we also observe increased protection to trypsin in mutations found in the P-arm domain (Cys^{361}, Cys^{367} and $Cys^{361/367}$) (Figure 4-3D). In particular, we observe increased protection in the double $Cys^{361/367}$ mutant showing strong, persistent presence of full-length calnexin up to 20 min (Figure 4-3D.) This implies that these residues in the P-arm may have a role in the coordination of Zn^{2+}. This is of interest as ERp57 binding has been mapped to the P-arm domain of calnexin [5] and that this may be a Zn^{2+}-dependent interaction [4]

In order to elucidate structural changes in the calnexin wild-type protein and mutants, I carried out intrinsic fluorescence analysis. Proteins all have a unique intrinsic fluorescence that is dictated by the three aromatic residues tryptophan, tyrosine and phenylalanine [12]. I measured the intrinsic fluorescence of calnexin mutants with increasing concentrations of the three cofactors ATP, Ca^{2+} and Zn^{2+}. Consistent with previous studies we found that with increasing concentrations of both Ca^{2+} and ATP I observed a decrease in intrinsic fluorescence of wild-type calnexin protein suggesting that both ATP and Ca^{2+} effect the conformation of the protein (Figure 4-5). Interestingly, all the mutants (His^{202}, His^{219}, Cys^{161}, Cys^{195}, $Cys^{161/195}$, Cys^{361}, Cys^{367} and $Cys^{361/367}$) showed very similar intrinsic fluorescence to increasing concentrations of ATP, Ca^{2+} and Zn^{2+} as the wild-type calnexin protein (Figure 4-5.) Although intensity of fluorescence differs, this is not very informative. Taken together with the limited trypsin proteolysis data, we can conclude that in the presence of ATP, Ca^{2+} and Zn^{2+} there are minor differences in the conformation of calnexin mutants however not enough to vastly impact the intrinsic fluorescence signal and tertiary structure.

Cysteine mutants lost their ability to prevent aggregation of IgY and not MDH – In order to investigate the roles of the residues His^{202}, His^{219}, Cys^{161}, Cys^{195}, Cys^{361} and Cys^{367} in chaperone activity, I measured their chaperone activity as a function of their ability to prevent thermal aggregation of two substrates, the non-glycosylated substrate, malate dehydrogenase (MDH), and the glycosylated substrate, IgY. MDH is a non-glycosylated, mitochondrial/cytosolic homodimer protein that can thermally aggregate at 45°C as measured as a function of light scattering [24]. Previous studies

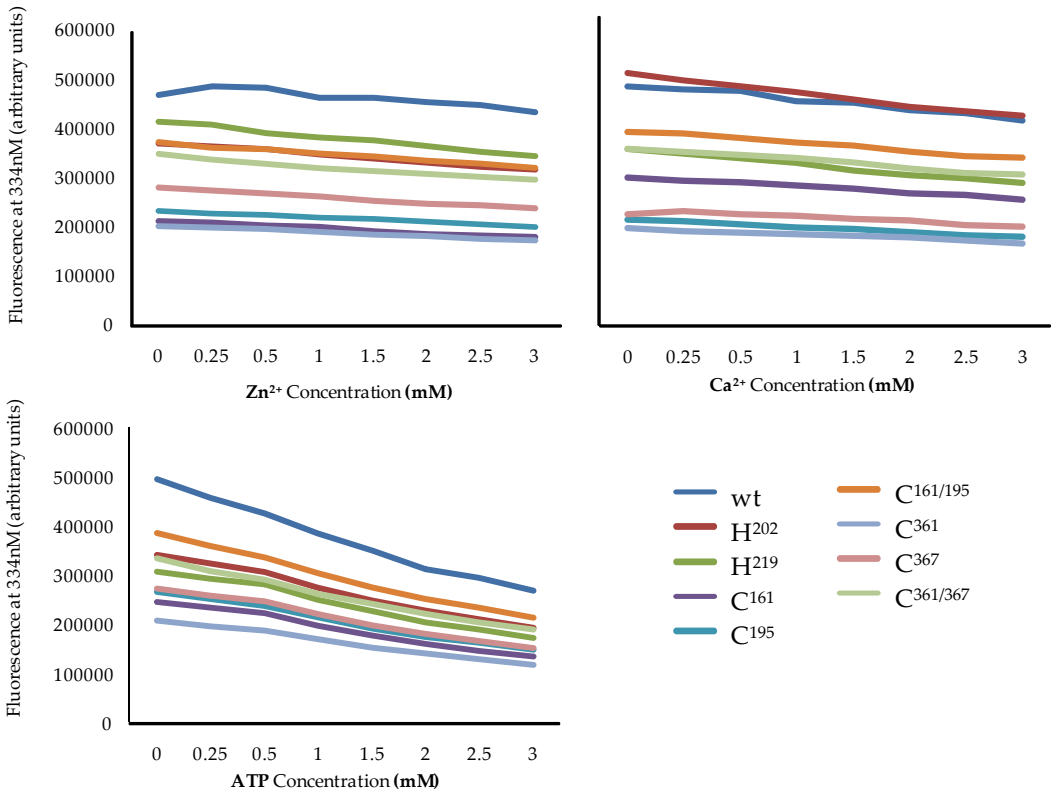

Figure 4-4

Figure 4-4 – Intrinsic fluorescence of wild-type calnexin and mutant calnexin. Intrinsic fluorescence analysis was carried out in the absence and presence of increasing Zn^{2+}, Ca^{2+} and ATP. The excitation wavelength was set to 286nm and the range of emission wavelength was set to 295nm-450nm. The 334nm wavelength fluorescence is plotted with increasing concentration.

have shown that in the presence of molecular chaperones, thermal aggregation of MDH can be partially prevented [10-12, 21, 24]. IgY is a soluble, glycosylated antibody of birds that can also thermally aggregate at 45°C and this aggregation can be slowed when molecular chaperones are present [21]. Using these assays, we can measure them impact calnexin mutants have on the folding of glycosylated versus non-glycosylated substrates.

Soluble, wild-type calnexin prevents thermal aggregation of the MDH substrate (Figure 4-5). Mutations to calnexin at His^{202}, His^{219}, Cys^{161}, Cys^{195}, Cys^{361}, Cys^{367} and $Cys^{361/367}$ are able to prevent thermal aggregation of MDH in a similar manner to wild-type calnexin (Figure 4-5A-D). However, the double mutant, $Cys^{161/195}$ in the N-globular domain of calnexin, shows slightly greater folding of the MDH substrate when compared to wild-type protein (Figure 4-5D). This suggests that the double mutation to the residues Cys^{161} and Cys^{195} positively impacts the folding abilities of calnexin on non-glycosylated substrates.

Next, when looking at the effect of calnexin mutations on interaction with the glycosylated substrate, I focused on the mutations that would break putative disulfide bonds. We looked specifically at double mutations in the N-globular domain, $Cys^{161/195}$, and in the P-arm domain, $Cys^{361/367}$, and used His^{202} as a control (Figure 4-6). I found that both double cysteine mutations were less able to prevent thermal aggregation of the IgY substrate while the histidine mutation was able to prevent aggregation in a similar manner to wild-type calnexin (Figure 4-6). Specifically, mutations to the N-globular domain cysteines ($Cys^{161/195}$) resulted in an expedited

A.

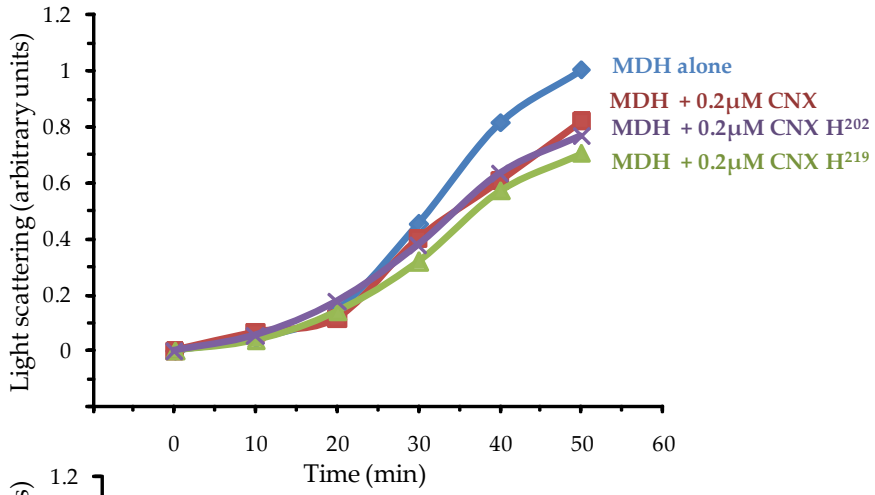

B.

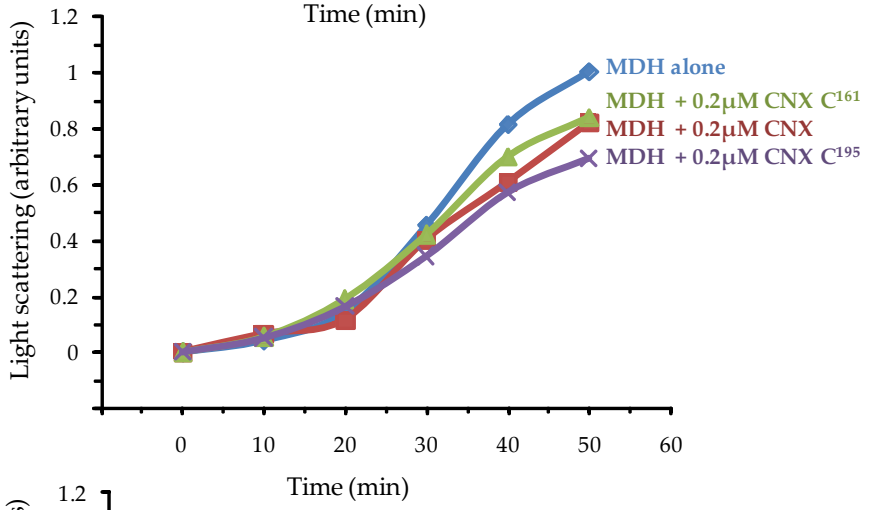

C.

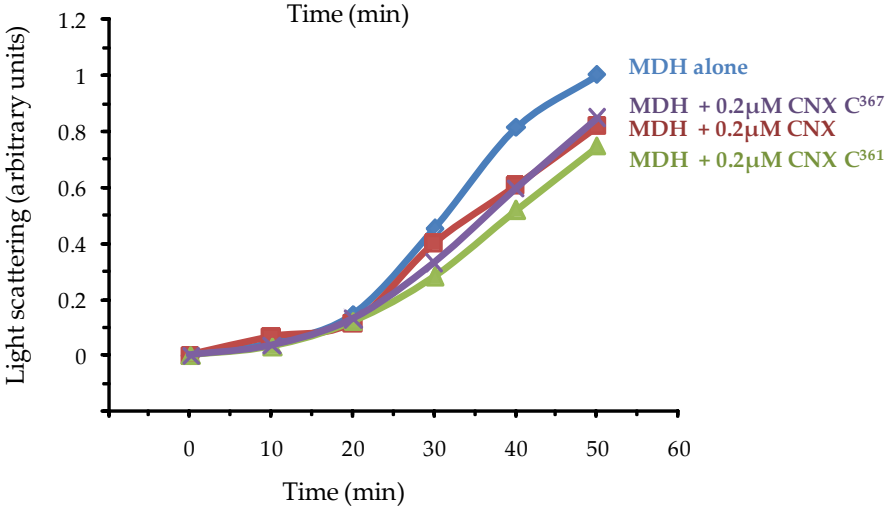

Figure 4-5 (continued on following page)

D.

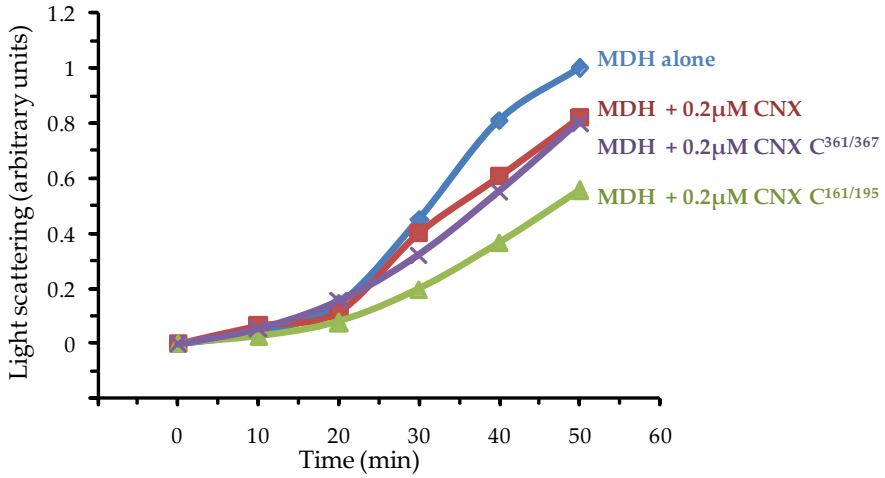

Figure 4-5

Figure 4-5 - Effect of soluble wild-type calnexin and calnexin mutants on the thermal aggregation of malate dehydrogenase (MDH) A. Wild-type, His^{202}, His^{219}, **B.** Cys^{161}, Cys^{195}, **D.** Cys^{361}, Cys^{367}, **E.** $Cys^{161/195}$ and $Cys^{361/367}$ calnexin mutants were incubated with heat-treated MDH and thermal aggregation was monitored over time at 360nm. All graphs were normalized to the same wild-type calnexin.

aggregation of IgY suggesting that this mutation positively impacts glycosylated substrate. Although, mutations to the P-arm domain cysteines ($Cys^{361/367}$) also result in loss of aggregation of IgY it does not result in an increase in aggregation beyond the thermal aggregation of IgY alone suggesting that $Cys^{361/367}$ residues are important for the chaperone activity of calnexin.

Taken together, I have found that the N-globular domain cysteine residues Cys^{161} and Cys^{195} together are important for the chaperone activity of calnexin on both glycosylated and non-glycosylated substrates. This is of particular interest because with non-glycosylated MDH substrate the $Cys^{161/195}$ mutation of calnexin increases chaperone activity while in the case of the non-glycosylated substrate, we observe a loss of chaperone activity implying that these residues may play a regulatory role in chaperone function which is dictated by substrate status. The cysteine residues 361 and 367 in the P-arm domain together have no impact on the chaperone activity on non-glycosylated.substrate but have a role in the chaperone activity for glycosylated substrate. Residues 361 and 367 are involved in the function of calnexin as a chaperone but only if the substrate is glycosylated

Calnexin mutants' interaction with ERp57- Cross-linking studies demonstrated a functional association of calnexin with ERp57 that brings ERp57 into proximity of newly synthesized proteins to carry out isomerisation of disulfide bonds [15, 25]. Genetic screens, NMR studies and mutagenesis analysis have shown that the C-domain of ERp57 interacts with the P-domain of calnexin [5]. The largest effects on ERp57 binding are seen in residues at the tip of the P-domain of calnexin (Trp^{343},

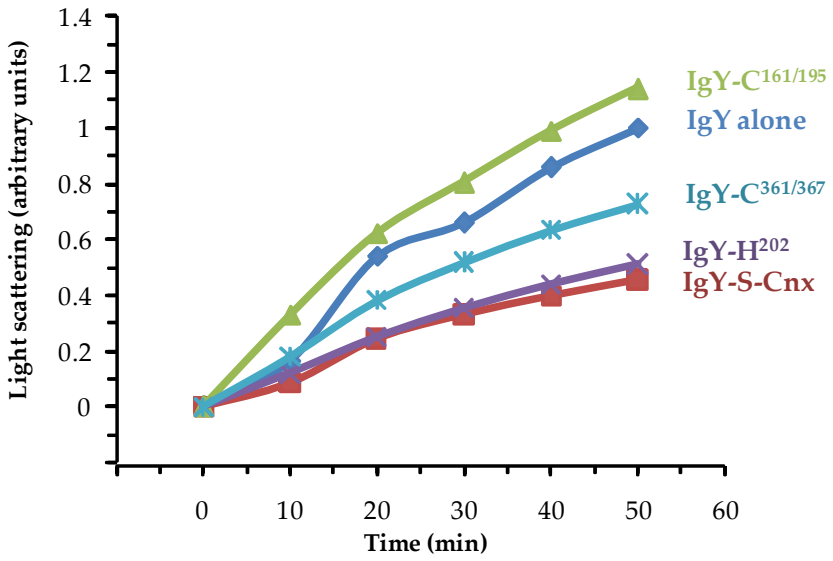

Figure 4-6

Figure 4-6 - Effects of soluble calnexin and calnexin mutants His^{202}, $Cys^{161/195}$ and $Cys^{361/367}$ on the thermal aggregation of glycosylated substrate IgY. Wild-type, His^{202}, $Cys^{161/195}$ and $Cys^{361/367}$ calnexin mutants were incubated with IgY and thermal aggregation was monitored over time at 360nm. All graphs were normalized to the same wild-type, soluble calnexin.

Asp^{344}, Gly^{349} and Glu^{352}) [5]. Therefore, we wanted to see if any of our mutated residues, specifically the Cys$^{361/367}$ in the P-domain, had any impact on ERp57 interaction. I used a Surface Plasmon Resonance (SPR) or BIAcore to investigate whether ERp57 binds to the calnexin mutants [10, 12]. BIACore technology exploits SPR to determine the affinity of two ligands, with one immobilized on a matrix and the other in a test solution. When these ligands associate, the result is an increase in mass and when the molecules disassociate, the mass decreases. Mass changes can be monitored by an SPR signal and binding and rate constants can be calculated [10, 12, 26].

Purified, soluble canine wild-type calnexin and calnexin mutants, His^{202}, Cys$^{161/195}$ and Cys$^{361/367}$ were covalently bound to dextran matrix sensor chip as the ligand and his-tagged ERp57 was in solution as the analyte (See "Materials and Methods"). Consistent with previous studies, an increase in mass was seen for wild-type calnexin and ERp57 showing an interaction between the two proteins [12]. Both the binding constants (association tendency, K_A and dissociation tendency, K_D) of ERp57 to wild-type and calnexin mutants are within the normal parameters not only confirming that the systems is working but also indicating middle level of affinity of ERp57 for calnexin (Table 4-1). The rate constants (k_a, k_d) of ERp57 for wild-type calnexin and calnexin mutants also fall within the normal parameters however, differences between the rate of association and disassociation of ERp57 to calnexin and calnexin mutants are observed (Table 4-1.) When comparing the rates of complex formation (K_a), I observed that the Cys$^{361/367}$, P-domain calnexin mutant has a slower complex formation then wild-type, His^{202} and Cys$^{161/195}$ calnexin (Table 4-1).

I also observed that all three calnexin mutants form a less stable complex with ERp57 when compared to wild-type with the $Cys^{361/367}$ having the least stable complex (Table 4-1). I also plotted the R_{max} values of wild-type, His^{202}, $Cys^{161/195}$ and $Cys^{361/367}$ calnexin in order to evaluate the amount of interaction of calnexin with ERp57 (Figure 4-7). These R_{max} were plotted taking into the following parameters: the predicted R_{max}, the molecular weight of both ligand and analyte and the valence of these two molecules. The wild-type:ERp57 binding was arbitrarily set to "1" and the obtained R_{max} values of the calnexin mutants was normalized to this. We determined that all three calnexin mutants bound more ERp57 than the wild-type calnexin protein (Figure 4-7). The His^{202} and $Cys^{161/195}$ N-globular domain mutants bound approximately 2.5-fold more ERp57 while the $Cys^{361/367}$ P-domain mutants bound approximately 5-fold more ERp57 when compared to wild-type (Figure 4-7). This His^{202} and $Cys^{161/195}$ mutations are found within the N-globular domain of calnexin which has not been shown to have a role in ERp57 binding. The observed increase in bound ERp57 may result from indirect effects on the interacting P-domain that could potentially expose residues involved in ERp57 binding. This phenomenon has been observed previously with both calnexin and calreticulin where N-domain mutations result in increased ERp57 binding [12] [10]. Interestingly, the $Cys^{361/367}$ results in a 5-fold increase in binding of ERp57 compared to wild-type calnexin (Figure 4-7). This suggests that mutation to these P-domain cysteines can result in some conformational changes that may expose residues involved in ERp57 binding causing increased accessibility and binding.

Table 4-1: Kinetic analysis of surface plasmon resonance of recombinant ERp57 binding to soluble wild-type calnexin and calnexin mutants.

Mutant	ka (1/Ms)	kd (1/s)	KA (1/M)	KD (M)
CNX-wt	**1.98e4**	**1.03e-2**	**1.93e6**	**5.19e-7**
CNX-His^{202}	**1.05e4**	**3.24e-3**	**3.25e6**	**3.07e-7**
CNX-$Cys^{161/195}$	**2.2e4**	**4.35e-3**	**5.06e6**	**1.97e-7**
CNX-$Cys^{361/367}$	**1.93e3**	**4.54e-4**	**4.36e6**	**2.3e-7**

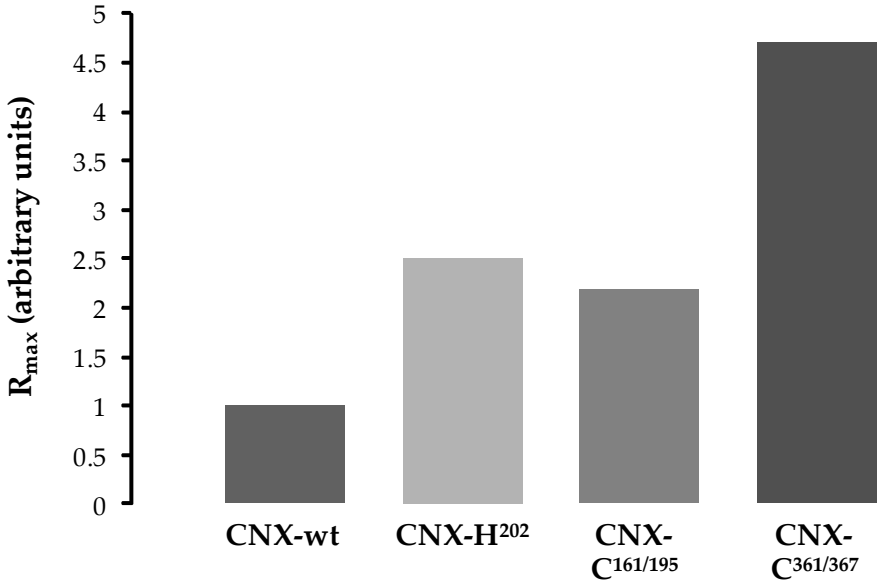

Figure 4-7

Figure 4-7 - Maximum interaction of soluble wild-type calnexin and His^{202}, $Cys^{161/195}$ and $Cys^{361/367}$ calnexin mutants with recombinant ERp57 by surface plasmon resonance (SPR) Purified soluble calnexin and calnexin mutants were covalently bound to a sensor chip and ERp57 injected over the chip and mass changes were recorded. The bar graphs are the R_{max} values of wild-type calnexin and calnexin mutants normalized for molecular weight and valence. R_{max} is plotted in arbitrary units as compared to wild-type. The graph is representative of two experiments.

Discussion

In this study I carried out functional and structural studies of N-domain and P-domain mutants of calnexin. I looked at the impact of specific cysteine and histidine mutants would have on the chaperone activity of calnexin on both non-glycosylated and glycosylated substrates, the impact on ERp57 binding and the impact on the structure of calnexin. I focused on the cysteine residues in the N-domain (Cys^{161}, Cys^{195}) as it has been predicted that they form a disulfide bridge that may be important for the function of calnexin [13, 14]. The P-domain cysteine residues (Cys^{361}, Cys^{367}) are also of interest in our studies because it has been predicted that they also form disulfide bonds [13, 14] and this may contribute to the structure of calnexin and impact on function. I was also interested in investigating the histidine residues in the N-globular domain, particularly His^{202} as the corresponding histidine in calreticulin (His^{153}) has been previously shown to be critical in the chaperone function of calrecticulin [11].

Consistent with earlier studies, I found that wild-type, soluble calnexin prevented aggregation of both glycosylated substrate (IgY) and, to a lesser extent, the non-glycosylated substrate (MDH) [12]. This further supports that calnexin may bind both glycosylated and non-glycosylated substrates while showing specificity for glycosylated substrates [12]. I report that both the $Cys^{361/367}$ and the $Cys^{161/195}$ residues are important for folding of glycosylated substrates as we observe loss of aggregation of IgY. The N-globular domain cysteines are conserved within calreticulin (Cys^{88} and Cys^{120}) and mutation to these residues resulted in partial disruption of chaperone activity of calreticulin [10] while mutations to the N-globular

domain $Cys^{161/195}$ of calnexin results in significant loss of chaperone activity. Structural studies on calnexin have modelled a putative carbohydrate binding site in the N-globular domain of calnexin with the third mannose residue of the carbohydrate wrapping around the Cys^{161}-Cys^{195} residues [13]. The involvement of the $Cys^{161/195}$ residues in the carbohydrate binding site [13] is further supported by evidence that there is increased aggregation of the non-glycosylated substrate, MDH. Taken together, our studies corroborate with structural studies providing further evidence that the Cys^{161}-Cys^{195} residues form an important part of the carbohydrate binding site and have a role in the folding of glycosylated substrate. Interestingly, we observe that the His^{202} residue has no role in the chaperone function of calnexin for either glycosylated or non-glycosylated substrate. Although this was surprising because the conserved histidine residue in calreticulin (His^{153}) has been found to be critical for chaperone function [10], this suggests that calnexin and calreticulin may chaperone differently and this may contribute to the specificity of their substrates. The His^{219} also did not impact thermal aggregation of glycosylated or non-glycosylated substrates further suggesting that histidine residues in the N-globular domain of calnexin do play a role in chaperone function.

The P-domain of calnexin is a flexible arm domain that contains 4 copies of two unique proline rich domains arranged in 1111222 pattern [3, 13]. The four copies of motif 1 and motif 2 extend away from the lectin domain and fold back on one another forming a large hairpin [13]. This domain, because of its unusual extended curved structure, is thought to have a role in substrate binding [3]. I have found that the cysteine residues 361 and

367 in the P-arm domain seem to be important in folding of glycosylated substrate, although to lesser extent then the N-globular domain cysteines. These cysteines are not conserved in calreticulin [13] and perhaps play a novel structural or functional role in calnexin. Interestingly, mutations to these residues do not impact the thermal aggregation of the non-glycosylated substrate but do partially prevent the thermal aggregation of glycosylated substrate.

The P-arm domain has also been show to mediate ERp57 interaction, specifically through residues located at the tip such as residues Trp^{343} and Asp^{344} in the 4^{th} repeat of motif 1 and Gly^{349} and Glu^{352} located in the 4^{th} repeat of motif 2 [5]. I have found that when I mutate the P-domain $Cys^{361/367}$ residues found in the 4^{th} repeat of motif 2, we increase the interaction with ERp57. Interestingly, I also observed that there is slower ERp57:calnexin complex formation and this complex is less stable in the $Cys^{361/367}$ mutant. This suggests that disruption of $Cys^{361/367}$ potentially results in local conformational changes that could expose the nearby established ERp57 interaction residues (see above) resulting in increased interaction, however, this interaction is not normal as revealed by the lack of propensity to form an unstable complex. This result also provides further evidence for the model of ERp57 binding to calnexin to fold substrates rather than binding to calnexin to help form disulfide bonds of calnexin [27]. Furthermore, we found that the N-globular domain His^{202} and $Cys^{161/195}$ residues also are involved in ERp57 binding and when mutated, interaction with ERp57 is enhanced forming a slow and less stable complex, although to a lesser extent then the P-domain mutant. Although ERp57 interaction with calnexin is not mediated through its N-

domain, previous studies have shown that mutations to the N-domain of calnexin [12] and calreticulin [10] can result in enhanced ERp57 binding suggesting that modifications to the carbohydrate binding site results in conformational changes and functional properties that ERp57 binding is affected. Limited trypsin proteolysis analysis showed that in the $Cys^{161/195}$ mutant there are differences in the accessibility of trypsin to calnexin. This indicates that there may be minor structural differences in this mutant that may affect ERp57 binding.

In conclusion, I have carried out site-specific mutagenesis to generate mutations to cysteines (Cys^{161}, Cys^{195}, $Cys^{161/195}$, Cys^{361}, Cys^{367} and $Cys^{361/367}$) and histidines (His^{202} and His^{219}). These studies have shown the cysteine residues in the N- and P-domain of calnexin are involved in the functioning of the protein. I have identified the N-globular cysteines Cys^{161} and Cys^{195}, near the carbohydrate binding pocket, as having a major role in the chaperone activity of glycosylated proteins while the P-domain cysteines Cys^{361} and Cys^{367} as having a more of a minor role in the chaperone activity of glycoyslated proteins. I also found that the Cys^{161} and Cys^{195} and His^{202} enhance ERp57 binding and Cys^{361} and Cys^{367}, located near residues involved in ERp57 binding, significantly increase ERp57 interaction and this all occurs presumably through minor conformational changes resulting from mutations to these residues.

References

1. Hebert, D.N. and M. Molinari, *In and out of the ER: protein folding, quality control, degradation, and related human diseases.* Physiol Rev, 2007. **87**(4): p. 1377-408.
2. Williams, D.B., *Beyond lectins: the calnexin/calreticulin chaperone system of the endoplasmic reticulum.* J Cell Sci, 2006. **119**(Pt 4): p. 615-23.
3. Jung, J., Coe, H., Opas, M., and Michalak, M., *Calnexin: An Endoplasmic Reticulum Integral Membrane Chaperone.* Calcium Binding Proteins, 2006. **1**(2): p. 67-71.
4. Leach, M.R., et al., *Localization of the lectin, ERp57 binding, and polypeptide binding sites of calnexin and calreticulin.* J Biol Chem, 2002. **277**(33): p. 29686-97.
5. Pollock, S., et al., *Specific interaction of ERp57 and calnexin determined by NMR spectroscopy and an ER two-hybrid system.* Embo J, 2004. **23**(5): p. 1020-9.
6. Kraus, A., et al., *Calnexin deficiency leads to dysmyelination.* J Biol Chem, 2010.
7. Denzel, A., et al., *Early postnatal death and motor disorders in mice congenitally deficient in calnexin expression.* Mol. Cell. Biol., 2002. **22**(21): p. 7398-7404.
8. Jung, J., Janowicz, A., Coe, H., Kraus, A. and Michalak, M. , *Specialization of Endoplasmic Reticulum Chaperones for the Folding and Function of Myelin Glycoproteins P0 and PMP22.* submitted, 2010.
9. Coe, H., et al., *Endoplasmic reticulum stress in the absence of calnexin.* Cell Stress Chaperones, 2008. **13**(4): p. 497-507.
10. Martin, V., et al., *Identification by mutational analysis of amino acid residues essential in the chaperone function of calreticulin.* J Biol Chem, 2006. **281**(4): p. 2338-46.
11. Guo, L., et al., *Identification of an N-domain histidine essential for chaperone function in calreticulin.* J. Biol. Chem, 2003. **278**: p. 50645-50653.
12. Groenendyk, J., Dabrowska, M., and Michalak, M., *Mutational analysis of calnexin.* Biochimica et Biophysica Acta, 2010.
13. Schrag, J.D., et al., *The structure of calnexin, an ER chaperone involved in quality control of protein folding.* Mol. Cell, 2001. **8**: p. 633-644.
14. Ou, W.J., et al., *Conformational changes induced in the endoplasmic reticulum luminal domain of calnexin by Mg-ATP and Ca2+.* J Biol Chem, 1995. **270**(30): p. 18051-9.
15. Zapun, A., et al., *Enhanced catalysis of ribonuclease B folding by the interaction of calnexin or calreticulin with ERp57.* J Biol Chem, 1998. **273**(11): p. 6009-12.
16. Corbett, E.F., et al., *Ca2+ regulation of interactions between endoplasmic reticulum chaperones.* J Biol Chem, 1999. **274**(10): p. 6203-11.

17. Coe, H., et al., *ERp57 modulates STAT3 signalling from the lumen of the endoplasmic reticulum.* J Biol Chem, 2009.
18. Milner, R.E., et al., *Calreticulin, and not calsequestrin, is the major calcium binding protein of smooth muscle sarcoplasmic reticulum and liver endoplasmic reticulum.* J. Biol. Chem., 1991. **266**: p. 7155-7165.
19. Nakamura, K., et al., *Changes in endoplasmic reticulum luminal environment affect cell sensitivity to apoptosis.* J. Cell Biol., 2000. **150**: p. 731-740.
20. Balakier, H., et al., *Calcium-binding proteins and calcium-release channels in human maturing oocytes, pronuclear zygotes and early preimplantation embryos.* Hum. Reprod., 2002. **17**(11): p. 2938-2947.
21. Saito, Y., et al., *Calreticulin functions in vitro as a molecular chaperone for both glycosylated and non-glycosylated proteins.* EMBO J., 1999. **18**: p. 6718-6729.
22. Lefevre, F., M.H. Remy, and J.M. Masson, *Alanine-stretch scanning mutagenesis: a simple and efficient method to probe protein structure and function.* Nucleic Acids Res, 1997. **25**(2): p. 447-8.
23. Corbett, E.F., et al., *The conformation of calreticulin is influenced by the endoplasmic reticulum lumenal environment.* J. Biol. Chem., 2000. **275**: p. 27177-27185.
24. Lee, G.J., et al., *A small heat shock protein stably binds heat-denatured model substrates and can maintain a substrate in a folding-competent state.* EMBO J., 1997. **16**(3): p. 659-671.
25. Oliver, J.D., et al., *ERp57 Functions as a Subunit of Specific Complexes Formed with the ER Lectins Calreticulin and Calnexin.* Mol. Biol. Cell, 1999. **10**: p. 2573-2582.
26. Phizicky, E.M. and S. Fields, *Protein-protein interactions: methods for detection and analysis.* Microbiol. Rev., 1995. **59**: p. 94-123.
27. Bedard, K., et al., *Cellular functions of endoplasmic reticulum chaperones calreticulin, calnexin, and ERp57.* Int Rev Cytol, 2005. **245**: p. 91-121.

Chapter Five
General Discussion

The objective of my thesis was to determine the critical functionality of calnexin and ERp57 with an emphasis on the expression throughout development and role in the quality control cycle and intracellular signalling. Major findings from this work included:

- expression of calnexin and ERp57 throughout embryonic development is restricted to neurological and cartilage tissue and to lung, liver and brain tissue, respectively.
- calnexin and ERp57 both have a role in the adaptive unfolded protein response to ER stress
- ERp57 modulates STAT3 signalling from the ER lumen in association with calreticulin
- cysteine residues in the N-globular domain of calnexin are involved in the binding of glycosylated substrate.

I investigated these two ER associated proteins at both the animal level as well as the cellular level. The expression of both proteins throughout embryonic development as well as post-natally was determined. The function of both ERp57 and calnexin in intracellular signalling was examined and residues important to the structure and function of calnexin as a chaperone in association with ERp57 were also looked at. This study suggested that ERp57 and calnexin may impact and be involved in the normal development of specific tissues. As well, I also used calnexin- and ERp57-deficient cell lines to investigate the role both calnexin and ERp57 have in intracellular signalling that could contribute to phenotype observed.

Calnexin and ERp57 Expression Throughout Development

The calnexin-deficient mouse model is viable but displays severely ataxic phenotype [1]. These mice are 30-50% smaller than their wild-type littermates and have severe gait disturbances [1, 2]. Electron micrographs show severe dismyelination of the spinal cord and sciatic nerve resulting in reduced nerve conduction velocity [2]. This phenotype suggests that the calnexin expression may be restricted to specific tissues during embryonic development. On the other hand universal deletion of ERp57 in mouse models results in embryonic lethality while tissue specific deletion of ERp57 in B cells results in a live mouse that has aberrant assembly of the peptide loading complex [3]. Understanding the tissue expression of ERp57 and calnexin throughout embryonic development will allow us to gain insight into critical role it plays in development in utero as we can learn where ERp57 and calnexin are expressed and potentially where they may play a developmental role.

My studies have revealed that calnexin is highly expressed early on in embryonic development in cartilage and neuronal tissue with later expression in the liver and little to no expression observed in the heart (Figure 2-1, 2-2, 2-3). The neuronal expression that we observed is not surprising as the calnexin-deficient mouse model exhibits motor disorders [1, 2]. The calnexin-deficient mice also have dismyelination of the peripheral nervous system (PNS) [2]. In *Caenorhabditis elegans* calnexin (CNX-1) is expressed in dorsal and ventral nerve cord and head and tail neurons throughout development [4]. *C. elegans* deficient in calnexin showed no gross morphological defects under normal conditions

however, under stress conditions, these animals showed decreased brood size as well as increased larval and embryonic lethality suggesting a role for calnexin in stress induced chaperone functions [4]. Further studies support a role of calnexin in neuronal development as calnexin has been shown to form functional complexes with myelin proteins, peripheral myelin protein 22 (PMP22) and protein zero (P0) [5, 6]. In the absence of calnexin, these proteins are misfolded, they escape quality control and are localized correctly but are non-functional as adhesion proteins of myelin [5]. Mutants of PMP22 are retained in the ER and have been linked to the human pathologies Charcot-Marie-Tooth Disease and Dejerine-Sottas syndrome [6]. Calnexin has also been found to interact with a mutant form of the ER transmembrane protein, sepien and it is has been implicated in several motor neuron pathologies including Silver's syndrome, variants of Charcot–Marie–Tooth disease type 2, dHMNV (distal hereditary motor neuropathy type V) and spastic paraplegia motor disorders [7, 8]. It is possible that the role of calnexin in development is neuroprotective and it has chaperone specificity for proteins involved in neurological development. How calnexin would mediate this specificity remains to be answered however, the localization of calnexin to neurological tissue provides further evidence for this theory. Interestingly, calnexin and calreticulin, a soluble ER resident homolog of calnexin, have very similar domain structure (Figure 1-4, 1-5) and have some redundant properties. However, the mouse model deficient phenotypes of both proteins are completely different. The calreticulin-deficient mouse model is embryonic lethal due to cardiac malformation resulting from impaired Ca^{2+} signalling (See '*2.2biii – Mouse Models*') [9]. Calreticulin is highly expressed in the

developing heart [9] while we see decreased calnexin expression in the heart throughout development (Figure 2-1, 2-2, 2-3). This study provides further evidence that calreticulin and calnexin do not have compensatory roles in terms of tissue development, as they are expressed in differently.

The difference in substrate specificity of calnexin and calreticulin may simply be a matter of one lectin being soluble (calreticulin) and the other being membrane bound (calnexin) [10]. In fact, when the soluble domain of calnexin is expressed, the pattern of substrate binding is very similar to that of calreticulin, however, soluble calnexin cannot replace calreticulin in all cases [10-12]. Calnexin and calreticulin may bind the same substrate, however, they bind different oligosaccharides or at different stages of the maturation process [10]. Another school of thought is that calnexin mediates specificity of substrates through its transmembrane domain by either promoting association of calnexin to membrane proteins by placing it at the ER membrane or it could directly bind the transmembranes of target proteins [13]. Studies with proteolipid protein (PLP) a non-glycosylated membrane protein that associates with calnexin have shown that calnexin binds the misfolded transmembrane domain [13]. Calnexin binds the membrane proteins PMP22 and P0 [5, 6] providing another example of calnexin binding membrane proteins. Both PMP22 and P0 are glycosylated proteins and calnexin presumably interacts through the carbohydrate binding domain found in the N-globular domain [14, 15], however, what mediates the interaction of PMP22 and P0 to calnexin over an interaction with the luminal chaperone calreticulin is unknown. It would be interesting to generate a luminal calnexin protein (N + P-domain) with no transmembrane or cytosolic C-

tail and determine if it is able to interact with both P0 and PMP22. If the interaction between calnexin and PMP22 or P0 was abolished, one could presume that the transmembrane domain and/or cytosolic tail play a role in the specificity of calnexin substrate binding.

Throughout embryonic development, we also observed calnexin expression in cartilage and vertebra (Figure 2-1). Proteoglycans, which are important structural components of the extracellular matrix of cartilage, are also found to be expressed in the central nervous system specifically the developing and mature brain [16]. Proteoglycans co-localize with a number of putative binding partners during differentiation of the central nervous system tissue suggesting that proteoglycans may also have a role in brain development [16]. This provides us with evidence of a link between skeletal and neuronal development. Together with our β-galactosidase staining of developing embryos (Figure 2-1) it is highlighted how important it is for us to investigate skeletal development in calnexin-deficient mice. Interestingly, DNA micro-array analysis has identified genes relevant for cartilage and bone formations that are developmentally regulated in myelinating nerves [17]. One of these up-regulated genes is collagen alpha type II (Col2α1) which is a key component of cartilage but has also been detected in other tissues, such as the notochord, during development [17]. The Col2α1-deficient mouse is viable but dies shortly after birth and develops skeletons with no endochondral bone (bone that replaces cartilage) [18]. Col2α1 is regulated by axonal signals, such as Sox9 and Maf-2, and was shown to be expressed in Schwann cell lineage as early as E14 of embryonic development and in both myelinating and nonmyelinating Schwann cells [17]. It is thought that Col2α1 binds specific

growth factors to divert early glia to other lineages [17]. Another transcription factor known to be involved in Schwann cell development and the myelination program *in vivo* is Krox-20 [17]. By looking at Krox-20-deficient embryos, Krox-20 has been shown to be important for hindbrain development and development of the peripheral nervous systems [19]. However, Krox-20-deficient mice also have skeletal abnormalities characterized by decreased length and thickness of newly formed bones [19]. The Col2α1- and Krox-20-deficient mouse models highlight the relationship between neuronal development and proper bone formation.

In this study, we also looked at the tissue specific expression of ERp57 throughout mouse embryonic development. We found that ERp57 is highly expressed in the inner cell mass of blastocysts, which is important for fetus formation [20], as well as the lung, liver and the brain during early stages of embryonic development (Figure 3-4 and 3-5). The *ERp57*$^{-/-}$ mouse is embryonic lethal at stage 13.5 post-coitum (Table 3-1) and the role it plays in these tissues may be of critical importance to survival. In the neonatal rat model of hyperoxia-induced lung injury as well as cultured cells, there is a down-regulation of ERp57 [21]. Additionally, siRNA studies to knockdown ERp57 expression in epithelial cells showed a decrease in tunicamycin- or hyperoxia-induced apoptosis (as measured by caspase-3 activation), however, there was an increase in the UPR (as measured by GRp78/BiP expression) [21]. Taken together, expression of ERp57 in the lungs of the developing embryo (Figure 3-4 and 3-5) as well as ERp57 providing cellular protection against hyperoxia-induced apoptosis in epithelial cells [21], suggests that ERp57 may have a

protective role to prevent paediatric lung injury. ERp57 expression in the brain is also of interest as siRNA studies performed on N2 neuroblastoma cells [22]. Neuroblastoma, a malignant neoplasm that arises from the sympathetic nervous system (SNS), is the most common solid tumour in children and has a very poor prognosis highlighting the need for new treatment and therapy [23]. N2 neuroblastoma cells are derived from the bone marrow of metastatic tumours of children and siRNA studies to knockdown ERp57 expression results in an increase in sensitivity to misfolded prion proteins (PrP^{SC}) whereas over-expression of ERp57 significantly protects cells against PrP^{SC} toxicity [22]. Furthermore, progression of murine scrapie results in an up-regulation of ERp57 which corresponds to the kinetics of prion replication in different brain areas, suggesting that ERp57 up-regulation is a specific cellular response induced by prion replication *in vivo* [22]. ERp57, with calreticulin, have been shown to be the carrier proteins that prevent aggregation of β-amyloids, a major component of toxic plaques found in the brains of Alzheimer's patients [24]. Together, these results suggest that ERp57 expression is an early event in pathology and perhaps has a role in modulating neurotoxicity [22]. ERp57 may be a novel target for transmissible spongiform encephalopathy (TSE) therapy and other neurodegenarative disease, such as Alzheimer's disease, that result from misfolded proteins [22]. Interestingly, in liver failure, resulting from inhalation of the anaesthetic halothane, ERp57 is triflouraceylated and non-functional resulting in an increase in misfolded proteins which contributes to liver toxicity [25, 26]. The expression pattern of ERp57 throughout development in the liver, lungs and brain (Figure 3-4 and 3-5) complements studies carried out on

cells derived from these tissues or from *in vivo* studies showing that ERp57 is protective in the health and survival of these specific organs [21, 22, 25].

The expression pattern of calnexin and ERp57 provide invaluable information about the potential organs and systems that could be affected by the absence of these proteins. Interestingly, calnexin and ERp57 have different expressions patterns then the ER chaperone, calreticulin. At early stages of embryonic development calreticulin is expressed primarily in the heart [9] while calnexin is expressed primarily in the brain (Figure 2-1 and 2-2) and ERp57 is expressed primarily in lung, liver and brain tissue (Figure 3-4 and 3-5). As well, the deficient-mouse models of these three proteins are different with calreticulin-deficient mouse being embryonic lethal at E12.5 due to cardiac malformation [9], calnexin-deficient mouse being viable but ataxic [1, 2] and ERp57-deficient mouse being embryonic lethal at E13.5 [3, 27]. Collectively, this suggests that although these three proteins that are known to function together in the quality control cycle of the ER, may have very specific roles in quality control or outside of this cycle that are important for the correct development of specific systems in utero and post-natally.

The Role of Calnexin and ERp57 in the Unfolded Protein Response

The ER is the primary protein folding compartment of the cell and, as such, during cell growth, differentiation and in response to environmental stimuli, it has to deal with different protein folding demands [28]. In response to developmental demands and physiological requests, the ER has developed the capacity to enhance protein folding and expedite secretion [28]. However, if the ER continues to be overwhelmed by protein

load, it has evolved the UPR (Figure 1-7) to deal with this accumulation [29]. Evidence suggests that long-lasting ER insult results in prolonged activation of UPR and this can contribute to the pathogenesis of many diseases [28]. Apoptotic pathways emanate from the ER and are extensions of UPR that are mediated by IRE1, caspase-12 and PERK/CHOP [28]. We found that both in the absence of calnexin and the absence of ERp57 there is an activation of the unfolded protein response (Figure 2-5 and 2-6 for calnexin and Figure 3-8 for ERp57.)

Although wild-type and calnexin-deficient cells seem to have the same capacity for ER stress induction (when stimulated by tunicamycin and thapsigargin) in non-stimulated cells, calnexin-deficient cells have increased UPR when compared to wild-type controls. Interestingly, the spine, cerebellum, brain and liver of calnexin-deficient mice showed no activation of UPR when compared to wild-type control littermates (Figure 2-8, 2-9). ER stress is a two-faced term encompassing both acute stress that is transient in nature such as chemical insult and chronic stress that is persistent such as a genetic mutation to a component of the quality control pathway [30]. Acute stress requires cells to tolerate a brief period of perturbation and then recover by restoring ER homeostasis while chronic stress requires long term adjustments to cellular function [30]. Calnexin-deficiency represents a chronic stress where a component of the quality control pathway is completely absent. Despite the increase in UPR observed in the calnexin-deficient cells, we do not observe an increase in cell death as these cells adhere to plastic and proliferate (Figure 2-4) [31]. One characteristic that is common amongst different kinds of chronic stresses (for example, viral infection that can designate the secretory

pathway for production of viral proteins or various neurodegenerative disorders of protein aggregation) is that they demand a cellular mechanism that can tolerate insult over longer periods of time so there is minimal cell death [30]. It appears that calnexin-deficient cells have evolved an adaptive response that allows them to survive and avoid apoptosis as they are able to survive *in vitro* in cell culture (Figure 2-4) [30-32]. It has been suggested that one adaptation of cells undergoing chronic stress is to improve the protein processing capabilities so as not to execute apoptotic cascades [30]. Indeed, calnexin-deficient cells have increased proteasomal activity (Figure 2-7) suggesting an increase in ER associated degradation (ERAD) to deal with constitutively misfolded proteins in the ER. However, this raises the question that if there is increased ERAD, is there a corresponding increase in protein secretion as another mechanism to deal with the burden of misfolded proteins on the ER? If so, what is the mechanism that decides which misfolded substrate is degraded and which is secreted? Recent studies have shown that there is a competition between ERAD and protein secretion machineries suggesting that the decision whether to degrade or transport a substrate is effected by a number of factors including cell stress [33, 34]. There is an adaptable model for protein transport that goes beyond the traditional school of thought that mutated proteins are degraded by ERAD if they are less stable then wild-type and sent for secretion if they are more stable then wild-type [35]. This adaptable model reveals that export efficiency is affected not only by folding and misfolding energetics but also by adjustable biological factors such as ERAD [35]. Very recent results from our laboratory indicate that calnexin substrates, PMP22 and P0, are transported to the cell surface in

the absence of calnexin [5]. Although both PMP22 and P0 have been shown to be non-functional at the cell surface they nevertheless, are properly localized [5]. Interestingly, they are not retained in the ER or sent for ERAD despite an increase in proteasomal activity in calnexin-deficient cells [32]. What we know, is that the absence of calnexin is a chronic type of ER stress and that this results in activation of the UPR. Calnexin-deficient cells, however, have an adaptive response where they have increased proteasomal activity to, presumably, clear rapidly accumulating proteins. Interestingly, in the absence of calnexin both PMP22 and P0 escape ERAD and are exported to the cell surface [5]. The adaptable model in the context of calnexin-deficient cells suggest that the absence of calnexin affects more than just the quality control cycle and, in fact, disrupts ER homeostasis and must make adjustments accordingly. This is not surprising as previous work has shown that in the absence of the chaperone calreticulin, ER intracellular Ca^{2+} stores are dramatically affected [9, 36]. Although this study has determined that one of these mechanisms is an increase in ERAD, recent evidence suggests that secretion of non-functional proteins may also be affected or even increased [5]. In order to fully understand the impact the absence of calnexin has on ER homeostasis in terms of degradation and secretion, we need to determine a several parameters: (i) how has calnexin-deficiency resulted in an increase proteasomal activity?, (ii) is there an increase in protein secretion in the absence of calnexin? and (iii) what are the mechanisms and factors that decide which proteins are degraded and which proteins are secreted in the absence of calnexin? The absence of calnexin resulting in both hyperactive proteasomal activity and non-functional but properly

localized proteins together with a neurological phenotype of mouse deficient models highlights the essential role calnexin plays within the ER and how its absences upsets this critical balance.

We also investigated the activation of the UPR in the absence of ERp57. ERp57-deficient cells also showed an increase in UPR, however, when we expressed full-length recombinant ERp57 in ERp57-deficient cells, we did not see a rescue of UPR (Figure 3-8). In the absence of ERp57, there seems to be a tolerable low level of UPR that does not activate the apoptosis pathway, impact ER morphology or expression of ER associated chaperones and foldases. Our results suggest that the ERp57-deficient cells may be considered, like the calnexin-deficient cells, a genetic example of chronic stress and they have adapted to this low-level of persistent stress [37]. The adaptive responses of cells deficient in calnexin and ERp57 are not surprising as a deficiency in UGGT1, another component of the quality control pathway, has been demonstrated as a genetic example of chronic ER stress that has evolved an adaptive response [37]. The ERp57-deficient cells have some of the hallmarks of an adaptive response because the cell population does not undergo apoptosis, proliferation still occurs despite activation of UPR however, they are not desensitized to stress introduced by a perturbant [37]. When both wild-type and ERp57-deficient cells lines are treated with the classical ER stress inducer, thapsigargin, there is an increased activation of the UPR in the absence of ERp57 (Figure 3-8). However, this is not rescued by expression of recombinant ERp57 in ERp57-deficient cells suggesting that ERp57-deficient cells have adapted to this low-level of UPR. In fact, when we treated wild-type and ERp57-deficient cells with thapsigargin and measure apoptosis by Annexin-V

binding, there was a significantly less cell death in the absence of ERp57 (Figure 3-9). This provides additional evidence that ERp57-deficient cells may have adapted to a low-level, tolerable of UPR.

Our studies provide further evidence for a model showing that cells are able to adapt to mild, chronic ER stress for survival which is different for constitutively active UPR that results in apoptosis [37]. This suggests that the calnexin and ERp57 may have other functions that contribute to the pathologies of their respective mouse model phenotypes. For example, calnexin has been shown to interact with myelin specific proteins P0 and PMP22 and it has been suggested that in the absence of calnexin they are non-functional and could contribute to the phenotype observed [2, 5]. ERp57 has also been shown to interact with STAT3 and loss of modulation of this transcription factor may also be implicated in the ERp57-deficient mouse embryonic lethality [27, 38-42].

ERp57 and STAT3 Signalling

Outside of its role as a foldase in the ER, ERp57 (GRp58) has also been reported to affect STAT3 signalling *via* interaction of STAT3 [38-40, 43, 44]. Indeed the absence of ERp57 results in an increase in STAT3 signalling and this phenomenon is mediated by the ER form of ERp57 (Figure 3-10). Additionally, STAT3 activity depends on the formation of ERp57-calreticulin complexes in the lumen of the ER (Figure 3-14, 3-15). Both of these findings were initially surprising however, this is not the first time that cellular events are controlled by "ER signalling" and it is also not the first time ERp57 has been shown to complex with calreticulin to impact biological events [45-49].

How ERp57, in complex with calreticulin, signals from the ER lumen to impact STAT3 signalling is not clear at present. There are several way that STAT can be activated including (i) the classical model of the JAK-STAT pathway that is activated in response to cytokines, (ii) direct phosphorylation by receptor tyrosine kinases, (iii) through non-receptor associated tyrosine kinases (iv) by G-coupled protein receptors or (v) by adaptor proteins bringing JAK proteins into close proximity to STATs [50]. STAT3 can be activated by the classical pathway through the binding of cytokines and growth factors, by chemokine binding to G-coupled protein receptors MIP-1 and RANTES and MEKK1-C and islet-25 acting as adaptors to bring STAT3 into close proximity of JAKs [50]. Now, it is emerging that aside from Tyr and Ser phosphorylation status to regulate STAT activation, Arg methylation, acetylation/deacetylation, isomerization, ubiquitination, SUMOylation, ISGylation, proteolysis, protein-protein interaction, have all been described to affect the activities of STATs [50]. The more we learn about STATs it becomes very clear how complicated regulation of activation is and we now wonder how ER localized proteins ERp57 and calreticulin fit into this puzzle. There, however, be some physiological relevant relationship between STAT3, ERp57 and calreticulin. Interestingly, in keloid scars, STAT3 is hyperphosphorylated and expressed suggesting that STAT3 may have a role in would healing, cell migration and collagen disposition [50]. Calreticulin is also found to promote wound healing and when calreticulin is applied to the wounds of diabetic mice; their wounds heal faster than wild-type controls [51]. As well, tissue specific deletion of STAT3 in bronchiolar and alveolar epithelial cells results in enhanced

apoptosis following adenoviral injection suggesting a cytoprotective function of STAT3 [50]. ERp57, has also been shown to be protective in hyperoxia-induced apoptosis in epithelial cells [21]. Taken together, the interplay between calreticulin and ERp57 may represent another branch of STAT3 activation and regulation whose fine control could be critical for proper development and cellular functioning.

STAT3-deficient mice are embryonic lethal at very early stages of embryogenesis between E6.5 and E7.5 post-coitum [42]. It is thought that lethality may be due to defect in the visceral endoderm function which is the principal site of nutrient exchange between the maternal and embryonic environments [52]. However, it remains unknown what the ligand is in the visceral endoderm that activates STAT3 signalling [52]. As discussed, STAT3 can be activated by a number of different cytokines and growth factors [50] and mouse-deficient models of a number of these factors have been shown to result in lethality [42]. However, these mice are lethal at different stages [42]. For example, LIF-receptor and CNFT-receptor deficient mice are lethal shortly after birth, gp130-deficient mice are embryonic lethal between E15.5-E18.5 and EGF-receptor deficient mice are embryonic lethal at E11.5 [42]. It is thought that the lethality observed may be due to loss of one or more of these signals [42]. This study has established embryonic lethality of ERp57-defiecient mice at E13.5 post-coitum [27]. This study has also shown that a complex between ERp57 and calreticulin formed in the ER lumen effects STAT3 signalling [27]. Although there are some discrepancies in terms of the time frame of lethality of the ERp57- or STAT3-deficient mouse model, this suggests that aberrant STAT3 signalling could contribute to the lethality observed in

ERp57-deficient mouse model. Constitutively active STAT3 (STAT3-C) has been known to be an oncogene and fibroblasts expressing STAT3-C developed malignant properties in culture and formed tumors in nude mice [53]. STAT3-C results in oncogenesis by conferring a survival advantage through inhibition of apoptosis [53]. Interestingly, in ERp57-deficient cells, we observe a decrease in apoptosis especially when exposed to a chemical perturbant (Figure 3-9). In ERp57-deficient cells we also observe an increase in STAT3 signalling suggesting that this inhibition of apoptosis could perhaps be due to an increase in STAT3 signalling (Figure 3-10).

Role of Disulfide Bonds in Calnexin Structure and Function

In this study, I have identified that the cysteines in the N- and P-domain of calnexin are critical to the chaperoning of glycosylated substrates. Mutation to these residues does not impact on calnexin structure suggesting that they have a direct role in the functioning of calnexin. This is interesting because it has been speculated that these cysteine residues form disulfide bonds and could potentially contribute to the maintaining the structural integrity of the N- and P- domain [14]. It has also been speculated that the N-terminal cysteine residues have a direct role in carbohydrate binding to calnexin [14].

Conclusion

In this study I examined the function of ER proteins calnexin and ERp57 by studying their expression throughout mouse development and their role in intracellular signalling. Both calnexin and ERp57 have been shown

to be critical for proper development in utero and this study has identified potential candidate tissues that these proteins impact. This study has also allowed us to gain thorough insight into the molecular mechanisms of both proteins both inside and outside their classical role in quality control. Together, this study has shown us that calnexin and ERp57 have unique functions. Insight into the critical functionality of both the calnexin and ERp57 gene will undoubtedly give us essential knowledge regarding the progression of devastating diseases. These ideas can be applied to novel strategies for early diagnosis and eventual treatment.

References:

1. Denzel, A., et al., *Early postnatal death and motor disorders in mice congenitally deficient in calnexin expression.* Mol. Cell. Biol., 2002. **22**(21): p. 7398-7404.
2. Kraus, A., et al., *Calnexin deficiency leads to dysmyelination.* J Biol Chem, 2010.
3. Garbi, N., et al., *Impaired assembly of the major histocompatibility complex class I peptide-loading complex in mice deficient in the oxidoreductase ERp57.* Nat Immunol, 2006. **7**(1): p. 93-102.
4. Lee, W., et al., *Caenorhabditis elegans calnexin is N-glycosylated and required for stress response.* Biochem Biophys Res Commun, 2005. **338**(2): p. 1018-30.
5. Jung, J., Janowicz, A., Coe, H., Kraus, A. and Michalak, M. , *Specialization of Endoplasmic Reticulum Chaperones for the Folding and Function of Myelin Glycoproteins P0 and PMP22.* submitted, 2010.
6. Dickson, K.M., et al., *Association of calnexin with mutant peripheral myelin protein-22 ex vivo: A basis for "gain-of-function" ER diseases.* Proc. Natl. Acad. Sci. U.S.A., 2002. **99**: p. 9852-9857.
7. Ito, D. and N. Suzuki, *Seipinopathy: a novel endoplasmic reticulum stress-associated disease.* Brain, 2009. **132**(Pt 1): p. 8-15.
8. Ito, D. and N. Suzuki, *Molecular pathogenesis of seipin/BSCL2-related motor neuron diseases.* Ann Neurol, 2007. **61**(3): p. 237-50.
9. Mesaeli, N., et al., *Calreticulin is essential for cardiac development.* J. Cell Biol., 1999. **144**: p. 857-868.
10. Molinari, M., et al., *Contrasting functions of calreticulin and calnexin in glycoprotein folding and ER quality control.* Mol. Cell, 2004. **13**(1): p. 125-135.
11. Gao, B., et al., *Assembly and Antigen-Presenting Function of MHC Class I Molecules in Cells Lacking the ER Chaperone Calreticulin.* Immunity, 2002. **16**: p. 99-109.
12. Danilczyk, U.G., M.F. Cohen-Doyle, and D.B. Williams, *Functional relationship between calreticulin, calnexin, and the endoplasmic reticulum luminal domain of calnexin.* J. Biol. Chem., 2000. **275**: p. 13089-13097.
13. Swanton, E., S. High, and P. Woodman, *Role of calnexin in the glycan-independent quality control of proteolipid protein.* Embo J, 2003. **22**(12): p. 2948-58.
14. Schrag, J.D., et al., *The structure of calnexin, an ER chaperone involved in quality control of protein folding.* Mol. Cell, 2001. **8**: p. 633-644.
15. Ou, W.J., et al., *Conformational changes induced in the endoplasmic reticulum luminal domain of calnexin by Mg-ATP and Ca2+.* J Biol Chem, 1995. **270**(30): p. 18051-9.

16. Bandtlow, C.E. and D.R. Zimmermann, *Proteoglycans in the developing brain: new conceptual insights for old proteins.* Physiol Rev, 2000. **80**(4): p. 1267-90.
17. D'Antonio, M., et al., *Gene profiling and bioinformatic analysis of Schwann cell embryonic development and myelination.* Glia, 2006. **53**(5): p. 501-15.
18. Li, S.W., et al., *Transgenic mice with targeted inactivation of the Col2 alpha 1 gene for collagen II develop a skeleton with membranous and periosteal bone but no endochondral bone.* Genes Dev, 1995. **9**(22): p. 2821-30.
19. Levi, G., et al., *Defective bone formation in Krox-20 mutant mice.* Development, 1996. **122**(1): p. 113-20.
20. Ghassemifar, M.R., et al., *Gene expression regulating epithelial intercellular junction biogenesis during human blastocyst development in vitro.* Mol Hum Reprod, 2003. **9**(5): p. 245-52.
21. Xu, D., et al., *Knockdown of ERp57 Increases BiP/GRP78 Induction and Protects against Hyperoxia and Tunicamycin-induced Apoptosis.* Am J Physiol Lung Cell Mol Physiol, 2009.
22. Hetz, C., et al., *The disulfide isomerase Grp58 is a protective factor against prion neurotoxicity.* J Neurosci, 2005. **25**(11): p. 2793-802.
23. Seeger, R.C., et al., *Morphology, growth, chromosomal pattern and fibrinolytic activity of two new human neuroblastoma cell lines.* Cancer Res, 1977. **37**(5): p. 1364-71.
24. Erickson, R.R., et al., *In cerebrospinal fluid ER chaperones ERp57 and calreticulin bind beta-amyloid.* Biochem Biophys Res Commun, 2005. **332**(1): p. 50-7.
25. Martin, J.L., et al., *Halothane hepatitis patients have serum antibodies that react with protein disulfide isomerase.* Hepatology, 1993. **18**(4): p. 858-63.
26. Khanal, R.C. and I. Nemere, *The ERp57/GRp58/1,25D3-MARRS receptor: multiple functional roles in diverse cell systems.* Curr Med Chem, 2007. **14**(10): p. 1087-93.
27. Coe, H., et al., *ERp57 modulates STAT3 signalling from the lumen of the endoplasmic reticulum.* J Biol Chem, 2009.
28. Zhang, K. and R.J. Kaufman, *The unfolded protein response: a stress signaling pathway critical for health and disease.* Neurology, 2006. **66**(2 Suppl 1): p. S102-9.
29. Schroder, M. and R.J. Kaufman, *ER stress and the unfolded protein response.* Mutat Res, 2005. **569**(1-2): p. 29-63.
30. Rutkowski, D.T. and R.J. Kaufman, *That which does not kill me makes me stronger: adapting to chronic ER stress.* Trends Biochem Sci, 2007. **32**(10): p. 469-76.
31. Groenendyk, J., et al., *Caspase 12 in calnexin-deficient cells.* Biochemistry, 2006. **45**(44): p. 13219-26.

32. Coe, H., et al., *Endoplasmic reticulum stress in the absence of calnexin.* Cell Stress Chaperones, 2008. **13**(4): p. 497-507.
33. Kincaid, M.M. and A.A. Cooper, *Misfolded proteins traffic from the endoplasmic reticulum (ER) due to ER export signals.* Mol Biol Cell, 2007. **18**(2): p. 455-63.
34. Vembar, S.S. and J.L. Brodsky, *One step at a time: endoplasmic reticulum-associated degradation.* Nat Rev Mol Cell Biol, 2008. **9**(12): p. 944-57.
35. Wiseman, R.L., et al., *An adaptable standard for protein export from the endoplasmic reticulum.* Cell, 2007. **131**(4): p. 809-21.
36. Lynch, J. and M. Michalak, *Calreticulin is an upstream regulator of calcineurin.* Biochem. Biophys. Res. Commun., 2003. **311**(4): p. 1173-1179.
37. Rutkowski, D.T., et al., *Adaptation to ER stress is mediated by differential stabilities of pro-survival and pro-apoptotic mRNAs and proteins.* PLoS Biol, 2006. **4**(11): p. e374.
38. Eufemi, M., et al., *ERp57 is present in STAT3-DNA complexes.* Biochem Biophys Res Commun, 2004. **323**(4): p. 1306-12.
39. Guo, G.G., et al., *Association of the chaperone glucose-regulated protein 58 (GRP58/ER-60/ERp57) with Stat3 in cytosol and plasma membrane complexes.* J Interferon Cytokine Res, 2002. **22**(5): p. 555-63.
40. Coppari, S., et al., *Nuclear localization and DNA interaction of protein disulfide isomerase ERp57 in mammalian cells.* J. Cell. Biochem., 2002. **85**(2): p. 325-333.
41. Ndubuisi, M.I., et al., *Cellular physiology of STAT3: Where's the cytoplasmic monomer?* J Biol Chem, 1999. **274**(36): p. 25499-509.
42. Takeda, K., et al., *Targeted disruption of the mouse Stat3 gene leads to early embryonic lethality.* Proc Natl Acad Sci U S A, 1997. **94**(8): p. 3801-4.
43. Wearsch, P.A. and P. Cresswell, *The quality control of MHC class I peptide loading.* Curr Opin Cell Biol, 2008. **20**(6): p. 624-31.
44. Grillo, C., et al., *The DNA-binding activity of protein disulfide isomerase ERp57 is associated with the a(') domain.* Biochem Biophys Res Commun, 2002. **295**(1): p. 67-73.
45. Horton, J.D., J.L. Goldstein, and M.S. Brown, *SREBPs: activators of the complete program of cholesterol and fatty acid synthesis in the liver.* J. Clin. Invest., 2002. **109**(9): p. 1125-1131.
46. Schroder, M. and R.J. Kaufman, *The mammalian unfolded protein response.* Annu Rev Biochem, 2005. **74**: p. 739-89.
47. Putney, J.W., Jr., *Recent breakthroughs in the molecular mechanism of capacitative calcium entry (with thoughts on how we got here).* Cell Calcium, 2007. **42**(2): p. 103-10.
48. Burns, K., et al., *Modulation of gene expression by calreticulin binding to the glucocorticoid receptor.* Nature, 1994. **367**: p. 476-480.

49. Panaretakis, T., et al., *The co-translocation of ERp57 and calreticulin determines the immunogenicity of cell death.* Cell Death Differ, 2008. **15**(9): p. 1499-509.
50. Lim, C.P. and X. Cao, *Structure, function, and regulation of STAT proteins.* Mol Biosyst, 2006. **2**(11): p. 536-50.
51. Gold, L.I., et al., *Overview of the role for calreticulin in the enhancement of wound healing through multiple biological effects.* J Investig Dermatol Symp Proc, 2006. **11**(1): p. 57-65.
52. Akira, S., *Roles of STAT3 defined by tissue-specific gene targeting.* Oncogene, 2000. **19**(21): p. 2607-11.
53. Redell, M.S., et al., *Conditional overexpression of Stat3alpha in differentiating myeloid cells results in neutrophil expansion and induces a distinct, antiapoptotic and pro-oncogenic gene expression pattern.* J Leukoc Biol, 2007. **82**(4): p. 975-85.

Chapter Six
Future Directions

This study has provided novel information regarding the expression of calnexin and ERp57 throughout embryonic development as well insight into the role these proteins play in intracellular signalling. These projects, however, can be extended and elaborated on in order to gain further insight into the function of ERp57 and calnexin and their involvement in disease.

The calnexin-deficient mice, as discussed earlier, have severe ataxic phenotype and are significantly smaller than their wild-type littermates. It would be interesting to monitor skeletal development of both wild-type and calnexin-deficient mice to determine whether there is any gross morphological skeletal abnormalities that could contribute to the smaller size of the deficient mice [1]. Aside from performing x-ray radiography, we could also perform alcian-blue/alizaine-red staining for acid mucopolysaccharides and glycosaminoglycans components of cartilage and for ossified bones (via forming calcium complexes) respectively. Again, this may indicate whether there is irregular bone formation in the absences of calnexin that could potentially contribute to the size differences observed.

In order to investigate the role calnexin may play in skeletal formation, we could isolate chondrocytes or cartilage cells from both wild-type and calnexin-deficient mice and measure whether there are any differences in expression of cartilage specific components [2, 3]. Chondrocytes are highly specialized cells that function to produce collagen types II, IX, X and XI as well as the large proteoglycan, aggrecan [3]. Studies using primary cultures of chondrocytes from wild-type and calnexin-deficient mice

would complement phenotypic studies and allow us to biochemically characterize these mice.

In order to fully understand why there is strict expression of calnexin to neuronal tissues as well as cartilage during embryonic development, it would be important to look at transcriptional regulation of the calnexin gene. Previous analysis of the calnexin promoter has shown that the transcription factor PAX6 (paired box gene 6), that has a role in neuronal development, activates the calnexin promoter (Qiu, Y, unpublished results.) Further studies need to be carried out to determine the site of binding of PAX6 on the calnexin promoter. However, we propose that there are other candidate transcription factors that contribute to the expression of calnexin including Krox-20. Krox-20 is of particular interest because it not only has a very important role in Schwann cell development but also in proper skeletal development (see Chapter 5 – General Discussion) [1, 4]. Calnexin is highly expressed in both neuronal and cartilage tissue of developing embryos and to understand how this specific expression is achieved by identifying transcription factors involved would allow us to gain insight into critical functionality of calnexin throughout development.

In order to investigate the potential protective role of ERp57 in paediatric lung injury, we propose to administer oxygen-induced bronchopulmonary dysplasia (BPD) to both wild-type and ERp57-heterozygote mice pups and measure response in terms of lung injury [5]. We cannot use ERp57-deficient pups because ERp57-deficieny is embryonic lethal [6, 7]. ERp57-heterozygote mice are viable and have no gross morphological differences when compared to their wild-type

littermates. In order to carry out oxygen-induced BPD in our wild-type and ERp57-heterozygote mice, we would perform experiments as described by Ladha, F. et al. [5]. We would subject our wild-type and ERp57-heterozygote mice pups randomly to normoxia conditions (21% O_2) or hyperoxia conditions (95% O_2, BPD-model) in sealed containers [5]. We would perform histological analysis of the lungs and look at number and size of air spaces and capillary density [5]. In oxygen-induced BPD mouse models there are fewer and enlarged air spaces as well as decreased capillary density [5]. We expect that the ERp57-heterozygote mice will be more susceptible to oxygen-induced BPD and will show more severe lung injury when compared to wild-type littermates. When ERp57 is expression is knocked down via siRNA in epithelial cells, we observe sensitivity to hyperoxia-induced apoptosis as well when neonatal rats are subject to hyperoxia-induced lung injury there is a down-regulation of ERp57 [8]. We propose that having 2 copies of ERp57 (in the wild-type mice) as compared to 1 copy of ERp57 (in the ERp57-heterozygote mice) will have a significant difference in the severity of outcome of oxygen-induced BPD further demonstrating the role of ERp57 in paediatric lung injury.

Although we know that the absence of ERp57, and calreticulin, impact STAT3 signalling (Figure 3-10 and 3-11) we do not know which downstream genes are affected in the absence of ERp57. Knowing genes that are up- or down-regulated in the absence of ERp57 should help gain insight into the mechanisms that result in embryonic lethality in these deficient mice. We propose to carry out gene expression profiling experiments or DNA microarray analysis on the wild-type and ERp57-deficient mouse embryonic fibroblasts to help identify genes that are

impacted by the absence of ERp57. We have established that ERp57 modulates STAT3 signalling and DNA microarrays of STAT3-deficient and over-expressing cells have identified hundreds of potential downstream gene targets [9-11]. STAT3 can act as a repressor and activator to mediate diverse biological processes including cell growth, oncogenesis and differentiation [9]. This leaves the door wide open for the candidate genes that ERp57 may modulate through STAT3 for development and survival.

In order to fully understand whether these cysteine residues contribute to the functionality of the calnexin *in vivo*, it would be interesting to link specific disease causing substrates to calnexin. Myelin specific proteins P0 and PMP22 are critical to the compaction and maintenance of myelin through hetero- and homo-philic interactions [12]. As discussed earlier, PMP22 and P0 have been shown to bind to calnexin [13, 14] and mutations to both of these proteins have been linked to neurological diseases such as Charcot-Marie-Tooth disease [15]. It would be interesting to determine whether calnexin mutants that we have generated are able to interact with P0 and PMP22 proteins. By directly looking at specific substrates of calnexin *in vivo*, not only would we be able to confirm thermal aggregation in vitro data this would provide us with some intriguing information. Although mutants of both P0 and PMP22 have been associated with human neuropathologies, calnexin is just recently being directly implicated in human disease [12, 13]. Recently, our lab showed that calnexin has a specific and detrimental effect on myelin formation in mice [12, 13]. Calnexin homologs, however, have been identified in human and the amino acid sequence of calnexin is highly conserved among

human and mouse sharing approximately 93-98% sequence identity [16]. Interestingly, a mouse model expressing calnexin with its carbohydrate binding pocket disrupted was phenotypically identical to that of the calnexin-deficient mouse [17]. Taken together this suggests that perhaps that human neuropatholgies are associated with mutant forms of calnexin that are unable to properly function as a molecular chaperone of PMP22 and P0. Our study has identified that both the N- and P-domain cysteines have a role in the chaperoning of glycosylated substrates suggesting that these mutants may be implicated in neuropathologies.

References

1. Levi, G., et al., *Defective bone formation in Krox-20 mutant mice.* Development, 1996. **122**(1): p. 113-20.
2. Bandtlow, C.E. and D.R. Zimmermann, *Proteoglycans in the developing brain: new conceptual insights for old proteins.* Physiol Rev, 2000. **80**(4): p. 1267-90.
3. Lefebvre, V., et al., *Characterization of primary cultures of chondrocytes from type II collagen/beta-galactosidase transgenic mice.* Matrix Biol, 1994. **14**(4): p. 329-35.
4. D'Antonio, M., et al., *Gene profiling and bioinformatic analysis of Schwann cell embryonic development and myelination.* Glia, 2006. **53**(5): p. 501-15.
5. Ladha, F., et al., *Sildenafil improves alveolar growth and pulmonary hypertension in hyperoxia-induced lung injury.* Am J Respir Crit Care Med, 2005. **172**(6): p. 750-6.
6. Coe, H., et al., *ERp57 modulates STAT3 signalling from the lumen of the endoplasmic reticulum.* J Biol Chem, 2009.
7. Garbi, N., et al., *Impaired assembly of the major histocompatibility complex class I peptide-loading complex in mice deficient in the oxidoreductase ERp57.* Nat Immunol, 2006. **7**(1): p. 93-102.
8. Xu, D., et al., *Knockdown of ERp57 Increases BiP/GRP78 Induction and Protects against Hyperoxia and Tunicamycin-induced Apoptosis.* Am J Physiol Lung Cell Mol Physiol, 2009.
9. Snyder, M., X.Y. Huang, and J.J. Zhang, *Identification of novel direct Stat3 target genes for control of growth and differentiation.* J Biol Chem, 2008. **283**(7): p. 3791-8.
10. Paz, K., et al., *Transformation fingerprint: induced STAT3-C, v-Src and Ha-Ras cause small initial changes but similar established profiles in mRNA.* Oncogene, 2004. **23**(52): p. 8455-63.
11. Clarkson, R.W., et al., *The genes induced by signal transducer and activators of transcription (STAT)3 and STAT5 in mammary epithelial cells define the roles of these STATs in mammary development.* Mol Endocrinol, 2006. **20**(3): p. 675-85.
12. Kraus, A., et al., *Calnexin deficiency leads to dysmyelination.* J Biol Chem, 2010.
13. Jung, J., Janowicz, A., Coe, H., Kraus, A. and Michalak, M. , *Specialization of Endoplasmic Reticulum Chaperones for the Folding and Function of Myelin Glycoproteins P0 and PMP22.* submitted, 2010.
14. Dickson, K.M., et al., *Association of calnexin with mutant peripheral myelin protein-22 ex vivo: A basis for "gain-of-function" ER diseases.* Proc. Natl. Acad. Sci. U.S.A., 2002. **99**: p. 9852-9857.
15. Shames, I., et al., *Phenotypic differences between peripheral myelin protein-22 (PMP22) and myelin protein zero (P0) mutations associated with Charcot-*

Marie-Tooth-related diseases. J Neuropathol Exp Neurol, 2003. **62**(7): p. 751-64.

16. Jung, J., Coe, H., Opas, M., and Michalak, M., *Calnexin: An Endoplasmic Reticulum Integral Membrane Chaperone.* Calcium Binding Proteins, 2006. **1**(2): p. 67-71.
17. Denzel, A., et al., *Early postnatal death and motor disorders in mice congenitally deficient in calnexin expression.* Mol. Cell. Biol., 2002. **22**(21): p. 7398-7404.

Appendix

IRE1α System Creation Study

Introduction

Calnexin is a type I integral endoplasmic reticulum (ER) membrane protein involved in quality control in the secretory pathway and in the folding of newly synthesized monoglucosylated proteins [1]. Calnexin associates with ERp57, an oxidoreductase belonging to a family of protein disulfide isomerase [2]. ERp57 catalyzes disulfide bond formation and exchange on the glycoproteins bound to calnexin [2].

Several studies have mapped the carbohydrate binding site to the N-domain and residues Tyr^{165}, Lys^{167}, Tyr^{186}, Glu^{217},Glu^{426}, Trp^{428}, Cys^{161} and Cys^{195} have all been implicated [3-5]. Recently, the Cys^{361} and Cys^{367} residues in the P-arm domain have also been shown to be involved in substrate binding (Chapter 4). The arm domain is not thought to be directly involved in substrate binding, however it has been shown to enhance the folding function of the globular domain and it is speculated to have a role in physically constraining the glycoprotein when bound to the N-domain [5]. The P-arm domain of calnexin is a proline-rich tandem repeat domain containing four copies of repeat domains arranged in a linear pattern of 11112222 [6]. The P-domain is responsible for mediating interactions of calnexin with ERp57 and mutagenesis studies have mapped the binding to the tip of the P-domain at residues Trp^{343}, Asp^{344}, Gly^{349} and Glu^{352} [5, 7, 8]. Recent studies in our lab also implicate Cys^{361} and Cys^{367} and N-domain residues His^{202}, Cys^{161} and Cys^{195} in ERp57 binding (Chapter 4) [3].

In vitro studies showing ERp57 binding to calnexin such as Surface Plasmon Resonance (SPR) Analysis and NMR structural analysis have

identified the P-arm domain of calnexin as being critical to ERp57 binding [3-5, 7]. The objective of this study was to identified amino acid residues and of calnexin critical for (i) ERp57-calnexin interactions and (ii) calnexin specific substrate binding in a cellular system. In this study, we exploit the IRE1 (inositol requiring enzyme 1) branch of the unfolded protein response pathway to measure protein interaction in a cellular system (Figure S1) [7]. We based our model after a yeast-system developed by the Thomas group [7]. They developed a novel membrane yeast two-hybrid system (termed MYTHS) that is able to detect interactions between ER proteins [7]. Through their model they confirmed that the C-terminal region of ERp57 is responsible for interaction with the tip of the P-domain of calnexin [7]. We have set out to adapt their yeast system to a mammalian system to investigate residues of calnexin that are important for ERp57 binding. In our model, we would use RT-PCR for Xbp1 splicing [9] as a qualitative readout and luciferase assay using an Xbp1-luciferase splicing plasmid [9, 10] as a quantitative readout to indirectly show interaction of two proteins. Developing a mammalian system where interaction of ER proteins can qualitatively and quantitatively be measured will provide us with a standard tool to investigate endless combinations of ER proteins.

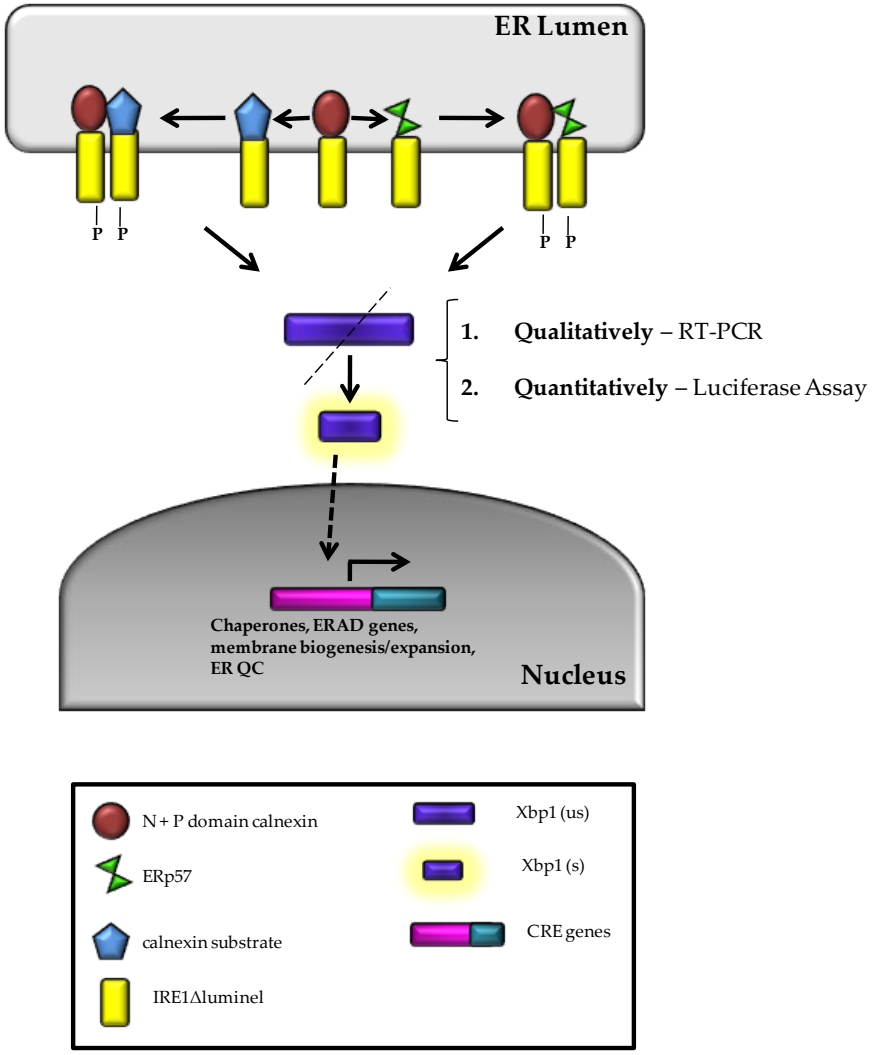

Figure S1

Figure S1 - Model of mammalian IRE1αΔluminal ER protein-protein interaction system. Fusions of proteins calnexin (*purple circle*), ERp57 (*green bowtie)* and a calnexin substrate (*blue pentagon)* in place of the substrate binding domain of IRE1α and to the transmembrane kinase/endoribonuclease domain of IRE1α. Interaction of two proteins results in oligermerization of IRE1α inducing autophosphorylation of the IRE1α kinase domains. This leads to activation of the IRE1α endoribonuclease domain which then leads t the processiing of the mRNA of the UPR transcriptional activator , Xbp1 –us (*purple rectangle)* to Xbp1-s (*glowing purple rectangle).* This splicing event of Xbp1 can be measured qualitatively by RT-PCR and quantitatively by luciferase assay.

Materials and Methods

Plasmids and DNA – Mouse IRE1α plasmid DNA was a generous gift from Dr.K. Myoshi. Mouse IRE1α is cloned into pcDNA3.1(+) at Kpn1 and Apa1 sites. p2K7-calnexin was derived previously (Chapter 4) and it contained full length mouse calnexin and the promoter EF1α (cellular polypeptide chain elongation factor 1 alpha) into the destination lentiviral vector $2K7_{bsd}$ (containing blasticidine resistance gene for cell selection.) GST containing plasmid (pGEX-3X) was obtained from GE Healthcare and contains one copy of GST. ERp57 template was generated previously [11] and briefly, is cDNA of full-length ERp57 generated from mouse brain library. Commercial pcDNA3.1/Zeo with a cytomegalovirus (CMV) promoter and zeocin resistance gene was used as the targeting vector (Invitrogen).

Mutagenesis – Using, methods from QuickChange XL Site-Directed Mutagenesis Kit (Stratagene) and *Pfu* DNA polymerase, restriction sites were engineered into the above template DNA. The following primers were used with restriction sites underlined and gene specific nucleotides in bold: to full-length IRE1α to clone in the mini-multiple cloning site (mini-MCS) forward 5′-GCTAGCTCTAGAGAATTCGATATC**ATGGCTACCATTATCCTGAGCACCTTCCTGC**-3′ and to clone in Apa1 reverse 5′-GGGCCC**GAGGGCTGCCCTAGCTCAGAGGGCATATGGAATCACTGG**-3′; to clone in restriction sites into calnexin Nhe1 forward 5′-GCTAGC**ATGGAAGGGAAGTGGTTAC**-3′ and EcoR1 reverse 5′-GAATTC**CAAAATGTAGACCACCCAAAGCC**-3′; to clone in restriction sites into ERp57 Xba1 forward 5′-

TCTAGA**ATGCGCTTCAGCTGCCTAG**-3′ and EcoRV reverse 5′-GATATC**GAGGTCCTCTTGTGCCTT**-3′; and GST Nhe1 forward 5′-GCTAGC**ATGTCCCCTATACTAGG**-3′ and GST Xba1 reverse 5′-TCTAGA**CGATGAATTCCCGGGGATC**-3′.

E.coli expression, restriction and ligation – All plasmid DNA templates were expressed in Stbl3.1 MTase-deficient *E.coli*. After mutagenesis, PCR purification was carried out (Sigma) and restriction digest performed using enzymes from New England Biolabs according to the specifications outlined. Digested products were run on a 1% agarose gel and gel purification of products performed using QIAquick Gel Extraction Kit (Qiagen). Ligation of digested products was carried out at 37°C overnight using T4 ligase and T4 ligation buffer (New England Biolabs) at a 1:10 ratio (based on DNA concentration) of vector to insert. 6ul of ligated product was transformed into DH5α *E.coli* and DNA isolated from resulting colonies using a Sigma mini-prep. Colonies were checked for insert via size on 1% agarose gels and performed DNA sequencing analysis.

Results

Engineering in restriction sites – In order to create fusion proteins of the cytoplasmic/active portion of IRE1 with our proteins of interest, calnexin, ERp57 and GST (control), we engineered in restriction sites to physically cut and ligate proteins together. Figure S2A shows the DNA plasmid templates that we will be utilizing for the study. Mouse IRE1α is an ER transmembrane protein with its N-terminal sensor domain that is responsible for detecting misfolded proteins located in the ER lumen [12].

In response to misfolded proteins, IRE1α oligermerizes and its C-terminal cytoplasmic domain autophosphorylates activating its endoribonuclease activity that specifically cleave 26 nucleotides from X-box-binding protein 1 mRNA (Xbp1-us) releasing the active transcription factor (Xbp1-s). Xbp1-s translocates to the nucleus to activate genes to deal with misfolded proteins in the ER [12]. Calnexin is also a transmembrane protein with its chaperone and ERp57 binding domains (N+P domains) located in the ER and its Ca^{2+} binding C-tail located in the cytoplasm [6]. ERp57 is an ER luminal protein that has catalytically active domains (*a* and *a'*) and calnexin binding domains (*b* and *b'*) [2]. The GST protein is used as a positive control as GST proteins will form dimers, thus, once fused to IRE1α, will result in a constitutively activated endoribonuclease activity [7].

When engineering in restriction sites for downstream use, two factors must be taken into consideration: (i) the restriction sites must be unique and (ii) the inserted restriction sites must be in frame. Keeping this in mind, we proceeded to select restriction sites to insert around our protein of interest followed by insertion of all used restriction sites, in sequence, in front of the transmembrane domain and endoribonuclease domain of IRE1α (Figure S2B). PCR was performed (See "Materials and Methods") to engineer these sites into the DNA templates (Figure S2C). We have obtained PCR products containing restrictions sites for IRE1α, calnexin, ERp57 and GST (Figure S2C) that are the correct size and also have been checked via DNA sequencing analysis.

Generation of the IRE1αΔluminal-mini-MCS - The first step of creating this system was to generate a targeting vector (IRE1αΔluminal-mini-MCS) that contains the transmembrane domain and endoribonuclease domain of IRE1α and a multiple cloning (mini-MCS) site containing restriction sites that have been engineered into the proteins of interest (Nhe1, Xba1, EcoRV and EcoR1) (Figure S2B and Figure S3A and B.) First, PCR was carried out to insert the mini-MCS in front of the transmembrane domain and endoribonclease domain and an Apa1 restriction site after the endoribonclease domain (Figure S2C). Next, restriction digest was carried out (see "Materials and Methods") using Apa1 and Nhe1 (the most N-terminal restriction site in the mini-MCS) in the resulting PCR product as well as a target vector (pcDNA3.1-zeocin) containing a multiple cloning site as well as a zeocin resistance gene which will be important for downstream selection (Figure S3A and B). Using a T4 ligase, we inserted the IRE1-mini-MCS product without the luminal domain into the pcDNA3.1 vector (Figure S2A and B). The product was transformed into DH5α *E.coli* and selected with ampicillin resistance and 7 positive colonies were selected (Figure S3B). The increase in size of DNA from colony number 5 compared to the other 6 colonies suggested that the insert had ligated into the vector and this was confirmed by digestion of the plasmid with Apa1 and Nhe1 enzymes as well as sequencing (Figure S3A and B). This resulting plasmid was named IRE1αΔluminal-mini-MCS and will be the target of insertion of proteins of interest including calnexin, ERp57 and GST.

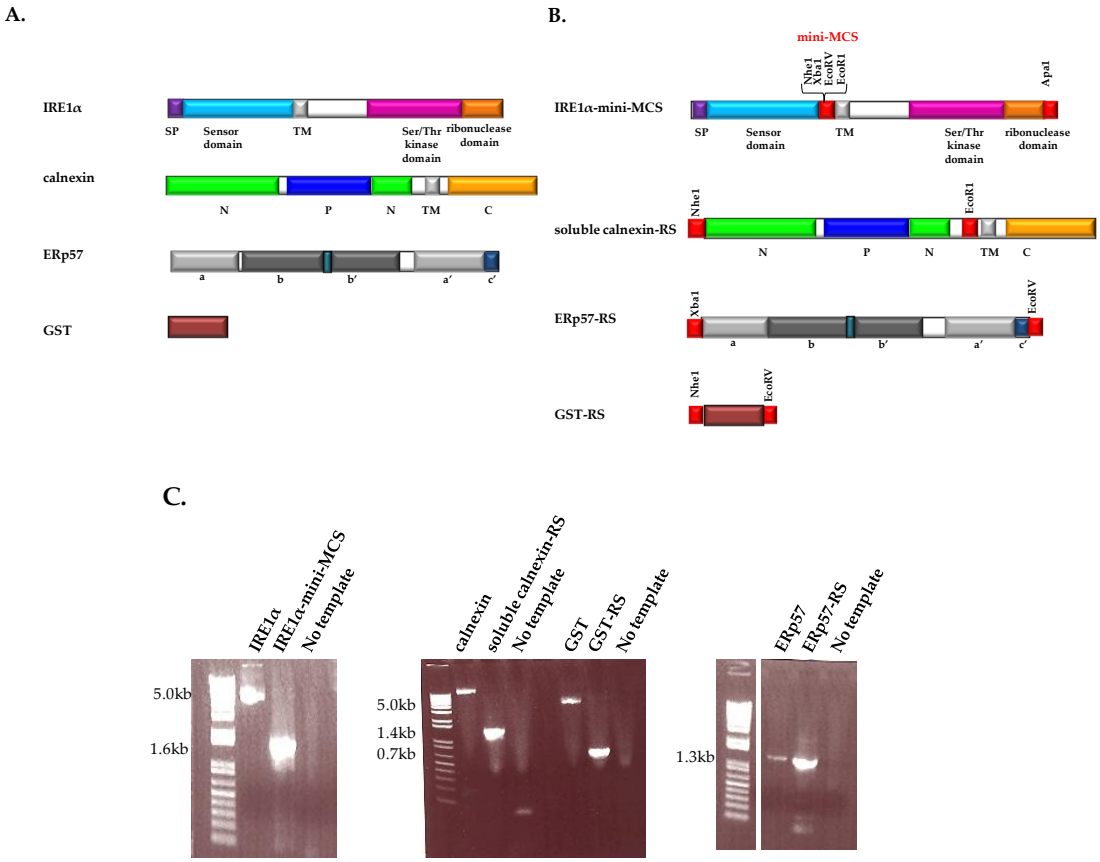

Figure S2

Figure S2 - Engineering in restriction sites A. Domain structure of IRE1*α* from mouse IRE1*α* pcDNA3.1(+), calnexin from p2K7-calnexin (Coe, et al. 2008), ERp57 from full-length ERp57 (Coe, et. al. 2010) and GST from pGEX-3x (GE Healthcare). Domains of each protein are color coded and the domain indicated below **B.** Restriction sites to be inserted into proteins are indicated above each protein. IRE1*α* has 4 restriction sites (*red box,* mini-multiple cloning site (MCS)) engineered between its transmembrane /kinase domain (*grey box*) and its sensor domain (*light blue box)* and is then termed IRE1*α*-mini-MCS. Calnexin has an Nhe1 site (*red box)* engineered at its N-terminal domain in front of the beginning of the N-domain (*green box)* and an EcoR1 site (*red box)* between the N-domain (*green box*) and the transmembrane domain (*grey box)* and is then termed soluble calnexin-RS (restriction sites). ERp57 has a Xba1 restriction site (*red box)* inserted in front of the *a* domain (*grey box)* and an EcoRV site (*red box)* behind its c′ domain (*navy blue*) and is then called ERp57-RS. GST is surrounded by a Nhe1 site and EcoRV site and is then known as GST-RS. **C.** Acrylamide gels showing the template (as in **A)** and the PCR product with engineered restriction sites (as in **B**).

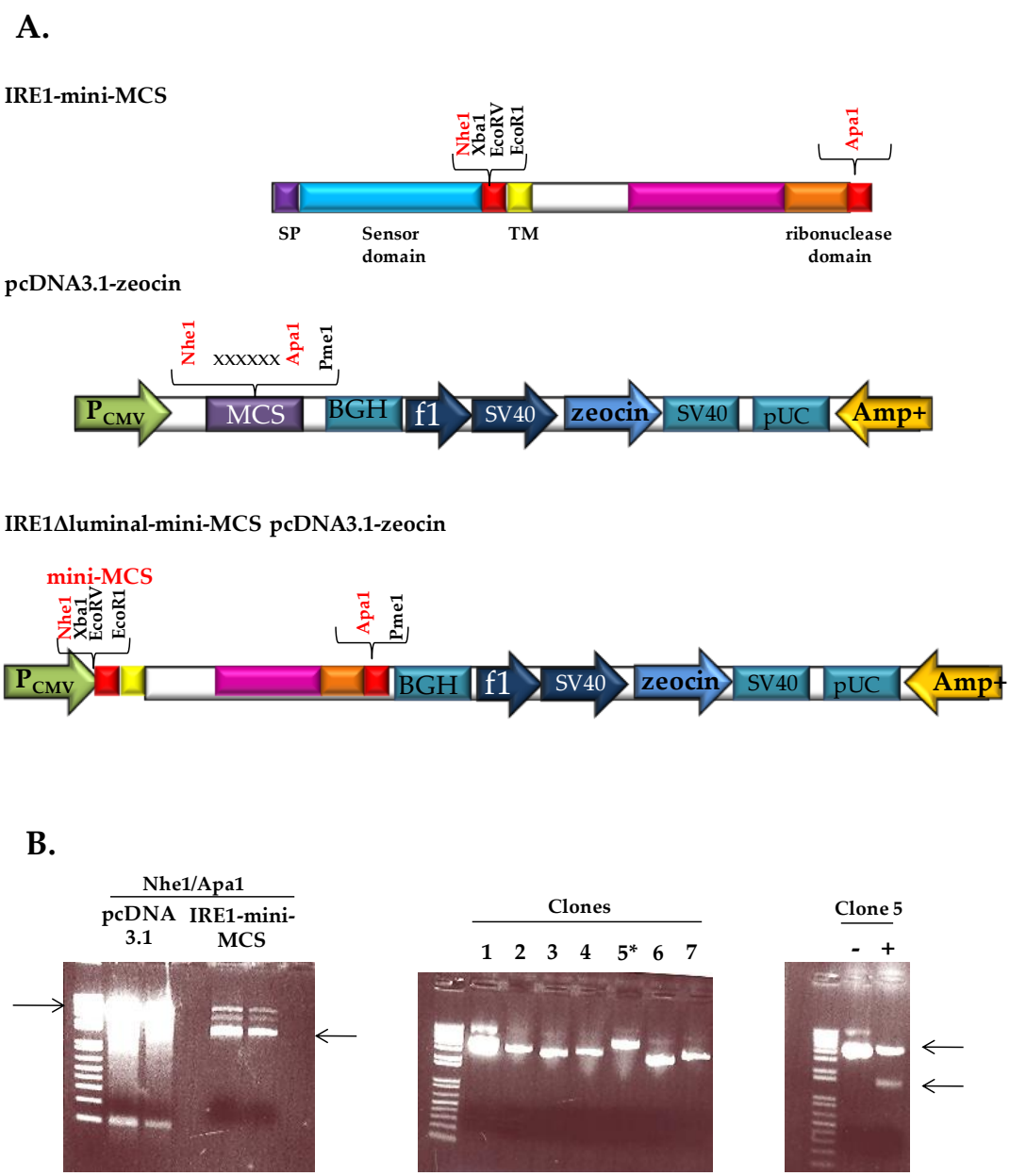

Figure S3

Figure S3 - Generation of the IRE1αΔluminal-mini-MCS pcDNA3.1-zeocin A. IRE1-mini-MCS, pcDNA3.1-zeocin templates were digested with Nhe1 and Apa1 and ligated to form IRE1αΔluminal-mini-MCS **B.** acrylamide gels with digestion products from Nhe1/Apa1 restriction (*top arrow*, vector and *bottom arrow*, insert). After ligation, clones from resulting colonies are shown with * indicates positive clone. Clone 5 was digested with Nhe1/Apa1 (+) or not digested (-) and top arrow indicates vector and bottom arrow indicates insert.

Insertion of calnexin into IRE1αΔluminal-mini-MCS – In order to insert calnexin into our target vector (IRE1αΔluminal-mini-MCS) we utilized the EcoR1 and Nhe1 restriction sites engineered surrounding the soluble domains of calnexin and in the mini-MCS of IRE1αΔluminal-mini-MCS (Figure S2B and Figure S4A). We digested with EcoR1 and Nhe1 and ligated the digested vector (Figure S4B, *lane 1*) and insert (Figure A2-S4B, *lane 2*) using a T4 ligase. We then transformed DH5α *E.coli* and isolated DNA from 4 colonies (Figure S4C, *lanes 2-5*) and analyzed on a 1% acrylamide gel (Figure S4C). DNA from clones 3 and 4 was isolated and we performed sequencing analysis and found to be positive for the N+P domains of calnexin and the transmembrane and endoribonuclease domain of IRE (Figure S4A).

Discussion

In this study, we have initiated work on a genetic system that can be utilized to measure both qualitatively and quantitatively the interaction between two ER resident proteins (Figure S1). We designed tools that will exploit the IRE1α branch of UPR signalling by replacing the sensor domain of IRE1α with proteins of interest (Figure S2). We have successfully created a target vector (IRE1αΔluminal-mini-MCS) that does not contain the luminal sensor domain of IRE1α but does contain a small multiple cloning site (mini-MCS) for insertion of proteins of interest as well as the endoribonulease domain of IRE1α (Figure S3). Using this vector, we inserted soluble calnexin (N+P domains) in front of endoribonuclease domain (Figure S4). We also have created mutants of full-length ERp57 that contain restriction sites Xba1 and EcoRV (ERp57-

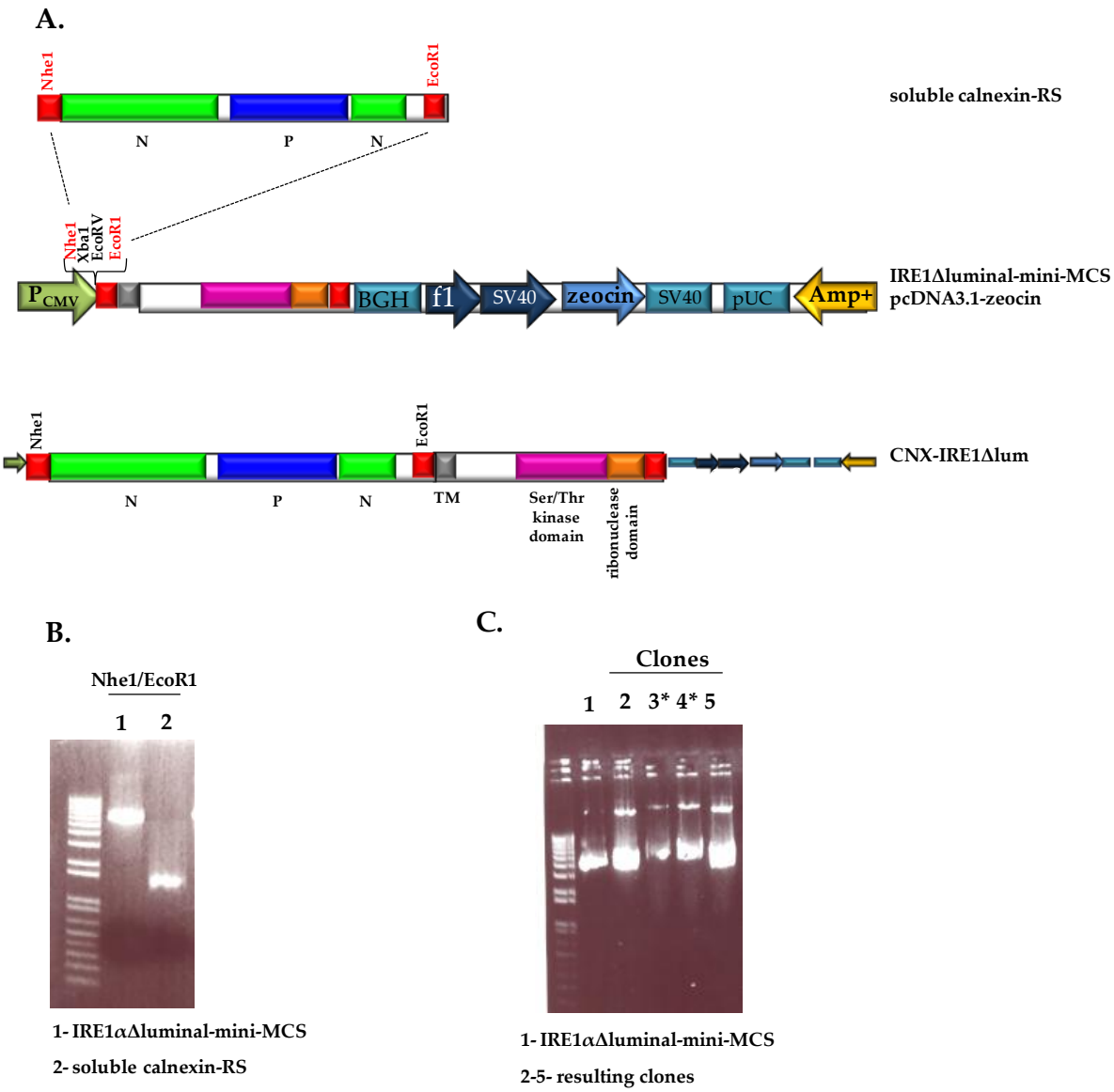

Figure S4

Figure S4 - Insertion of calnexin into IRE1Δluminel-mini-MCS. **A.** Linear diagrams of the insert (soluble calnexin-RS) and the vector (IRE1Δluminal-mini-MCS-pcDNA3.1zeocin) with the enzymes used highlighted in red (Nhe1/EcoRI). A linear diagram of the resulting fusion protein is also shown (CNX-IRE1Δlum). **B.** Acrylamide gels showing digestion of vector (*lane 1)* and insert (*lane 2*) with Nhe1/EcoR1. **C.** DNA of 4 clones after ligation (* represents positive).

RS) and GST that contain restriction sites Nhe1 and EcoRV (GST-RS) (Figure S2). Additional work will need to be carried out on this project specifically, insertion of both GST and ERp57 into the IRE1$\alpha\Delta$luminal-mini-MCS and determination if the system works. For qualitative protein interaction analysis we will use RT-PCR to look at Xbp1 splicing and luciferase reporter assay for Xbp1 splicing to obtain quantitative information [9]. This system has the potential to be a powerful tool that can confirm the in vitro studies showing the interaction between ERp57 and calnexin and the amino acid residues that are critical for this interaction. Furthermore, this system could also be used to confirm the *in vitro* interaction between calnexin and substrates, such as PMP22, and elucidate the amino acid residues important for these functional interactions. An infinite number of combinations of ER protein can be engineered into this system and their interactions qualitatively and quantitatively measured.

References

1. Trombetta, E.S. and A.J. Parodi, *Quality Control and Protein Folding in the Secretory Pathway.* Annu. Rev. Cell Dev. Biol., 2003(19): p. 649-676.
2. Coe, H. and M. Michalak, *Molecules in Focus ERp57, a multifunctional endoplasmic reticulum resident oxidoreductase.* Int J Biochem Cell Biol.
3. Groenendyk, J., Dabrowska, M., and Michalak, M., *Mutational analysis of calnexin.* Biochimica et Biophysica Acta, 2010.
4. Schrag, J.D., et al., *The structure of calnexin, an ER chaperone involved in quality control of protein folding.* Mol. Cell, 2001. **8**: p. 633-644.
5. Leach, M.R., et al., *Localization of the lectin, ERp57 binding, and polypeptide binding sites of calnexin and calreticulin.* J Biol Chem, 2002. **277**(33): p. 29686-97.
6. Jung, J., Coe, H., Opas, M., and Michalak, M., *Calnexin: An Endoplasmic Reticulum Integral Membrane Chaperone.* Calcium Binding Proteins, 2006. **1**(2): p. 67-71.
7. Pollock, S., et al., *Specific interaction of ERp57 and calnexin determined by NMR spectroscopy and an ER two-hybrid system.* Embo J, 2004. **23**(5): p. 1020-9.
8. Oliver, J.D., et al., *ERp57 Functions as a Subunit of Specific Complexes Formed with the ER Lectins Calreticulin and Calnexin.* Mol. Biol. Cell, 1999. **10**: p. 2573-2582.
9. Coe, H., et al., *Endoplasmic reticulum stress in the absence of calnexin.* Cell Stress Chaperones, 2008. **13**(4): p. 497-507.
10. Back, S.H., et al., *Cytoplasmic IRE1{alpha}-mediated XBP1 mRNA Splicing in the Absence of Nuclear Processing and Endoplasmic Reticulum Stress.* J Biol Chem, 2006. **281**(27): p. 18691-706.
11. Coe, H., et al., *ERp57 modulates STAT3 signalling from the lumen of the endoplasmic reticulum.* J Biol Chem, 2009.
12. Schroder, M. and R.J. Kaufman, *The mammalian unfolded protein response.* Annu Rev Biochem, 2005. **74**: p. 739-89.